Patrick Romano, Dipl.-Ing.

Ground Station Engineering and Operations of Nanosatellite Missions

DOCTORAL THESIS

to achieve the university degree of

Doktor der technischen Wissenschaften

submitted to

Graz University of Technology

Supervisor

Univ.-Prof. Dipl.-Ing. Dr. Otto Koudelka
Institute of Communication Networks and Satellite Communications

Second Advisor

Univ.-Prof. Dr. rer.nat. Dr.-Ing. e.h. Ernst Messerschmid
Universität Stuttgart, Institut für Raumfahrtsysteme

Graz, September 2015

EIDESSTATTLICHE ERKLÄRUNG

AFFIDAVIT

Ich erkläre an Eides statt, dass ich die vorliegende Arbeit selbstständig verfasst, andere als die angegebenen Quellen/Hilfsmittel nicht benutzt, und die den benutzten Quellen wörtlich und inhaltlich entnommenen Stellen als solche kenntlich gemacht habe. Das in TUGRAZonline hochgeladene Textdokument ist mit der vorliegenden Dissertation identisch.

I declare that I have authored this thesis independently, that I have not used other than the declared sources/resources, and that I have explicitly indicated all material which has been quoted either literally or by content from the sources used. The text document uploaded to TUGRAZonline is identical to the present doctoral dissertation.

Datum / Date

Unterschrift / Signature

Abstract

BRITE-Austria is the first Austrian satellite and part of the Bright Target Explorer (BRITE) mission, the world's first constellation of nanosatellites to observe the brightness oscillations of massive luminous stars by differential photometry. Up to now, six satellites (two each from Austria, Poland, and Canada) are part of the constellation.

To operate the constellation, a network of ground stations has been established, including ground stations in Austria (Graz), Canada (Toronto), and Poland (Warsaw). The operations concept for the mission foresees the use of a master station for each satellite, which is co-located with the respective mission control centre and has full control over the spacecraft, while the other stations are available as download, relay and/or backup stations.

While various nanosatellite ground stations systems are available, they mostly operate in the amateur radio bands and have low performance and availability requirements. The demanding scientific objectives of BRITE-Austria for a mission of this size require a professional ground segment and operations concept, capable of operating in regulated frequency bands and of providing high performance, high availability and reliability, while staying in line with a low-cost budget.

In the context of this thesis, a dedicated BRITE-Austria master ground station has been developed at the Institute of Communication Networks and Satellite Communications of Graz University of Technology. The design and configuration of the ground station are presented, showing a cost-effective approach for establishing a professional nanosatellite ground station. Subsequently, the mission operations concept with the existing ground station network is described, including operations support procedures such as ground station automation, remote access, as well as routine maintenance tasks.

A crucial aspect in the establishment of the ground station is the assessment of its performance. For this purpose, modelling and extended characterisation of the ground station with respect to its performance in both up- and downlink has been carried out, including measurements taken with comparable spacecraft in both the uplink and the downlink paths. Synergies and comparisons between simulations and measurements are presented.

The validation of the ground station and link performance took place during the commissioning and operations phase of the BRITE-Austria/TUGSAT-1 satellite after its launch in February 2013. Results of long term measurements to assess the communication link performance of the spacecraft with the ground station are presented. The results show high performance achievements of the system with high availability and reliability, significantly exceeding the mission requirements.

Finally, enhancements to the current system as well as an outlook are provided. Enhancements are considered on the ground station configuration as well as on the communication protocol side to increase the data throughput and to counteract link impairments. As an outlook, concepts of using the ground station for operating multiple nanosatellite missions are described.

The established ground segment and operations concept represents a professional approach for operating scientific small satellite missions. In addition, the distributed ground software concept makes the system scalable for multi-mission operations.

Kurzfassung

BRITE-Austria ist der erste österreichische Satellit und Teil der Bright Target Explorer Mission, der weltweit ersten Nanosatelliten-Konstellation zur Messung von Helligkeitsschwankungen massiver heller Sterne durch differentielle Photometrie. Die Konstellation besteht bisher aus sechs Satelliten, und zwar je aus zwei österreichischen, kanadischen und polnischen.

Die derzeit verfügbaren Nanosatelliten-Bodenstationen werden meist in Amateurfunkbändern betrieben und haben geringe Anforderung in Bezug auf Leistungsfähigkeit und Verfügbarkeit. Die hohen wissenschaftlichen Anforderungen der BRITE-Austria Mission erfordern jedoch ein professionelles Bodensegment, welches auch in lizenzierten Frequenzbändern operiert, hohe Leistungsfähigkeit, Verfügbarkeit und Zuverlässigkeit gewährleistet sowie zur gleichen Zeit in einem geringen Kostenrahmen realisiert werden kann.

Für den Betrieb der BRITE-Konstellation wurde daher ein eigenständiges Bodenstationsnetzwerk mit Stationen in Österreich (Graz), Kanada (Toronto) und Polen (Warschau) errichtet. Das Betriebskonzept basiert auf der Verwendung einer eigenen Master-Bodenstation für jeden Satelliten, die räumlich mit dem entsprechenden Kontrollzentrum vereint ist und Vollzugriff zum jeweiligen Satelliten bereitstellt, während die übrigen Stationen als Relais oder Backup dienen.

Im Rahmen dieser Dissertation wurde die BRITE-Austria Master-Station am Institut für Kommunikationsnetze und Satellitenkommunikation der Technischen Universität Graz entworfen und entwickelt. Das vorgestellte Bodenstationskonzept stellt eine kostengünstige Lösung für eine professionelle Kleinsatelliten-Bodenstation dar. Das angewandte Betriebskonzept ermöglicht die Vernetzung mit den anderen BRITE Bodenstationen sowie einen hohen Grad an Automatisierung und Fernwartung.

Ein wesentlicher Aspekt bei der Errichtung einer Bodenstation ist Feststellung der Funktion bzw. ihrer Leistungsfähigkeit. Es wurde daher eine detaillierte Modellierung und Charakterisierung der Bodenstation durchgeführt, inklusive Messungen mit vergleichbaren Satelliten. Eine Gegenüberstellung der Simulationen und Messergebnisse wird in der Arbeit präsentiert.

Die Beurteilung der Bodenstation und des Kommunikationslinks erfolgte in der Kommissionierungs- und Betriebsphase von BRITE-Austria/TUGSAT-1 nach dessen Start im Februar 2013. Ergebnisse von Langzeitmessungen zeigen eine hohe Effizienz, Verfügbarkeit und Zuverlässigkeit des Systems, welche die ursprünglichen Anforderungen um ein Vielfaches übertrifft.

Abschließend werden mögliche Erweiterungen des Systems beschrieben. Diese betreffen hauptsächlich mögliche Erweiterungen der Bodenstationskonfiguration sowie die Verwendung von effizienten Kommunikationsprotokollen zur Erhöhung des Datendurchsatzes und als Maßnahme zur Erkennung bzw.

Beseitigung von Störungen. Als Ausblick werden Konzepte vorgestellt, um die Bodenstation für den Betrieb unterschiedlicher Nanosatelliten-Missionen einzusetzen.

Das im Rahmen dieser Arbeit errichtete Bodensegment und erarbeitete Betriebskonzept stellt einen innovativen professionellen Ansatz für den Betrieb von wissenschaftlichen Kleinsatellitenmissionen dar. Das verteilte Kontrollsoftwarekonzept ermöglicht die Erweiterung des Systems für den Parallelbetrieb unterschiedlicher Missionen.

Contents

List of Figures

List of Tables

to my father

Acknowledgements

The author wishes to thank Prof. Otto Koudelka, Head of the Institute of Communication Network and Satellite Communications at Graz University of Technology, as advisor of this thesis for the valuable support in the realisation of this work.

The author is grateful to Prof. Ernst Messerschmid, professor at the University of Stuttgart, as co-reviewer of this thesis for his comments.

Further, the author is indebted to all people who provided support or contributed to the realisation of this thesis:

Prof. Martin Friedrich for the language revision of the thesis.

The colleagues at the Institute of Communication Networks and Satellite Communications for their co-operation and support in the BRITE-Austria project and the related thesis work.

The colleagues at UTIAS/SFL and the University of Vienna for the excellent cooperation in the BRITE-Austria project.

Special mention goes to my colleague Manuela Unterberger, systems engineer of BRITE-Austria, for the appreciated collaboration in the project.

Finally, I wish to thank my family for their unconditional support.

Chapter 1

Introduction

Space missions can be divided in three segments: the space segment, the ground segment, and the user segment [1]. The space segment includes one or more spacecraft with its payloads as well as the respective platforms with all the subsystems. The ground segment includes one or more ground stations and is responsible for communication with the space segment as well as for mission operations. In addition, the ground segment acts as interface to the user segment. The user segment represents the customers of the mission which benefit from applications and data products. The different outcomes of the mission are delivered to the user segment without the need to know all the underlying technicalities.

The relation and basic interaction between space segment, ground segment, and user segment is shown in Figure 1.1.

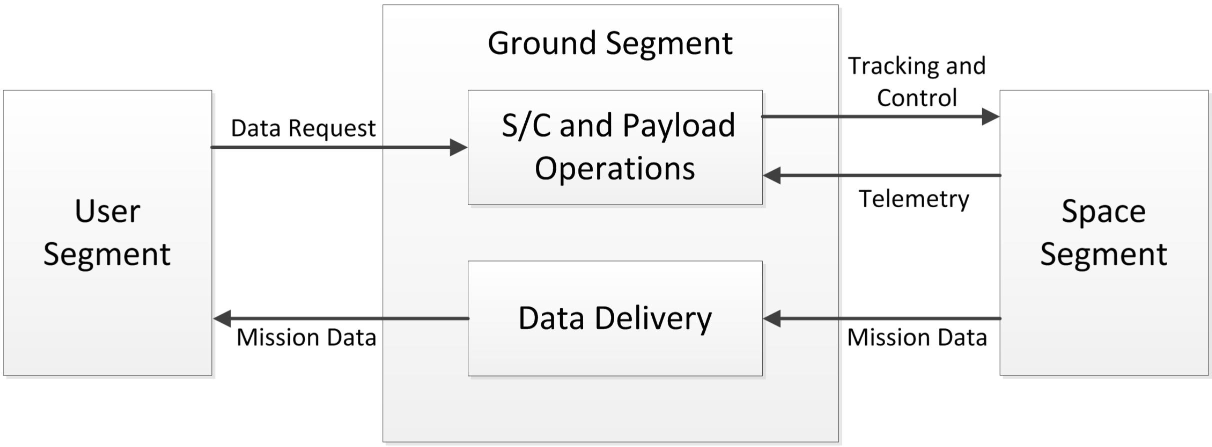

Figure 1.1: Relation between space mission segments. The relation between space, ground, and user segment is shown. The ground segment serves as interface to the space segment for spacecraft and payload operations. In addition, it processes requests from the user segment and forwards the requested data to the users.

This thesis deals with the ground segment and operations of nanosatellite missions. This chapter serves as an introduction to the topic of the thesis. After the provided overview of the different segments of a space mission, the next sections focus on the role of the ground segment. General considerations are outlined before going more into detail on the characteristics of ground segments for nanosatellite missions. Different considerations for the planning of a nanosatellite ground segment are discussed and examples are provided. Finally, the motivation and scope of this work are presented.

1.1 Ground Segment for Satellite Missions

The ground segment or ground system of a satellite mission consists of ground stations and mission control centres which cooperate to operate a space mission. A ground station is part of the ground segment of a mission and is used as physical communications interface with the space segment for command upload, and data download. Depending on the mission requirements, ground station networks rather than a single ground station are used to increase availability and to provide redundancy. A ground station or a ground station network can be of exclusive use for a particular mission, or share capacity among different missions. An example for the latter is the ESA tracking station network (ESTRACK), a worldwide network of ground stations allowing satellite operations from the European Space Operations Centre (ESOC) [2].

The main purpose of the ground segment of a satellite mission is to provide a communication link to the spacecraft. This includes uplink capabilities for satellite telecommand and tracking as well as downlink capabilities for satellite payload data and housekeeping telemetry download. The main tasks of the ground segment include [1]:

- **Mission planning and operations**

  Mission planning includes long term preparatory tasks for operating a mission, including implementation of the mission timeline, as well as scheduling and resource management tasks. Mission operations provide communication links with the spacecraft for telemetry, tracking, and control (TT&C) tasks. These tasks include the upload of spacecraft and payload commands, telemetry download and monitoring of spacecraft and payloads health status, as well as anomaly detection and assessment. In addition, mission operations provides capabilities for tracking one or multiple spacecraft and for operating with a ground station network (if applicable).

- **Mission data relay**

  Mission data relay deals with the provision of mission data to the users. The subtasks mainly include data handling, dissemination, archiving, and distribution.

- **Ground station maintenance**

  Ground station maintenance is crucial to keep the station operational to serve the mission. The tasks include routine maintenance as well as repairing capabilities and redundancy in case of outages.

1.2 Ground Segment for Nanosatellite Missions

The ground segment for a nanosatellite mission fulfils the same purpose as the ground segment for larger missions. The difference mainly lays in the usually lower budget and complexity. For example, re-use of Assembly, Integration, and Verification (AIV) systems for operations is a common approach for smaller missions for complexity and cost effectiveness [3].

1.2.1 Ground Segment Topology Considerations

When planning the ground segment for a nanosatellite mission, an important initial consideration is whether to use a single ground station or a ground station network. As nanosatellite missions usually operate in low Earth orbit (LEO), contact windows to the satellite are therefore limited. For a single ground station, depending on the satellite orbit and ground station location, possibly only a few contacts per day of about 10-15 minutes can be established. Therefore, a ground station network would always be desirable for operating the mission, since it increases availability by increasing the amount of contacts with the satellite. In addition, a ground station network provides redundancy, as temporary outage of a station can be compensated by other stations in the network. On the other hand, the use of a ground station network increases complexity in terms of interfaces, contact scheduling, personnel resources, and operations costs.

1.2.2 Ground Segment Implementation Options

An important step in the operations planning process for a nanosatellite mission is to decide if the mission will be operated by own ground station(s) or if operations are outsourced to suitable existing stations or networks.

The first possibility for operating a nanosatellite mission is to establish an own ground segment consisting of one or several ground stations. This approach allows customisation of the ground segment to the mission needs. In addition, it gives full control and autonomy for mission operations, as there is no need to coordinate the usage of the ground segment with other teams or organisations. The main drawback of this approach is the large expertise and effort required in the establishment of the ground segment. Development, establishment, verification, as well as operations and maintenance of a ground segment require substantial resources in terms of budget, time, expertise, and personnel power. While the establishment of a dedicated ground segment for a single mission represents considerable effort and introduces significant costs, this approach ensures sustainability if put in the context of a small satellite program development aiming at multiple mission operations. In this case, the main focus has to be laid on defining common ground segment requirements for the current and any future planned missions, as well as to provide modularity and flexibility in the design of the ground segment [4].

The second possibility for operating a nanosatellite mission is to buy excess capacity from existing ground stations or networks. This approach saves time and reduces complexity, as the infrastructure is already available and there is no need for development. However, interoperability has to be ensured, i.e. the mission has to be compliant with existing interfaces and standards applicable to the ground segment used. In addition, availability may be limited, because the ground segment is shared with other missions. Finally, this approach is not sustainable, as it is merely beneficial for the current mission; in case of follow-up activities planning of the ground segment has to be reconsidered.

1.2.3 Frequency Band Selection

Another important aspect in the planning process of nanosatellite missions is the selection of frequency bands [5]. At present, no dedicated International Telecommunication Union (ITU) [6] frequency band assignments for nanosatellites exist. Therefore, in order to obtain a license for a dedicated frequency band to operate a mission, the whole ITU coordination process has to be performed. This process can be quite extensive and time-consuming and in addition, expensive.

Therefore, nanosatellite missions often use amateur radio frequency bands for operations as it simplifies the frequency coordination process. It has to be noted that, if amateur radio frequencies are used, the coordination process has to go through the International Amateur Radio Union (IARU) [7] in addition to ITU [8]. Amateur radio equipment for the ground station is widely available and cheap, however, amateur radio bands impose many restrictions. The application range is very limited, as amateur radio bands can only be used for non-commercial purposes or for testing new technology. The frequency band allocations are also limited in usable bandwidths and RF power. In addition, many amateur radio bands are not for exclusive use - in certain cases even only for secondary use - exposing the mission's operation success at risk by potential radio interference issues.

1.2.4 Example 1: ESA Global Education Network for Satellite Operations (GENSO)

The Global Education Network for Satellite Operations (GENSO) is an ESA initiative aiming to develop a world wide ground station network for nanosatellite missions by the use of a common software standard, compatible with low cost off-the-shelf amateur radio equipment. In fact, GENSO is based on amateur radio frequency bands, simplifying the process of frequency coordination and utilisation. The idea of GENSO is to provide a tool for serving nanosatellite missions for educational purposes [9] [10].

The concept is based on the participation of many amateur radio ground stations which implement the software standard and serve as relay stations for various nanosatellite missions. This approach provides users access to their satellite without the need of having to set up an own ground station. Users can log in remotely to a GENSO station and establish contact to their satellite. Limitations of GENSO apply mainly due to the usage of amateur radio frequencies, affecting the nanosatellite applications (non-commercial), available bandwidths, and data rates.

The showcase for the GENSO network were the seven CubeSats launched as secondary payloads on the VEGA maiden flight in February 2012 [11]. Those satellites were using the GENSO network in addition to their own ground stations for operating their missions. In turn, those missions also served as testbed

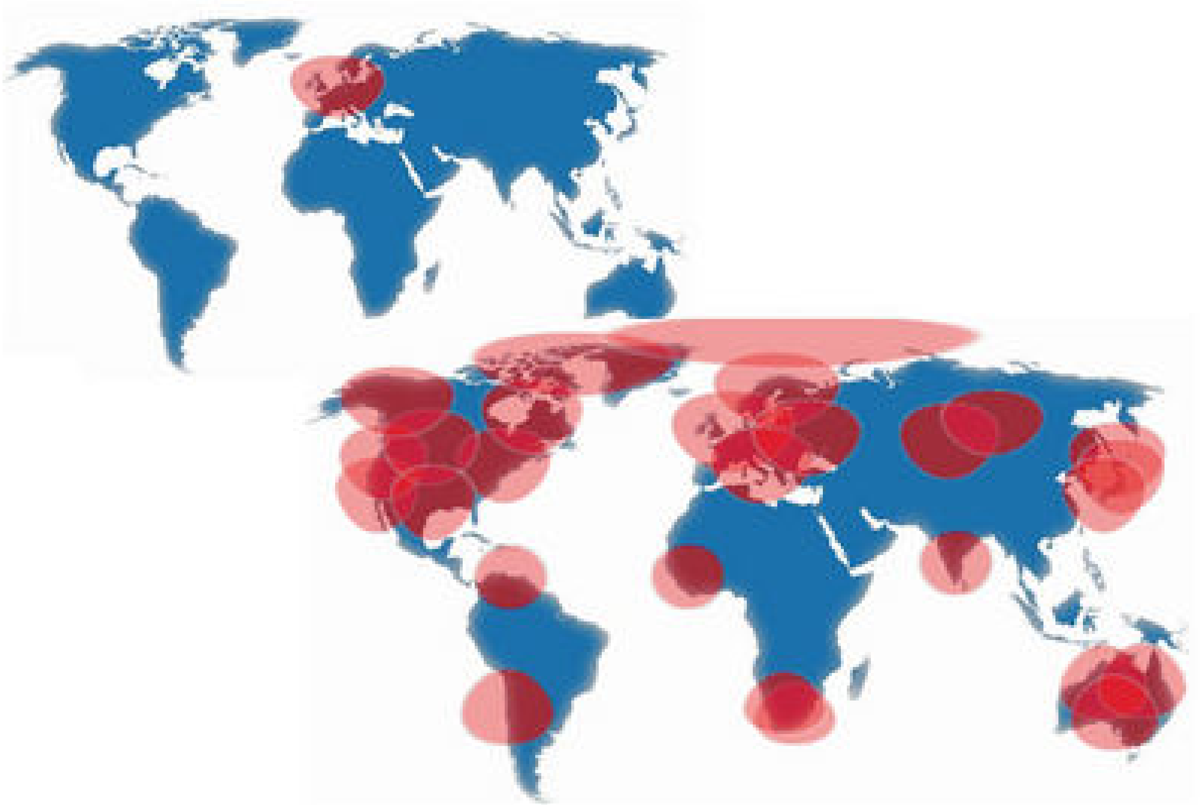

Figure 1.2: GENSO ground station network coverage. Coverage by educational satellite network in 2010 vs. proposed coverage by GENSO network with 30 nodes. The proposed network guarantees worldwide coverage and multi-mission operations. (image credit: ESA)

for the GENSO software.

Recently, due to outstanding developments and delays in the implementation, the GENSO approach has been losing interest and will no longer be supported. However, the GENSO idea and basic concept served as precursor to other approaches for nanosatellite ground station networks, more tailored to specific missions, that are now being pursued.

1.2.5 Example 2: Nanosatellite Ground Station Networks for the QB50 Mission

The QB50 mission is an FP7 project lead by the von Karman Institute for Fluid Dynamics (VKI). The project foresees the simultaneous launch of up to 50 double / triple CubeSats on the same launcher to carry out measurements in the Earth's lower thermosphere (90-320km), re-entry research, and in-orbit demonstration of miniaturised sensors and technologies [12].

The simultaneous operations of all 50 CubeSats and the short mission lifetime (about 6 months) represent a challenging endeavour. The data download requirements for the mission are *2 Mbit/day* (*1/8* of the nominal BRITE data download requirements). To ensure the data return, concepts to establish small ground station networks have been proposed. While the basic idea was to use the GENSO network, by

2013 it was determined that this approach would not be suitable for operating the mission. Therefore, two alternative ground station network concepts have been proposed.

1.2.5.1 QB50 Mini Ground Station Network

The QB50 mini ground station network is based on the idea of having a small number (typically 3) of ground stations available for a CubeSat within QB50, geographically distributed in a meaningful way for allowing efficient operations of the satellite given the challenge of operating a large number of CubeSats overlapping in their ground track for a short lifetime mission. The ground stations can be used for operating several CubeSats within QB50 and will be shared according to scheduling and prioritisation schemes.

The proposed network is based on the operations concept for the SwissCube mission by the École Polytechnique Fédérale de Lausanne (EPFL). The participating ground stations will be using a Satellite Control Software (SCS) for QB50 [13] which allows interconnection of the ground stations as well as centralised data management by a single mission control centre.

The SCS will support telecommand upload to the spacecraft, as well as housekeeping and science data download which will be stored to a mission server repository on the QB50 server and made available to the respective satellite team.

From the hardware requirements, a compatible telemetry and telecommand (TMTC) frontend is needed. The amateur packet radio standard based on the AX-25 protocol is used for data transmission.

1.2.5.2 ESA/ESOC CubeSat Ground Station Network

An alternative to the mini ground station networks using the satellite control software for QB50 is represented by the ESOC CubeSat Ground Station Network concept [14].

Unlike having a network of ground stations with both up- and downlink available for satellite operations, this concept is based on the use of a network of downlink-only ground stations which can be booked by the QB50 teams. A graphical user interface provides a map view of all the participating ground stations along with their availability and compatibility for the mission as well as the current schedules and timeline. When booking a ground station, the requesting CubeSat team has to ensure that the ground station schedule is compatible with the time-tagged scheduled data download on the spacecraft. The downloaded data will be made available to the respective team on an FTP server. The team then can use the partially downloaded files to fill holes from its own control station via telecommand requests.

The system is set up and running at ESA/ESOC and is currently being validated with the QB50 precursor flight missions launched in June 2014.

1.3 Motivation and Scope of This Work

This thesis has been realised in the context of the BRIght Target Explorer (BRITE) mission. The main motivation of this work was the participation in an international space project with an ambitious scientific objective. The BRITE mission has had a considerable response in the scientific community, showing that the selected nanosatellite platform provides excellent capabilities for performing first class science. The performance of the BRITE constellation in orbit exceeds the mission requirements - both in terms of attitude control performance and instrument sensitivity, thus considerably increasing the science return.

The demanding scientific objectives of BRITE-Austria for a mission of this size requires a professional ground segment and operations concept, capable of operating in regulated bands and of providing high performance, high availability and reliability, while staying in line with a low-cost budget. Therefore, the establishment of a dedicated ground station for BRITE-Austria represented a crucial task for operating the mission. In order to guarantee the mission data return, after the ground station establishment its performance had to be validated. The performance has been validated by simulations and several measurements prior to the satellite's launch and verified during its commissioning and early operations phase. During BRITE-Austria operations, improvements to the current system have been continuously investigated and implemented to extend the capabilities of the ground station. Furthermore, the possible extension of the ground station to serve as generic ground station for multiple nanosatellite mission operations has been investigated, including interoperability with well established space communication standards.

Commissioning and operations of a satellite mission are challenging but also very fascinating tasks. Besides the ambitious scientific goal and technical challenges, BRITE-Austria as the first Austrian satellite built and tested at the Institute of Communication Networks and Satellite Communications is also a matter of prestige. The ground station developed in the context of this work is the first ground station co-located with the mission control centre in Austria operating its own mission autonomously, providing an end-to-end space-to-ground interface for the mission to the users.

The rest of the thesis is structured in the following manner: **Chapter 2** gives an overview about the BRITE-Austria mission and the BRITE-Austria/TUGSAT-1 satellite. Special focus is laid on the communication subsystem as the space-to-ground interface, including test results of both functional as well as environmental tests of the spacecraft's communication subsystem.

Chapter 3 deals with the design and establishment of the BRITE-Austria master ground station, which is co-located with the mission control centre, including a detailed description and rationales for the design choices and selected components.

Simulations and measurements carried out to characterise the ground station performance are presented in **Chapter 4**. Validation of the ground station design at unit and system level is described along with the respective methods and results. In addition, measurements with comparable spacecraft in both uplink and downlink are presented, as well as comparisons between measured values and extended simulations of the communication links are provided.

In **Chapter 5**, the mission operations concept for BRITE-Austria is illustrated, including mission planning, execution, and evaluation strategies. In addition, various measurements for the verification of the link performance between the BRITE-Austria satellite and the ground station are presented.

Chapter 6 deals with possible enhancements to improve the performance of the current ground station design and provides an outlook for multiple nanosatellite mission operations scenarios.

Conclusions and an outlook for future work are provided in **Chapter 7**.

Chapter 2

The BRITE-Austria Nanosatellite and Its Communication System

The BRIght Target Explorer (BRITE) nanosatellite mission has the scientific objective of investigating the brightness oscillations of massive luminous stars with a visual magnitude V down to $V = +3.5$ by differential photometry [15] [16]. The mission is operated as nanosatellite constellation, the so-called BRITE-Constellation, which currently consists of five nanosatellites in orbit:

- 2 Austrian nanosatellites: BRITE-Austria (TUGSAT-1) and UniBRITE
- 2 Polish nanosatellites: BRITE-PL1 (Lem) and BRITE-PL2 (Heweliusz) [17]
- 2 Canadian nanosatellites: BRITE-Toronto and BRITE-Montreal [1] [18]

The satellites are designed to operate in pairs as listed above. Each spacecraft carries a photometric instrument, an optical camera with a high resolution charge coupled device (CCD) taking star images[19]. To fulfil the mission goals precise three-axis stabilisation down to arc minute level is used. Each satellite pair comprises one spacecraft with an optical filter sensitive in the red spectral range and the other spacecraft with an optical filter sensitive in the blue spectral range.

The operation of a constellation provides a significant improvement to the scientific output of the mission compared to a single spacecraft, as two spectral channels can be used. In addition, the more satellites in the constellation, the better the time and spatial coverage that can be achieved [20] [21].

The work presented in this chapter has been carried out in the context of the *BRITE-Austria/TUGSAT-1 Phase 1* Contract in the Framework of the *Austrian Space Applications Programme (ASAP)* funded by the *Austrian Research Promotion Agency (FFG)* of the Austrian *Ministry of Transport, Innovation, and Technology (BMVIT)* [22], entitled: *”BRIght Target Explorer - Austria mission (BRITE-Austria)”*, dedicated to the development of BRITE-Austria/TUGSAT-1 up to its flight readiness.

[1] BRITE-Montreal suffered a deployment failure on the DNEPR rocket and is not operational

2.1 The BRITE-Austria Nanosatellite

The BRITE-Austria/TUGSAT-1 project started in 2006. It was funded by the Austrian Research Promotion Agency (FFG) of the Austrian Ministry of Transport, Innovation, and Technology (BMVIT) in the framework of the Austrian Space Applications Programme (ASAP). BRITE-Austria is the first Austrian satellite and part of BRITE-Constellation. The satellite has been built at the Institute of Communication Networks and Satellite Communications of Graz University of Technology (TU Graz/IKS) in close cooperation with the Space Flight Laboratory of the University of Toronto, Institute for Aerospace Studies (UTIAS/SFL) and the scientific lead of the Institute of Astrophysics of the University of Vienna (UV/IfA). In addition, the Institute of Telecommunications of the Vienna University of Technology (TUV/ITC) was involved in the project with an additional ground station in the beginning [23] [5].

The BRITE-Austria spacecraft is a nanosatellite cube of *20x20x20 cm* and *6.9 kg*, carrying a photometric instrument sensitive in the blue spectral range as scientific payload [23].

The following paragraphs give an overview of the BRITE-Austria subsystems. The description of the satellite subsystems is based on the *BRITE-Austria Detailed Design Document* [24].

2.1.1 Structure and Thermal Control Subsystem

The BRITE-Austria structure consists of a dual-tray system accommodating all internal satellite components. The launch rails of the satellite run along two parallel edges of each tray. The trays are positioned on opposing sides of the satellite leaving a large volume (approx. *8x13x17 cm*) between them (at the centre of the satellite), which is available for the payload and startracker. Figure 2.1 shows the dual tray structure with the payload.

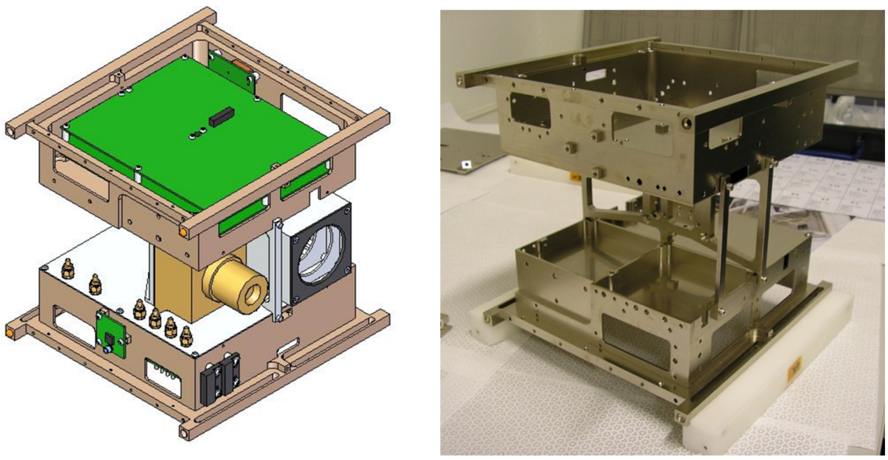

Figure 2.1: BRITE-Austria dual tray structure with payload. The two trays accommodate the different subsystems of the satellite bus, while the space in between serves as envelope for different mission specific payloads. For BRITE, this envelope is used for the photometric instrument payload as well as for the startracker. (image credit: UTIAS/SFL and TU Graz/IKS)

Once the trays and payload are fully integrated, the structure is completed with six aluminium panels that are used to mount components external to the spacecraft (e.g. solar cells, and antennas).

Thermal control is performed passively by thermal coating applied on the panel surfaces according to the final orbit definition. Temperatures are monitored by thermocouples applied on the inside of the panels as well as temperature sensors on most printed circuit boards. The only active thermal control is performed by heaters for the payload to keep the CCD temperature relatively constant as well as for the batteries to prevent them from dropping below $0°$ C.

2.1.2 On-board Computer Subsystem

The BRITE-Austria/TUGSAT-1 spacecraft comprises three on-board computers (OBCs), each responsible for dedicated tasks:

- House-Keeping On-board Computer (HKC): The HKC is used for housekeeping, communication with ground and inter-OBC communication, collection and storage of telemetry data, as well as the implementation of the mission timeline (time tag queue)
- Attitude Determination and Control System On-board Computer (ADCC): The ADCC runs the attitude software. It interfaces with the attitude sensors and actuators as well as with the HKC
- Science Instrument On-board Computer (IOBC): The IOBC is used for controlling the scientific payload

The HKC and ADCC share an identical hardware design for redundancy in case of failure of one of them although during nominal operations each performs dedicated tasks. The IOBC is used to operate the photometric instrument. The computers provide different interfaces for inter-OBC communication as well as for the different sensors and actuators. Each OBC provides *256 MByte* external flash storage for science and housekeeping telemetry data. The operating environment is layered in two levels:

- Bootloader: provides basic functionality for monitoring and control of the vital spacecraft systems and for communication with the ground station
- Application Code: actual operating system providing all functionality required to operate the spacecraft, from housekeeping and on-board data handling to attitude control and payload operations.

Communication with the ground station is performed by a dedicated network layer protocol, the Nanosatellite Protocol (NSP), for which the data packets are encapsulated in High-Level Data Link Control (HDLC) protocol frames. BRITE-Austria therefore uses the first three of the seven layers in the classical Open Systems Interconnection (OSI) architecture as defined in [25].

2.1.3 Attitude Control Subsystem

The mission requirements require that precise attitude knowledge and control attitude are provided to meet the performance objectives. The attitude determination and control system (ADCS) design is shown in Figure 2.2. An ADCS cycle with a minimum duration of 2 seconds is performed in three steps:

1. determination : measurements of the attitude sensors are performed
2. software processing: solving the attitude problem and calculate control efforts
3. control: implementation of the control commands

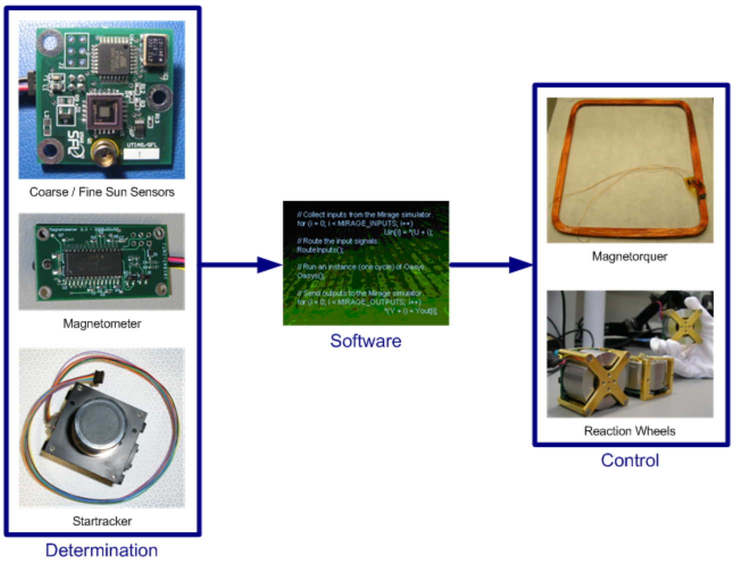

Figure 2.2: BRITE-Austria attitude control subsystem. The attitude software processes the readings acquired from the attitude sensors (sun sensors, magnetometer, startracker) and controls the attitude actuators (magnetorquers and reaction wheels) accordingly to achieve the desired attitude performance. (image credit: UTIAS/SFL)

To determine the attitude, the spacecraft uses six sun sensors (each comprising a coarse and fine sun sensor), mounted on every face of the spacecraft, a three-axis magnetometer, and a startracker. The coarse sun sensors are used to determine the illuminated panels of the spacecraft, for which then two dimensional sun sensor profiles are read out with the fine sun sensors. In combination with the magnetic field readings of the magnetometer, attitude can be determined with a precision of about $2-3°$. For fine three-axis pointing as required for payload operations, a startracker is used, providing an attitude determination precision of better than *70 arcseconds* in all three axes.

For attitude control, three reaction wheels and three magnetorquers are used. The magnetorquers, which consist of electromagnetic coils, provide coarse attitude control in all three axes and are used for detumbling the spacecraft and for momentum dumping of the wheels. The reaction wheels are used for fine three-axis control to meet the pointing requirements for payload operations. The pointing performance of the spacecraft achieved in orbit is *73 arcseconds* RMS, which is significantly better than the *2 arcminutes* as specified in the mission requirements.

2.1.4 Electrical Power Subsystem

Power generation is performed by triple junction gallium arsenide ($GaAs$) solar cells (26.8% efficiency, *967 mW* peak power) mounted on all faces of the spacecraft (36 in total).

For controlling the power switches of the spacecraft, a power board is used. The power board operates at a nominal bus voltage of *4.2 V*, performs voltage regulation for different sensors (*3 V*, *5 V*, and *10 V*) and power distribution to the subsystems, as well as provides over-current protection.

For energy storage, the spacecraft accommodates two *5300 mAh* lithium-ion batteries, only one of which is primarily used. Each battery has a Battery Charge and Discharge Regulator (BCDR) attached, used for peak power tracking for the solar arrays and regulation of the current entering the battery to prevent it from overcharging. In addition, the battery is equipped with a heater to prevent the battery temperature from dropping below $0°C$.

2.1.5 Communication Subsystem

In its first design phase, the communication suite for BRITE-Austria comprised the following items [26], also shown in Figure 2.3.

- **VHF beacon:** The beacon is used to obtain a quick snapshot of the spacecraft health and operates in the VHF amateur radio band (2 metre) in Morse code.
- **UHF uplink:** The UHF uplink represents the sole method of commanding the spacecraft and operates in the UHF amateur radio band (70 cm).
- **S-band downlink:** The S-band downlink is the primary downlink capability for the BRITE-Austria satellite. Because a substantial amount of scientific data has to be downloaded via this link, the chosen downlink frequency is ITU-regulated, according to the Space Research Space-to-Earth (SRS) S-band spectrum assignment. The main advantage is the availability of a dedicated bandwidth protected from interference leading to degradations in the link performance.

Later in the design phase the VHF beacon was discarded because of potential interference issues with the UHF receiver, which is the sole method for commanding the spacecraft from the ground station. Therefore, only the S-band telemetry downlink and the UHF telecommand uplink were implemented. The VHF beacon transmitter design is not further considered in this section.

The UHF uplink is the only one method for commanding the spacecraft. All commands and software are uploaded via this link. Therefore, the UHF receiver must be active at all times when power is available at the spacecraft. After launch, when the spacecraft is in the so-called kick-off mode (only power subsystem

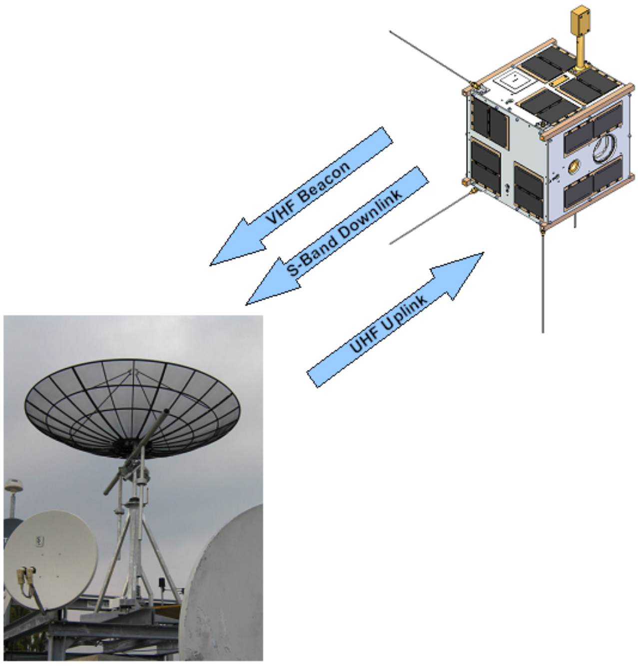

Figure 2.3: BRITE-Austria communication links. The satellite telecommand is performed via UHF uplink, while the primary downlink for satellite telemetry and science data is performed via S-band. (image credit: UTIAS/SFL)

and UHF receiver active) the UHF receiver listens to basic HDLC commands from the ground station, the so-called *"Firecodes"*, to turn on the on-board computers.

The UHF design is actually a transceiver capable of bidirectional communications. However, within the BRITE-Austria mission, only the receiver part is populated and used. The receiver's antenna interface comprises four antenna inputs for the UHF antennas. A matching / filtering network is used for combining the incoming signal of the four ports and a low noise amplifier is used for signal amplification. Subsequently, the receiver demodulates and descrambles the incoming GMSK modulated signal and forwards the incoming commands to the respective computer. The UHF receiver is connected with both the housekeeping and the attitude determination and control computer for redundancy reasons, and in addition to the power board for triggering a system reset of the entire spacecraft from ground.

An $RG316$ coaxial cable interconnects the radio electronics with the four canted monopole antennas, mounted as shown in Figure 2.4. The purpose of this configuration is to establish a more omni-directional pattern than is normally available from just a single monopole or dipole in order to allow communications with the spacecraft from ground independently from its attitude.

The S-band telemetry transmitter consists of two commercial off-the-shelf (COTS) components boards: a core board, which contains the baseband processing up to the modulator output, and an output board, containing the power amplification chain and the RF-front end.

The transmitter allows on-the-fly selection of different modulation schemes and data rates. Convolution coding (Viterbi, $K = 7$) with forward error correction (FEC) is used with a fixed coding rate configuration of $CR = 1/2$ .The default downlink configuration for operations is Binary Phase Shift Keying (BPSK) with a data rate of *32 kbit/s*. Depending on the link quality, the data rate can be increased by commands from the ground station. The supported modulation schemes are Binary Phase Shift Keying (BPSK) and Quadrature Phase Shift Keying (QPSK), and the supported data rates range from *8 kbit/s* to *1 Mbit/s* in 2^k steps. Due to restrictions in the downlink bandwidth allocation for BRITE, a maximum data rate of *256 kbit/s* with QPSK modulation can be used.

The power amplifier provides an output power of *500 mW*. The antenna interface at the transmitter's output filters the harmonic content of the power amplifier with a low-pass filter and equally splits the signal to feed the two antennas. Two patch antennas with circular polarization, mounted on opposite faces of the satellite are used and the antennas are fed in-phase with the same power level. The antenna radiation characteristics are very broad, which in combination form a near omnidirectional beam in order to communicate with the spacecraft independently of its orientation. Figure 2.4 illustrates the placement of the UHF and S-band antennas on the BRITE-Austria spacecraft.

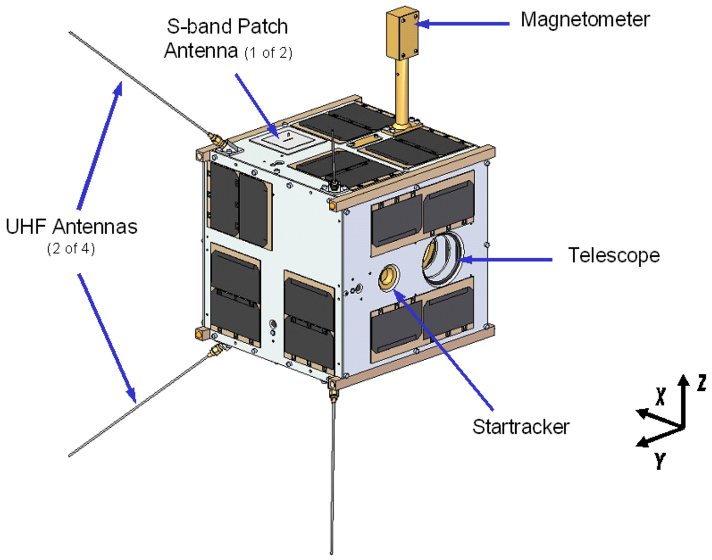

Figure 2.4: BRITE-Austria antennas on the spacecraft. Four monopole UHF antennas and two S-band patches on opposite faces guarantee nearly omnidirectional antenna patterns in UHF and S-band to ensure communications with the spacecraft in any attitude. (image credit: UTIAS/SFL)

2.1.6 Photometric Instrument (Payload)

The BRITE-Austria payload is a photometric instrument sensitive in the blue visual spectral range (*390-460 nm*) [16]. BRITE-Austria observes bright massive stars (> 8 solar masses). The surface temperatures of those massive stars are around *30.000 K* for blue giants and around *20.000 K* for blue supergiants.

The instrument consists of three main parts: the header tray containing the CCD and header board, mounted on a small PCB attached at the rear of the telescope, the optical cell containing the lenses, and the baffle. The total length of the instrument is approximately *190 mm*, with a maximum diameter of the optical cell of *54 mm*, while the baffle width is *65 mm*. Figure 2.5 illustrates the main parts of the BRITE-Austria telescope including the lens design.

BRITE-Austria's full assembly was completed in March 2011. Subsequently, the spacecraft has undergone environmental testing including vibration testing, thermal vacuum testing, electromagnetic compatibility testing, attitude control testing, and open field testing to finally obtain its flight readiness in autumn 2011. Figure 2.6 shows the fully assembled BRITE-Austria spacecraft in the cleanroom.

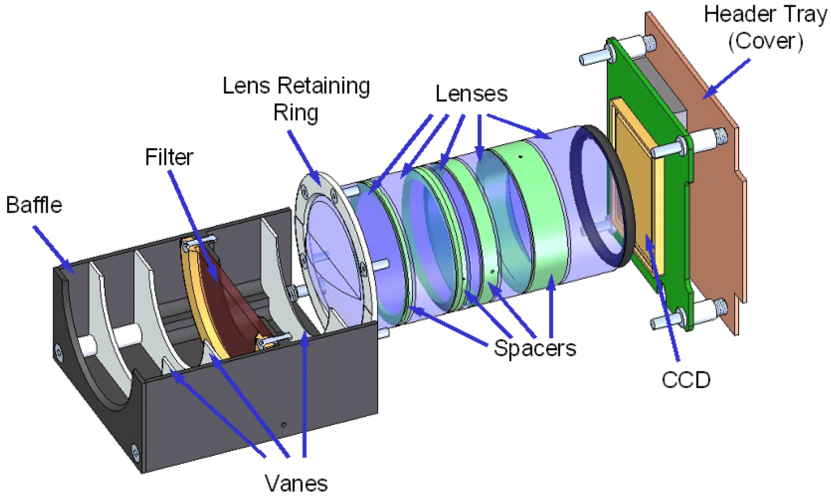

Figure 2.5: BRITE-Austria telescope design. The telescope consists of a CCD mounted on a header board, a five lens system with fixed focus, an optical filter sensitive to the blue visual spectral range, as well as a baffle for protecting the telescope from stray light. (image credit: UTIAS/SFL)

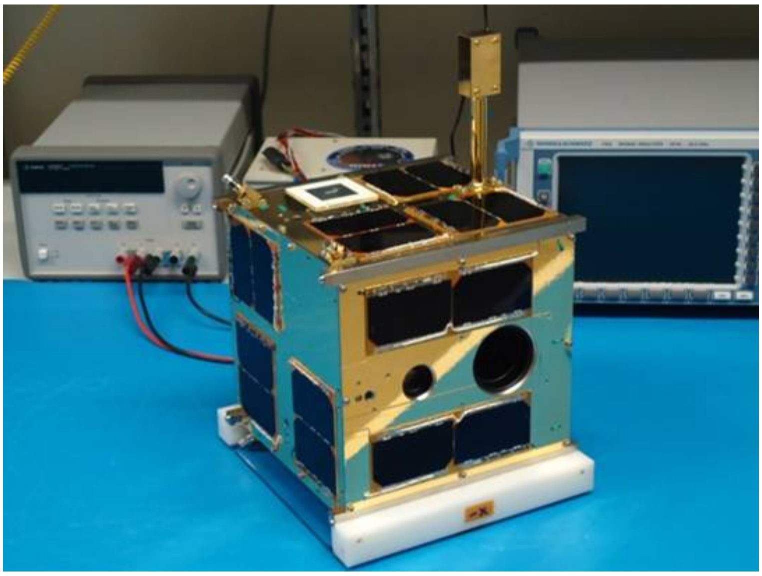

Figure 2.6: Fully assembled BRITE-Austria spacecraft in the cleanroom. The fully assembled spacecraft ready for the functional test is shown.

2.2 Communication Subsystem Functional Testing

This section describes the functional testing performed on the BRITE-Austria communication subsystem as part of unit and system level testing of the spacecraft. Figure 2.7 depicts the BRITE-Austria UHF receiver and S-band transmitter integrated in their tray.

In order to verify the performance of the system, functional tests have been performed at unit and system level. The test results were compared to reference values and checked for compliance with the requirements. The following sections describe the performed tests and the results.

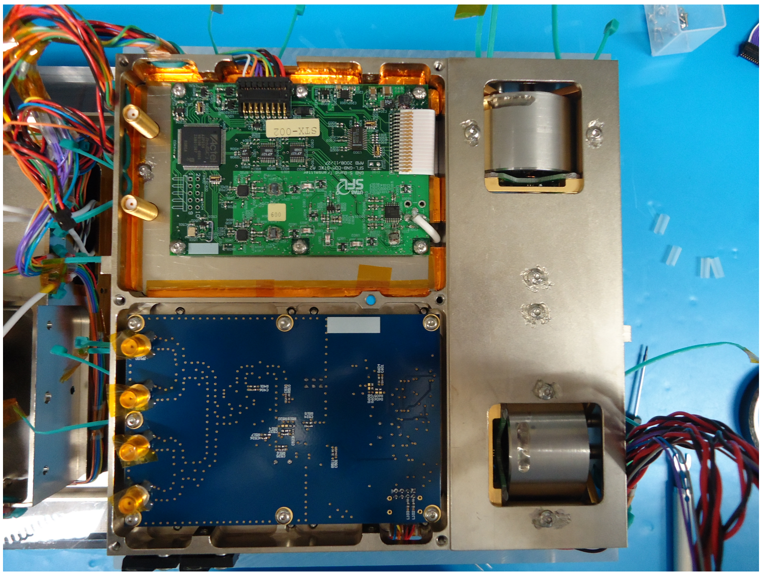

Figure 2.7: BRITE-Austria communication subsystem integrated in the spacecraft. The S-band transmitter (top) and UHF receiver (bottom) integrated in their tray are shown.

2.2.1 UHF Receiver Unit Level Test

The unit level test of the UHF receiver was carried out to characterise the unit's stand-alone performance and verify that it met the design criteria to operate the spacecraft. The test results are presented according to the UHF receiver unit level test report [27].

The test consisted of two essential parts: a bandwidth sweep and a sensitivity sweep. Both tests were carried out by measuring the receiver's bit error rate at different frequencies / input power levels. Figure 2.8 shows the test setup for the UHF receiver unit level test. The test was performed with the receiver mounted on the rotating table in the anechoic chamber of the Institute of Microwave and Photonic Engineering of Graz University of Technology (TU Graz/IHF).

In the used test setup, one receiver port used for all tests was connected to a calibrated coaxial cable in the chamber with a known attenuation of *12.5 dB*. In order to verify the amplitude balance and connectivity of each antenna port, a measurement for each port with the same setting was performed.

The GMSK modulated input signal to the receiver was generated by the terminal node controller (TNC), as well as upconverted and amplified by the UHF transceiver (*2 W* out). Between transceiver and receiver three stages of attenuation were used: a first fixed attenuation stage of $60dB$, a second variable attenuation stage (*0-31 dB* in *1 dB* steps) with a power splitter for measuring the power level, and a third fixed attenuation stage of *20 dB*. The bit error rate (BER) was measured with a logic signal analyser connected to the Transistor-Transistor Logic (TTL) levels of the receive clock and data lines of the UHF receiver.

The bit error measurements were performed by generating a constant transmit signal of all logic ones by setting the TNC to idle mode. At the logic signal analyser, a count of the incoming zeros was performed, representing the errors occurred during the transmission. For statistical evaluation of the bit errors a minimum of *300 bit* errors per measurement had to be collected; the measurement times for different bit error rates had to be adapted accordingly in order to collect at least the minimum amount of errors.

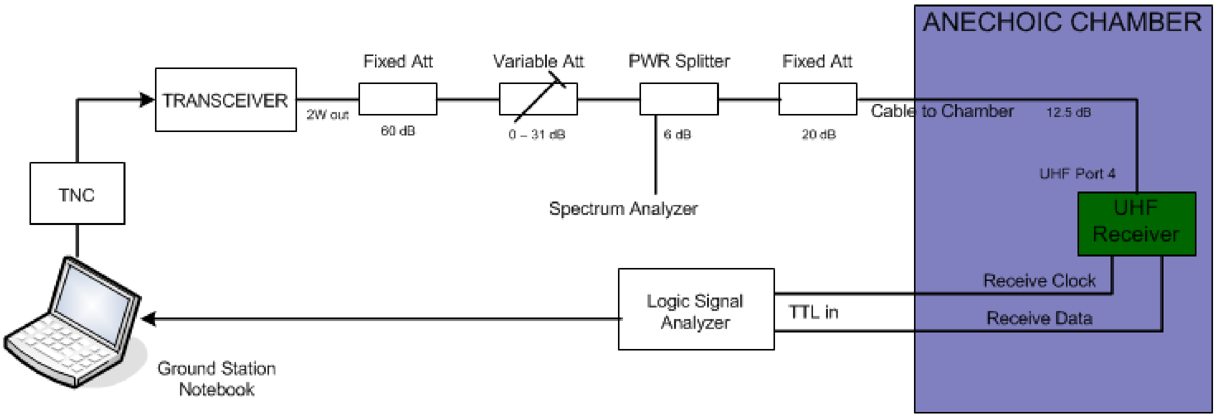

Figure 2.8: BRITE-Austria UHF receiver unit level test setup. Measurements of the receiver's sensitivity, bandwidth, and bit error rates were performed.

The bandwidth sweep test was performed to verify the receiver's approximate centre frequency and bandwidth. The centre frequency is defined as the centre of the usable bandwidth and generally does not correspond to the peak performance point. First, a suitable input level for the receiver to obtain a bit error rate of 10^{-3} was determined. Subsequently, a frequency sweep starting at *65 kHz* below and finishing at *65 kHz* above the nominal centre frequency was performed in *5 kHz* steps, and the bit error rate was recorded. Figure 2.9 shows the measured UHF receiver's passband. It can be seen that, within ± 30 *kHz* from the centre frequency, the signal rejection of the receiver is *15 dB*.

The receiver's sensitivity was verified by testing. The test had to be performed at the nominal centre frequency because no a priori knowledge for the spacecraft temperature (main contributing factor to a drift in the receiver's passband) is available. The test was performed by taking several bit error rate measurements for different receiver input power levels. Starting with a configuration for an input power level of *-114 dBm*, the power was raised in *1 dB* steps until at least a bit error rate of 10^{-5} was obtained. The input power level for which the equivalent bit error rate is 10^{-5} corresponds to the sensitivity of the receiver. In addition, a measurement of the BER at a receiver input power level of *-60 dBm* was performed to determine the performance at the approximate saturation level of the receiver. The measurement results presented in Table 2.1 and Figure 2.10 show that the receiver sensitivity is *-102 dBm*.

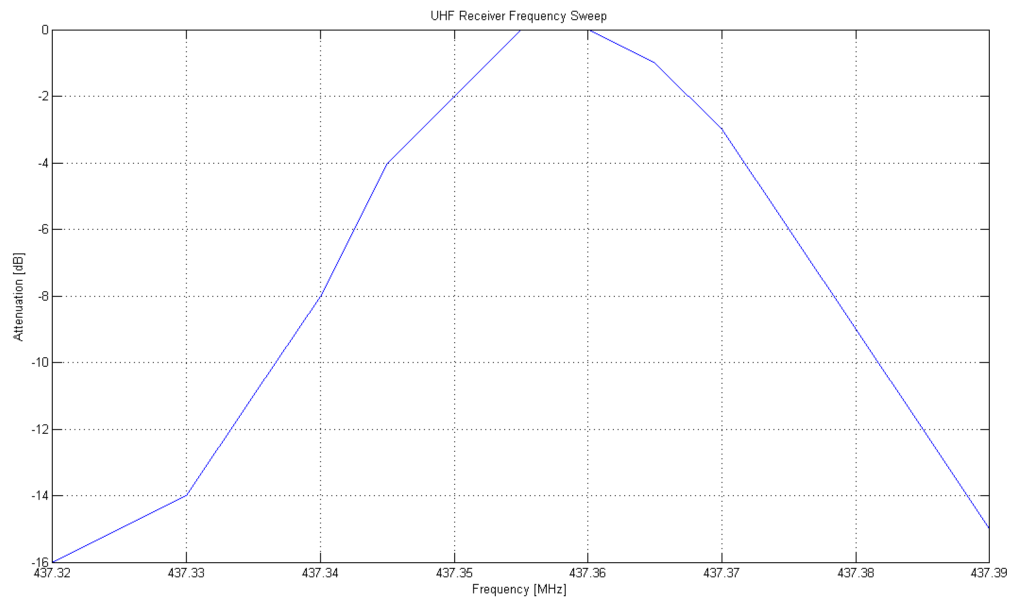

Figure 2.9: BRITE-Austria UHF receiver passband. Within ± 30 *kHz* from the centre frequency, the signal rejection is *15 dB*.

RX Signal Level [dBm]	BER	RSSI [V]
-114	$3.83*10^{-3}$	0.65 V
-113	$1.85*10^{-3}$	0.66 V
-112	$9.03*10^{-4}$	0.67V
-111	$4.47*10^{-4}$	0.67 V
-110	$4.0*10^{-4}$	0.68 V
-109	N/A	0.69 V
-108	$5.77*10^{-5}$	0.70 V
-107	$4.88*10^{-5}$	0.72 V
-106	$4.2*10^{-5}$	0.74 V
-105	$3.99*10^{-5}$	0.75 V
-104	$2.15*10^{-5}$	0.77 V
-103	$2.05*10^{-5}$	0.79 V
-102	$1.18*10^{-5}$	0.80 V
-101	$2.64*10^{-5}$	0.81 V
-100	$2.96*10^{-5}$	0.83 V
-60	$1.5*10^{-5}$	1.67 V

Table 2.1: BRITE-Austria UHF receiver sensitivity. The sensitivity was specified as the signal level for which the receiver achieves a bit error rate of 10^{-5} and is therefore *-102 dBm*.

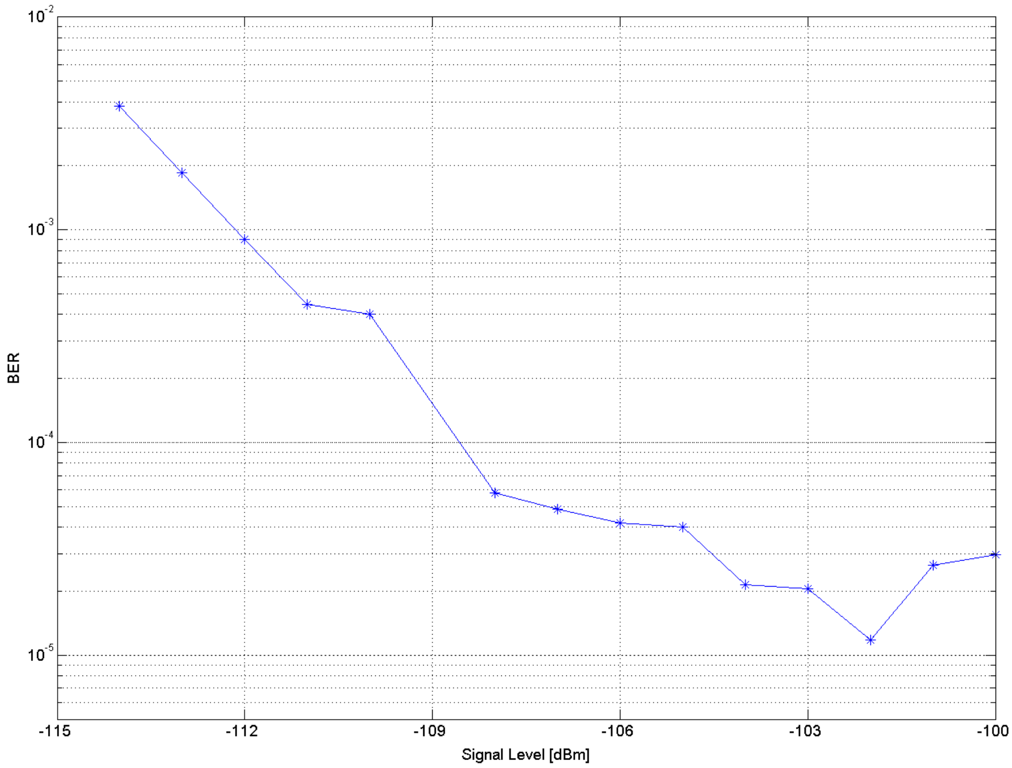

Figure 2.10: BRITE-Austria UHF receiver sensitivity. The sensitivity was specified as the signal level for which the receiver achieves a bit error rate of 10^{-5} and is therefore *-102 dBm*.

2.2.2 S-band Transmitter Unit Level Test

The unit level test of the S-band transmitter was carried out to characterise the unit's stand-alone performance and to verify that it matched the design criteria to operate the spacecraft. The test results are presented according to the S-band transmitter unit level test report [28].

The test was performed on the so-called flatsat. The flatsat is a configuration of all (or a subset of) satellite components populated on a mounting plate next to each other and interconnected with test harness as in flight. This setup is used to verify the overall satellite performance at system level prior to spacecraft assembly. For the S-band transmitter unit level test, the setup included the housekeeping on-board computer for commanding the transmitter and the power board for powering the units as well as for connecting to the test port interface.

For the RF-signal measurement, one output port of the transmitter was connected - with suitable attenuation - to a vector signal analyser, while the second port was terminated.

As the S-band transmitter consists of two boards, a core board and a power output board, the first action during unit level testing was powering up and checking telemetry of the boards sequentially to verify that each board powers up correctly and that the returned telemetry was nominal. Once telemetry had been verified, the main performance tests of the unit could be carried out, including spectrum measurements, modulation analysis, power analysis, and link tests.

Spectrum measurements were performed to verify the transmitter's performance concerning spurious signals (<*-40 dBc* required), harmonic output levels (<*-40 dBc* required), and interference at the UHF frequency (<*-130 dBm/Hz* required), as it is relevant for the mission. All requirements were met. Figure 2.11 shows the spectrum of the transmitter for QPSK with *8 kbit/s* at *1 MHz* frequency span.

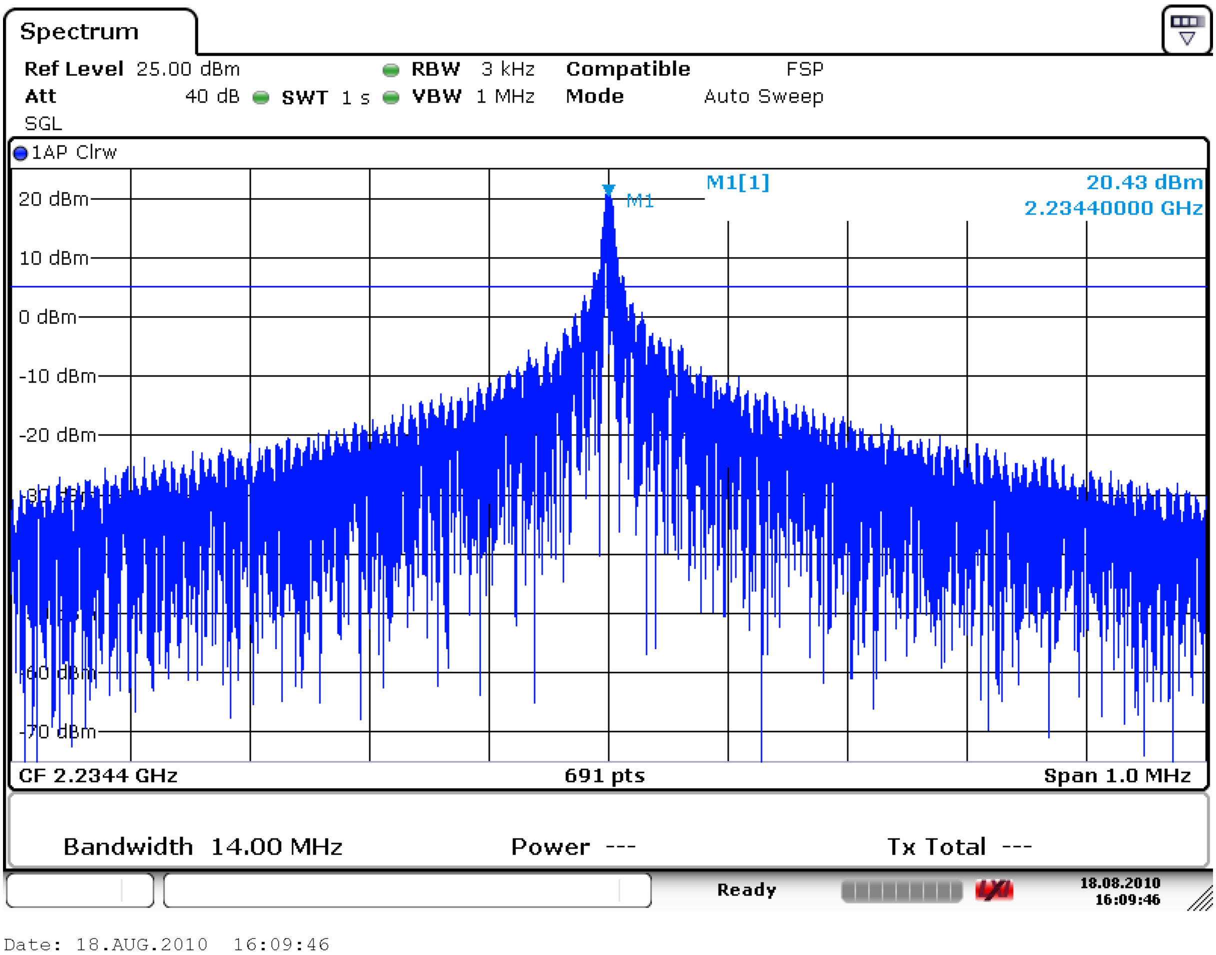

Figure 2.11: BRITE-Austria S-band transmitter spectrum. A spectrum measurement for the QPSK modulated S-band signal with data rate *8 kbit/s* is shown.

Modulation analysis was performed to verify the quality of the transmitter's output signal for different modulation and data rate settings. The measurement parameters and pass criteria are listed in Table 2.2.

Figure 2.12 shows a screenshot from the vector signal analyser for the modulation analysis measurement at the nominal modulation setting of BPSK and the nominal data rate setting of *32 kbit/s*. The results show an error vector magnitude of 6.44%, a magnitude error of 3.77%, a phase error of 3.50°, as well as a frequency error of *-152.78 Hz* (corresponding to *-6.83 ppm*). Hence, all requirements for the measurement parameters described in Table 2.2 are met.

Measurement	Requirement
RMS Error Vector Magnitude (EVM)	10%
RMS Magnitude Error	5%
Phase Error	5 degrees
Frequency Error	$\pm 10ppm$

Table 2.2: BRITE-Austria S-band transmitter modulation analysis. The measurement parameters specified as pass criteria for the test are listed.

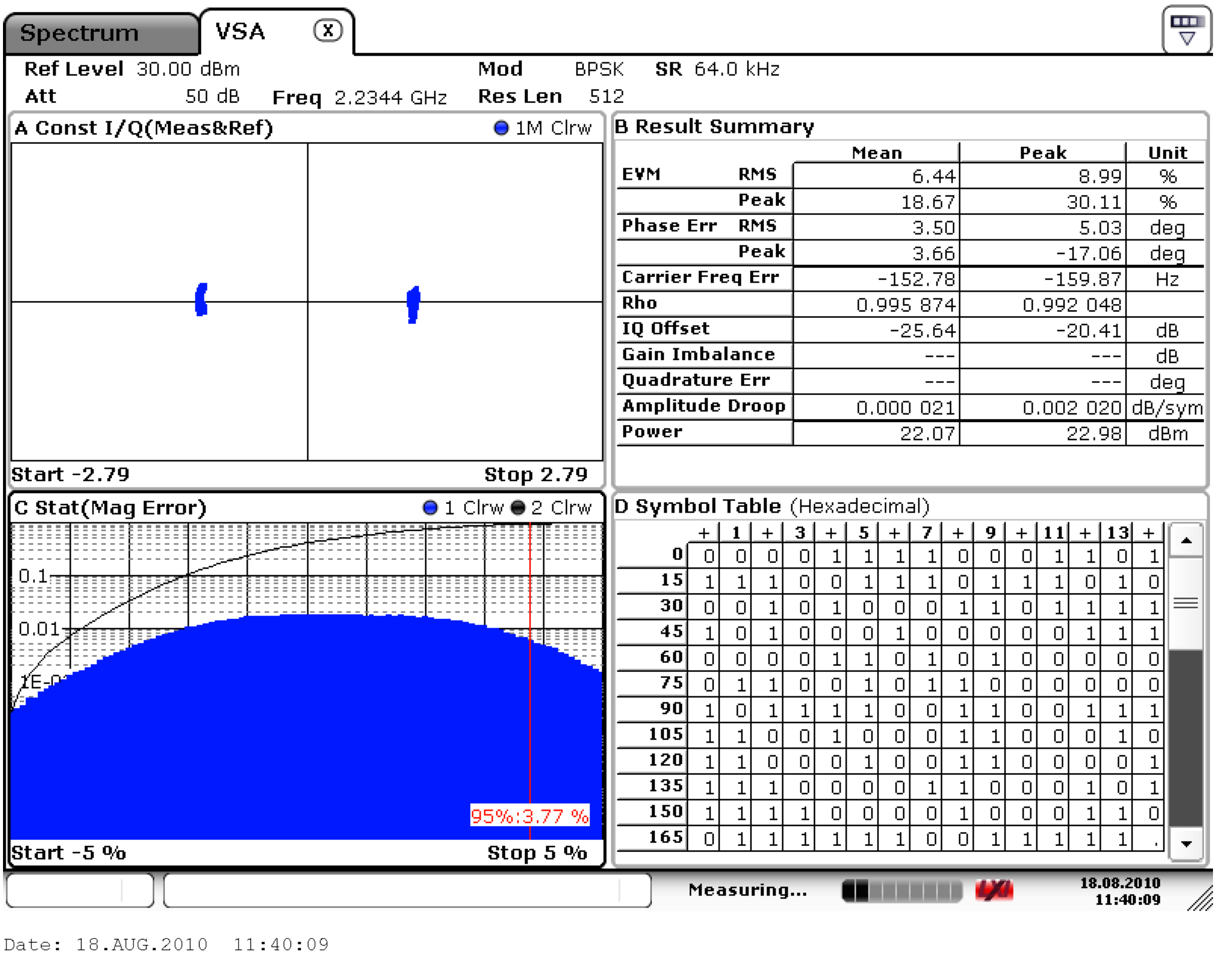

Figure 2.12: BRITE-Austria S-band transmitter modulation analysis. The screenshot shows a modulation analysis measurement for BPSK and the data rate set to *32 kbit/s* (default configuration). The results show an error vector magnitude of 6.44%, a magnitude error of 3.77%, a phase error of 3.50∘, as well as a frequency error of *-152.78 Hz* (corresponding to *-6.83 ppm*), fulfilling all requirements according to Table 2.2.

Finally, a power Complementary Cumulative Distribution Function (CCDF) analysis was performed to verify the Crest Factor (peak to average power ratio) for different modulation and data rates. The crest factor requirement for the typical modulation and data rate settings was $<$*3 dB* and could be met for each of the settings. Figure 2.13 depicts a vector signal analyser screenshot of the crest factor measurement for the BPSK *32 kbit/s* setting. The result shows that the measured crest factor is *1.08 dB*, which is substantially lower than the *<3 dB* requirement.

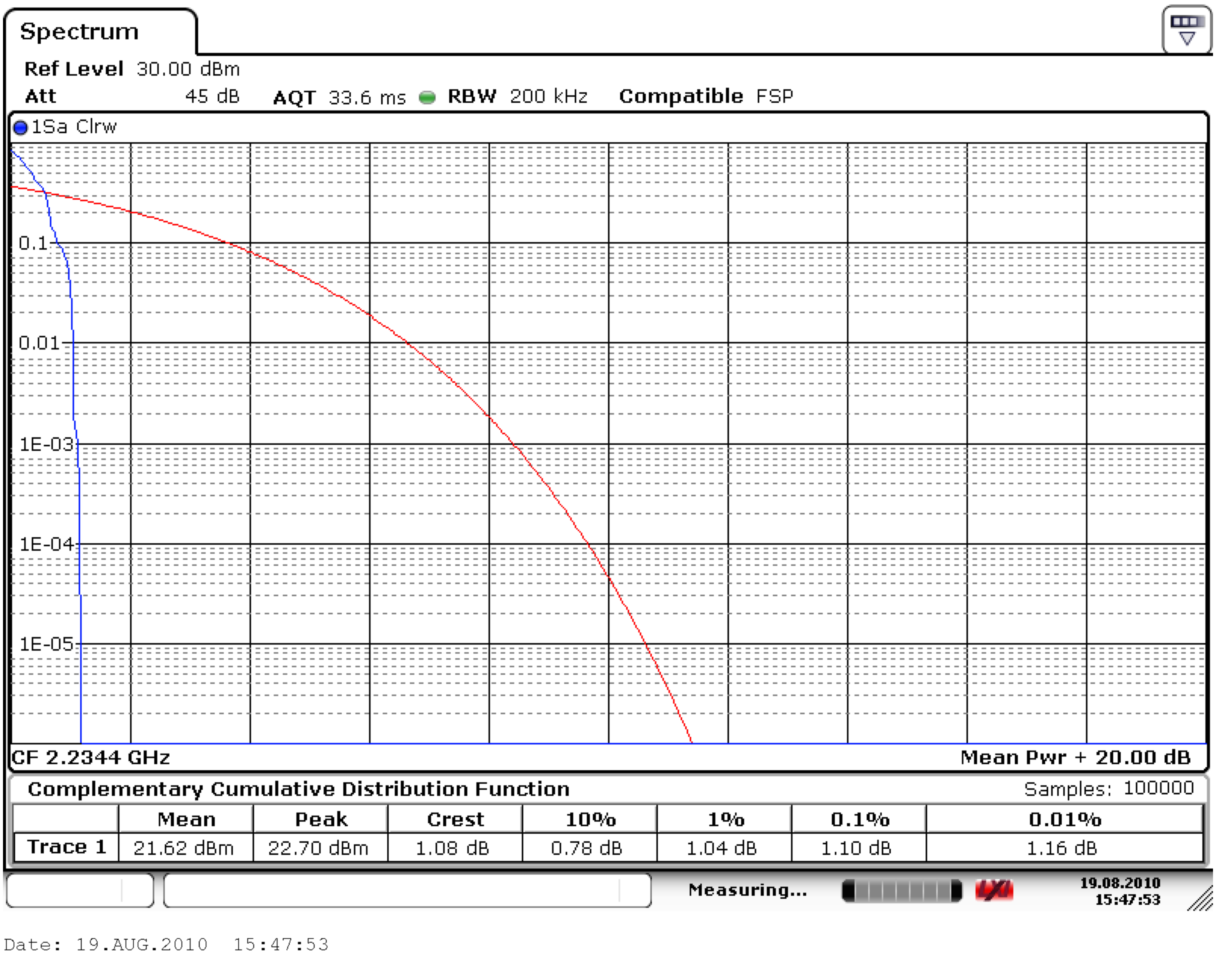

Figure 2.13: **BRITE-Austria S-band transmitter CCDF measurement.** The measurement result for BPSK *32 kbit/s* shows a crest factor of *1.08 dB*, which is well within the *<3 dB* requirement.

Once the performance of the stand-alone unit had been verified, link tests for each configurable modulation and data rate setting were carried out to verify the ability of the transmitter to correctly send data. The transmitted data packets were analysed while performing basic operations such as ping commands or telemetry queries.

2.2.3 Communication Subsystem System Level Tests

System level tests were carried out on the BRITE-Austria flatsat. For BRITE-Austria, only a flatsat of the protoflight model was used. Figure 2.14 depicts the fully populated flatsat in the clean room.

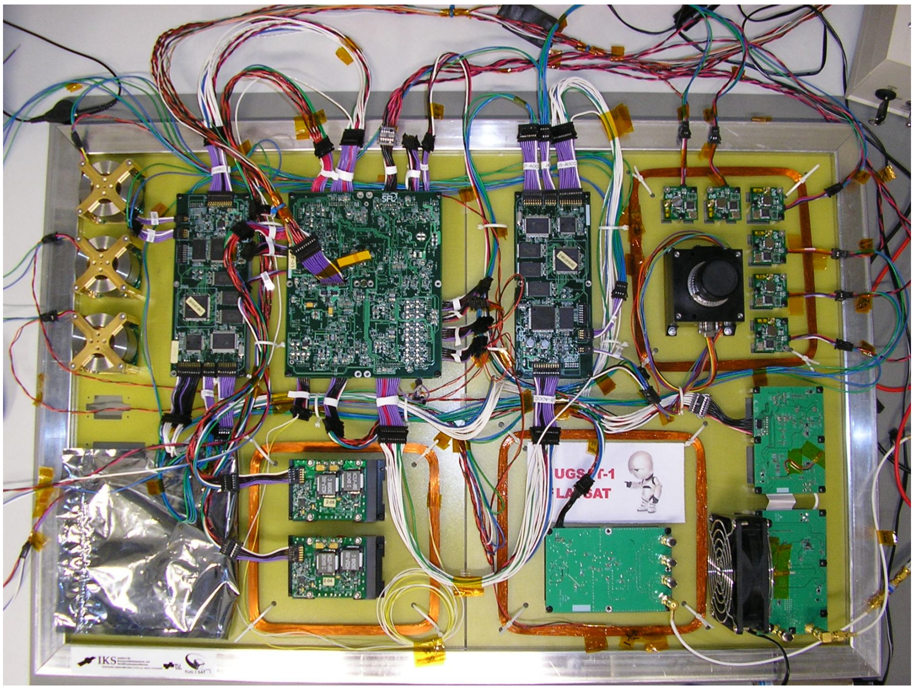

Figure 2.14: BRITE-Austria fully populated flatsat in the cleanroom. All satellite subsystems were interconnected as in flight to verify their functionality at system level (communication subsystem in the lower right corner).

For the communication subsystem, system level tests were performed in the long form functional test (LFFT) part of the flatsat tests [29]. This test is used to verify the overall spacecraft performance and consists of several tests for each unit. The test was carried out during all phases of assembly, integration, and testing (AIT) of the spacecraft.

The communication part of the LFFT consists of an UHF receiver test and an S-band transmitter test. The test setup required the use of the essential parts of the ground station: the Terminal Node Controller (TNC), the UHF transceiver connected to an UHF transmit antenna, an S-band receiving antenna, the S-band downconverter, and the satellite modem as ground station receiver. A detailed description of the ground station design and its components is provided in Chapter 3.

The UHF receiver test is performed by sending special commands, the so-called firecodes, to the spacecraft. The firecodes are basic commands which allow to turn on/off or reset the housekeeping and attitude determination and control computers, and to perform a power system reset of the entire spacecraft. These commands are essential to start-up the spacecraft after launch, and to reset the system in case of unexpected behaviour. The OBC on/off firecodes were performed by issuing ping commands after sending a firecode and checking if a response could be obtained. The ping responses were also observed when issuing OBC reset firecodes, but this time also the timestamps were analysed. Since the OBCs boot with the initial $J2000$ timestamp, after a reset the timestamp of the computers is also reset. For the power system reset firecode test, all switches are turned on (including the second battery), and after issuing the firecode it is verified that all switches have turned off (except the default battery charge/discharge regulator).

The S-band test was performed by enabling the transmitter as in the flight configuration, checking the communication link with the spacecraft by reading out housekeeping telemetry, and recording the receiving parameters of the satellite modem (carrier level, E_b/N_0, and the received intermediate frequency). The test was repeated for three representative modulation and data rate settings used in flight:

- BPSK, 32 kbit/s (nominal signal acquisition setting)
- QPSK, 8 kbit/s (lowest data rate and minimal bandwidth setting)
- QPSK, 128 kbit/s (representative high data rate configuration)

In addition, each configuration was tested by commanding the transmitter from both the housekeeping and the attitude determination and control computer to check that the link could be established by both OBCs.

Finally, a readout of the spacecraft core telemetry was obtained by the radio links for all configurations mentioned above as end-to-end check of the communication subsystem performance. All test results passed, showing that the basic performance of the communication link is suitable to operate the spacecraft.

2.3 Integrated Spacecraft Environmental Testing

The unit level tests of the communication system had the purpose to verify the single unit performance against the requirements. System level tests were carried out on a flatsat to verify the overall satellite performance prior to assembly. After assembly, several tests with the integrated satellite were performed to obtain flight readiness. For BRITE-Austria, these tests included [30]:

- vibration testing
- thermal vacuum (TVAC) testing
- electromagnetic compatibility (EMC) testing
- attitude determination and control (ADCS) testing
- open field testing

These tests are known as spacecraft environmental tests.

From the communication system point of view, two among the environmental tests were of main interest: the electromagnetic compatibility (EMC) test, and the open field test. These two tests are described in detail in the following sections.

2.3.1 Electromagnetic Compatibility Test

Electromagnetic compatibility (EMC) testing is performed [31]:

1. to ensure that emissions from the spacecraft meet the requirements imposed by the launch vehicle
2. to ensure that the spacecraft does not produce electromagnetic interference (EMI) that interferes with its own operation

As the satellite was launched in an off configuration, no testing requirements had been imposed by the launcher. Therefore, emission testing was not performed for the BRITE-Austria satellite.

Concerning the self-compatibility of the spacecraft, different requirements were applicable. When connected to the antennas, the UHF receiver operation is mainly affected by background thermal noise level. To determine the true sensitivity of the receiver any type of non-thermal environmental noise had to be removed, as it degrades the performance results by masking self-compatibility issues. Therefore, next to parts of the UHF receiver unit level testing, the EMC tests of the integrated spacecraft were performed in a calibrated anechoic chamber for high frequency antenna measurements at the Institute of Microwave and Photonic Engineering of Graz University of Technology (TU Graz/IHF).

Figure 2.16 shows the BRITE-Austria satellite in the anechoic chamber for the electromagnetic compatibility test, while Figure 2.15 shows the test setup for the electromagnetic compatibility test of BRITE-Austria. The ground station for command control and telemetry reception was established in the control room next to the anechoic chamber to avoid long cable lengths.

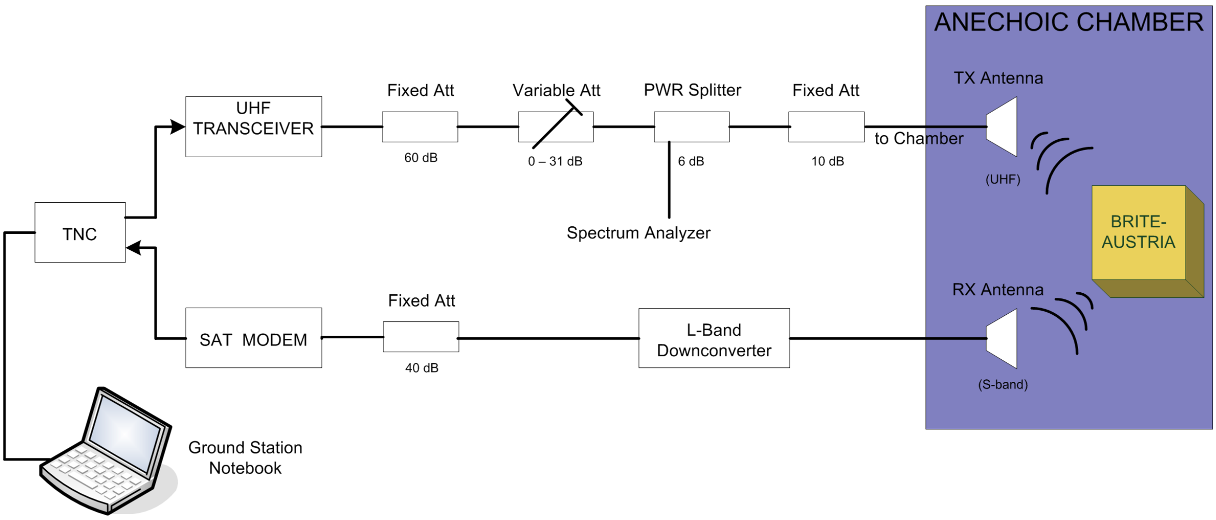

Figure 2.15: Electromagnetic compatibility test setup. The spacecraft was placed in the anechoic chamber and the respective ground station elements in the chamber's control room nearby. The UHF sensitivity and packet error rate were measured for different satellite operational modes to confirm the receiver's performance was unaffected.

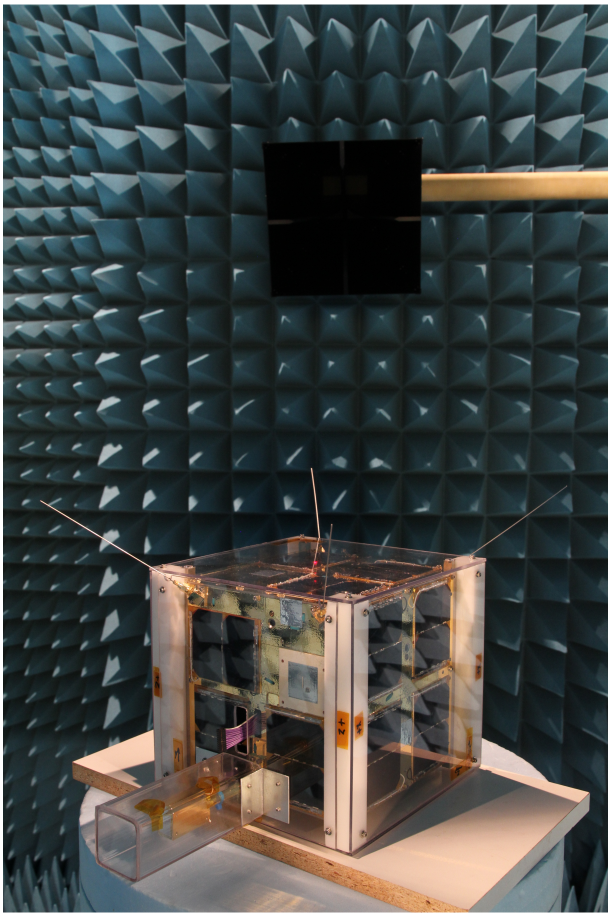

Figure 2.16: BRITE-Austria EMC testing in the anechoic chamber. The purpose of the test was to verify that the UHF receiver on the spacecraft is unaffected by any other subsystem to ensure proper functionality of the satellite's uplink.

The performance of the receiver was tested for different representative operational modes. The following cases were investigated:

1. Safe-Hold mode [2]
2. ADCS - OASYS [3] Passive [4]
3. ADCS - OASYS B-dot [5]

Table 2.3 shows the test results for the different modes. The relevant measurements were performed at low received signal strength indicator (RSSI) levels to determine the levels where the packet failure rate significantly increases. The results show that the measured RSSI values are consistent for the different selected spacecraft operational modes.

[2] Safe-Hold mode without attitude determination and control
[3] OASYS is the attitude control software thread running on the BRITE-Austria application software
[4] Passive attitude determination mode with only sensors active (sun sensors and magnetometer) but no actuators
[5] Detumbling mode - high magnetic distortion expected due to high magnetorquer currents

RX Signal Level [dBm]	RSSI Spec [V]	RSSI Safe Hold [V]	RSSI OASYS Passive [V]	RSSI OASYS B-dot [V]
-104.5	0.76	0.75	0.75	0.74
-106.2	0.74	0.74	0.74	0.73
-107.2	0.72	0.71	0.72	0.71
-108.5	0.69	0.68	0.68	0.68
-109.7	0.68	N/A	0.68	N/A

Table 2.3: Electromagnetic compatibility testing - Test results for different spacecraft operational modes. A comparison of the measured Received Signal Strength Indicator (RSSI) for a given input signal level is provided. The results show that the measured RSSI values are consistent for the different spacecraft operational modes considered and meet the specifications measured during unit level testing.

Figure 2.17 depicts the performance of the UHF receiver at different operational modes. The packet failure rate in dependence of the received signal strength indicator is shown. The results show that the packet failure rates are comparable for different operational modes and there is only little influence on the receiver's performance.

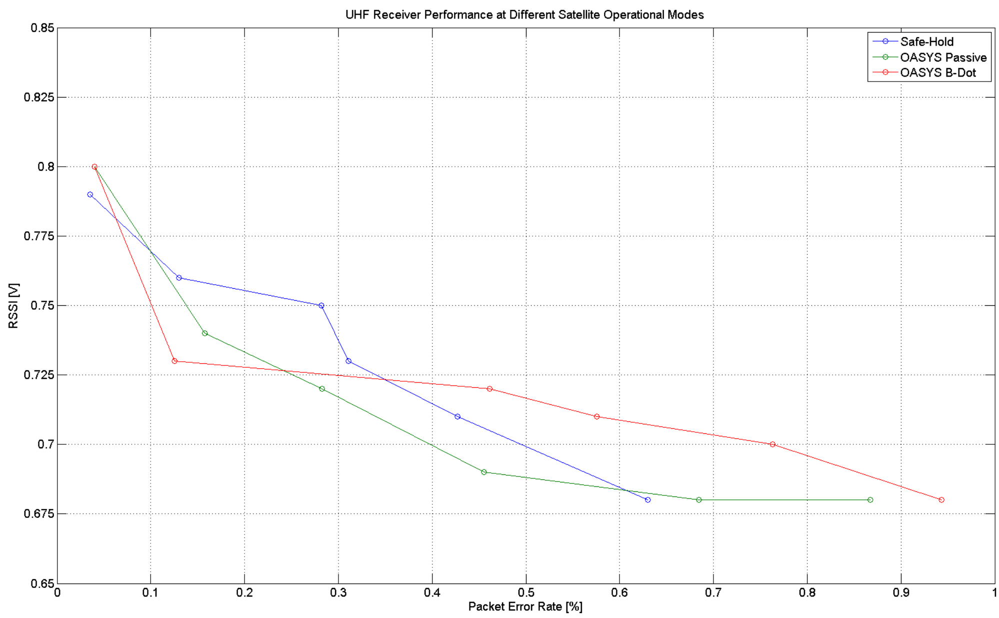

Figure 2.17: Electromagnetic compatibility - receiver performance at different operational modes. The curves show that the packet failure rates for different operational modes are comparable and there is almost no influence on the receiver's performance.

After measuring the sensitivity and packet error rates for different operational modes of the satellite, UHF sensitivity measurements were performed. The test was carried out to verify the approximate sensitivity on the nominal centre frequency of the receiver in the fully assembled spacecraft. The RSSI was measured with a cable, which was directly connected at one UHF antenna input port of the satellite. To avoid any interference the remaining three antennas were removed and their ports were terminated with 50 Ω. The TX signal level was measured with the channel power measurement function of a spectrum analyser.

Starting at a power level of *-70 dBm*, the input signal level was gradually decreased by increasing the attenuation in steps of *1 dB* and the corresponding RSSI was logged. The result of this measurement was the creation of a table matching power levels in $[dBm]$ with RSSI values in $[V]$ as a reference for the satellite operations phase.

2.3.1.1 Spacecraft S-band Antenna Pattern Measurements

During Electromagnetic Compatibility Testing, as described in Section 2.3.1, the S-band antenna pattern of the fully assembled spacecraft was recorded to characterise the radiation behaviour of the two S-band antenna patches. Figure 2.18 and Figure 2.19 show the two-dimensional radiation patterns - with horizontal and vertical receiving polarisation, respectively - of the spacecraft. The plots show that the radiation characteristics of the combined patch antennas on the assembled spacecraft result in a near omnidirectional beam.

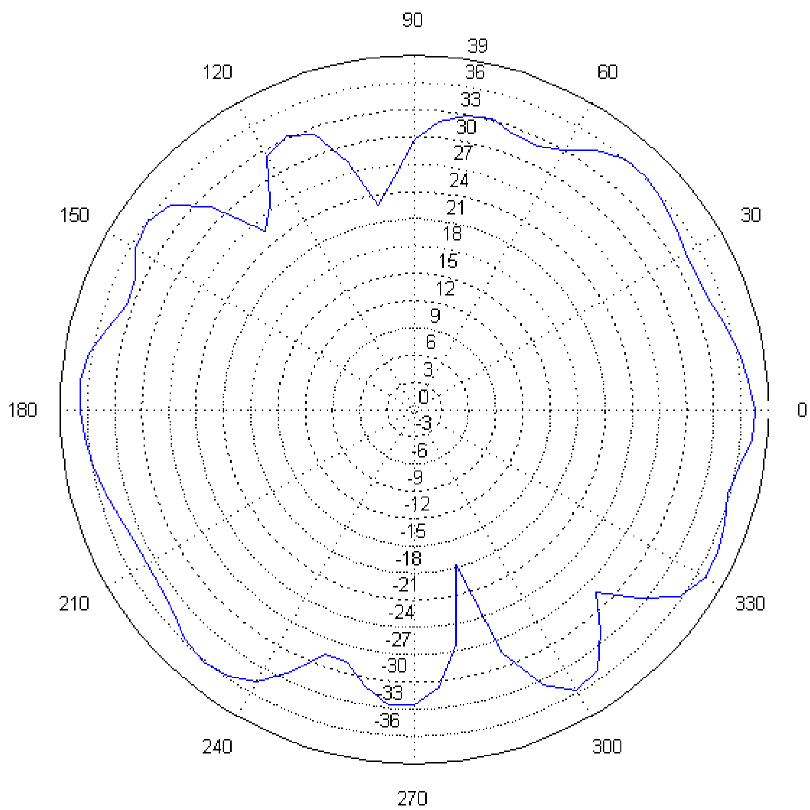

Figure 2.18: BRITE-Austria S-band horizontal antenna pattern. The pattern is almost omnidirectional, ensuring good communications with the spacecraft in any attitude with respect to the ground station.

For this measurement, the spacecraft was mounted on the rotating table in the anechoic chamber, rotating with respect to the calibrated measuring antenna of the chamber in $5°$ steps, while the measuring antenna was set to fix pointing towards the spacecraft at $0°$ elevation. At the starting point of the measurement, the satellite was facing the measurement antenna with its -Z face, with one of the S-band patches directly pointed towards the receiving antenna.

The results show that the horizontal antenna pattern is almost omnidirectional, ensuring good communications with the spacecraft in any attitude with respect to the ground station. As expected there are sharp nulls at about $\pm 90°$ (Y faces of the spacecraft), yielding a minimum antenna gain of *-16 dBi*.

In contrast, the vertical pattern reveals a less omnidirectional characteristic. This behaviour is not unexpected, as right hand circular polarisation is used, denoting the main signal portion in the horizontal polarisation domain.

The patterns show that even in the worst case orientations minimum communication capabilities are still provided.

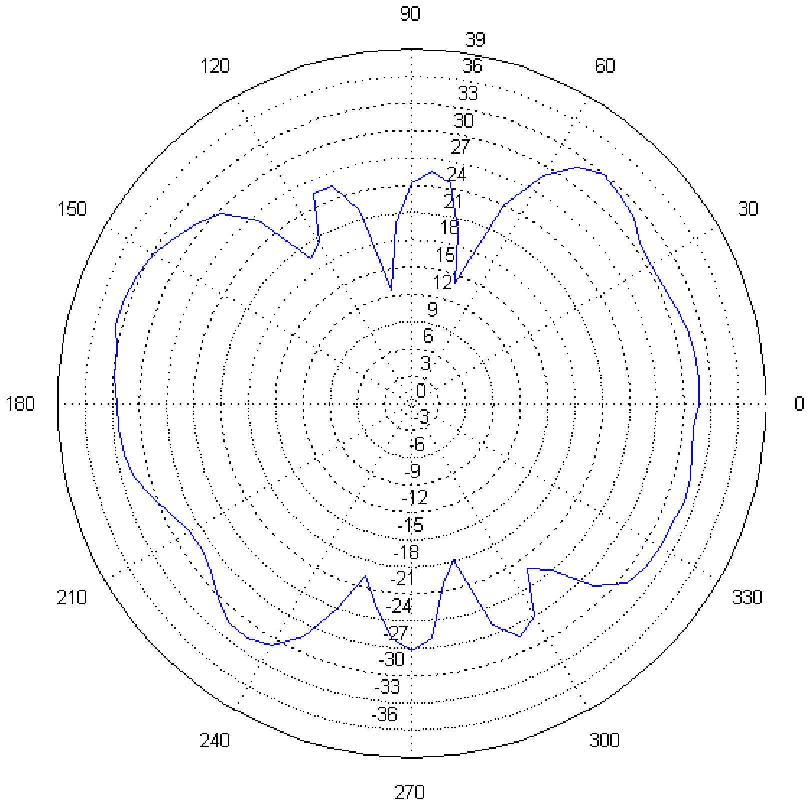

Figure 2.19: BRITE-Austria S-band vertical antenna pattern. In this plane, the omnidirectional characteristic of the pattern is not as optimal as for the horizontal plane. However, it still guarantees acceptable communications with the spacecraft even in the worst case orientation.

Concerning the S-band EIRP, the measurement results are shown in Table 2.4. The EIRP values were obtained by subtracting the known losses of the test setup from the measured values. It can be seen that the EIRP is higher in the horizontal polarisation, which is expected as the S-band antennas are right hand circularly polarised.

Parameter	EIRP [dBm]
Horizontal Polarisation Maximum	27.00
Horizontal Polarisation Minimum	7.20
Horizontal Polarisation Mean	22.74
Horizontal Polarisation Median	24.00
Vertical Polarisation Maximum	23.20
Vertical Polarisation Minimum	2.10
Vertical Polarisation Mean	17.54
Vertical Polarisation Median	19.75

Table 2.4: **Satellite S-band EIRP.** The EIRP values were obtained during the measurements of the antenna pattern. The maxima and minima as well as the mean and median values for both horizontal and vertical received polarisation are listed, showing that the EIRP for the horizontal polarisation is higher.

2.3.2 Open Field Test

The purpose of the open field test for BRITE-Austria was to test the correct operation of different subsystems in a representative environment [32]. The spacecraft was taken outside to test the functionality of the solar arrays and sun sensors under real sunlight, the operation of the startracker and the optical instrument with the night sky, as well as communications with the ground station. In these sections, only the communications part of the test is described. Because the satellite had to be taken outside for this test, special handling procedures were applied to ensure safety and cleanliness of the spacecraft. (The spacecraft was put into a sealed, air-tight plexiglass box including desiccant packets.)

The tests were performed at the observatory Lustbühel in Graz. The satellite was mounted on a tripod to avoid obstruction during communication with the ground station. The BRITE-Austria ground station at TU Graz/IKS, at a line of sight distance of *2.7 km*, was used to operate the satellite during the test.

Figure 2.20 depicts the block diagram of the open field test setup, while Figure 2.21 shows the test configuration with the spacecraft at the observatory Lustbühel.

The communications portion of the test is intended to verify that the spacecraft can communicate in the nominal configuration with the ground station. This is one of the few times before launch when the full communications chain, including all ground antennas and spacecraft antennas, was used to communicate with the satellite.

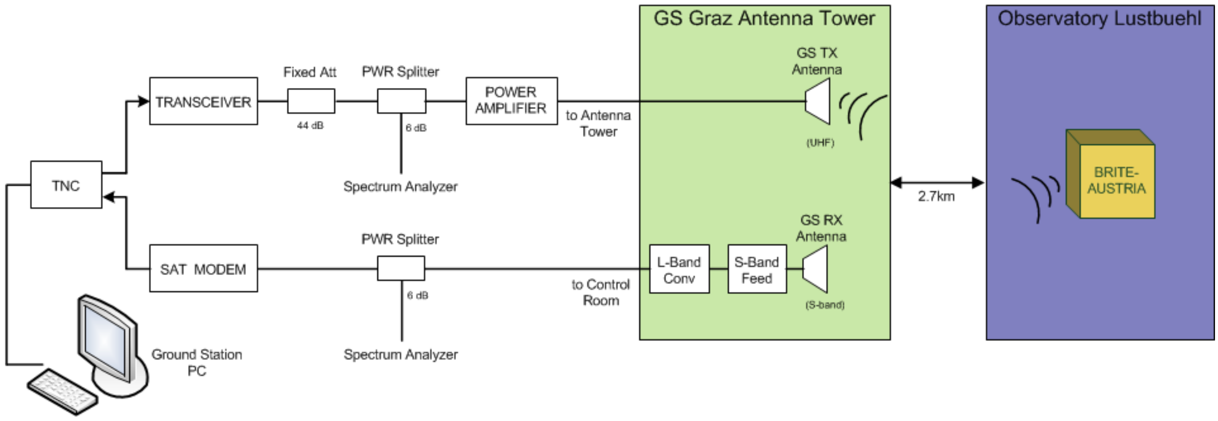

Figure 2.20: Open field test setup block diagram. Communication with the satellite was tested by using the real ground station (with suitable attenuation) communicating with the flight model of the spacecraft located outdoors at the Lustbühel observatory at *2.7 km* line of sight distance.

Figure 2.21: Open field test setup. The flight model of the spacecraft was mounted outdoors on a tripod at the observatory Lustbühel for the test.

Suitable attenuation on the UHF uplink was applied at the ground station to prevent saturation of the receiver input of the satellite during the test. The attenuation used during the testing was *50 dB*, resulting in an effective isotropic radiated power (EIRP) of *10.75 dBm*, suitable to operate the satellite at an adequate receiving power level of about *-90 dBm*, more than *10 dB* above its receiver's sensitivity level.

According to the test outline for the communication part of the open field test the following actions were performed, for which the test results are summarized in Table 2.5:

- Firecodes: try out all satellite firecodes to verify the ability to command the spacecraft
- Application software load: command the spacecraft from kick-off mode up to full application mode (by loading the housekeeping application code via uplink and not from on-board memory)
- Units activation: activate each unit on the spacecraft
- Whole Orbit Data (WOD) collection: Record whole orbit data for 30 minutes; download and verify that the whole orbit data is complete and free from anomalies.
- System reset: Issue a Spacecraft Power Cycle firecode and confirm that the spacecraft reboots in Kick-Off mode.

Test	**Pass/Fail**
Firecodes	Pass
Kick-off to full application mode	Pass
Load HKC software over radios	Pass
Activation of all switches	Pass
Whole Orbit Data Recording and Download	Pass
Power Cycle Firecode	Pass

Table 2.5: Open field test communication test results. All tests performed were successful, demonstrating the functional performance of the communication link.

During the test, the received S-band spectrum was recorded. Figure 2.22 shows the received S-band signal spectrum at the ground station during the open field test.

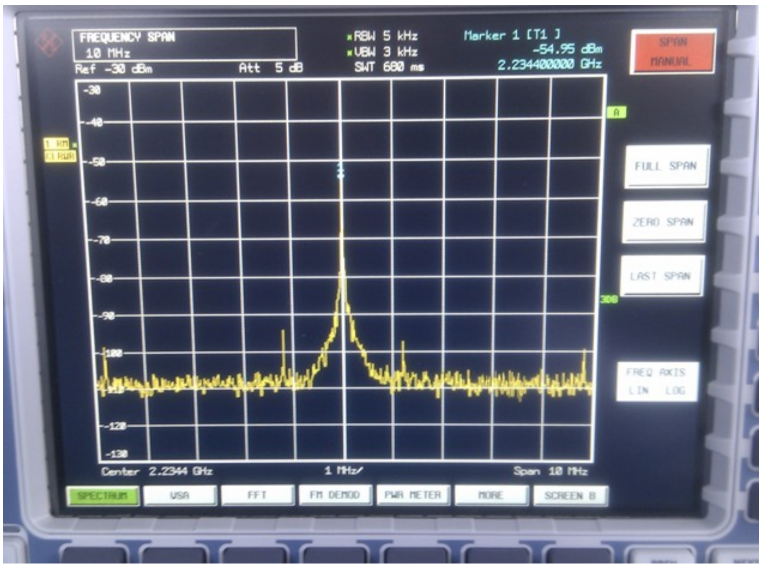

Figure 2.22: Open field test received S-band signal spectrum. The transmitter was set to QPSK modulation and a data rate of *8 kbit/s* for the test.

After confirming stable communications with the satellite and suitable power levels for testing, a verification of the link budget was performed. For that purpose, several measurements of the downlink and uplink signal were performed. It has to be noted that due to the short link distance and low elevation, additional effects such as partial shadowing of the link due to obstacles (especially for the S-band path) as well as partial obstructions of the Fresnel zone (especially for the UHF path), resulting in multipath signal components, may have been introduced.

At the beginning, the satellite was facing the ground station with the -Z panel. In this configuration, one S-band patch and all four UHF antennas are oriented towards the ground station, providing the best conditions for communications. Subsequently, the satellite was rotated clockwise by approximately 45 degrees at time, and a new measurement was recorded.

The measurements were then compared to the calculated values according to the link budgets, described in Section 4.2 to verify the accuracy of the calculations. For the uplink, an output power of *-5.4 dBm* was measured at the power amplifier output, resulting in an EIRP of *10.75 dBm*. At the spacecraft, a received signal power of *-90 dBm (1.04 V RSSI)* was expected. For the downlink, a received signal power of about *-4 dBm* was expected. The test results are summarised in Table 2.6.

The results show that, when optimally pointed towards the ground station, the measured and calculated values for the downlink agree quite well, while for the uplink the measured value is even better than the calculated one. At other orientations of the spacecraft, the signal measurements fluctuate according to the satellite antenna pattern characteristics. Averaging of the measurement results show good agreement of the calculated and measured values for the uplink, while a few decibel are missing in the measured downlink values. This behaviour can be explained with the previously described additional effects present on the link (partial shadowing and obstructions in the Fresnel zone).

Satellite Position [deg]	**S-band RX Signal [dBm]**	**UHF RSSI [V]**	**UHF Equivalent Signal Level [dBm]**
Expected	-4.0	1.04	-90.0
0	-5.5	1.09	-87.1
45	-5.7	0.94	-94.9
90	-10.0	1.14	-84.2
135	-15	1.04	-90.0
180	-5.5	0.93	-95.5
225	-6	0.95	-94.5
270	-7	1.02	-91.0
335	-5.6	1.08	-88.0
360	-5.5	1.08	-88.0
Average	-7.3	1.03	-90.36

Table 2.6: Open field test link budget verification. Despite possible signal distortion due to obstacles in the test path, the results show that the measured values agree quite well with the calculated ones in both the up- and downlink.

Chapter 3

The BRITE-Austria Master Ground Station Design

As part of BRITE-Constellation, the BRITE-Austria satellite is operated by the BRITE ground station network. Each satellite in the constellation has a master ground station, which is responsible for the respective satellite and primarily used for operations. Within BRITE, a master ground station is co-located with the mission control centre (MCC) for the corresponding spacecraft. A detailed description of the BRITE ground station network can be found in Chapter 5. For BRITE-Austria, the master ground station and mission control centre have been established at the Institute of Communication Networks and Satellite Communications of Graz University of Technology.

As part of this thesis, the Graz ground station has been established, validated, and operated during the commissioning and operations phases of the BRITE-Austria spacecraft.

The following sections provide detailed information about the establishment of the Graz ground station. The topics include the ground station requirements, the ground station preliminary and final design, the rationales for the design choices, as well as possible design alternatives, planned and performed upgrades, including backup scenarios.

3.1 Ground Station Requirements

The requirements for the BRITE-Austria ground station in Graz mainly derive from the satellite orbit and from the produced science data amount to be downloaded. Additional requirements derive from the fact that the ground station in Graz is co-located with the mission control centre for BRITE-Austria.

3.1.1 Satellite Orbit and Tracking Requirements

The general orbit requirement for the BRITE-Austria ground station in Graz was the tracking capability of a satellite in sun-synchronous Low Earth Orbit (LEO) with altitudes between *500 km* and *900 km* [33]. This general orbit requirement derives from the scientific mission requirements, as these characteristics were found to be optimal for performing the envisaged science tasks.

A sun-synchronous orbit (SSO) is a satellite orbit with consistent Sun lighting conditions. A satellite in SSO passes the equator and each latitude at the same time every day. The orbit has an inclination that causes the satellite orbital plane to rotate (drift) by approximately *1°/day* towards the East. This way, the satellite moves along with the Earth's rotation around the sun, maintaining a fixed orientation of the orbital plane with respect to the sun's direction [34]. Therefore, a SSO is very suitable for Earth observation applications, and as well for an astronomy mission such as BRITE. The two extreme types of SSO used for LEO satellite missions are:

1. Dawn-dusk SSO (LTAN/LTDN 06:00): The satellite passes the equator at dawn or dusk
2. Noon-midnight SSO (LTAN/LTDN 12:00): The satellite passes the equator at noon or midnight

In order to track the spacecraft, the ground station needs to control the antenna rotators according to the current satellite position during a pass. For operating BRITE, satellite tracking is based on program track by the use of NORAD Two-Line Element (TLE) data. The ground station shall use these data to determine the contact windows with the satellite and to calculate the required antenna pointing angles accordingly.

A crucial aspect for satellite tracking is time synchronization. The ground station must use a time reference allowing a precision of one second or better.

3.1.2 Data Download Requirements

The selected BRITE-Austria satellite orbit yields an orbital period of about 100 minutes, with typical contact times of $8-15$ minutes with the ground station per pass, and about 6 trackable passes in total per day. Hence, the ground station must be capable of uploading the necessary satellite commands and of downloading science data and housekeeping telemetry during these limited contact windows. Therefore, the command upload is not the limiting factor, as during nominal operations the spacecraft operates autonomously, requiring only uploads of command sequences for scheduling long-term operational tasks. In addition, the upload data amount is very limited (only a few kBytes). Similarly, during operations the housekeeping telemetry data to be downloaded represent a small amount compared to the collected scientific data to be downloaded. Hence, the main driver for the data download requirements is the collected amount of scientific data.

In the requirements phase, the typical science data amount to be downloaded was estimated with at least *2 MByte/day* and up to *10 MByte/day*. The minimum guaranteed data rate for the downlink is *32 kbit/s* per requirement. With this data rate the upper bound of the data download requirements can be met, as it would take about 42 minutes per day to download all the required scientific data. Having typically six passes a day of $8 - 15$ minutes contact time each available provides sufficient margins to meet this requirement. In addition, the data rate can be adaptively increased during a pass provided that good link quality is available. The data download requirements are summarised in Table 3.1.

Data Download Requirements	
Main driver	Science data download
Data amount	up to *10 MByte/day*
Data rate	*32 kbit/s* minimum

Table 3.1: Ground station data download requirements. The main driver for the data download is the amount of science data collected.

3.1.3 Space-to-Ground Interface Requirements

In order to operate the BRITE satellites, the ground station needs to be compatible with the spacecraft in hardware and software and fulfil the communication standards and protocols used [33].

The ground station shall be compatible with the frequency bands used for satellite operations. The ground station shall provide uplink capabilities in the UHF amateur radio satellite band for satellite telecommand with sufficient margins for the target uplink data rate of *9.6 kbit/s*. The ground station shall provide downlink capabilities in the Space Research Services (SRS) S-band spectrum for satellite telemetry download, with sufficient margins to allow operations at data rates between *32 kbit/s* and *256 kbit/s* (minimum guaranteed and maximum allowed data rates, respectively).

The ground station shall be compatible with the generic nanosatellite bus (GNB) physical layer, i.e. the ground station hardware equipment must be compatible with the spacecraft communication subsystem. In addition, the ground station shall implement the ground segment software suite and shall be compatible with the GNB software protocols in order to allow data up- and download with the spacecraft [33].

3.1.4 Mission Control Centre Requirements

The ground station in Graz is co-located with the mission control centre for the BRITE-Austria satellite and is also the primary ground station for operating the spacecraft. The ground station is in charge of BRITE-Austria and has full control over the satellite. From this ground station, commissioning and operations of the satellite shall be carried out including corrective actions or contingency procedures.

The ground station shall implement the full version of the ground segment software, including ground station specific software, control software for the spacecraft and the payload for command upload and payload setup, as well as software for data download, processing, evaluation, and dissemination for both science data and satellite telemetry [33].

The ground station shall provide raw data storage of the BRITE-Austria data as well as ensure data integrity. Furthermore, it shall be integrated in the BRITE ground station network for constellation operations and data distribution.

Last but not least, an additional requirement for the establishment of the ground station was cost effectiveness. The whole ground station has been set up for less than *50,000 €*.

3.2 Graz Ground Station Design

This section deals with the design of the BRITE-Austria master ground station in Graz, providing detailed descriptions of the components used and their interaction. In addition, upgrades to the initial design applied in a later step are presented as well as possible further improvements are discussed.

The BRITE-Austria master ground station has been established at the Institute of Communication Networks and Satellite Communications of Graz University of Technology (TU Graz/IKS). The outdoor installations including the antennas are located on the roof of TU Graz/IKS, while the mission control centre including all ground station indoor equipment is located in a dedicated room underneath the roof platform. This allows to keep the cabling lengths to a minimum, and has the advantage of being co-located to the outdoors equipment for quick assessment in case of anomalies.

Figure 3.1 shows the block diagram of the Graz ground station with the main components in the uplink and downlink path. Common ground station components are illustrated in blue boxes, uplink components in orange boxes, and downlink components in green boxes. The items in the block diagram are divided in outdoor equipment on the antenna platform and indoor equipment in the mission control room. All outdoor equipment is mounted on the same antenna tower, including the antennas as well as an outdoor box for RF-equipment. The indoor equipment is assembled in a *19"* rack in a suitable configuration.

3.2.1 Ground Station Components and their Interaction

The Graz ground station comprises different components, which are detailed in the following sections. The description provided is based on the *Ground Station Hardware Critical Design Document* [35] and the *BRITE-Austria Ground Station Hardware Manual* [36].

3.2.1.1 Common Components for Uplink and Downlink

This section provides an overview of the main ground station components used in common by the uplink and downlink.

Antenna Tower

The antenna tower is installed on the roof of the TU Graz/IKS building, which is located at the TU Graz Campus Inffeldgasse. The ground station geographical information is summarised in Table 3.2:

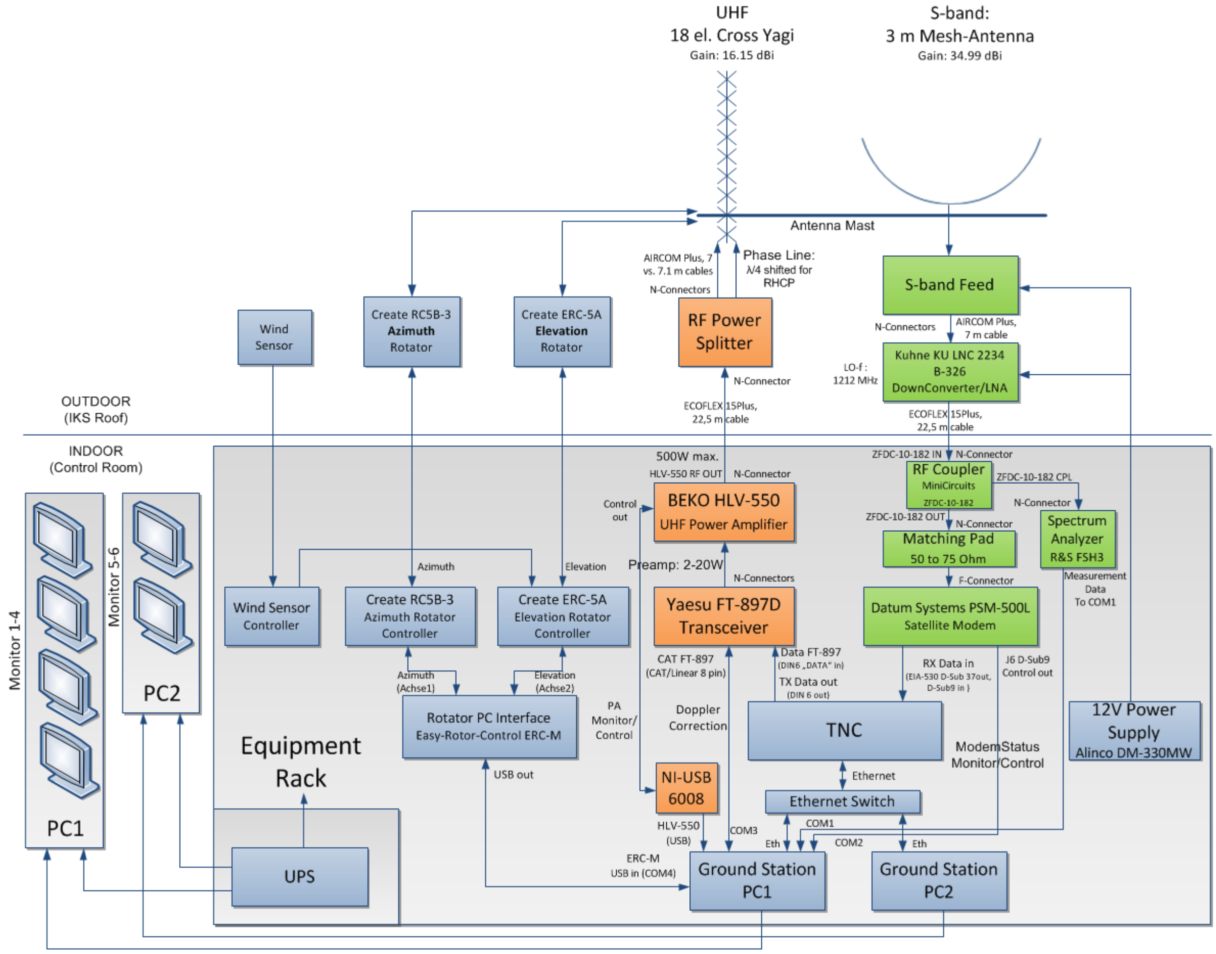

Figure 3.1: Graz ground station functional block diagram. Common ground station components are illustrated in blue boxes, uplink components in orange boxes, and downlink components in green boxes, respectively.

Latitude	47.05917 N
Longitude	15.45972 E
Altitude	360 m
Height above ground	25 m
min. Elevation	5 deg

Table 3.2: Graz ground station geographical information. The parameter of main relevance for satellite operations is the minimum elevation required to communicate with the spacecraft.

Installed on the highest point of the building on the 4th floor, the ground station antenna tower location is well suited to operate a LEO satellite mission. The visible horizon limit in every antenna's azimuth orientation is 5° or less. In addition, the selected location allows having the ground station control room (which also serves as mission control centre for BRITE-Austria) directly underneath the roof platform, with relatively short cabling distances of about *20* to *25 m*. Furthermore, the entire ground station is located in the same building as TU Graz/IKS, which is advantageous as the operating team for BRITE-Austria is formed by staff members of TU Graz/IKS.

Two antennas are used for operating the satellite: a *3 m* parabolic S-band antenna for the satellite downlink and an 18 element UHF crossed Yagi antenna for the satellite uplink. Both antennas are mounted on the same antenna tower and use the same rotators. Therefore, the same tracking performance for uplink and downlink can be achieved.

Figure 3.2 shows the antenna tower of the Graz ground station, while Figure 3.3 shows the ground station control room with the workstation for the operators and the indoors equipment rack.

Figure 3.2: Graz ground station antenna tower. The UHF crossed Yagi uplink antenna (left) and the 3m S-band parabolic downlink antenna (right) are mounted on the same antenna tower on the roof of the TU Graz/IKS building.

Figure 3.3: BRITE-Austria mission control centre (MCC). The MCC is located underneath the roof with the antenna tower and contains the ground station equipment as well as the workstation for the satellite operators.

Un-interruptible Power Supply (UPS)

The ground station is equipped with an un-interruptible power supply (UPS) to prevent unavailability of the ground station in case of power outage. The UPS provides *3 kW* backup for all ground station components assembled in the indoor equipment rack (including the PC monitors), as well as for the power supply of the antenna platform. In addition, a web-based remote control interface is available for configuration. The UPS is shown in Figure 3.4.

Figure 3.4: Ground station UPS. The UPS is used to provide power margins in case of power outage to prevent unavailability of the ground station.

12 V Power Supply

A *12 V* power supply is used for powering outdoor equipment on the antenna tower. Currently, the supply is only used for downlink components, providing constantly *12 V DC* voltage to the S-band feed box (for the low noise amplifier). The unit is switchable from the control room to the fixed mounted box on the antenna tower (not rotating), where, apart from the feed, additional devices such as the S-band downconverter can be powered. In addition, the *12V DC* voltage is used to power the Terminal Node Controller (TNC) in the control room. Figure 3.5 illustrates the *12 V* power supply.

Figure 3.5: Ground station 12V voltage supply. The supply is used for powering outdoor equipment on the antenna tower such as the S-band LNA and downconverter.

Ground Station PCs

For operating the ground station, two redundant PCs are used. The main PC provides the interfaces to the hardware and is used for satellite control; all hardware components are physically connected to this PC. The second PC is used for mission planning and documentation tasks during nominal operations, but can fully take over the functionality of the main ground station PC if required, as it includes all interfaces in the same configuration as the primary PC. Therefore, if required, the hardware devices can be connected to this PC and accessed in the same manner as in the nominal configuration. Backups of the PCs are obtained on a regular basis for quickly restoring the most up-to-date configuration in case needed. Figure 3.6 shows one of the ground station PCs, while Table 3.3 lists the interfaces and items connected to the primary ground station PC.

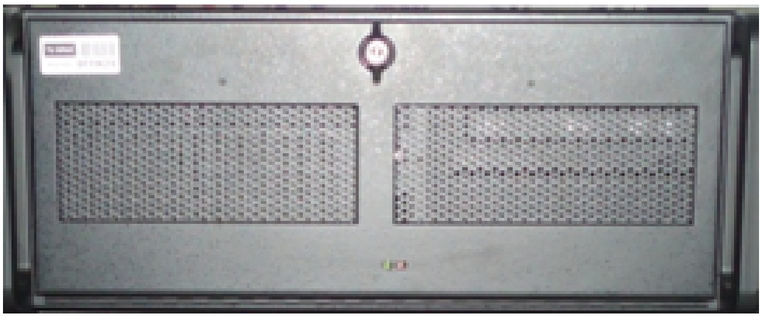

Figure 3.6: Ground station PCs. Two identical PCs are used in the ground station; the main PC is used for interfacing with the ground station hardware and operating the spacecraft, the second PC for mission planning and documentation tasks.

Manufacturer / Part No.	Schneid, 19” PCs
Function	Ground Station Control satellite / mission operations with ground segment software
Interfaces	COM1 Port: Spectrum Analyser RS FSH3 connection COM2 Port: satellite modem remote connection COM3 Port: transceiver CAT-interface (PTT On/Off, Doppler correction, power level setting) COM4 Port: ERC-M rotator-interface connection static IP addresses for remote control private IP addresses for connection with the TNC

Table 3.3: Ground station PCs facts. A description of the ground station hardware interfaces and functionality is provided.

Antenna Rotators

For tracking the spacecraft, two different rotators for azimuth and elevation are used. The same rotator set is used for both up- and downlink. A second set of rotators including their controllers is available as a backup. Figure 3.7 shows the azimuth and elevation rotator on the antenna platform, while Figure 3.8 shows the correspondent rotator controllers and rear connections. Table 3.4 describes the rotator interfaces and operation characteristics.

Figure 3.7: Antenna azimuth and elevation rotators. The same rotators are used for the uplink and downlink antenna, allowing to achieve the same tracking precision.

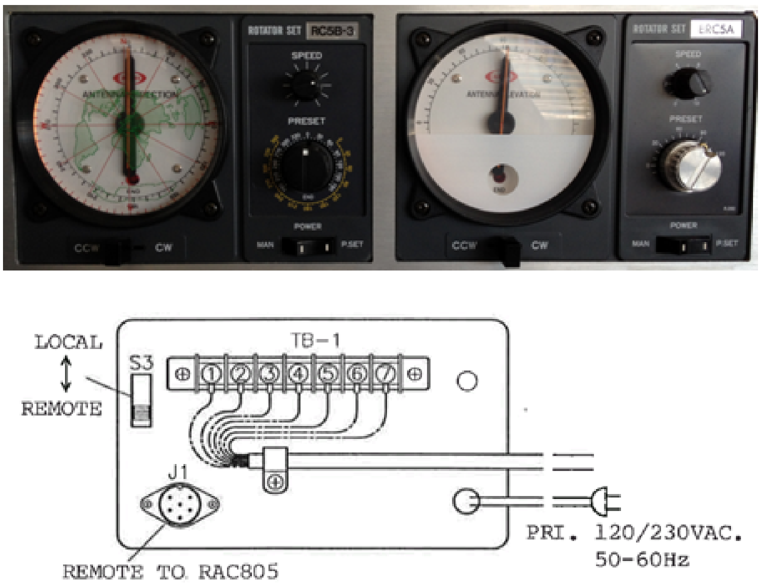

Figure 3.8: Antenna azimuth and elevation rotator controllers and connections. The controllers are commanded remotely by the tracking software to operate the satellite according to its passes over the ground station.

Manufacturer / Part No.	Create RC5B-3 Azimuth Rotator / Create ERC5A Elevation Rotator
Function	Rotators for antenna pointing to the desired position for satellite tracking
Interfaces	TB-1 connector: 7-pin cable from the controller to the rotator J1 DIN6 Pin connector for rotator PC-Interface (remote connection) S3 Local/Remote: Remote connection of elevation-rotator to the wind sensor
Operation / Characteristics	Nominal operation: Power Switch set to “P.SET” for remote operation by the PC tracking software “Tracker” Manual operation: Power Switch set to “MAN”, the correspondent rotator can be controlled with the CCW/CW switch Wind sensor: If wind sensor threshold value reached, elevation rotator moves to the manually set preset-position (90° elevation)

Table 3.4: Antenna rotators and controllers facts. The interfaces and operations characteristics are presented.

Rotator Interface

The rotator interface allows remote control of the azimuth and elevation rotator from the ground station PC. As the rotators can only be commanded by their dedicated control units, an additional interface to command these units from the ground station PCs is required. The rotators are controlled by the tracking software *Tracker*. The software determines the satellite position based on its two line elements (TLE) data, calculates the corresponding contact windows with the spacecraft, and sets the correspondent antenna pointing angles during a pass. Therefore, for operating the BRITE-Austria mission, a program track-based solution for satellite tracking is used.

To operate the BRITE-Austria mission with the *Tracker* software, a rotator interface from *EasyRotor* was installed. It provides an USB interface for the controlling ground station PC and establishes a connection to a COM port by the USBtoRS232 Future Technology Devices International (FTDI) chip on the controller board. The interface communicates with *Tracker* via the *Yaesu GS232-A* protocol.

This interface replaced the previously installed IF100 interface, which used a parallel port for communicating with the controlling PC. In addition, the former tracking software (SatPC32) only allowed the identification of the parallel port on the controlling PC by fix hardware addresses, making the use of USB to parallel port converters or even parallel PCI PC-cards impossible.

In the new configuration, the *EasyRotor* interface is connected to the remote port of the original rotator controllers, which additionally allow manual control of the rotators by using an analogue display of the rotators' position. For each of the two rotators (azimuth and elevation), a separate controller is used.

The elevation controller is further connected to a wind sensor which is actively included in the system when the controller is in remote operation mode. The wind sensor measures the wind speed on the antenna tower and checks it against a threshold. In case the threshold value is reached, a relay switch is activated, triggering the switch of the elevation rotator to return back to its parking position (90°), to protect the antenna from wind loads. The rotator interface including cable pin-outs is shown in Figure 3.9, while a description of the main facts of the interface can be found in Table 3.5.

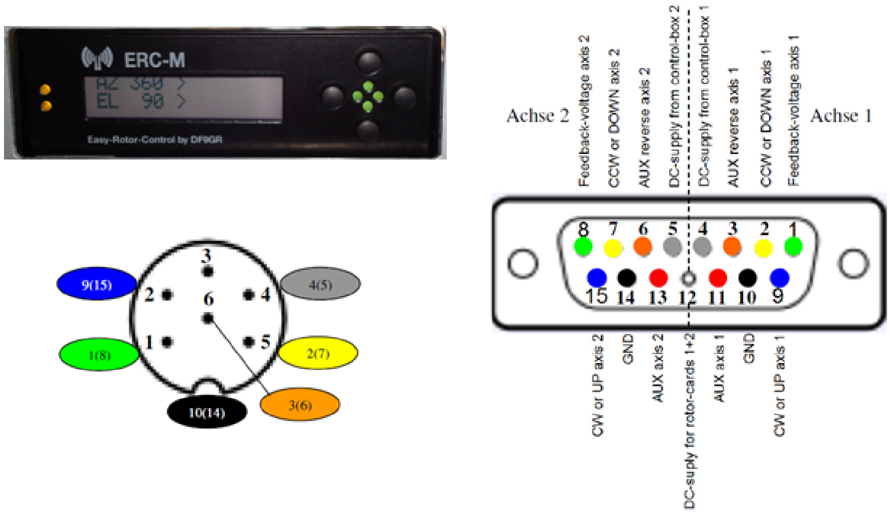

Figure 3.9: Antenna rotator PC interface. The PC interface allows the tracking software to remotely control the rotators.

Manufacturer / Part No.	Easy-Rotor-Control ERC-M
Function	Interface between rotator controller and ground station PC
Interfaces	USB to USB -COM4 Port of ground station PC (USB RS-232 FTDI driver required) D-Sub 15 Pin cable to rotator controllers: Achse 1: azimuth controller connection Achse 2: elevation controller connection
Software Interface	Tracker (operation) Easy Rotor ERC-M Service Tool V2.0 (calibration)

Table 3.5: Antenna rotator PC interface characteristics. The main interface characteristics are listed, including interface configurations and software used.

Terminal Node Controller (TNC)

The core component in the ground station for communications with the spacecraft is the Terminal Node Controller (TNC). This device is used as interface between the ground station specific hardware and the ground segment software. The TNC provides baseband processing functionalities, performing data scrambling and GMSK modulation in the UHF uplink as well as data descrambling in the S-band downlink. The UHF interface of the TNC is the transceiver, the S-band interface is the satellite modem.

The TNC radio interface board is connected to a commercial *200 MHz* ARM based embedded Linux computer board, which interfaces with the ground station PCs via Ethernet. A Linux-based TNC software allows the ground segment software to connect to the TNC and communicate with the spacecraft.

In the nominal configuration, the ground station PCs connect to the TNC with a private IP-address. Alternatively, a remote connection with a public IP-address can be established. Figure 3.10 shows the TNC front panel with its control light emitting diodes (LEDs), and Table 3.6 lists the TNC key facts.

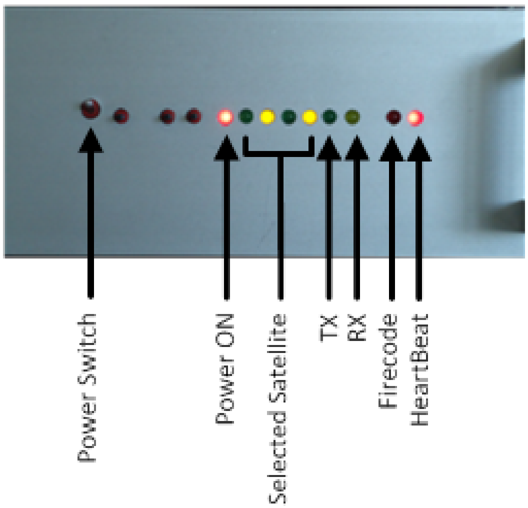

Figure 3.10: Terminal node controller front panel. The terminal node controller is used as interface between the ground station hardware and ground segment software in both up- and downlink.

Manufacturer / Part No.	UTIAS/SFL
Function	Communication for Up- and Downlink; Interface between GS hardware and GS software(via GS PC) GMSK modulator and scrambler for Uplink Descrambler (base band) for downlink
Interfaces	DIN 6 connector for data TX to transceiver (uplink) DB9 connector for data RX from modem (downlink) Ethernet connector for communication with GS-PC
Software Interface	FTP: for software upload Telnet: for configuration MUX/TIP: for satellite operations
Operation / Characteristics	Automatic software load and run on startup Satellite selection LEDs 2. to 5. HeartBeat LED flashing indicates operative state Software: Connection to MUX/TIP: TNC Control, TNC Uplink, TNC Downlink

Table 3.6: Terminal node controller facts. The operations principle is based on the TNC software which acts as interface between the ground segment software and the ground station hardware in both up- and downlink.

3.2.1.2 S-band Downlink

The S-band RF downlink chain comprises the S-band parabolic antenna with an antenna feed box (including the feed, a lown noise amplifier, and a bandpass filter), a downconverter to the intermediate frequency of the receiver, and the satellite modem as the receiving unit in the chain.

For receiving the S-band downlink signal of the satellite, a *3 m* parabolic meshed antenna is used. The antenna has a gain of *35 dBi* and a half power beamwidth of 3.13°.

Figure 3.11: S-band antenna and feed. A 3 m meshed parabolic antenna with *35 dBi* gain is used for the satellite downlink.

Components	S-band antenna: 3m parabolic antenna, 35dBi gain S-band antenna feed box: - Linear polarisation patch antenna feed (custom built) - LNA (Kuhne KU 222 AH-HEMT): 31dB gain, 0.5dB NF - Bandpass filter (Reichl Funkzubehör): 2170-2290 MHz -30dB
Function	S-band downlink signal reception at 2234.4MHz
Interfaces (feed)	RF- output: N-connector 12V supply: BNC-connector

Table 3.7: S-band antenna and feed facts. The S-band antenna and feed components are listed. An LNA and bandpass filter are directly attached to the feed (patch antenna).

The S-band antenna feed box is mounted on the antenna's focal point. It contains a patch antenna feed, a low noise amplifier (LNA) and a receive bandpass filter. The LNA is directly connected to the receiving patch antenna and used to amplify the receive signal to provide sufficient signal level to the rest of the downlink chain and to limit the influence of the noise temperature of the following items in the chain. The LNA has a gain of *31 dB* and a noise figure (NF) of *0.5 dB*. The bandpass filter is connected to the LNA with a low loss cable (*0.3 dB* attenuation) and is used to eliminate interference and intermodulation products. It has a passband of *60 MHz* between *2.1 GHz* and *2.7 GHz* and a noise figure (NF) of *1.2 dB*. The inside of the feed box with the connections between the components is shown in Figure 3.12.

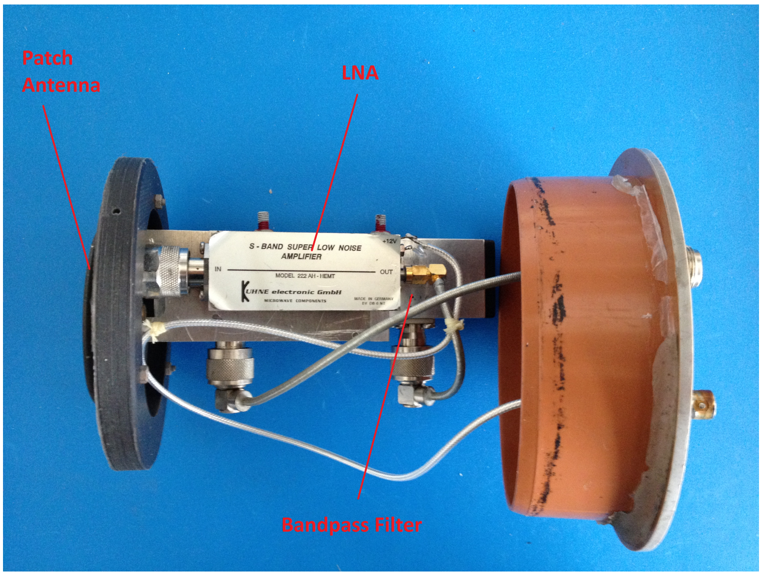

Figure 3.12: S-band feed box with patch antenna, LNA, and bandpass filter. The received signal is first amplified to minimise the system noise temperature, and subsequently filtered.

The feed box is connected to a downconverter through a low loss cable (*1.25 dB*). The downconverter has a local oscillator (LO) frequency of *1212 MHz* and converts the S-band signal to a suitable L-band intermediate frequency of *1022.4 MHz* as input to the satellite modem. The converter has a gain of *40 dB* and a noise figure of *0.7 dB*. In addition to the downconverter, another LNA with a gain of *15 dB* is available in case the input signal at the modem input should be too weak. Both devices are supplied with *12 V* from the outdoor box on the antenna tower, and can be switched from the control room. Figure 3.11 shows the 3 m S-band antenna with the S-band feed box mounted in its focal point, while Table 3.7 provides the main facts of the components.

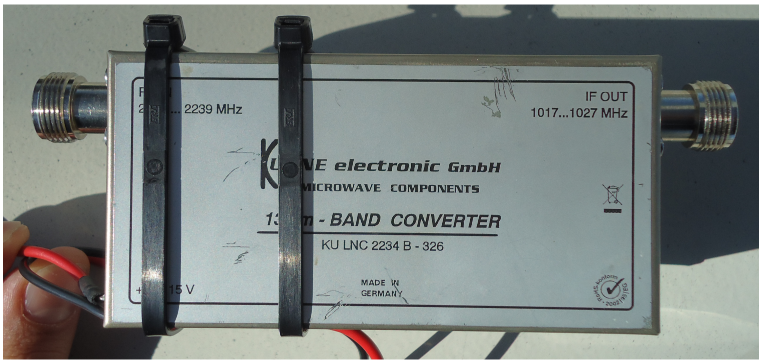

Figure 3.13: S-band downconverter. The received S-band signal is downconverted to the L-band intermediate frequency of the satellite modem (receiver).

Manufacturer / Part No.	Kuhne KU LNC 2234 B-326
Function	Down conversion of received S-band RF signal to L-band modem IF Amplification of down converted signal: *40 dB* gain, *0.7 dB* NF
Interfaces (feed)	RF- input and IF-output: N-connector 12V Supply: V+ and GND connections in outdoor box

Table 3.8: S-band downconverter characteristics. The downconverter has a low noise figure and additionally amplifies the signal after conversion from S-band to L-band.

For the connection from the antenna tower to the control room, a *22.5 m* low loss RF cable (*Ecoflex 15 Plus*; *L = 3.2 dB* at *1022 MHz*) is used. This cable connects the output of the S-band downconverter to the satellite modem. Since the L-band input of the satellite modem has an impedance of 75 Ω, but the incoming signal from the antenna tower has an impedance of 50 Ω a matching pad is used. The matching pad also serves as adapter between the N-connector of the RX cable and the F-connector input of the modem and has a loss of *5.7 dB*.

Satellite Modem

The receiver in the S-band downlink chain is the *Datum Systems PSM505L* satellite modem. It demodulates and decodes the incoming signal, and provides the resulting baseband signal to the TNC via serial interface (RS422). The TNC descrambles the received baseband signal from the modem and forwards the data via Ethernet to the ground station PC. Figure 3.14 illustrates the front panel of the satellite modem, and Table 3.9 provides the main modem facts.

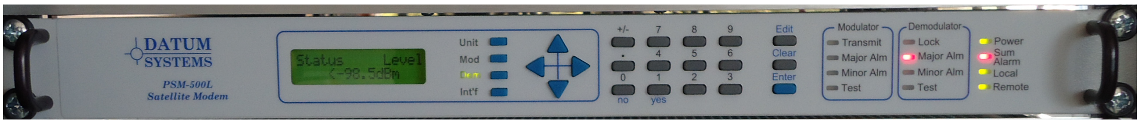

Figure 3.14: Satellite modem. The modem is used as receiver in the downlink chain; its modulation and data rate settings are changed dynamically according to the measured link quality by the ground software.

Manufacturer / Part No.	Datum Systems PSM500L
Function	Receiver in the downlink chain, demodulator
Interfaces	J9 RCV IF IN (L-band, F-Connector): RF Signal input J3 Data Interface (RS-422): Data output to TNC J6 Control (RS-232): Remote Control connection for GS software
Software Interfaces	MUX/TIP + PSM Pass Thru LabView Logging Software

Table 3.9: Satellite modem characteristics. The modem characteristics including interfaces and the software used for remote control are listed.

The main ground segment software BRITE Multiplexer (MUX), connected to the TNC via Ethernet, demultiplexes the incoming data stream into packets and forwards them to the respective requesting ground software modules. A detailed description of the BRITE ground segment software is provided in Chapter 5.

3.2.1.3 UHF Uplink

The uplink commands generated by the ground software are transmitted via Ethernet to the terminal node controller (TNC). The TNC performs GMSK modulation and scrambling of the data and forwards them via a serial interface (DIN 6 pin connector) to the data input of the transceiver.

The UHF indoor components comprise the UHF transceiver and the UHF power amplifier.

Transceiver Yaesu FT-897D

The Yaesu FT-897D transceiver is used for upconversion of the incoming modulated signal from the TNC to the desired uplink frequency (*437.365 MHz*) and for pre-amplification (*2 - 20 W*) of the output radio signal. For the data transmission, packet mode is used. The UHF transceiver is shown in Figure 3.15; the relevant transceiver facts are listed in Table 3.10.

Figure 3.15: UHF transceiver (front and rear view). The transceiver is used for upconversion of the already modulated uplink signal to the desired uplink frequency as well as for pre-amplification (*2 - 20 W*).

Manufacturer / Part No.	Yaesu FT-897D
Function	Upconversion of the modulated TNC signal to UHF uplink frequency: *437.365 MHz* Pre-amplification of the UHF uplink signal (*2 - 20W*)
Interfaces	DATA in (DIN 6 Pin connector): Data input from TNC CAT/Linear (RS232): Doppler correction from ground station PC ANT-144/430 MHz (N-connector): RF-output to power amplifier

Table 3.10: UHF transceiver facts. The transceiver is remotely controlled by the ground software to enable/disable transmission, as well as for Doppler correction of the uplink frequency.

UHF Power Amplifier

The BEKO-HLV550 UHF linear power amplifier (PA) shown in Figure 3.16 takes the pre-amplified RF signal from the transceiver and generates the desired output power depending on the input power provided by the transceiver. It has a constant amplification factor of about 25. For the BRITE-Austria mission, the power amplifier provides suitable output power levels to operate the spacecraft with sufficient margins to compensate for low elevation contacts as well as with certain levels of noise signal interference from ground. The maximum output power available is around *500 W*. The operation characteristics of the amplifier are listed in Table 3.11.

Figure 3.16: **UHF power amplifier.** The PA is used for amplification of the uplink signal to a level suitable for operating the spacecraft.

Manufacturer / Part No.	BEKO HLV-550
Function	Amplification of UHF TX signal (50-500W)
Interfaces	RF IN (N-connector): RF input from transceiver RF OUT (N-connector): RF output (amplifier) for antenna Remote Control (DIN6-connector): via NI-USB 6008 interface
Operation / Characteristics	Nominal operations TX on (visual verification): Power ON LED on, PTT LED on, OUTPUT POWER shows desired output power Alarm: Protection and triggering alarm LED on: - Antenna: antenna mismatch / too high SWR - Overdrive: too high input power - Temperature: temperature threshold reached ATTENTION: Reset only if alarm is - Overdrive (after reduction of input power) - Temperature (after cool down period) If ”Antenna” Alarm verify antenna, cabling and PA SWR

Table 3.11: **UHF power amplifier facts.** The power amplifier is remotely controlled by the ground software to enable transmission, as well as to detect alarm states.

RF power measurements have been performed at different stages of the uplink chain. For the power amplifier, the amplification curve at each settable power level was measured. In addition, the power levels were measured at the input of the outdoor unit (RF power splitter input) as well as at the input of the horizontal and vertical input of the UHF crossed Yagi antenna. The resulting power levels are shown in Figure 3.17.

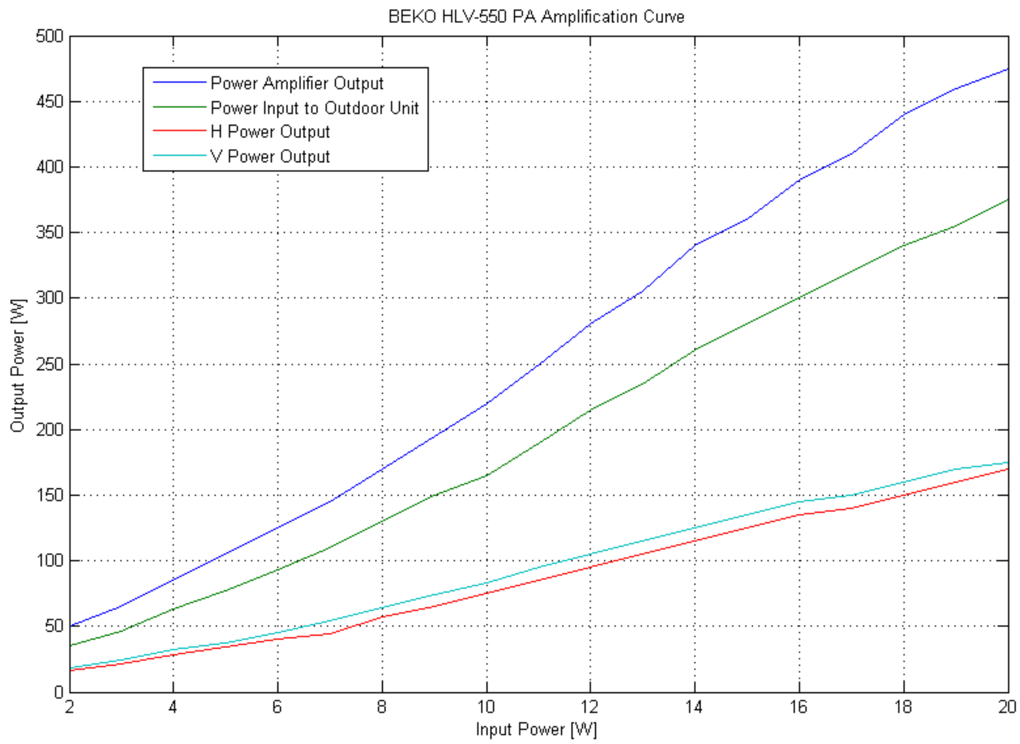

Figure 3.17: BEKO HLV-550 UHF power amplifier amplification curve. A comparison of the power levels at the output of the amplifier, the input to the power splitter, and the effective power input to the antenna dipoles is shown. It can be seen that the power level at the input of the power splitter is attenuated by *1.35 dB*, and the power distribution of the power splitter to the horizontal and vertical signal path is nearly identical.

Power Splitter and Phased Lines

The output signal of the power amplifier is fed into a *3 dB* power splitter with a *22.5 m* low loss cable (L = *1.35 dB*) to the antenna tower. The power splitter distributes the power to the two antenna dipoles of the crossed Yagi antenna. In addition, the two feed cables of the dipoles have different lengths. The feed line for the horizontal polarisation denotes an offset length of $\lambda/4$ compared to the feed line for the vertical polarisation, in order to generate right hand circular polarisation (RHCP). Therefore, the uplink to the spacecraft is always performed by using RHCP. Figure 3.18 shows the UHF outdoor equipment, which include the power splitter with the phased feed lines connected as well as the UHF crossed Yagi antenna.

The UHF antenna itself has been mounted on the antenna tower in a fashion to be as close as possible to the S-band antenna due to constructional constraints and to minimise unwanted movements as well as wind loads while tracking. The minimum required spacing of the UHF antenna to the S-band antenna was calculated according to the UHF antenna beam width (28°) with a margin of 2°. Considering 30° as the minimum beam width to be unobstructed, the minimum distance of the UHF antenna to the S-band antenna results in 115 cm. Figure 3.19 shows all relevant measures, where the angle α denotes the 30° beamwidth. The UHF antenna was mounted to the tower according to these considerations.

Figure 3.18: UHF antenna and phased feed lines. Right hand circular polarisation (RHCP) is generated by introducing a phase shift of 90° between the feed lines to the dipoles by different line lengths.

Appropriate phased line cables have been manufactured; the difference in length between them in order to obtain the right phase shift of 90° was performed by calculating the mechanical length difference according to the electrical length difference using the velocity factor of the cable used. The velocity factor is defined as the relation between the mechanical length l_L and the electrical length l_0:

$$V = \frac{l_L}{l_0} \tag{3.1}$$

The velocity factor can further be expressed as the relation between the electrical wavelength, travelling at speed of light c, and the mechanical wavelength, travelling through the cable medium:

$$V = \frac{\lambda_L}{\lambda_0} \tag{3.2}$$

The electrical wavelength λ_0 for the nominal used uplink frequency f_0 = *437.365 MHz* is *0.6855 m*. The correspondent electrical length difference l_0 between the two cables needed to result in a phase shift of 90 degrees is therefore $l_0 = \frac{\lambda_0}{4} = 0.17136\ m$. For the *Aircom Plus* cable used with a known velocity factor of $V = 0.83$ the resulting mechanical length offset for the two cable results in $l_{L,offset} = \frac{\lambda_L}{4} = V \cdot \frac{\lambda_0}{4} =$

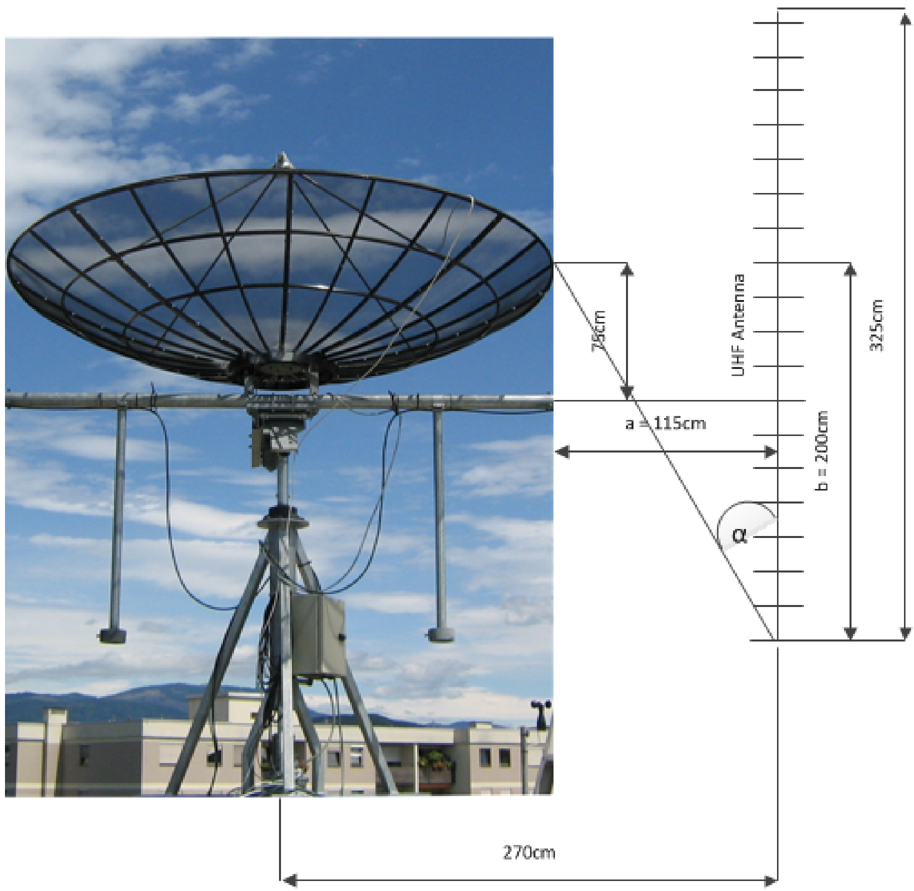

Figure 3.19: **UHF antenna spacing.** The UHF antenna was mounted on a boom at a distance of *115 cm* from the S-band antenna to ensure an unobstructed 30° for the UHF antenna radiation pattern (3dB-bandwidth of the antenna).

0.1422 *m*. However, the distance between the antenna dipoles of the crossed Yagi antenna has also to be taken into account, adding an additional phase shift. The plane distance between the dipoles is *0.24 m*, which equals to a phase shift of 125°. Therefore, the total phase shift required is $90 + 125 = 215°$, yielding an offset length of $l_{L,offset} = 0.3414$ *m*.

The cables were manufactured in-house with a suitable base length to reach the antenna connectors corresponding to a multiple of the mechanical wavelength for the cable $\lambda_L = V \cdot \lambda_0 = 0.569$ *m*, for a total of $l_L = 14 \cdot \lambda_L = 7.966$ *m*, with one of the two cables being longer by the offset length $l_{L,offset}$.

The precision of the manufactured cables in phase shift was verified by measurements with a network analyser as shown in Figure 3.20. A three-port measurement with the power splitter input and the cables connected to the two outputs of the splitter was performed. The phase between the nominal cable and the input (*S21*), as well as the phase between the cable with the offset length and the input (*S31*) were measured. The resulting network analyser plot shows that the phase shift between the two cables is 144.47°. Since the network analyser displays the phase between −180° and +180°, a subtraction of the measured value from 360° has to be performed to obtain the desired result, yielding a phase shift of 215.53°, which is ideal for generating right hand circular polarisation in this configuration.

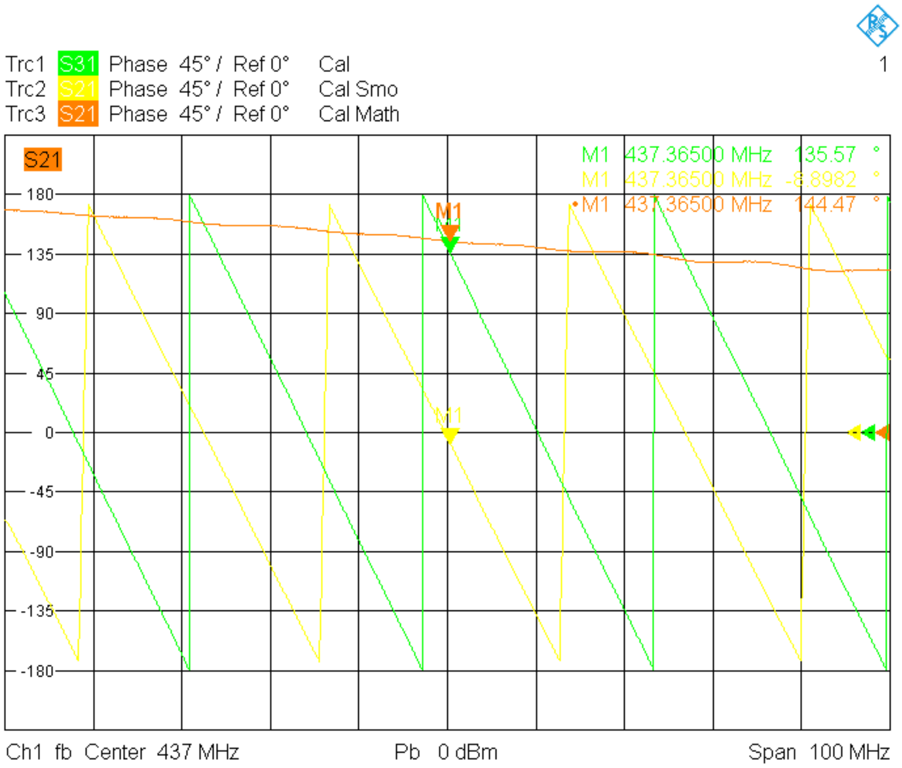

Figure 3.20: Phase shift of UHF antenna cables. The measured phase shift is $144.47°$. Since the network analyser displays the phase between $-180°$ and $+180°$, a subtraction of the measured value from $360°$ has to be performed to obtain the desired result, therefore the phase shift is $215.53°$, which is ideal for generating right hand circular polarisation in this configuration (the required phase shift is $90 + 125 = 215°$ due to the spacing of the dipoles relative to each other).

UHF Crossed Yagi Antenna

A single 18-element crossed Yagi antenna with a length of *3.25 m* is used for transmitting the uplink signal to the satellite. The antenna gain is *16.15 dBi* (*14 dBD*) and the half power beamwidth is 28°. The antenna is mounted on the same tower as the 3m S-band parabolic antenna, and can therefore be operated by the same set of rotators with the same tracking performance for both the uplink and downlink path.

3.2.2 Ground Station Design Considerations and Rationales

The essential BRITE-Austria ground station design criteria were robustness, low-complexity, and low-cost, to provide a suitable configuration for operating the mission. The concept was to pursue a semi-professional approach by using low-cost commercial off the shelf (COTS) components, either for professional use (e.g. the satellite modem) or from the high end radio amateur sector (e.g. the UHF power amplifier). Although there is room for improvement and for potential upgrades of the current configuration, these upgrades are limited by certain constraints. The most significant design choices and constraints are described in the following paragraphs.

3.2.2.1 S-band Downlink Design Choices

A 3m parabolic antenna provides a high antenna gain of about *35 dBi* in S-band, which makes it very suitable for the mission needs.

Concerning the downconversion of the received S-band signal to a suitable intermediate frequency for the satellite modem, two options are presently available: the downconversion from S-band to L-band (default) as well as a backup option a downconversion from S-band to VHF (cold redundancy), which is compatible with a second (spare) satellite modem with an VHF intermediate frequency input. The choice in favour of the downconversion to L-band as default configuration was made after several measurements, showing that the VHF converter was affected by substantial interference from the surroundings due to the fact that the operated VHF intermediate frequency is in the radio amateur band, which is not the case for the L-band intermediate frequency used. In addition, despite the higher cable attenuation to the control room, the downconverter also provides an amplification of *40 dB*, and considering the amplification of the S-band LNA and its short path to the downconverter, the noise temperature increase due to cabling is negligible. The backup option of a second intermediate frequency for downconversion not only represents an alternative configuration, but also introduces redundancy. A second downconverter and modem are available for that purpose.

The choice of the selected satellite modem was based on the fact that UTIAS/SFL had successfully used predecessor series of this modem in other GNB missions and the modem ensured maximal compatibility with the TNC (with respect of the configuration options provided) and the ground segment software.

3.2.2.2 Ground Station Tracking Performance

The installed antenna rotators are from the high-end amateur radio domain and provide acceptable performance, although for S-band better precision would be desirable. Given that the half power beamwidth of the S-band antenna is $3.13°$and the precision of the rotators is $3°$, fluctuations of the downlink signal due to rotator tracking lag can occur. This behaviour has been characterised and countermeasures with offsets in the tracking software as well as with feed readjustments have been performed and are described in detail in Chapter 4. The chosen rotator solution represents a compromise between performance, mechanical/electrical compatibility, and restrained costs. However, to improve the tracking performance, in January 2015 an upgrade to rotators with better precision has been implemented.

3.2.2.3 Antenna Tower Mechanical / Constructional Constraints

The height and limited area of the antenna tower represents a constraint for possible upgrade configurations of the current system. Possible design scenarios include the use of an UHF uplink antenna group of up to 4 crossed Yagi antennas, in order to distribute the output power and allow increasing the overall Effective Isotropic Radiated Power (EIRP). However, the present antenna tower is not suitable to accommodate 4 antennas; this configuration would imply a new tower construction which would need to be investigated in terms of feasibility, construction, and costs.

3.2.2.4 UHF Uplink Power / Complexity Constraints

Besides mechanical constraints, additional constraints for the UHF uplink design derive from available power levels as well as from the complexity of potential upgrades. In the following, constraints and adopted countermeasures are listed.

- Antenna groups introduce complexity despite the fact that the output power can be distributed among them - multiple polarisation switches and/or power splitter are required, multiple feed lines which must be very precise in length with respect to each other for the circular polarisation etc.
- Power constraints: The maximum allowed input power for the available polarisation switches in the amateur radio community is only specified as peak envelope power (PEP). The available switches at the institute can survive up to *600 W* PEP. However, during nominal operations of BRITE-Austria, the output power used will be continuous. Tests have shown that the switch cannot sustain more than *150 W* continuous power. Therefore it was decided to stick to a fixed circular polarisation mode, generated by phased lines from a power splitter (maximum RF power: *2 kW*) to the antenna dipole inputs rather than use the limited power available when using the polarisation switch.
- Power amplifier: In the initial configuration a power amplifier with a maximum output power of about *280 W* was used. It was replaced by the more powerful amplifier because of the fact that there is substantial background noise over Europe which interferes with the satellite's receiver (shown by measurements with comparable spacecraft). With the new amplifier, up to *500 W* RF power is available, providing substantial power margins for operations. The former power amplifier is still available at the ground station as backup option for redundancy purposes.
- TX cable from control room to the roof: The original cable for the uplink (RG213) introduced an attenuation of $> 3\ dB$ in the uplink path, which means that half of the TX power was dissipated on its way to the roof. Therefore, it was replaced by a ECOFLEX 15 cable with an attenuation of *1.35 dB*.
- Antenna dipoles: the standard dipoles are designed for *200 W* (PEP) maximum RF output power, therefore, they were replaced with high power dipoles which can survive *800 W* (PEP) maximum each.

3.2.3 Ground Station Improvements and Outlook

According to the current ground station design, available resources, and the constraints presented in the previous section, the following upgrades of the ground station have been investigated in detail, and have finally been implemented:

- Upgrade of the power amplifier to 1kW: The new BEKO-550 power amplifier has the option to be upgraded to 1kW. This upgrade could be beneficial for having larger margins available in case of signal interference from ground.

- Installation of a second UHF crossed Yagi antenna to form an antenna group in the uplink. While a group of 4 antennas represents a complex effort as described in the previous section, the installation of a group of 2 antennas would be feasible on the available antenna tower. A second antenna would allow to distribute the output power and increase the uplink EIRP.
- Upgrade of the antenna rotators to improve the tracking performance.

Due to strong ground based interference in the UHF uplink starting from October 2013, significantly limiting the uplink performance for operating the BRITE-Austria spacecraft, the upgrade of the power amplifier and to a dual UHF configuration were performed in March 2014 as countermeasures. A detailed description of the UHF uplink interference along with measurement results are presented in Chapter 5.

3.2.3.1 Upgrade of the UHF Uplink to a Dual Antenna Configuration

The purpose of upgrading the UHF uplink configuration to a group of two antennas is to increase the EIRP by up to *3 dB* as well as allowing to distribute the transmit power among the two antennas. In this configuration, the ground station could be operated with up to *1 kW* uplink power instead of the currently available *500 W*, providing an additional uplink margin of *+3 dB*. In combination, the available EIRP would therefore ideally be increased by *+6 dB*.

The optimal spacing distance A between two crossed Yagi antennas can be calculated according to Equation 3.3 [37]:

$$A = \frac{\lambda}{2 \cdot sin(\frac{\alpha}{2})} \tag{3.3}$$

where λ denotes the frequency used, and α the half beamwidth angle of the antenna in the spacing plane. For the Graz ground station configuration, this yields an optimal spacing distance of *1.41 m*. This distance between the antennas represent a challenge in accommodating both on the same tower with the S-band antenna. Different options have been investigated and are presented in the following paragraphs.

Figure 3.21 shows a possible configuration of two UHF crossed Yagi antennas on opposite faces with respect to the S-band antenna. The minimum suitable distance between the antennas in this configuration would be *540 cm*, in order to allow the minimum spacing between each UHF antenna and the S-band antenna required to avoid obstruction of the antenna pattern. The main drawback of this approach is that the two antennas would be mounted on opposing sides with the S-band antenna in between, thus distorting the combined antenna pattern of the antenna group. The impact of the S-band antenna to the UHF pattern and overall performance of the two UHF antennas would require further investigation. In addition, the spacing would be much larger than the optimal distance, leading to a reduction or even loss of the combined antenna gain.

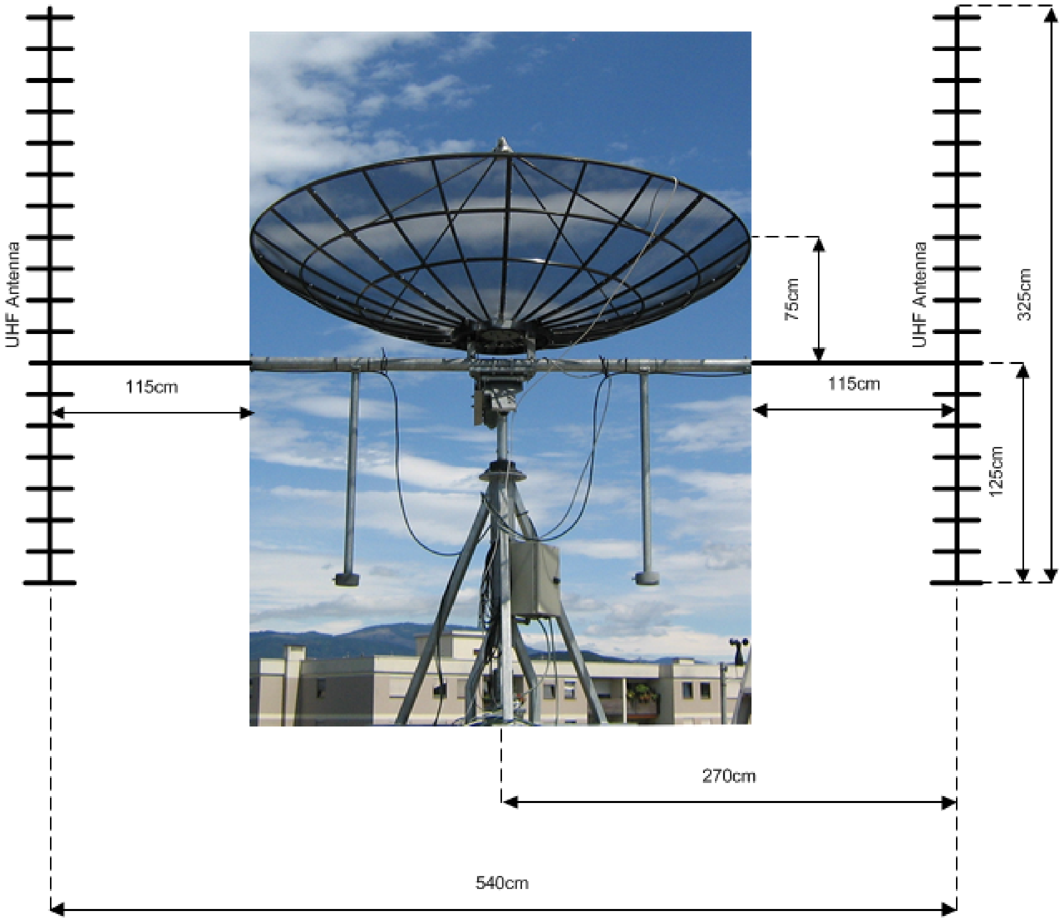

Figure 3.21: UHF antenna spacing with two antennas on opposite sides of the S-band antenna. The minimum spacing of each antenna with respect to the S-band antenna is *115 cm* to prevent obstruction of the UHF radiation pattern. This yields a total spacing distance of the two UHF antenna of *540 cm* relative to each other, which is not optimal for achieving a combined radiation characteristic. In addition, the S-band antenna in between would further distort the UHF radiation pattern of the two antennas.

Therefore, an alternative setup has been considered, with two UHF crossed Yagi antennas vertically spaced on the same side with respect to the S-band antenna, as shown in Figure 3.22. In this configuration the antennas are mounted on a rod transverse to the main rod. As the minimum distance between the S-band antenna and each UHF antenna needs to be *115 cm* to avoid obstruction of the main antenna lobe, in this configuration the main mounting rod length can be reduced to *90 cm* reducing the mechanical stress during tracking. In addition, considering the combined directivity of the two antennas leading to an increase in the transmit gain and hence, to a reduction of the half power beamwidth angle, this distance could be further reduced.

The advantage of this approach is the feasibility of the optimal spacing distance between the antennas, as well as the optimal directivity since there is less influence/distortion by the S-band antenna compared to the configuration shown in Figure 3.21. The main drawbacks are the mechanical construction, requiring substantial counterbalance on the opposite face of the S-band antenna, as well as the increased wind load. Luckily, Graz is not subject to frequent and heavy wind loads, so this approach was considered feasible.

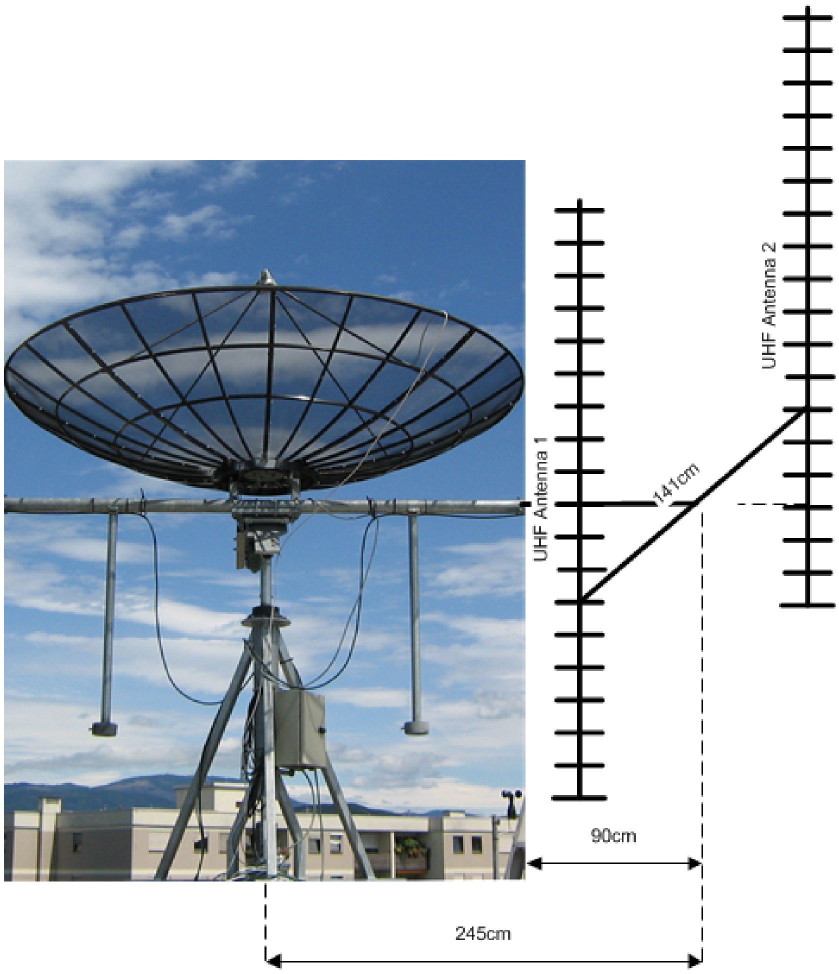

Figure 3.22: UHF antenna spacing with two antennas on one side with respect to the S-band antenna. This configuration ensures the optimal spacing between the antennas (*141 cm*) to achieve a combined group antenna characteristic with up to *3 dB* more gain.

In March 2014, the upgrade of the Graz ground station by a second UHF uplink antenna, identical to the one already installed crossed Yagi antenna, has been successfully performed in the second presented configuration and is shown in Figure 3.23. The uplink performance in this configuration and a comparison with the single antenna performance have been carried out by measurements with the BRITE-Austria spacecraft during operations. The results are presented in Chapter 5.

In addition, in the same time frame the BEKO HLV-550 UHF power amplifier has been upgraded to *1 kW*, providing an additional uplink margin of *+3 dB* to the ground station.

The maximum available EIRP of the Graz ground station after the upgrade is now *43 dBW*.

Figure 3.23: Graz ground station antenna tower after upgrade to two UHF transmit antennas. The UHF antenna group on the same side with respect to the S-band antenna provides an increase of the EIRP of about *+3 dB*.

3.2.3.2 Upgrade of the Antenna Rotators

The original rotators used at the Graz ground station specify a precision of $\pm 3°$ (for each individual rotator). As a result, pointing offsets of a few degrees will occur while tracking the spacecraft. While these offsets are almost negligible for the uplink performance (the half power beamwidth of the UHF transmitting antenna is $28°$), the offsets limit the downlink performance, as the half power beamwidth of the S-band receiving antenna is only $3.13°$.

While the applied countermeasures described in detail in Chapter 4 (offset definitions in the tracking software as well as S-band antenna feed re-alignment to increase the half power beamwidth) represented an effective way to improve the tracking performance, it was decided to upgrade the antenna rotators to a configuration that provides better tracking precision.

The new selected rotators are from *M2 Antenna Systems* and provide the following key features:

- Pointing precision of down to $0.1°$ (in both azimuth and elevation)
- Typical tracking precision of about $0.5°$ to $1°$.
- Rotator controller compatible with the tracking software used for operations
- Autocalibration of the rotators supported by the tracking software used for operations

The upgrade to the new rotators was performed in January 2015. Figure 3.24 shows the Graz ground station antenna tower after upgrade of the rotators. The new rotators have improved the tracking performance considerably, avoiding the need to apply rotator offset corrections for optimization. In addition, the nominal S-band feed alignment could be applied, ensuring the maximum available G/T.

An additional improvement is the autocalibration functionality supported by the tracking software. The new rotators are calibrated automatically before every pass, which increases reliability and avoids degradation of the tracking performance by misalignments.

Figure 3.24: Graz ground station antenna tower after upgrade of the rotators. The new rotators provide a tracking precision of about $0.5°$ to $1°$.

Chapter 4

Ground Station System Performance Evaluation

For assessing the performance of the established BRITE-Austria ground station in Graz, several measurements and simulations were carried out. The purpose of these measurements was to characterise the performance of the ground station at both component and system level. In addition, the obtained measurement results were used as inputs for further calculations and simulations of the overall ground station performance to predict its behaviour during nominal operations.

At component level, the measurements were carried out at the ground station antennas and the correspondent RF components, mainly focusing on the downlink chain (antenna patterns, system noise temperature, gain and figure of merit, noise signal interference). At system level, measurements with in-orbit spacecraft comparable to BRITE-Austria were carried out for both the up- and the downlink.

Link budget calculations for both uplink and downlink were performed to verify that sufficient margins are available. In this respect, the preliminary calculated budgets were refined by taking into consideration the measured values of the spacecraft and ground station components. Further, simulations for modelling the overall ground station performance were carried out including the measured values. These values include:

- The system noise temperature as a function of elevation angles
- The pointing loss due to tracking lag of the rotators
- The antenna patterns for the uplink and downlink antennas
- Atmospheric condition effects

The developed simulation tools allow to predicting the performance of the ground station for selected contacts with the satellite and to carry out comparisons between simulated and measured values collected during real contacts with the satellite. Therefore, these simulations can be used for long-term prediction of the link performance with respect to available data rates and data download volumes.

4.1 Antenna Measurements

The antenna usually provides the best amplification in a communication chain. Therefore, several measurements of the Graz ground station antennas have been carried out to assess their performance. The focus was laid on the S-band antenna used for the BRITE-Austria downlink. The measurements included:

- Antenna patterns of both the uplink and the downlink antennas
- System noise temperature as a function of elevation angles and atmospheric conditions for the S-band antenna
- Figure of merit (G/T) and gain of the S-band antenna
- Relevant neighbouring interference sources which have an impact on the S-band receive chain and determination of the S-band radio horizon

4.1.1 S-band and UHF Antenna Patterns

For both the UHF uplink and S-band downlink antennas used in the ground station the respective patterns were measured. The purpose of these measurements was to verify the antenna radiation characteristics and to obtain the respective diagrams of the patterns, which were used as part of the required documentation in the frequency coordination process.

For the S-band antenna, measurements of the radiation characteristics were needed as the antenna was customised, and hence no pattern from the manufacturer was available. For the UHF antenna, an antenna pattern from the manufacturer was available. Nevertheless, a measurement of the UHF antenna pattern was performed to verify the provided figures as well as to take into account potential effects from the environment, in particular the influence in the radiation characteristics by the S-band antenna mounted on the same tower.

The antenna patterns of the *3 m* S-band receiving antenna as well as of the UHF crossed-Yagi transmitting antenna were measured on a test path of *2.7 km* line of sight between the antenna tower on the roof of the TU Graz/IKS building and the Lustbühel observatory.

For measuring the S-band antenna pattern, a calibrated transmitter with an omnidirectional patch antenna attached was installed at the observatory. The transmitter was operated at constant RF output power of *0 dBm (1 mW)*, while varying the orientation of the S-band antenna on the TU Graz/IKS building in both azimuth and elevation, respectively. The received RF signal level was measured at the ground station control room with a spectrum analyser and recorded for every set position of the antenna, resulting in two antenna diagrams of the S-band antenna, an azimuth pattern and elevation pattern (both shown in Figure 4.1), respectively.

For the UHF crossed-Yagi antenna, a different setup on the same test path between TU Graz/IKS and the Lustbühel observatory was used. The UHF output signal involving the whole communication chain was

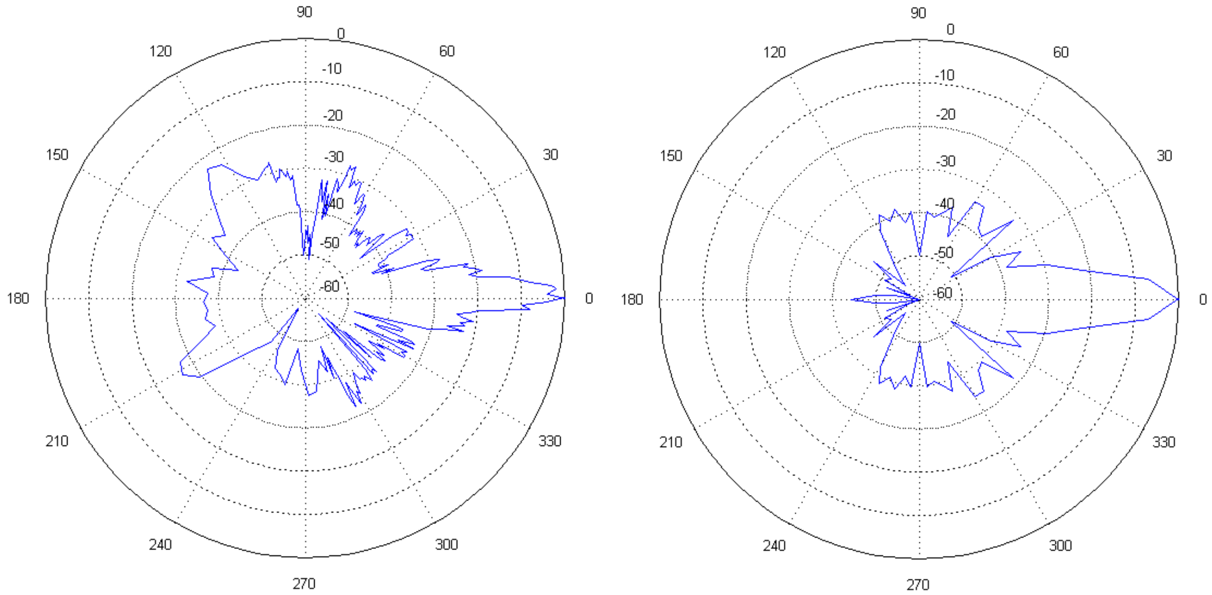

Figure 4.1: S-band antenna azimuth and elevation pattern. The azimuth pattern is shown on the left, while the elevation pattern is shown on the right. The patterns were recorded by measuring the received signal level at the antenna from a fixed transmitter location while moving the antenna in its azimuth. The pattern shows a narrow half power beamwidth of the antenna (around *3-3.5 dB*) as expected.

fed into the UHF transmitting antenna of the ground station. At the observatory the received signal power was measured with a spectrum analyser connected to a calibrated antenna with known characteristics. Due to the short distance of the test path, the output power was reduced to a suitable level for the receiving antenna.

At the ground station, a continuous output signal was generated by setting the data pattern of the TNC to an idle state (all 1's). This baseband signal was modulated by the TNC (GMSK), subsequently up-converted to the nominal UHF transmitting frequency and preamplified to *5 W* RF power by the UHF transceiver, and finally amplified to approximately *100 W* RF output power by the high power amplifier and fed into the transmitting antenna.

At the observatory, a calibrated antenna with linear polarisation was used. Since the incoming signal from the UHF antenna is circular polarised, two measurements were recorded for the received signal power at each azimuth/elevation position: one with vertical and one with horizontal polarisation. In addition, to observe the circular polarisation characteristic, additional measurements were collected by rotating the receiving antenna by 45°. The received signal power was measured with a spectrum analyser in channel power measurement mode.

Figure 4.2 and 4.3 show the measured horizontal and vertical antenna patterns for the UHF crossed-Yagi antenna. Concerning the azimuth patterns, the received vertical polarised pattern shows rather large side-lobes of relatively high signal power when moving the antenna towards left with respect to the receiver. A possible explanation for this behaviour is the influence of the S-band antenna co-located with the UHF antenna on the same tower, distorting the pattern in the direction where the UHF antenna is obstructed by the S-band antenna. For the azimuth pattern measured with receiving horizontal polarisation, this effect can only partly be recognised. In contrast, the elevation patterns are less affected by this behaviour.

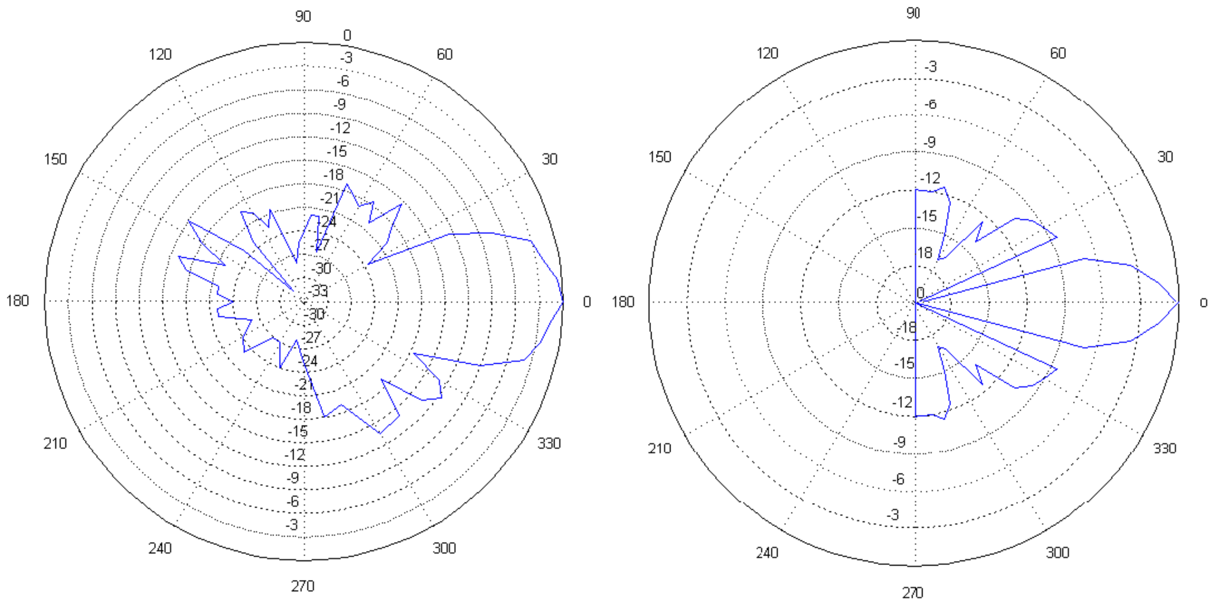

Figure 4.2: UHF antenna horizontal azimuth and elevation pattern. The azimuth pattern is shown on the left, while the elevation pattern is shown on the right. The patterns were recorded by measuring the received signal level with a calibrated antenna at a fixed receiving location with horizontal polarisation while moving the UHF TX antenna in its azimuth.

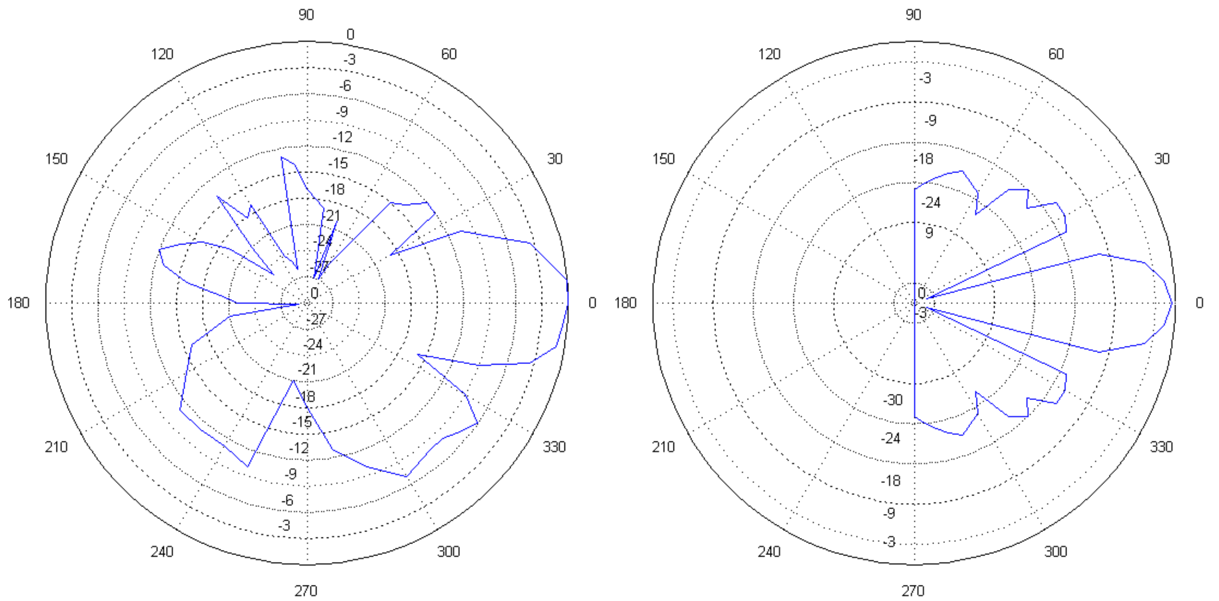

Figure 4.3: UHF antenna vertical azimuth and pattern. The azimuth pattern is shown on the left, while the elevation pattern is shown on the right. The patterns were recorded by measuring the received signal level with a calibrated antenna at a fixed receiving location with vertical polarisation while moving the UHF TX antenna in its azimuth.

4.1.2 System Noise Temperature Measurements

The system noise temperature is a measure for the noise contribution of all elements along a communications chain, including both sky noise and noise of the microwave components involved. The main noise contribution in this respect is thermal noise. Rather than the physical temperature, thermal noise expresses the noise power generated by thermal movement of electrons in passive elements, e.g. resistors [38]. The noise power N is defined by the Nyquist Equation (4.1) [38], and is dependent on the Boltzmann constant k, the equivalent noise temperature of the source T, and the noise bandwidth B:

$$N = k \cdot T \cdot B \tag{4.1}$$

A measure for the noise power which affects (degrades) the signal to noise ratio (SNR) is the noise figure F. For better characterisation, instead of the noise figure the equivalent noise temperature T is typically used. The noise figure F is the noise power of a microwave component at room temperature $T_0 = 290K$. The relation between noise figure and noise temperature is shown in equation (4.2) [39].

$$T = (F - 1) \cdot T_0 \tag{4.2}$$

The system noise temperature is the sum of the receiving antenna noise temperature and the noise temperature of the microwave components up to the receiver. It can be calculated by the *Friis* formula as shown in equation (4.3) [39].

$$T_{sys} = T_{ant} + T_1 + \frac{T_2}{G_1} + \frac{T_3}{G_1 \cdot G_2} + \cdots + \frac{T_n}{G_1 \cdot G_2 \cdots G_{n-1}} \tag{4.3}$$

The antenna noise temperature T_{ant} depends on the atmospheric absorption due to rain/gaseous attenuation A, the physical temperature of the rain medium T_m, as well as the cold sky temperature T_c, and can be calculated according to equation (4.4) [40].

$$T_{ant} = T_m \cdot (1 - 10^{\frac{-A}{10}}) + T_c \cdot 10^{\frac{-A}{10}} \tag{4.4}$$

Based on the presented equations, calculations of the system noise temperature for the Graz ground station S-band downlink chain were performed.

The antenna temperature T_{ant} was calculated according to Equation (4.4). In this equation, A denotes the total rain and gaseous attenuation absorption, T_m is the rain medium temperature and T_c is the cold sky temperature. According to [41], the values of T_m vary between *275 K* and *290 K*, while the values for T_c range from *3 K* to *10 K*.

Taking into account the maximum values for the rain medium temperature $T_m = 290$ *K* and cold sky temperature $T_c = 10$ *K* as described in [42], and assuming a gaseous attenuation value of $A = 1$ *dB* for S-band [43], the result for the S-band antenna temperature is *67.6 K*.

For the rest of the system, the total noise figure was calculated and the correspondent noise temperature was derived accordingly. Figure 4.4 shows the components with their noise figures and losses for the S-band downlink chain. The main contribution to the system noise temperature comes from the low noise amplifier (LNA), as it represents the first element in the downlink chain. To minimise the system noise temperature, an LNA with a low noise figure (*0.5 dB*) was selected and mounted right after the receiving patched antenna feed. This way, according to the *Friis* equation (4.3), the noise contribution of the subsequent elements in the downlink chain become negligible due to the high gain of the LNA (*31 dB*).

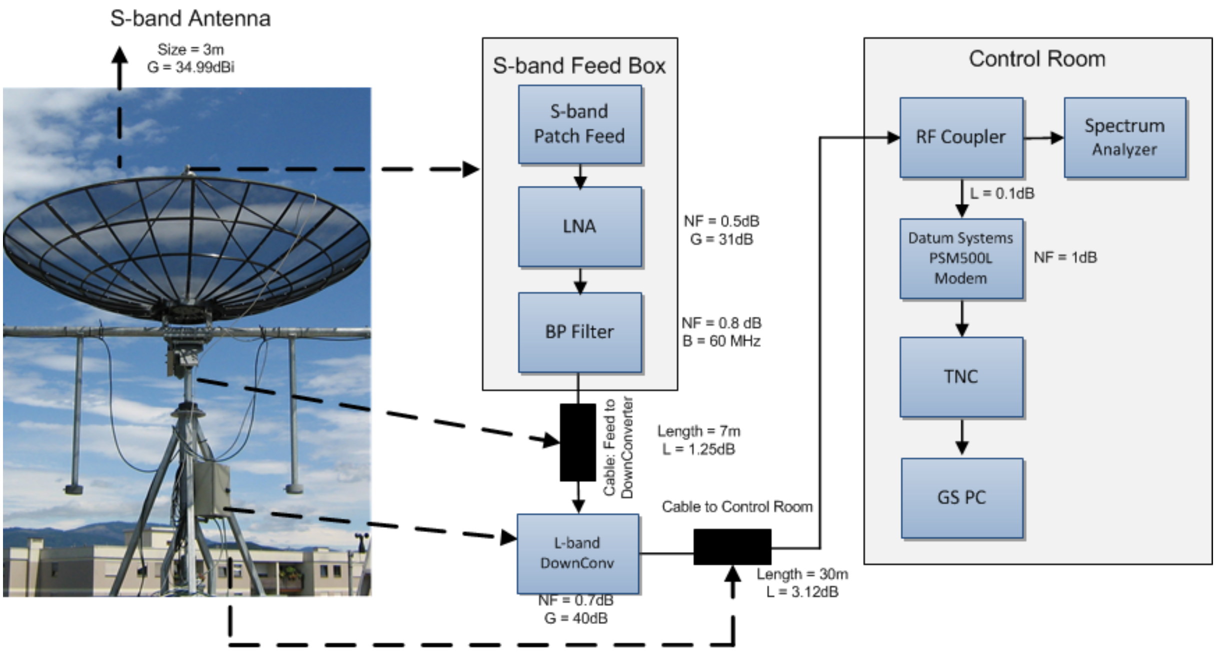

Figure 4.4: S-band downlink chain noise figures and losses. The main noise contribution for the system noise temperature comes from the LNA noise figure. A low noise LNA was chosen therefore to minimise the system noise temperature.

Table 4.1 lists the noise figures and losses of the individual components that have been used for the system noise temperature calculation.

Item	Gain [dB]	Noise Figure / Loss [dB]
Low Noise Amplifier (LNA)	31	0.5
Cable LNA to Bandpass Filter		0.5
Bandpass Filter		0.8
Cable Feed to Downconverter		1.25
L-band Downconverter	40	0.7
Cable to Control Room		3.12

Table 4.1: Gains and noise figures of the downlink system components. The contribution of the noise figures of the elements after the LNA are of little importance to the system noise temperature thanks to the high gain of the LNA.

The corresponding noise temperatures in K calculated with Equation (4.2) are shown in Table 4.2. The used value for the room temperature in the calculations was $T_0 = 290$ *K*.

Item	Noise Temperature [K]
S-band Antenna Temperature	67.6
Low Noise Amplifier (LNA)	31.7
Cable LNA to Bandpass Filter	35.4
Bandpass Filter	58.7
Cable Feed to Downconverter	96.7
L-band Downconverter	50.7
Cable to Control Room	304.8

Table 4.2: Equivalent noise temperature for the noise figures of the downlink system components. This shows once more why it is important to have the LNA directly attached to the antenna feed.

According to Equation (4.3), the system noise temperature for the Graz ground station results in:

$$T_{sys} = T_{ant} + T_{LNA} + \frac{T_{Filter}}{G_{LNA}} + \frac{T_{FeedCable}}{G_{LNA}} + \frac{T_{DownConv}}{G_{LNA}} + \frac{T_{ControlRoomCable}}{G_{LNA} \cdot G_{DownConv}} = 115.9K = 20.6dBK \tag{4.5}$$

The system noise temperature of the Graz ground station at zenith for clear sky conditions is therefore *115.9 K* or, in logarithmic representation, *20.6 dBK*.

The system noise temperature T_{sys} further depends on the elevation angles and on different atmospheric conditions. Quantitative measures of the latter are expressed in cumulative distributions (CD), for which according to [44] the most common CDs can be expressed as follows:

- CD = 0.00 clear dry, lowest weather effect
- CD = 0.25 average clear weather
- CD = 0.50 clear humid, or very light clouds
- CD = 0.90 very cloudy, no rain
- CD = 0.95 very cloudy, with rain

Therefore, a characterisation of the system noise temperature dependence on the antenna elevation and different atmospheric conditions was performed.

This characterisation is based on measurements of the received noise power and the calculation of relative offsets to determine the equivalent noise temperature. A spectrum analyser with a root mean square

(RMS) detector was used as receiver, and by own developed software several measurements of the received noise power were performed for each antenna position (in $3°$ steps). The measurements for each position were averaged and the resulting values were normalised to the minimum received noise power value (measured value at zenith) to obtain the relative offset (in dB) from the ideal value at zenith for each antenna position. These values were then added to the calculated system noise temperature for the S-band downlink chain of *115.9 K* according to Equation (4.5) to determine its dependence on different elevation angles.

The measurements were repeated for different atmospheric conditions for comparison and to obtain a more complete characterisation of the ground stations receiving system noise temperature. The following four atmospheric conditions were investigated:

- Clear sky
- Light clouds
- Rain
- Snow

Figure 4.5 shows the S-band antenna noise temperature as a function of elevation for the described weather conditions, while Figure 4.6 shows the corresponding system noise temperature.

The results show that, at the S-band downlink frequency used to operate BRITE-Austria, the considered atmospheric conditions have little impact on the system noise temperature (< 10 *K* between extremes). By contrast, the dependence on the antenna temperature and as a result, of the system noise temperature, from different antenna elevation angles have a significant impact. This can be recognised especially at elevations below 6 degrees due to the thermal noise picked up by the antenna from ground.

4.1.3 Sun Noise Measurements and Figure of Merit Calculation

A qualitative measure for the receiving communications chain is given by the figure of merit G/T, describing the ratio between the receiving antenna gain and the system noise temperature [38]. While the figure of merit of the S-band downlink of the Graz ground station has been calculated according to an assumed S-band antenna gain of *34.99 dBi* as described in Section 4.1.4 and the system noise temperature of *20.6 dBK* as determined in Section 4.1.2, measurements have been performed for comparison and confirmation.

Therefore, in order to determine the figure of merit G/T of the ground stations S-band downlink chain, an Y-factor method (also known as Hot/Cold method) measurement of the sun noise vs. the cold sky was performed. By knowing the solar flux density at the day of the measurement, the difference between the two measurements can be used to calculate the G/T of the station. The measurements and calculations were performed according to the procedure and equations described in [45] and [46], and reported hereafter.

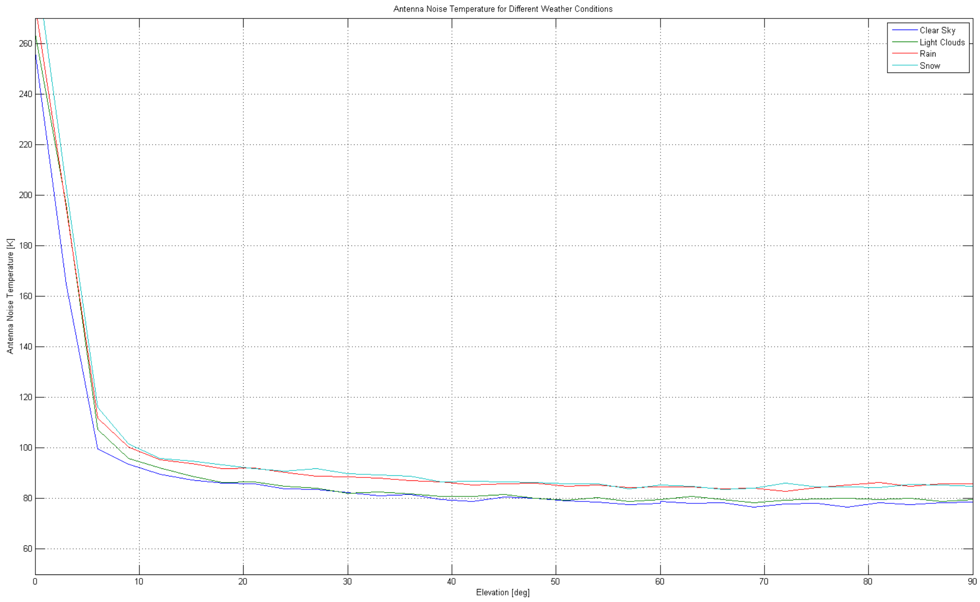

Figure 4.5: Antenna noise temperature vs. elevation. Antenna noise temperature vs. elevation of the Graz ground station S-band antenna for different weather conditions. It can be seen that the considered weather conditions have little impact on the system noise temperature, while the dependence of the antenna temperature on elevation angles due to thermal ground noise has a significant impact, particularly at low elevations below 6 degrees.

The Y-factor method is based on the measurement of the noise power of two noise sources at two different temperatures, the hot temperature and the cold temperature for the device under test (DUT). The Y-factor is defined as the relation between the two noise powers (4.6).

$$Y = \frac{P_{hot}}{P_{cold}} \tag{4.6}$$

For the hot temperature, the sun noise power was measured, while for the cold temperature the cold sky noise power was measured. Therefore, Equation (4.6) can be rewritten as (4.7).

$$Y = \frac{P_{sun}}{P_{coldsky}} \tag{4.7}$$

Under consideration of the noise power according to Equation (4.1) as presented in Section 4.1.2, the received noise power for the cold sky measurement can be defined as the power generated by the receiving system itself (4.8), where T_S denotes the system noise temperature.

$$P_{coldsky} = k \cdot T_S \cdot B \tag{4.8}$$

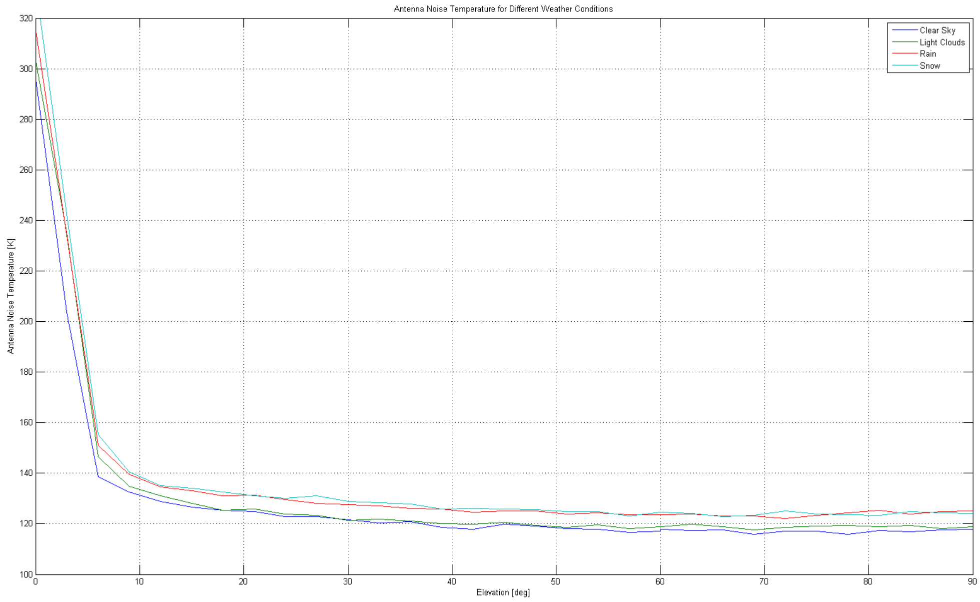

Figure 4.6: System noise temperature vs. elevation. System noise temperature vs. elevation of the Graz ground station S-band antenna for different weather conditions. Compared to the antenna noise temperature, the system noise temperature increases by the noise temperature of the RF components.

When pointed towards the Sun, the received noise power is increased by the solar radiation (4.9):

$$P_{sun} = k \cdot T_S \cdot B \cdot \frac{F_{sun}}{2} \cdot A_e \cdot B \cdot L_B \tag{4.9}$$

where F_{sun} is the solar flux density at the measured frequency, B is the measurement bandwidth, A_e is the effective antenna area (4.10), and L_B is the beamsize correction factor (4.11). Further, the solar flux density is divided by 2 to encounter the single polarisation state of the receiver as the solar radiation is randomly polarised.

$$A_e = \frac{G \cdot \lambda^2}{4 \cdot \pi} \tag{4.10}$$

$$L = 1 + 0.38(\frac{\Theta_{sun}^2}{\Theta_A}) \tag{4.11}$$

Θ_{sun} denotes the diameter of the radio Sun at the receiving frequency, while Θ_A denotes the 3 dB antenna bandwidth at the receiving frequency. Under consideration of the solar radiation, Equation 4.7 can be rewritten as (4.12):

$$Y = \frac{P_{sun}}{P_{coldsky}} = \frac{k \cdot T_S \cdot B \cdot \frac{F_{sun}}{2} \cdot A_e \cdot B \cdot L}{k \cdot T_S \cdot B} \tag{4.12}$$

Finally, by substituting the antenna area A_e with the equivalent term in Equation 4.10, Equation 4.12 can be rewritten for calculating the G/T (4.13):

$$\frac{G}{T_S} = \frac{8 \cdot \pi \cdot k}{F_{sun} \cdot L \cdot \lambda^2} \cdot (Y - 1) \tag{4.13}$$

The value of the solar flux density at the respective day of the measurement was taken from the recordings of the Australian Space Weather Agency at Learmonth Observatory [47]. As the recordings are only present for standard frequencies, the value for the measuring S-band frequency was obtained by interpolation.

Figure 4.7 shows the measured spectrum for the sun noise compared with the measured spectrum of the cold sky for a measurement on August 23rd 2012. Both measurements were performed in the control room at the input of the receiver, thus including all components in the S-band downlink chain.

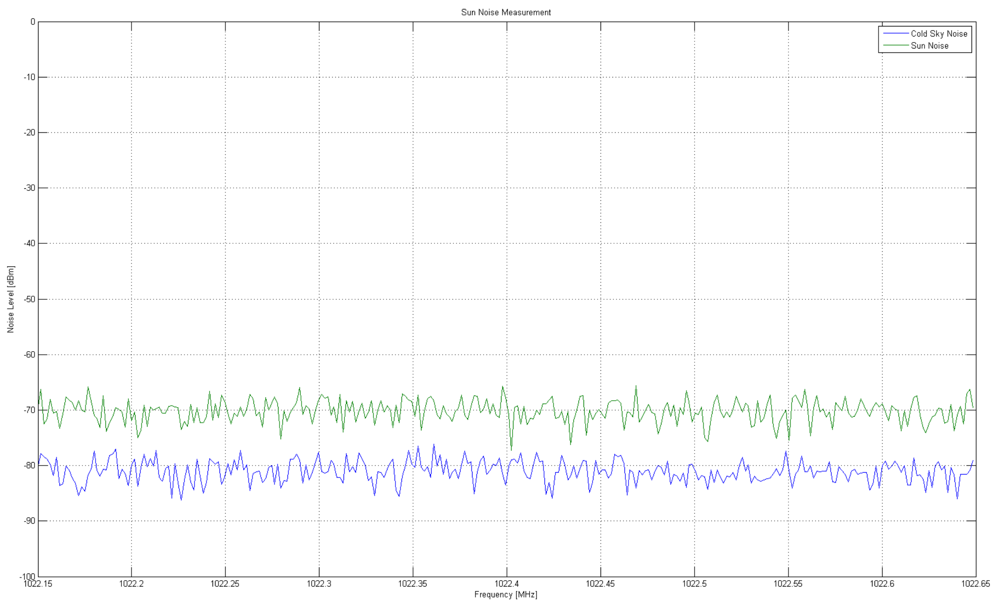

Figure 4.7: Sun noise vs. cold sky noise spectrum. The measurement has been performed on August 23rd 2012. A difference of 12 *dB* was measured.

Table 4.3 shows the measurement results for a representative sun noise measurement performed on August 23rd 2012, listing the Y-factor measurement result, the solar flux density on the measured day, and the resulting G/T. For determining the G/T of the ground station, several measurements were performed, and the results were essentially in agreement.

Parameter	Value
Y	12.34
Y [dB]	10.93
Solar flux density for RX frequency (interpolated)	88.84
G/T	24.68
G/T [dB]	13.92

Table 4.3: Sun noise measurement results. The measurement was performed on August 23rd, 2012. The results show that the measured G/T value matches quite well with the calculated result of *14.35 dB*.

The measurement results were finally averaged to obtain the G/T value of the ground station. The measurement result for the figure of merit (G/T) of the Graz ground station S-band antenna (mean value for several measurements performed) is *14 dB*. A comparison with the calculated G/T result of *14.35 dB* as described in the link budget calculations in Section 4.2 shows that the difference is only *0.35 dB*, showing that the performed Y-Factor measurement method is relatively accurate.

4.1.4 Antenna Gain and Efficiency Measurements

The antenna gain is a crucial parameter for assessing the antenna performance. Since the S-band parabolic meshed antenna is a modified C-band antenna with a customised S-band feed, a value for the gain of the modified antenna was not available from the manufacturer. Although an estimation of the antenna gain has been performed, resulting in a value of *34.99 dBi* based on an assumed antenna efficiency of 0.64, for better characterisation it was decided to validate this estimation by a measurement.

The S-band antenna gain was determined by carrying out two simultaneous measurements with a calibrated transmitter at the Lustbühel observatory and measuring the received RF signal power at the ground station with

- The S-band ground station antenna
- A calibrated S-band antenna with known characteristics

The measurement setup with the two antennas on the roof of TU Graz/IKS is shown in Figure 4.8.

With these two measurements, the antenna gain of the ground station antenna can be derived from the received power flux density described in Equation (4.14):

$$\Phi_{RX} = \frac{P_{RX} \cdot G_{RX}}{4 \cdot \Pi \cdot D^2} \tag{4.14}$$

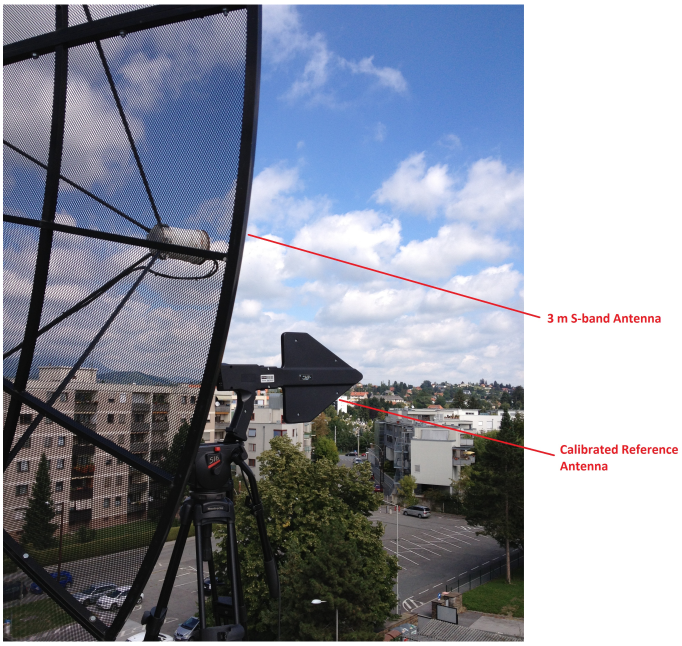

Figure 4.8: S-band antenna gain measurement setup. A simultaneous measurement of the received signal from a calibrated transmitter with the S-band downlink antenna and a calibrated measurement antenna were recorded and used to determine the S-band antenna gain from the received power flux density.

The known values for the reference antenna were the antenna gain and the antenna factor available from the data sheet for the receiving S-band frequency. The calculation of the power flux density and the antenna area D had to be determined via the electromagnetic field strength E_{Ref}(at 377 Ω, corresponding to the impedance of free space) (4.15), which in turn was calculated according to the equivalent voltage level U_{Ref} (at 50 Ω) for the measured RF-power of the reference antenna as well as the antenna factor AF_{Ref} (4.16) [48].

$$\Phi_{Ref} = \frac{E_{Ref}^2}{377} \tag{4.15}$$

$$E_{Ref} = U_{Ref} \cdot AF_{Ref} \tag{4.16}$$

From the knowledge of the calibrated antenna area, gain, and measured signal power, the power flux density of the reference antenna was calculated. As the power flux density at one particular receiving point is constant, by the knowledge of the antenna area and the measured received signal power of the ground station antenna, the gain of the ground station antenna was calculated according to Equation (4.17).

$$G_{RX} = \frac{P_{Ref} \cdot D_{RX}^2 \cdot G_{Ref}}{P_{RX} \cdot D_{Ref}^2} \tag{4.17}$$

According to the calculated antenna gain, the antenna efficiency η could further be determined (4.18):

$$\eta = \frac{G_{RX} \cdot \lambda^2}{\Pi^2 \cdot D^2} \tag{4.18}$$

The resulting measured values for the S-band antenna gain and efficiency are:

- S-band receiving antenna gain: *35.5 dBi*
- S-band receiving antenna efficiency: 0.72

The results show that there is half a decibel difference between the calculated gain value of *34.99 dBi* for the antenna, based on an assumed efficiency of 0.64, and the measured value of *35.5 dBi*. This difference can be explained by a combination of measurement uncertainties and possible distortions due to the short distance and possible atypical propagation effects due to low elevations / obstacles on the measured link path.

4.1.4.1 Gain Reduction due to Pointing Errors

Since the rotator precision of the Graz ground station is limited to $\pm 3°$ for each rotator, pointing offsets of a few degrees will occur while tracking the spacecraft. While these offsets are almost negligible for the uplink performance, since the half power beamwidth of the UHF transmitting antenna is $28°$, they limit the downlink performance, as the half power beamwidth of the S-band receiving antenna is only $3.13°$, thus reducing the receiving antenna gain.

To better characterise the above stated behaviour, the gain reduction vs. pointing errors has been calculated according to Equation (4.19) as described in [49].

$$\Delta G(\Theta)_{[dB]} = 10 \cdot log \cdot (e^{\frac{2.773 \cdot \Theta^2}{HPBW^2}}) \tag{4.19}$$

In this equation, Θ denotes the pointing error in degrees, while $HPBW$ denotes the half power beamwidth in degrees. Figure 4.9 shows the gain reduction vs. pointing errors for the S-band and UHF antennas of the Graz ground station. The figure shows that in the worst case of a rotators pointing offset of $4.2°$ the S-band antenna gain is reduced by *49.9 dB*, while the UHF antenna gain is only reduced by *0.6 dB*.

As countermeasure the definition of rotator offsets is applied during operations. The tracking software has been upgraded accordingly to define rotator offsets for both azimuth and elevation rotators in all directions. By a definition of an offset of $1°$, the maximum occurring pointing offset is limited to $2°$ degrees for each rotator, resulting in a maximum combined rotator offset of $2.8°$. However, in this worst case the S-band antenna gain is still reduced by *22.2 dB*.

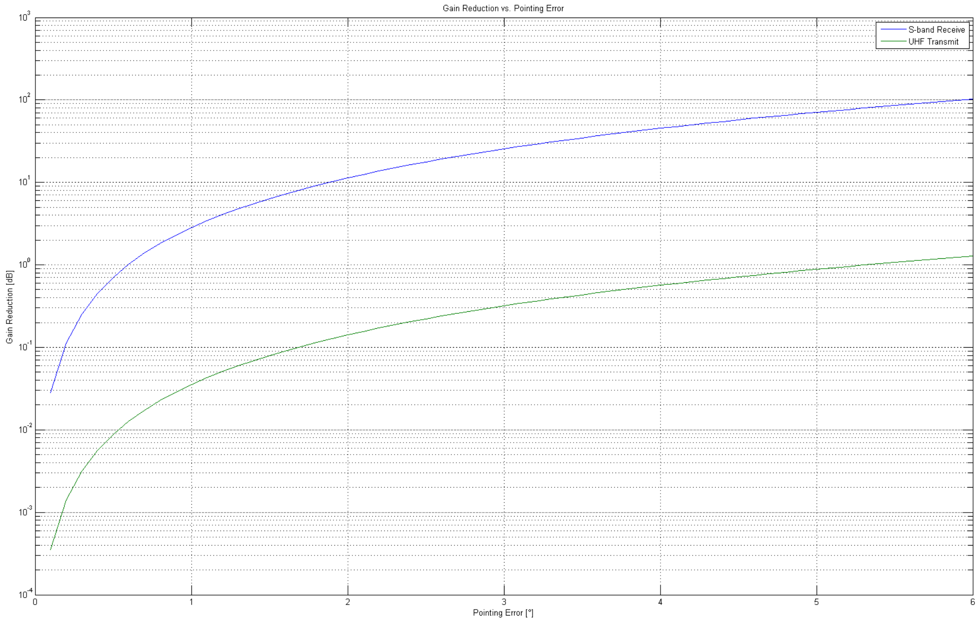

Figure 4.9: S-band and UHF antenna gain reduction vs. pointing offsets. By applying pointing offsets in the tracking software, the maximum pointing offset could be reduced from 4.2° to 2.8°.

Therefore, as additional countermeasure to cope with the lack of precision of the rotators a re-alignment of the S-band feed was performed. The aim of this new alignment was the intentional defocusing of the feed to increase the half power beamwidth angle of the S-band antenna at the expense of a reduction of the antenna gain. For this re-alignment, the feed was moved for about *10 cm* closer towards the antenna. The effect of this modification and a comparison of the former configuration with optimal feed alignment in the focal point of the antenna is shown in Table 4.4. This approach was found reasonable, since a significant downlink margin of *10.88 dB* according to the link budget is still available.

	Optimal Feed Alignment	**New Feed Alignment**
Antenna Gain	35 dBi	32.5 dBi
Half Power Beamwidth	3.13 deg	4.17 deg
G/T	14.35 dB	11.85 dB
Available Downlink Margin	13.38 dB	10.88 dB

Table 4.4: S-band feed alignment comparison The optimal S-band feed alignment is compared with the new alignment configuration. Although around *2.5 dBi* gain is lost, the feed re-alignment increases the half power beamwidth angle by about 1°, allowing to effectively counteract the lack in tracking precision of the rotators and improve the overall downlink performance.

In terms of gain reduction, a comparison of the optimal alignment performance vs. the new alignment performance is shown in Figure 4.10. For the worst case rotator pointing offset of $4.2°$ (without rotator offset definition in the tracking software), the gain is reduced by *28.13 dB* instead of *49.9 dB* as in the old configuration. Furthermore, by applying the offset correction in the tracking software, the worst case pointing offset for the maximum of $2.8°$ leads to a gain reduction of *12.5 dB* rather than *22.2 dB* as for the optimal aligned feed. Hence, by the combined countermeasures of feed re-alignment and definition of an offset correction for the rotators in the tracking software, in the worst case an S-band antenna gain of about *20 dB* is still available.

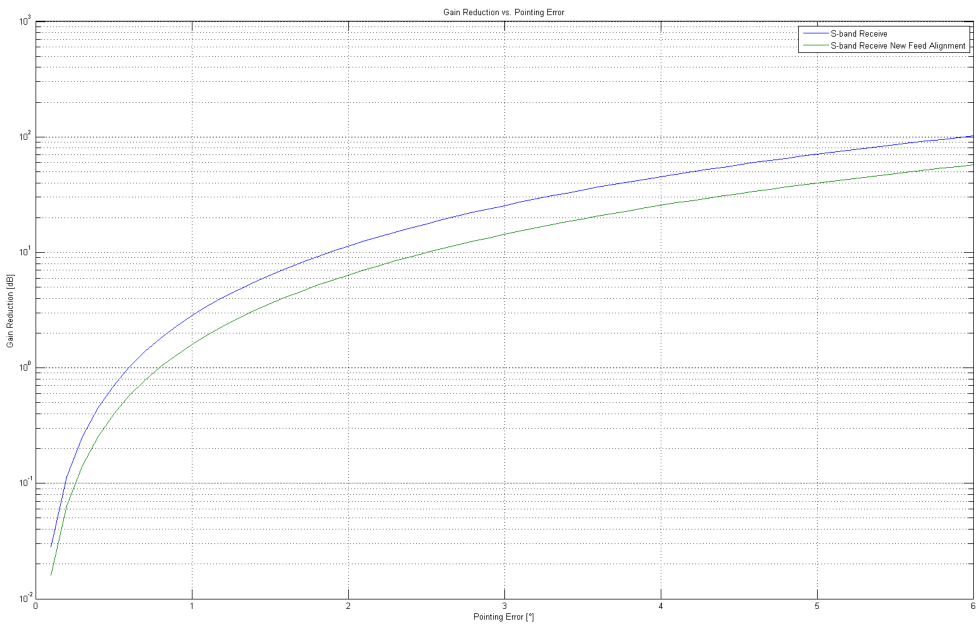

Figure 4.10: S-band antenna gain reduction vs. pointing offsets feed alignment comparison. For the reduced maximum pointing offset of $2.8°$ by the tracking software, with the new feed alignment the gain reduction leads to *12.5 dB* instead of *22.2 dB* as for the optimal aligned feed due to the larger half power beamwidth.

Despite the significant improvements achieved in the tracking performance by offset definition in the tracking software and re-alignment of the S-band feed, better tracking precision of the antenna rotators would be desirable. Therefore, an upgrade to antenna rotators with better tracking precision (about $0.5°$ to $1°$ in both azimuth and elevation) was carried out in January 2015. This upgrade has improved the tracking performance significantly and hence lowered the gain reduction. The gain reduction due to the worst case combined pointing error of the azimuth and elevation rotator ($1°$ worst case pointing error each, combined error $1.41°$) with the optimal aligned S-band feed is *5.6 dB*, which represents an improvement of *6.9 dB* compared to the best performance of the old rotators (tracking offsets and S-band feed re-alignment to increase the half power beamwidth).

4.1.4.2 S-band Feed Measurements

The S-band antenna feed consists of a patch antenna for the receiving S-band signal, which is connected to a low-noise amplifier (LNA) and bandpass filter for amplification and filtering of the received signal. These components are assembled together in an antenna feed box and mounted at the antenna's focal point.

To characterise the S-band feed, frequency sweep measurements of the entire feed box were performed in the anechoic chamber . The frequency sweep curve is shown in Figure 4.11, and illustrates the combined characteristics of the bandpass filter and low noise amplifier mounted in the feed box. The figure shows that the passband of the feed is about *50 MHz*.

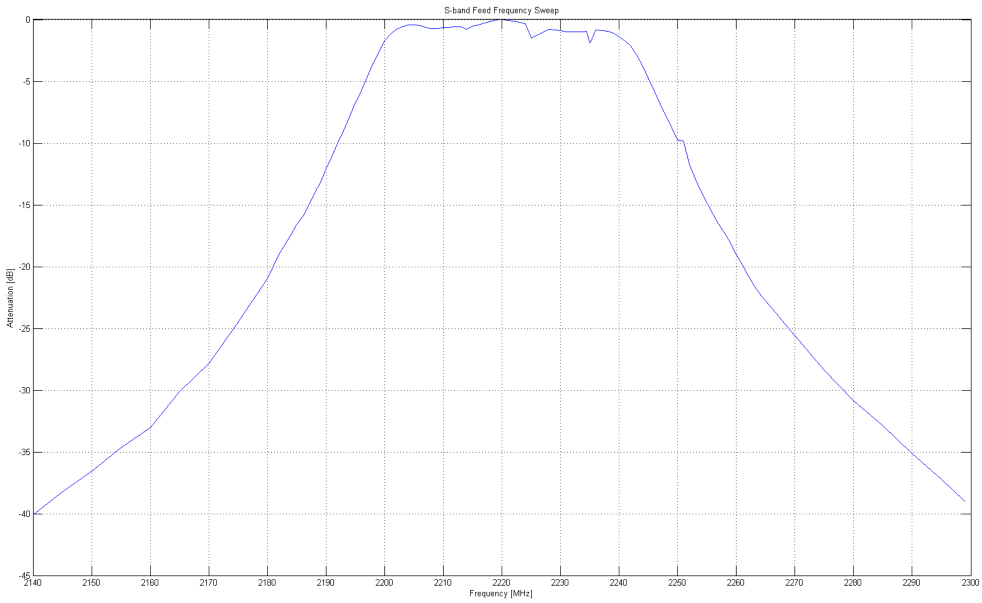

Figure 4.11: S-band feed characteristics. The measurement shows that the combined passband of the S-band feed, LNA and bandpass filter assembled in the feed box is about *50 MHz*.

In addition, the characteristic of the bandpass filter has been measured and is shown in Figure 4.12. The results show that the RX centre frequency denoted by *Marker 1* in the plot resides close to the upper passband end, which is a bit unfortunate since the UMTS spectrum ends at around *60 MHz* below the RX centre frequency and has significant influence in the S-band receive chain. Therefore, tuning of the bandpass filter (by adjustment of trimming screws) has been performed to improve the passband characteristic. The result of this re-tuning is shown in Figure 4.13. Compared to the previous configuration, it can be seen that the RX centre frequency has moved towards the centre of the filter's passband, and that the filter suppression at the UMTS spectrum bound of *2170 MHz* (*Marker 3*) has increased by from *27.9 dB* to *30.5 dB*.

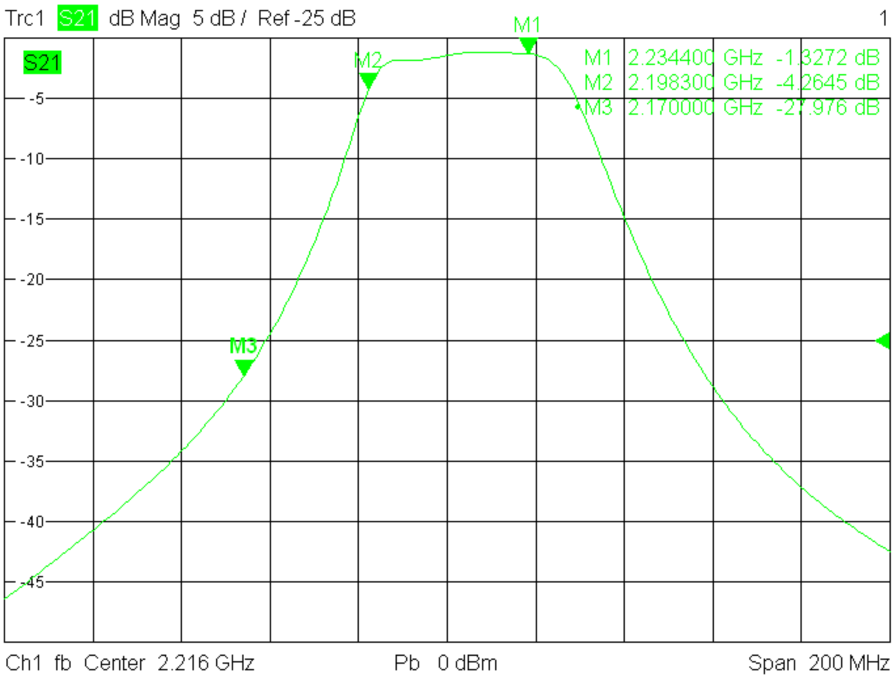

Figure 4.12: S-band bandpass filter characteristic. The measurement shows that the insertion loss at the receiving S-band frequency is *1.32 dB*, and that the rejection at the upper UMTS boundary is *26.6 dB*.

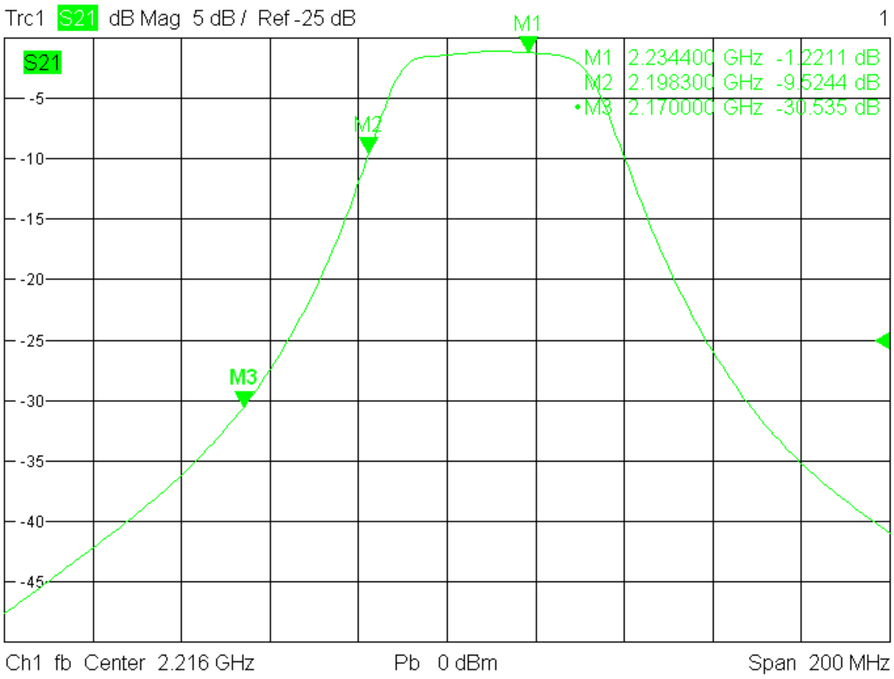

Figure 4.13: S-band bandpass filter characteristic after re-tuning. The measurement shows that the insertion loss at the RX frequency is *1.22 dB* (*0.1 dB* better than before), and that the rejection at the upper UMTS boundary is *29.3 dB* (*2.7 dB* better than before).

4.1.5 Interference Signal Measurements

To determine degradation of the S-band downlink performance by interference signals from the surroundings, measurements and characterisation of potential interference sources were performed. The main focus in the measurements has been laid at low elevations for all azimuth positions, as these are the relevant measurement points.

The result of these measurements is a radio frequency horizon mask shown in Figure 4.14, defining positions subject to interference with the correspondent interference signal magnitude. The 2-D plot shows the maximum detected interference signal at each azimuth position independently from the elevation.

A more detailed characterisation of the interference signals can be seen in the 3-D plot depicted in Figure 4.15, showing the interference signals for each azimuth and elevation position. Table 4.5 shows the interference signal peaks for the five most significant interference sources with the corresponding azimuth and elevation positions. In addition, the affected azimuth positions and the minimum required elevation to avoid the interference signal are listed. The table shows that the relevant interference signals are located South East (row 2) and South West (row 4) with respect to the ground station location. The other interference signals are not particularly relevant since they affect the receiving performance only below $4°$ of elevation, where tracking of the satellite is not always possible due to terrain limitations.

Azimuth [°]	Elevation [°]	Signal Level [dBm]	Azimuth Range [°]	min. Elevation [°]
86	0	-70,79	80-86	4
122	2	-55,32	117-129	10
166	0	-67,53	166-176	4
230	1	-57,63	229-234	8
326	1	-70,99	329-332	4

Table 4.5: S-band noise interference positions and signal levels. The relevant directions and minimum elevation values required to avoid the interference are listed. The relevant interference signals are located South East (row 2) and South West (row 4) with respect of the ground station location.

Taking these data into consideration, contacts with the spacecraft can be better characterised and better estimations about effective contact times when the spacecraft crosses the ground station at positions subject to interference can be made. In some cases, for low elevation passes over affected azimuth directions, it can be even decided to skip tracking to save resources.

In the context of a related Bachelor Thesis [50], a simulation with the software *AGI Satellite Toolkit (STK)* ® was used to model known potential interference sources and simulate their effect on the link performance between the BRITE-Austria satellite and the Graz ground station. By analysing the existing transmitters in a radius of about *1 km* around the ground station, it was determined that the interference for the downlink in all directions is caused by mobile base stations providing Universal Mobile Telecommunications System (UMTS) and High Speed Packet Access (HSPA) services.

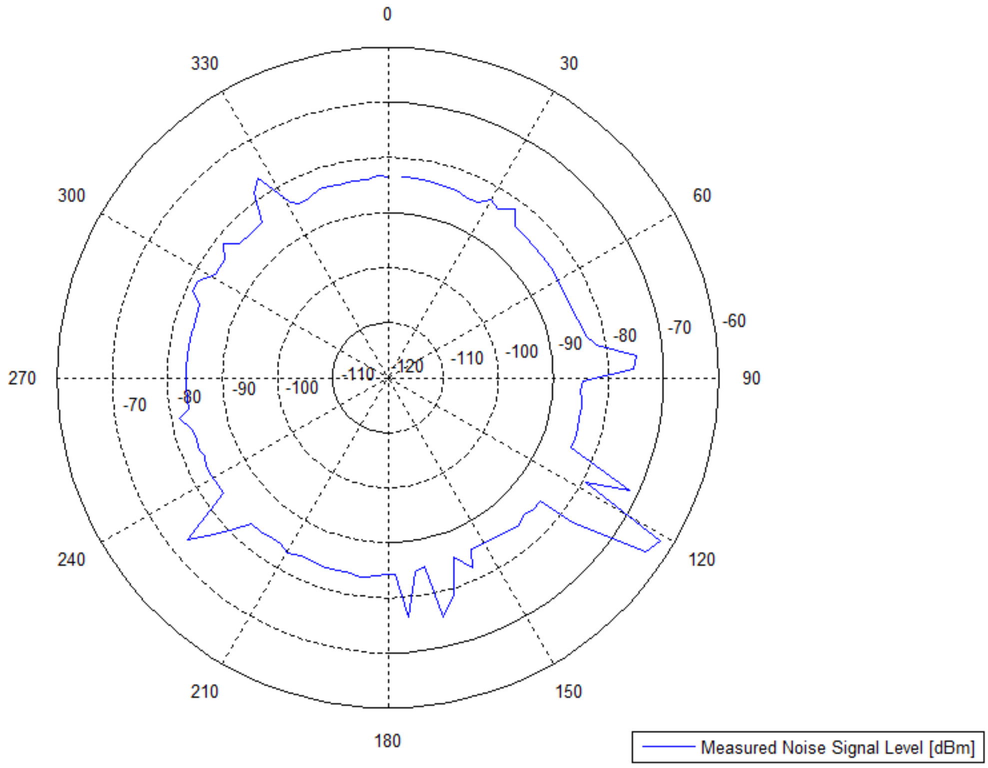

Figure 4.14: 2D interference signal mask for the S-band RX antenna. The plot shows the interference level at each azimuth and elevation position of the S-band antenna (not taking into account a specific elevation value).

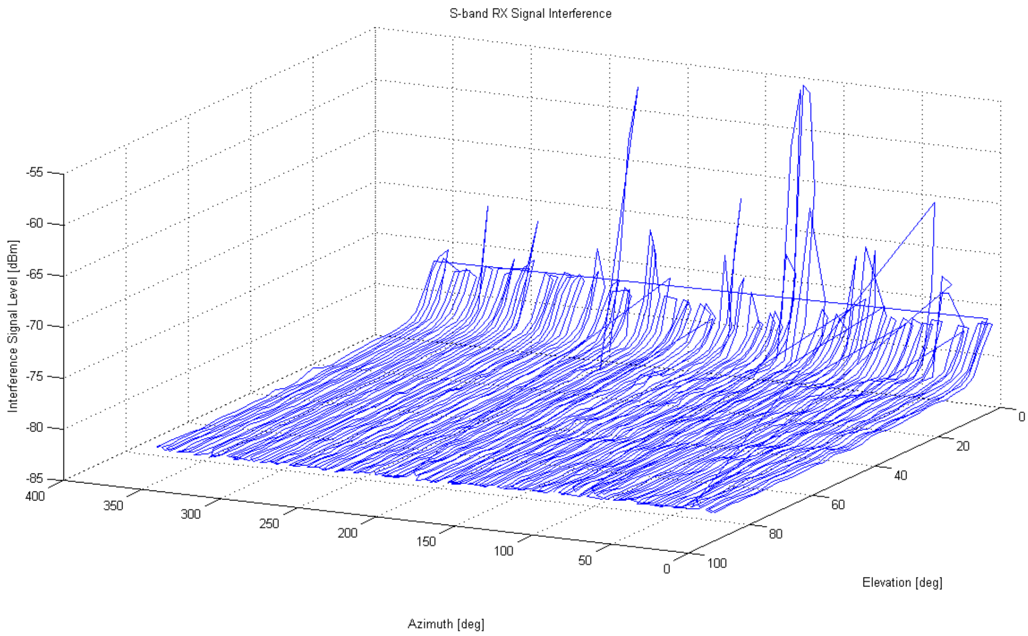

Figure 4.15: 3D interference signal mask for the S-band RX antenna. The maximum interference level at each azimuth and elevation position of the S-band antenna is shown.

Figure 4.16 shows all considered mobile base stations in the simulation. The impact of the base stations during a contact of BRITE-Austria with the ground station is shown, where the lines to the base stations indicate potential interference in the downlink during the contact. Furthermore, the simulation determines the main interference source at any moment during the contact, highlighted by the red line.

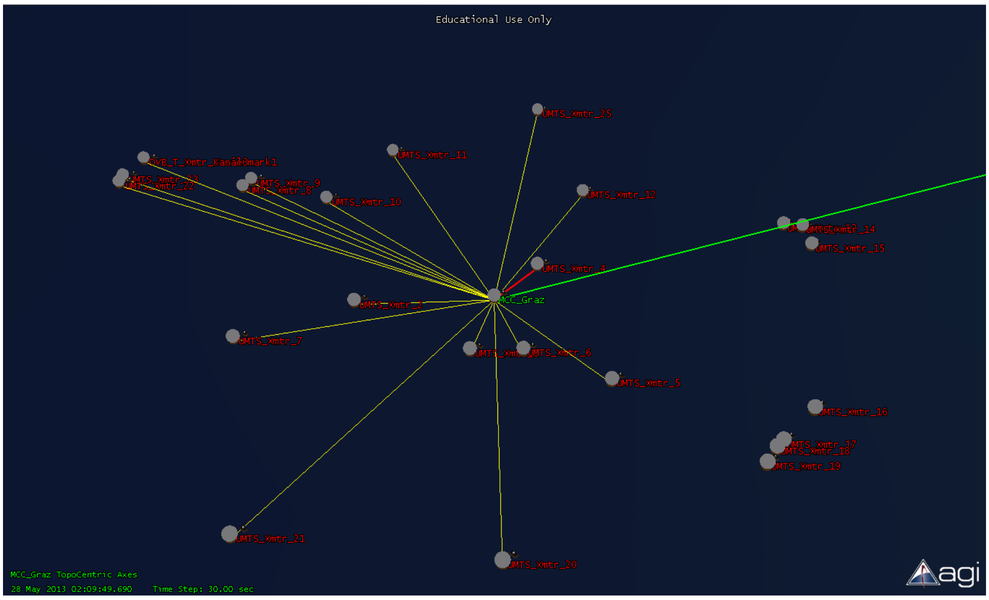

Figure 4.16: Simulated UMTS interference sources for the S-band RX Antenna. The simulation shows the affecting interference sources (yellow lines) during a particular contact of BRITE-Austria with the ground station (the green line shows the access). The main source of interference at this particular moment during the contact is illustrated by the red line. (image courtesy: STK)

A detailed analysis of the interference impact of the base stations in the context of [50] has confirmed that all measured interference signals can be attributed to the mobile base stations. In particular, it was confirmed that the main interference source is a mobile base station located South-East with respect the ground station on the roof of a building adjacent to the TU Graz Campus.

For this main source of interference, additional measurements have been performed with both the ground station S-band antenna as well as with a calibrated reference antenna for better characterisation.

Figure 4.18 shows a comparison between the measured signal spectrum of the S-band antenna pointed at zenith (0° Azimuth, 90° Elevation) and the received signal spectrum when pointed at the main interference source maximum, corresponding to the UMTS signal from the cellular network base station located at 122° Azimuth, 2° Elevation, according to Table 4.5. The figure shows that the interference lead to an increase of the noise level at the satellite downlink centre frequency of about *25 dB*, thus impeding communications with the spacecraft. In addition, Figure 4.17 shows the UMTS signal measured with a reference antenna at the antenna tower, showing the UMTS channels in the allocated downlink spectrum between *2110* and *2170 MHz* [51]. It can be seen that the strongest UMTS signals received are located between *2140* and *2150 MHz*, sufficiently separated from the BRITE-Austria S-band RX frequency.

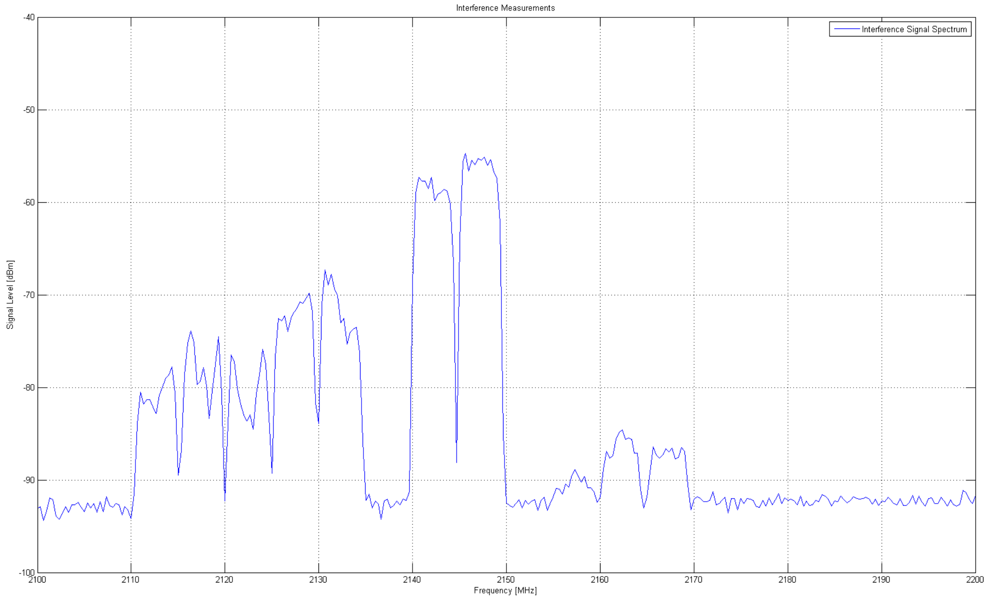

Figure 4.17: UMTS interference signal spectrum measured with a calibrated reference antenna. The strongest UMTS downlink signal in the surroundings next to the S-band RX frequency for BRITE-Austria is up between *2140* and *2150 MHz*.

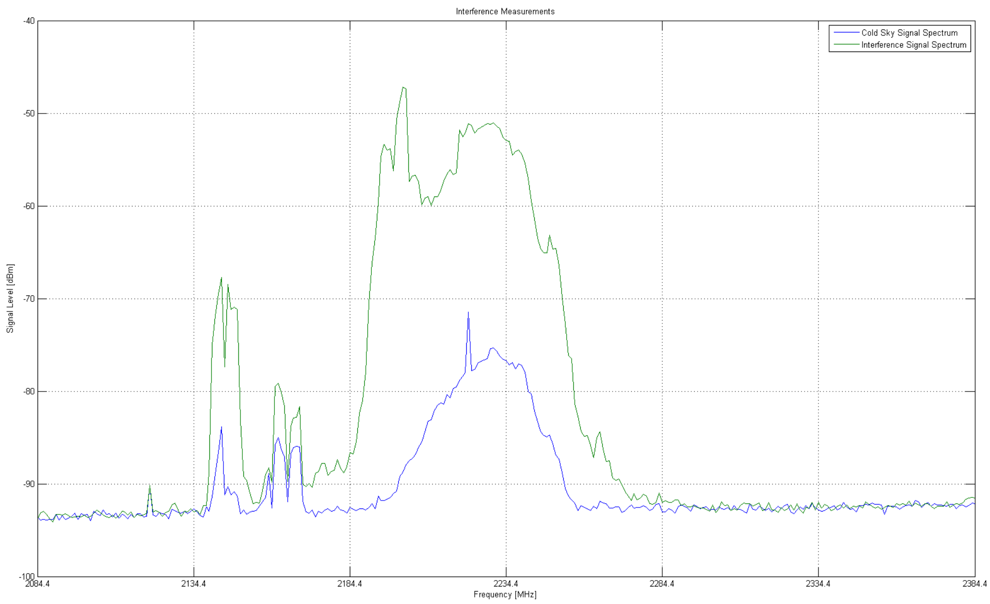

Figure 4.18: Ground station received signal spectrum minimum/maximum interference comparison. The received signal spectrum of the ground station antenna at zenith and at the major interference orientation is shown. A significant increase of the background noise level when pointing towards the interference source can be seen.

4.1.5.1 Upgrade of the S-band Feed Configuration

As part of the S-band upgrades of the Graz ground station, in September 2014 the S-band feed box was replaced with a new configuration. The purpose of this replacement was to get rid of terrestrial interference sources in the surroundings characterised in Section 4.1.5, as well as to avoid potential interference from the own uplink signal when operating at high power due to signal reflections at low elevation, an effect observed in particular after the upgrade to a dual UHF uplink antenna configuration.

A possible explanation for these interference effects is that, although a bandpass filter was used in the previous feed box installation, the interference signals were amplified by the S-band antenna to an extent to overload the LNA, and as a result an already distorted signal was filtered in the affected antenna positions, causing intermodulation.

Therefore, for the new feed box a bandpass filter with higher rejection and low insertion loss was selected. This allows to installing the bandpass filter directly after the patched feed and before the LNA (reverse order compared to the previous installation). This way, the interference signal components are filtered effectively before amplifying the received signal, thus preventing the LNA from overdrive effects. The trade-off of this configuration is a reduction of the figure of merit G/T due to an increase of the system noise temperature T_{Sys}. The new feed box configuration includes the following components:

- A new patched S-band feed covering the entire SRS S-band spectrum (*2200 - 2290 MHz*)
- A bandpass filter with higher rejection compared to the previous installation and low insertion loss
- An identical copy of the LNA used in the previous installation

To characterise the new bandpass filter, measurements with a network analyser were performed to determine the passband as well as the insertion loss. A screenshot of the measurement plot is shown in Figure 4.19. The measurement result shows that the insertion loss at the receiving S-band frequency is *0.63 dB* (around half compared to the old bandpass filter), and that the rejection at the upper UMTS boundary is *48.19 dB* (almost *20 dB* better than the old bandpass filter). Therefore, due to the low insertion loss, an installation of the bandpass filter before the LNA was considered suitable in order to keep the reduction of the G/T to a minimum compared to the previous configuration. To characterise the new S-band feed performance the following measurements were carried out:

- The sun noise measurements as described in Section 4.1.3 to determine the G/T
- The noise signal measurements as described in Section 4.1.5 for the receiving signal bandwidth at every S-band antenna orientation

With regard to the G/T, the measurement results showed that the G/T for the new S-band feed configuration is *13 dB*, which is only *1 dB* less compared to the old feed configuration.

The results of the noise signal measurements for the receiving signal bandwidth at every antenna orientation are shown in Figure 4.20.

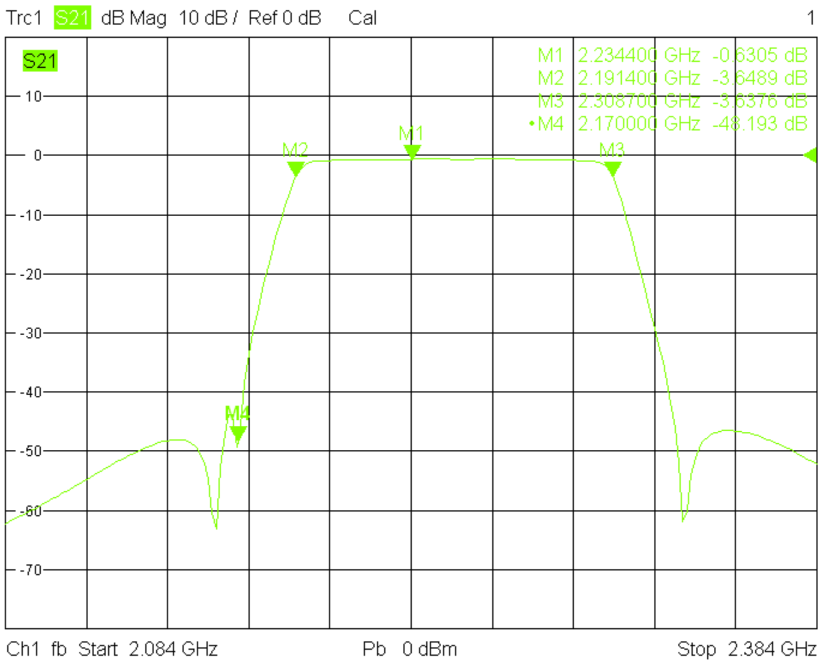

Figure 4.19: New S-band bandpass filter characteristics. The measurement result shows that the insertion loss at the receiving S-band frequency is *0.63 dB* (around half compared to the old bandpass filter), and that the rejection at the upper UMTS boundary is *48.19 dB* (almost *18 dB* better than the old bandpass filter).

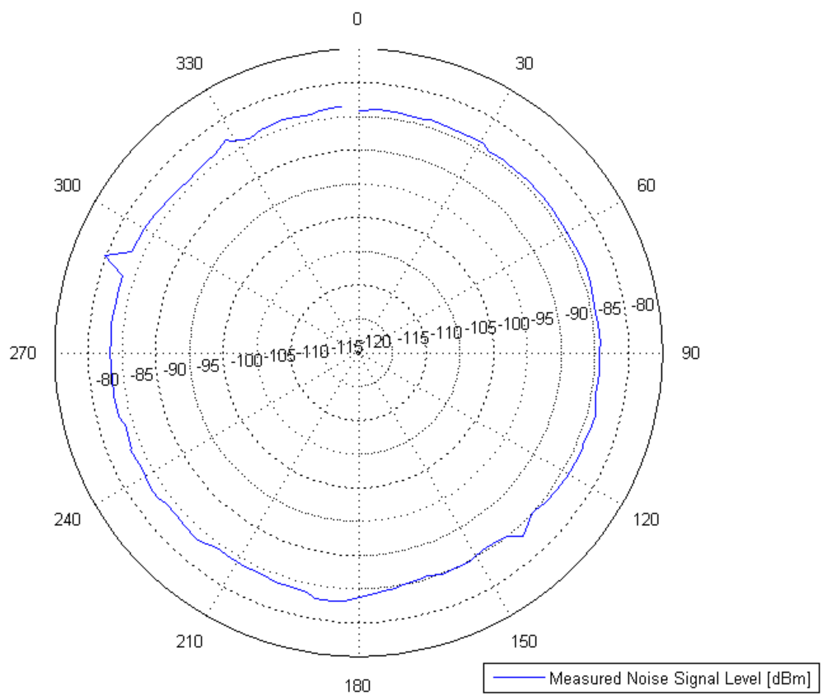

Figure 4.20: 2D interference signal mask for the S-band RX antenna with the new feed configuration. The interference level at each azimuth and elevation position of the S-band antenna with the new feed configuration is shown (not considering a specific elevation). There are no longer noticeable interference signals at any antenna orientation.

The plot shows that there are no longer noticeable interference signals at any antenna orientation, even at low antenna elevations during operations of the BRITE-Austria satellite at high uplink power levels. Therefore, as the new configuration allows to significantly reduce the interference signals at the expense of losing *1 dB* of G/T due to the increased system noise temperature T_{Sys}, the new S-band feed configuration was found to be more suitable for operating the ground station S-band downlink.

4.2 Link Budget Calculations

The link budget is a powerful tool in a satellite communication system design to estimate the link performance. It includes all relevant characteristics such as transmit powers, gains, and losses of the different links in the system and provides good estimations of the overall system performance. The equations used for the link budget calculations presented hereafter are based on [38], [52], and [53].

The main parameter for evaluating the link performance is the available carrier to noise ratio C/N at the receiver, and further the available link margin by comparison of the available C/N and the minimum required C/N for nominal operations.

The essential parameters for the calculation of the carrier to noise ratio, and hence essential for the link budget calculations and link performance assessment are the effective isotropic radiated power ($EIRP$), the free space loss (L_{FS}), and the receiving figure of merit gain over system noise temperature (G/T).

The carrier power C (4.20) is proportional to the product of the effective isotropic radiated power (EIRP), and effective antenna aperture A_{eff}, and indirectly proportional to the square of the link distance:

$$C = \frac{P_T \cdot G_T}{4 \cdot \pi \cdot R^2} \cdot A_{eff} \tag{4.20}$$

Considering the definition of $A_{eff} = \frac{G \cdot \lambda^2}{4 \cdot \Pi}$, the equation for the incoming carrier power at the receiver can be rewritten as

$$C = \frac{P_T \cdot G_T}{4 \cdot \pi \cdot R^2} \cdot \frac{G_R \cdot \lambda^2}{4 \cdot \pi} \tag{4.21}$$

This equation yields the definition of the free space loss L_{FS} (4.22):

$$L_{FS} = (\frac{\lambda}{4 \cdot \pi})^2 \tag{4.22}$$

The receiving noise power is dependent on the receiving channel bandwidth B, the system noise temperature T, and the Boltzmann constant k according to Equation (4.1). The Boltzmann constant expresses the temperature of a resistance delivering the same noise power as the considered noise source [39].

By simplification of the essential parameters the carrier to noise ratio C/N can therefore be calculated according to Equation (4.23), or after transformation in logarithmic representation according to Equation

(4.24). In addition to the free space loss as the main attenuation loss in the chain, the sum of the other losses ΣL (e.g. atmospheric, polarisation, pointing losses) has also to be considered.

$$\frac{C}{N} = \frac{P_T \cdot G_T \cdot G_R \cdot (\frac{1}{L_{FS}+\Sigma L})}{k \cdot T_{sys} B} \tag{4.23}$$

$$\frac{C}{N} = EIRP_{[dBW]} - L_{FS[dB]} - \Sigma L_{[dB]} + \frac{G}{T}_{[dB/K]} - k_{[dBJ/K]} - B_{[dBHz]} \tag{4.24}$$

After normalization of the receiving channel bandwidth B_N, the carrier to noise power density ratio C/N_0 can be derived from Equation (4.23), yielding Equation (4.25).

$$\frac{C}{N_0} = \frac{P_T \cdot G_T \cdot G_R \cdot (\frac{1}{L_{FS}+\Sigma L})}{k \cdot T_{sys}} \tag{4.25}$$

Finally, for a quantitative comparison of the performance independently of the coding scheme used, the energy per information bit E_b is used, yielding the calculation of the signal to noise ratio of E_b/N_0 as shown in Equation (4.26), where r_b denotes the net bit rate.

$$\frac{E_b}{N_0} = \frac{C}{N} \cdot \frac{B}{r_b} \tag{4.26}$$

According to the presented equations, four link budgets have been calculated and are presented: two for the downlink and two for the uplink. In the downlink budgets, the standard case for the minimum guaranteed data rate according to the requirements of *32 kbit/s* with BPSK modulation (Table 4.6) and the case for the maximum available data rate of *256 kbit/s* with QPSK modulation (Table 4.7) have been considered. In the uplink, link budgets are presented for the single UHF antenna (Table 4.8) and for the dual UHF antenna configuration (Table 4.9). The antenna gain increase of *1.9 dB* for the dual antenna configuration is based on uplink measurements performed with the spacecraft as presented in Chapter 5. A transmit power of *300 W* has been assumed as typical value used for operating the spacecraft.

For all link budgets, the maximum distance for the mean satellite altitude of *775 km* has been considered and the worst case free space loss at an elevation of $5°$ with respect to the ground station as the typical radio horizon limitation by terrain. In addition, all gains, noise figures, and losses, have been adapted to the effective determined values during the previously described measurements whenever available.

The results show that substantial link margins are available for all calculated budgets:

- *15.89 dB* for the S-band downlink budgets with BPSK *32 kbit/s*
- *6.86 dB* for the S-band downlink budgets with QPSK *256 kbit/s*
- *21.73 dB* for the UHF uplink budgets with a single transmitting antenna
- *23.68 dB* for the UHF uplink budgets with two transmitting antennas

S-band - Downlink	Inputs	Calculations	Units
Frequency	2234.4		MHz
Transmit power (mW)	175	22.43	dBm
Feed harness loss	0.5	-0.50	dB
Antenna gain		2.10	dBi
EIRP		**24.03**	**dBm**
Satellite orbital altitude (circular orbit)	775		km
Maximum distance to satellite	2782.63		km
Free space loss		-168.14	dB
polarisation and atmospheric losses		2	dB
Total propagation loss		-170.14	dB
Isotropic signal power at antenna input		-146.11	dBm
Antenna size	3		m
Antenna efficiency	64		%
Antenna gain		34.99	dBi
Antenna beamwidth (half power)	3.13		degrees
Pointing error	2		degrees
Feed loss	0.8	-0.8	dB
Feed LNA noise figure	0.5	-0.5	dB
Feed LNA gain	31		dB
Downconverter LNA noise figure	0.7		dB
Downconverter LNA gain	40		dB
Cable losses	4.37		dB
System noise temperature (K)	115.87	20.64	dBK
G/T		**14.35**	**dB/K**
Receiver signal power		**-116.52**	**dBm**
Receiver noise power		**-126.89**	**dBm**
C/N_0		66.84	dB
Information data rate	32000	45.05	bps
Coding rate	0.5	-3.01	dB
Channel data rate	64000	48.06	bps
Receive bandwidth	128000	51.07	dBHz
C/N		15.77	dB
Implementation losses	1	1.00	dB
E_b/N_0 (relative to channel data rate)		17.78	dB
E_b/N_0 **(relative to information data rate)**		**20.79**	**dB**
Required E_b/N_0 for 10E-6 BPSK	10.6	10.60	dB
Coding gain	5.7	5.70	dB
Coded required E_b/N_0 for 10E-6 BPSK		4.90	dB
Downlink margin		**15.89**	**dB**

Table 4.6: BRITE-Austria S-band downlink budget with default settings. The default settings are a data rate of *32 kbit/s* and BPSK modulation.

S-band - Downlink	Inputs	Calculations	Units
Frequency	2234.4		MHz
Transmit power (mW)	175	22.43	dBm
Feed harness loss	0.5	-0.50	dB
Antenna gain		2.10	dBi
EIRP		**24.03**	**dBm**
Satellite orbital altitude (circular orbit)	775		km
Maximum distance to satellite	2782.63		km
Free space loss		-168.14	dB
Polarisation and atmospheric losses		2	dB
Total propagation loss		-170.14	dB
Isotropic signal power at antenna input		-146.11	dBm
Antenna size	3		m
Antenna efficiency	64		%
Antenna gain		34.99	dBi
Antenna beamwidth (half power)	3.13		degrees
Pointing error	2		degrees
Feed loss	0.8	-0.8	dB
Feed LNA noise figure	0.5	-0.5	dB
Feed LNA gain	31		dB
Downconverter LNA noise figure	0.7		dB
Downconverter LNA gain	40		dB
Cable losses	4.37		dB
System noise temperature (K)	115.87	20.64	dBK
G/T		**14.35**	**dB/K**
Receiver signal power		**-116.52**	**dBm**
Receiver noise power		**-126.89**	**dBm**
C/N_0		66.84	dB
Information data rate	256000	54.08	bps
Coding rate	0.5	-3.01	dB
Channel data rate	512000	57.09	bps
Receive Bandwidth	512000	57.09	dBHz
C/N		9.75	dB
Implementation Losses	1	1.00	dB
E_b/N_0 (relative to channel data rate)		8.75	dB
E_b/N_0 **(relative to information data rate)**		**11.76**	**dB**
Required E_b/N_0 for 10E-6 QPSK	10.6	10.60	dB
Coding gain	5.7	5.70	dB
Coded required E_b/N_0 for 10E-6 QPSK		4.90	dB
Downlink Margin		**6.86**	**dB**

Table 4.7: BRITE-Austria S-band downlink budget for high data rate. The highest available data rate setting is *256 kbit/s* with QPSK modulation.

UHF - Uplink	Inputs	Calculations	Units
Frequency	437.365		MHz
Transmit power (mW)	300000	54.77	dBm
Feed harness loss	1.34	-1.34	dB
Power splitter and phased feed lines loss to antenna	0.7	-0.7	dB
Antenna gain		16.15	dBi
Antenna half power beamwidth	28		deg
Antenna mismatch	1.60	-0.24	dB
Pointing loss		-0.38	dB
EIRP		**68.26**	**dBm**
Satellite orbital altitude (circular orbit)	775		km
Maximum distance to satellite	2728.63		km
Free space loss		-153.98	dB
Polarisation and atmospheric losses		2	dB
Total propagation loss		-155.98	dB
Isotropic signal power at spacecraft		-87.72	dBm
Antenna gain		-3.00	dB
Antenna mismatch loss (VSWR)	1.48	-0.17	dB
Power splitter loss	0.9	-0.9	dB
Feed harness loss	0.8	-0.8	dB
Preamplifier noise figure	1.5		dB
Preamplifier gain	15		dB
Receiver noise figure	10		dB
System noise temperature (K)	603.08	27.80	dBK
G/T		**-30.97**	**dB/K**
Receiver signal power		**-90.89**	**dBm**
Receiver noise power		**-120.38**	**dBm**
C/N_0		79.73	dB
Receive bandwidth	110000	50.41	dBHz
C/N		29.32	dB
Channel data rate (= information data rate)	9600	39.82	bps
Modulation index	0.5		Hz/Hz
Occupied bandwidth	19200	42.83	Hz
Implementation losses	1	1.00	dB
E_b/N_0		**31.33**	**dB**
Required E_b/N_0 for 10E-5 GMSK	9.60	9.60	dB
Coded required E_b/N_0 for 10E-5 GMSK	9.60	9.60	dB
Uplink margin		**21.73**	**dB**

Table 4.8: BRITE-Austria UHF uplink budget. This link budget considers the single UHF uplink antenna.

UHF - Uplink	Inputs	Calculations	Units
Frequency	437.365		MHz
Transmit power (mW)	300000	54.77	dBm
Feed harness loss	1.34	-1.34	dB
Power splitter and phased feed lines loss to antenna	0.7	-0.7	dB
Antenna gain		18.10	dBi
Antenna half power beamwidth	28		deg
Antenna mismatch	1.60	-0.24	dB
Pointing loss		-0.38	dB
EIRP		**70.21**	**dBm**
Satellite orbital altitude (circular orbit)	775		km
Maximum distance to satellite	2728.63		km
Free space loss		-153.98	dB
Polarisation and atmospheric losses		2	dB
Total propagation loss		-155.98	dB
Isotropic signal power at spacecraft		-85.77	dBm
Antenna gain		-3.00	dB
Antenna mismatch loss (VSWR)	1.48	-0.17	dB
Power splitter loss	0.9	-0.9	dB
Feed harness loss	0.8	-0.8	dB
Preamplifier noise figure	1.5		dB
Preamplifier gain	15		dB
Receiver noise figure	10		dB
System noise temperature (K)	603.08	27.80	dBK
G/T		**-30.97**	**dB/K**
Receiver signal power		**-88.94**	**dBm**
Receiver noise power		**-120.38**	**dBm**
C/N_0		81.68	dB
Receive bandwidth	110000	50.41	dBHz
C/N		31.27	dB
Channel data rate (= information data rate)	9600	39.82	bps
Modulation index	0.5		Hz/Hz
Occupied bandwidth	19200	42.83	Hz
Implementation losses	1	1.00	dB
E_b/N_0		**33.28**	**dB**
Required E_b/N_0 for 10E-5 GMSK	9.60	9.60	dB
Coded required E_b/N_0 for 10E-5 GMSK	9.60	9.60	dB
Uplink margin		**23.68**	**dB**

Table 4.9: BRITE-Austria UHF uplink budget with two antennas. This link budget considers the dual UHF uplink antenna configuration.

4.3 Downlink Tests with the MOST Satellite

In order to assess the downlink performance, signal measurements with the Canadian Microvariability and Oscillations of STars (MOST) satellite have been performed. The MOST spacecraft is a microsatellite carrying a small astronomical telescope. It represents a predecessor of the BRITE mission, as its mission goal is the measurements of brightness oscillations of stars, which can be used to determine fundamental properties of the observed stars [54] [55].

Besides sharing a common mission goal with BRITE-Austria, the MOST satellite is particularly interesting for assessing the ground station performance of the Graz ground station because it is very similar to BRITE-Austria regarding the orbit and the downlink transmission parameters. MOST operates in an *830 km* altitude sun-synchronous, dawn-dusk orbit [43], which is very similar to the BRITE-Austria orbit. Therefore, contact times, the ground station antenna azimuth/elevation positions for tracking and directions of the contacts, as well as the distances to the satellite are representative.

MOST uses very similar downlink frequencies and transmitting parameter as BRITE-Austria. The effective isotropic radiated power (EIRP) and the radiation characteristics of the downlink beam are almost identical to the ones of BRITE-Austria. In addition, MOST is being tracked by a ground station in Vienna. Therefore, due to the advantageous geographic location of Graz, sharing almost the same satellite footprint as Vienna, the MOST downlink signal can be received from the Graz ground station during nearly the entire duration of the contact, as the transmitter is being turned on and off from the Vienna ground station.

With the courtesy of the colleagues of Vienna University of Technology (TUV) providing the relevant downlink parameters required for the configuration of the receiving satellite modem, signal measurements with the modem (down to data lock) could be performed.

The measurements have been performed by own-developed automated software, interfacing with a spectrum analyser and with the satellite modem to measure the relevant signal parameters. The following signal parameters were recorded:

Spectrum Analyser

- Spectrum, recording the spectrum analyser's trace samples
- Actual Signal Centre Frequency, by Doppler shift correction performed by the satellite modem
- Average Signal Level, by averaging the incoming signal over the signal bandwidth
- Average Noise Level, by averaging the surrounding noise floor

Satellite Modem

- Modem Lock State
- Signal level

- E_b/N_0
- Frequency offset
- Bit Error Rate (BER)

Figure 4.21 shows the measurement software in action during a MOST pass.

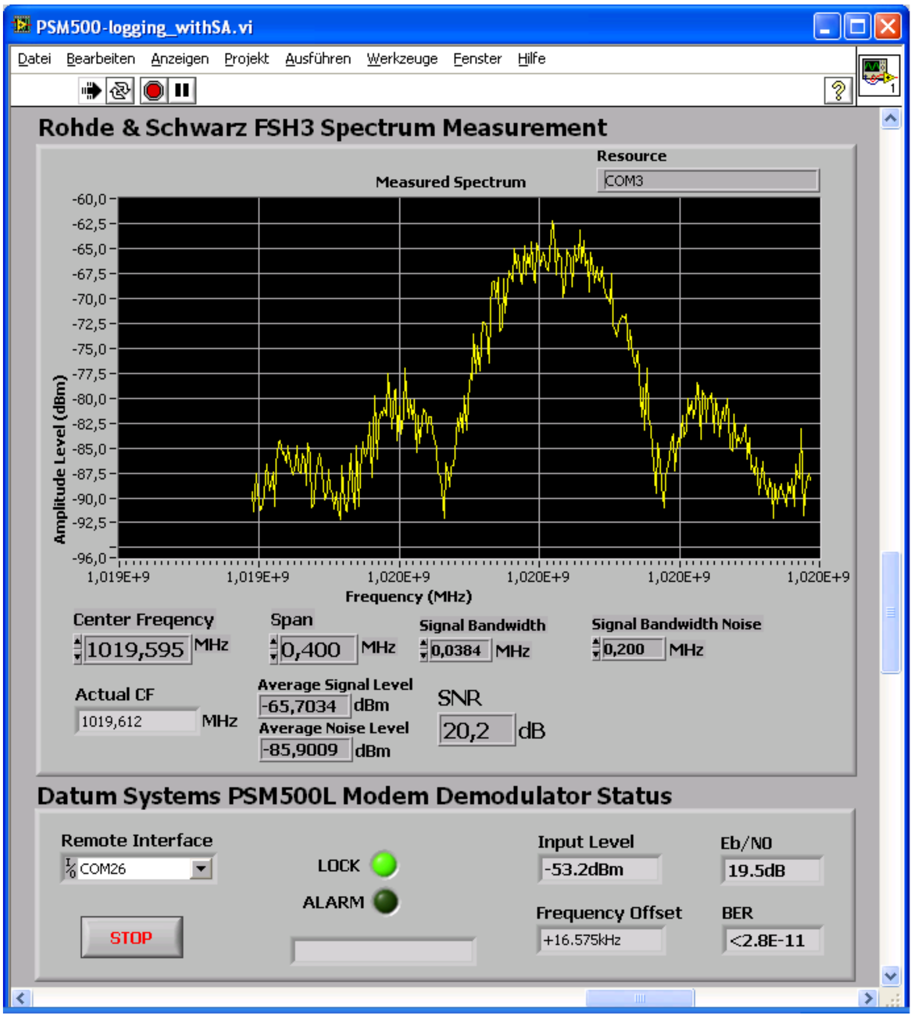

Figure 4.21: MOST S-band RX signal measurement software. The software captures the signal spectrum from a spectrum analyser as well as the key signal parameters from the satellite modem.

Figure 4.22 shows measurement results for a typical afternoon MOST pass over Graz, tracked on October 10th, 2012. The plot shows the average received signal level compared to the average received noise level over the pass duration. The contact time with the satellite was around 550 seconds, during which the modem had a stable data lock. While signal fluctuations can be detected mainly due to tracking lag of the rotators, the signal to noise ratio was mostly sufficient to guarantee bit error rates (BER) of 10^{-9}. To achieve this BER, an $E_b/N_0 = 7\ dB$ is required, as described in Section 4.5.

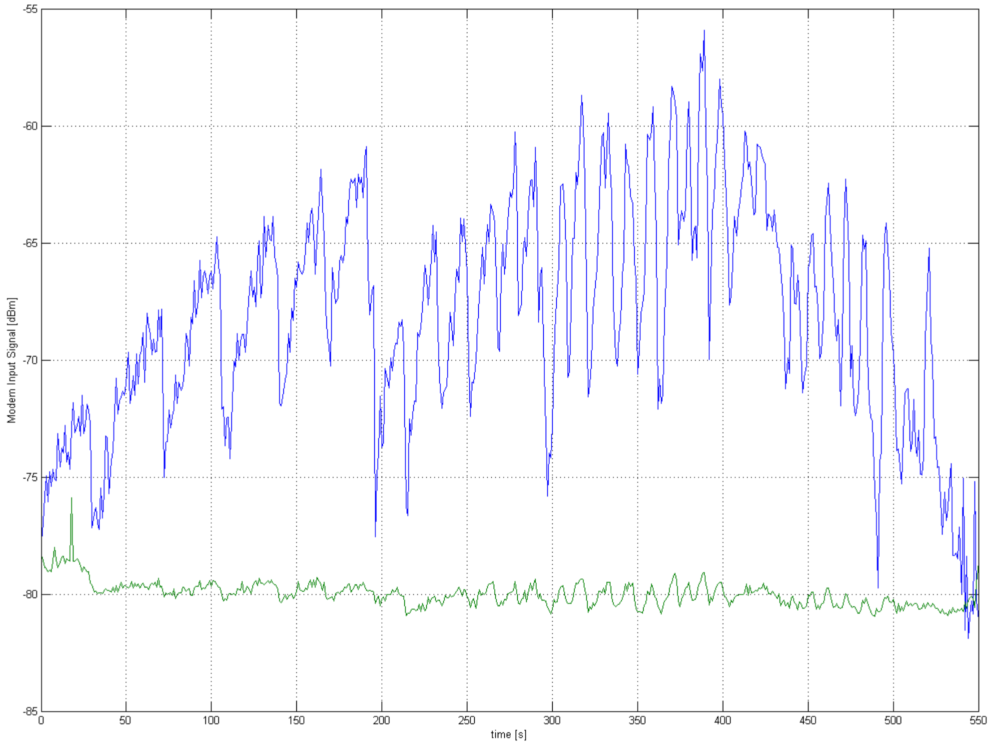

Figure 4.22: MOST S-band RX signal to noise ratio. S-band signal to noise ratio measurement results for a MOST pass over the Graz ground station on October 10th, 2012. During the measurement the modem had a stable data lock and the signal to noise ratio was mostly sufficient to guarantee bit error rates of 10^{-9} by an $E_b/N_0 > 7$ *dB*.

4.4 Uplink Tests with the NTS Satellite

Similar to the downlink measurements with MOST, tests for the uplink were performed with a representative satellite to assess the uplink performance. These tests were carried out with the Canadian CanX-6/NTS satellite.

CanX-6/NTS is one of the predecessor satellites of BRITE, developed and operated by UTIAS/SFL in cooperation with COM DEV International Ltd., with the purpose of technology demonstration and gaining of space heritage for the generic nanosatellite bus (GNB) components for usage in future missions. In particular, the technology demonstration of Automatic Identification System (AIS) detection was a key asset of the mission [56].

NTS flies a predecessor design of the BRITE UHF receiver which operates at the same uplink frequency. In addition, the ground software for NTS is compatible with the BRITE terminal node controller (TNC) and transmission schemes. Therefore, after proper configuration of the ground station and the definition of suitable test cases, uplink tests from the Graz ground station could be performed. As NTS uses the same downlink frequency band as BRITE, a bidirectional test would have been technically possible. Unfortunately, as the downlink frequency is part of an ITU regulated spectrum band and the service area defined in the Advanced Publication Information (API) does not include Europe, no downlink signal was available at the Graz ground station for the test. Instead, uplinked packets from Graz were stored on-board the spacecraft and downloaded from the UTIAS/SFL ground station in Toronto to evaluate the test results.

The tests were performed by continuously transmitting a test packet sequence to different adjacent on-board memory locations during selected contacts with the Graz ground station. Subsequently, during later contacts with the Toronto ground station, the data from the written memory locations were downloaded and a comparison of received vs. sent packets was made to evaluate the uplink performance. The test setup is shown in Figure 4.23.

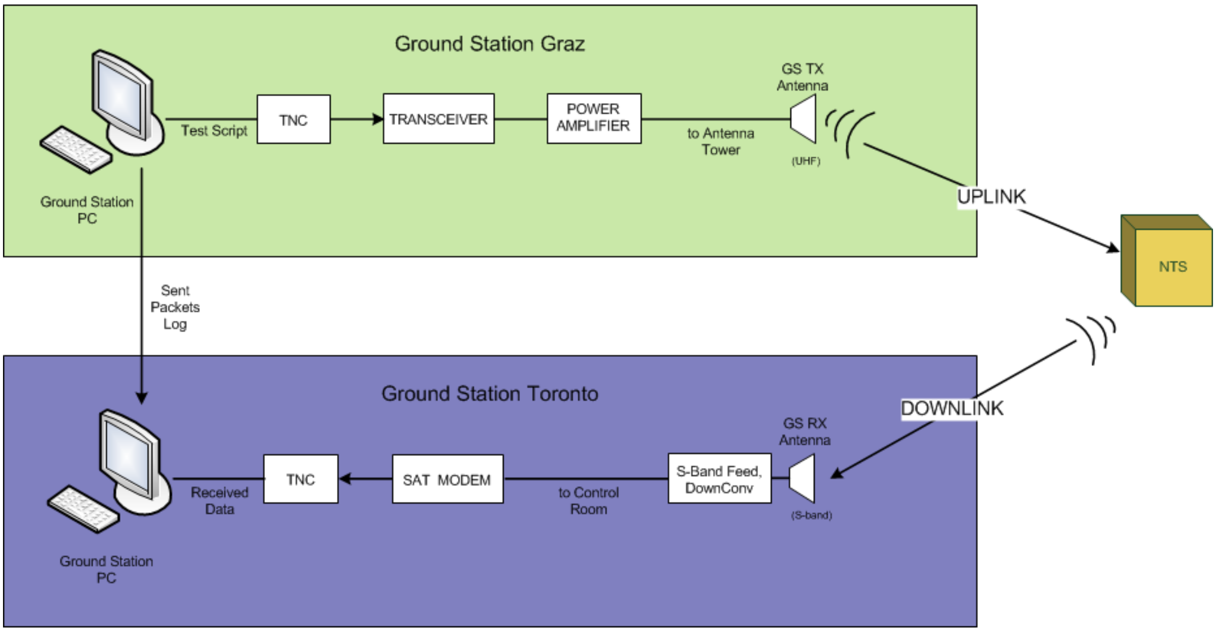

Figure 4.23: NTS uplink test setup. Test packets were uplinked from the Graz ground station and stored to a specific memory location on the spacecraft. Later, during a contact from Toronto, the correspondent memory location data were downloaded from the spacecraft.

At this point it is required to mention that while operating another GNB spacecraft from a European ground station it was noticed that noise interference in the amateur radio uplink band was significantly higher than in the Northern American area around Toronto, affecting the uplink performance in Europe. The NTS UHF receiver implements a wider receive filter and its sensitivity level is several dB higher compared to the BRITE UHF receiver. The substantial noise interference in combination with the design characteristics of the NTS receiver, resulted in an undistinguishable received signal strength indicator to determine whether contact with the Graz ground station had been established. As a result, the performance of the uplink measured during the tests was very poor, with success rates of $10-15\%$. Figure 4.24 shows the received packet statistics for one of the NTS passes tracked from Graz on August 22nd, 2012.

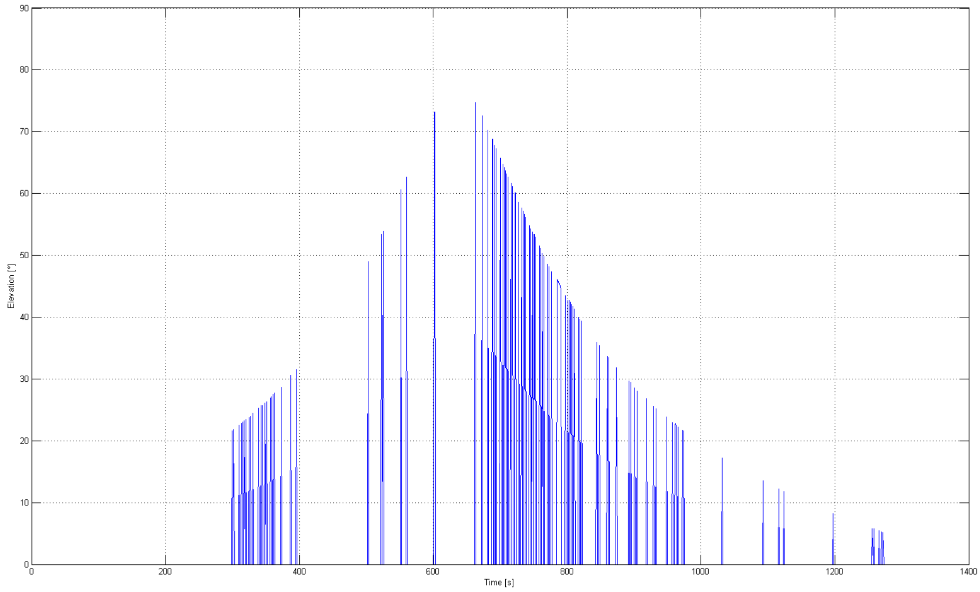

Figure 4.24: NTS packet uplink statistics. The statistics are presented for a pass tracked from the Graz ground station on August 22nd, 2012. The results show a rather poor packet success rate of about 10% due to interference in the UHF band over Europe.

However, with the better specifications of the BRITE receiver, no significant performance degradation for mission operations was expected at this point. In addition, besides the poor packet success rate results of the test, the positive aspect was to verify that the ground station had the capability of establishing contact with a real spacecraft and hence that the uplink chain is fully operative.

4.5 Ground Station Downlink Performance Modelling

Taking into account all the previous measurements, modelling and characterisation of the ground station downlink performance has been carried by the use of *Matlab*® simulations. Figure 4.25 shows the inputs and outputs of the simulation.

The simulation includes several ground station downlink parameters determined during the measurements described in the previous sections, including the system noise temperature results at different elevation angles, the measured figure of merit, the S-band antenna pattern and characteristics of the downlink chain, cumulative distributions for atmospheric conditions, as well as the radio horizon and the rotator's tracking performance. These values are used to predict the received signal strength and its characteristics (e.g. E_b/N_0) and to derive data download capabilities (e.g. data rates) during equivalent simulated BRITE-Austria passes. Besides the calculated values, the measured values from long term signal measurements with the MOST satellite were also imported in the simulation to compare the simulated and measured values from a real satellite contact to better evaluate the simulation performance.

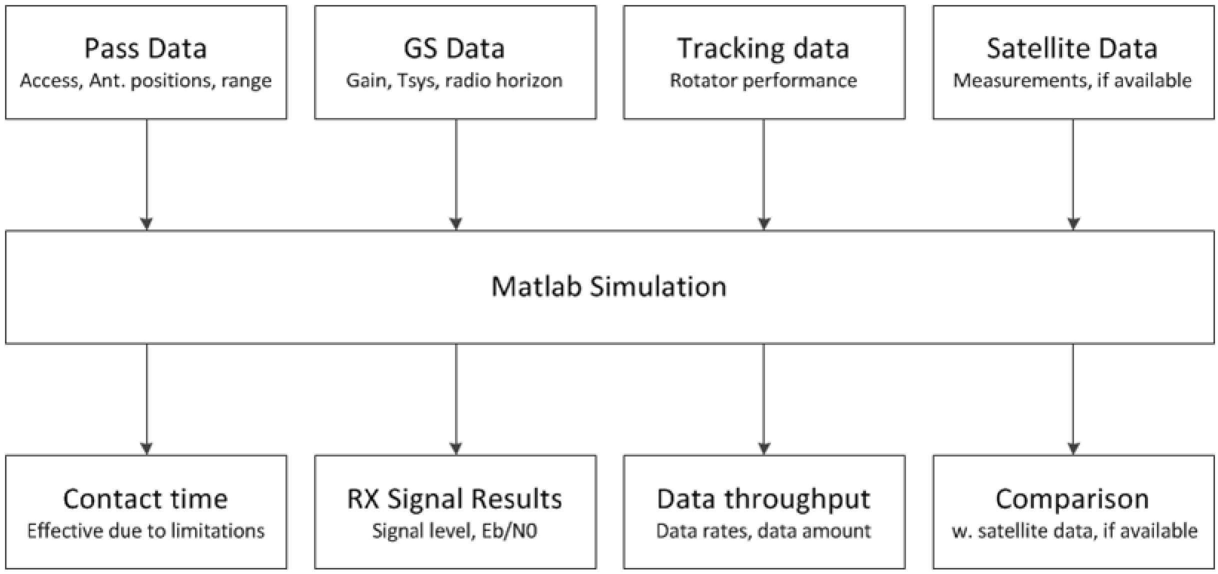

Figure 4.25: Ground station performance modelling inputs and outputs of Matlab simulation. The model reads in available ground station, contact, and satellite measurement data (if available) and returns available contact time, satellite downlink performance results (signal performance and data throughput), as well as comparison between simulated and measured data.

Next to the fixed characteristics of the ground station and the satellite (e.g. antenna gain or system noise temperature), to evaluate the link performance for a particular simulated satellite pass the correspondent contact information is required as input to the model, including the pass timestamps with the correspondent antenna pointing angles. According to the information provided, the simulation calculates:

- The estimated effective contact time with the satellite
- The effective antenna positions compared to the calculated ones (based on the rotators precision)
- The estimated incoming signal level at the modem (including a plot function)
- The estimated modem's E_b/N_0 (including a plot function)
- The maximum feasible data rates at each time during the pass according to the link quality
- The corresponding estimated maximum data download amount during the pass

The contact times of the satellite with the Graz ground station as well as the azimuth and elevation antenna values for tracking and the distance to the spacecraft were calculated with an *AGI Systems Toolkit (STK)* ® simulation. The used simulation includes the spacecraft with its nominal orbital parameters according to the launch provider, and the Graz ground station as tracking facility with its precise location and a defined elevation mask of $5°$ as the minimum radio horizon limit. For each simulated pass, the time step selected was 1 second, as it was found to provide reasonable accuracy for the calculations performed.

Besides providing the described input parameters to the calculations, the STK simulation was useful for observing preliminary contact times with the satellite on the long term and derive preliminary operations schedules. In addition, the two line elements (TLEs) for the spacecraft were generated and used as input for the tracking software for preliminary configuration. On a later step, the additional ground stations of the BRITE ground station network were also added to the simulation to extend the access statistics for BRITE-Austria when operating with the network.

The antenna positions provided by the STK simulation for a BRITE-Austria pass are ideal. However, due to the limited rotator performance of the ground station rotators the effective antenna positions of the ground station differ from the ideal, calculated ones according to the satellite movement. The rotator precision is $\pm 3°$, enabling the rotator to change its current position only when an offset of $3°$ with respect to the last position set is reached. The performance could be improved by the provision of rotator offsets in the tracking software as well as by re-alignment of the antenna feed as described in detail in Section 4.1.4. In the simulation however, the worst case offset of $3°$ was considered.

The measured values of the downlink chain described previously in this chapter were also included in the simulation. For instance, all the gains and losses as well as the measured G/T were considered. In addition, the calculated system noise temperature and its dependence from elevation angles was also included in the simulation according to the measured values for different atmospheric conditions.

For the data rate calculations, a threshold value for the minimum required E_b/N_0 for a bit error rate of 10^{-9} was taken into account. The value was calculated by comparing the E_b/N_0 for an ideal Viterbi decoder bit error rate curve ($K = 7$, $CR = 1/2$) with the actual E_b/N_0 values of the modem, including the implementation loss [57]. Since the specifications of the modem were only given for bit error rates down to 10^{-7}, the value for 10^{-9} was calculated by interpolation with the ideal curve. The minimum calculated value for the required E_b/N_0 was *7 dB*.

Figure 4.26 shows a screen shot of the downlink simulation software graphical user interface. The main menu allows to select the functions to calculate pass statistics or different predefined plot functions. In this figure, the representation of the pass statistics and a plot for the selected data set are shown.

Figure 4.27 and 4.28 show a comparison between simulated and measured results for a MOST pass tracked from the Graz ground station. The pass data was derived from an STK simulation with up to date orbital parameters of the spacecraft.

The results show that:

- The calculated and measured downlink signal values for the selected MOST pass agree quite well; even the signal fluctuations due to the tracking lag of the rotators can be mapped quite consistently.
- The E_b/N_0 comparison between calculated and measured signal agrees only partially due to the strong fluctuations introduced in the calculation by the tracking offsets.

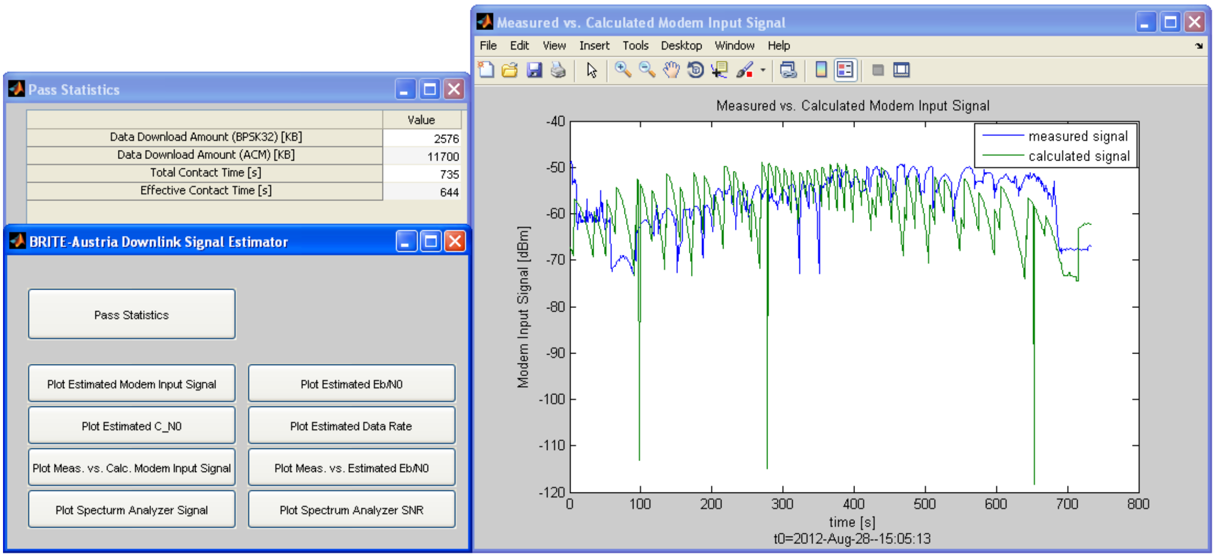

Figure 4.26: Downlink simulation software screenshot. The software provides general pass statistics such as contact time and data throughput, and allows to select between predefined plot functions such as estimated signal parameters for the downlink signal, spectrum analyser measurements, as well as comparisons between simulated and measured data.

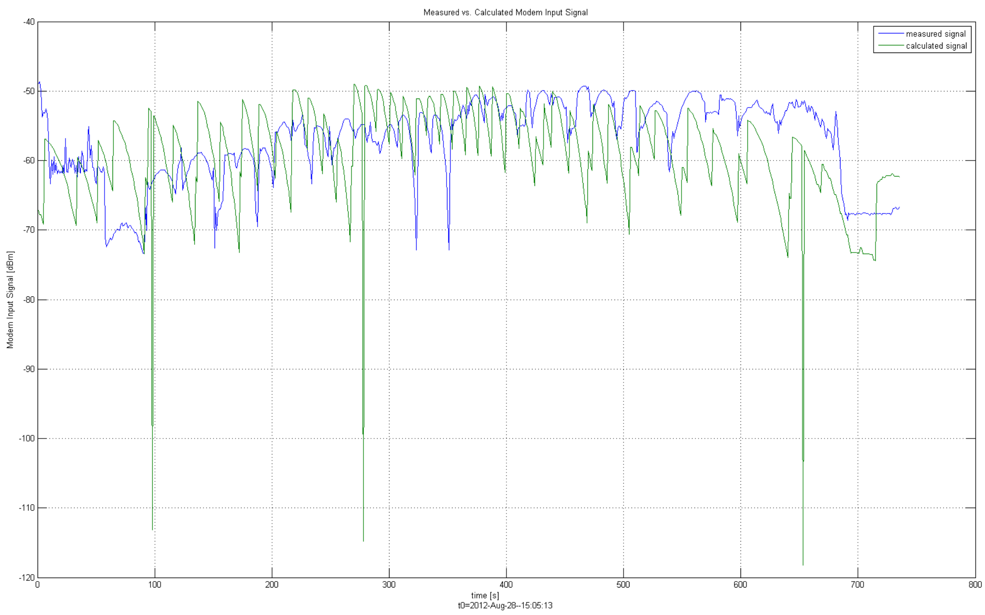

Figure 4.27: Comparison between calculated and measured downlink signal for a MOST pass. The plot shows that the simulation data agrees quite well with the measured data.

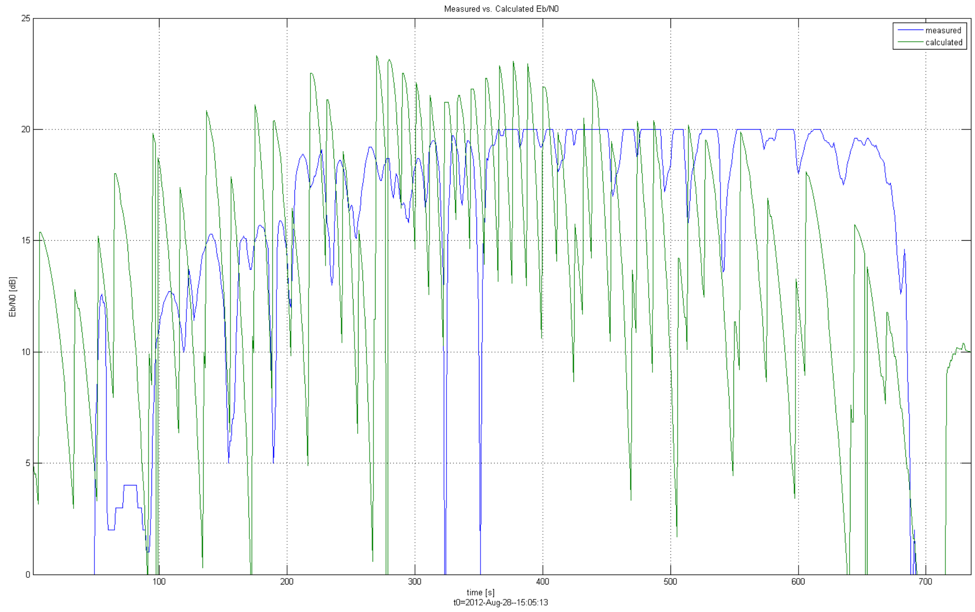

Figure 4.28: Comparison between calculated and measured E_b/N_0 for a MOST pass. The values agree only partially due to the tracking offset considered in the simulation which is partly corrected by the tracking software for the measured data.

Figure 4.29 to 4.31 show the simulation results for a sample simulated BRITE-Austria pass over the Graz ground station assuming clear sky conditions. As baseline for the pass data an STK simulation with the preliminary orbital parameters of the spacecraft was used.

The results show that:

- The calculated downlink signal values for the simulated BRITE-Austria pass are more than acceptable for the considered BPSK modulation and data rate of *32 kbit/s*. The signal fluctuations in the simulation map the tracking lag of the rotators.
- By comparison of the E_b/N_0 between the static data rate setting of *32 kbit/s* (BPSK) and the implemented Adaptive Coding and Modulation (ACM) switching between BPSK *32 kbit/s* and QPSK *256 kbit/s* (minimum and maximum data rate settings) sufficient margins available to operate at the higher data rate.
- By analysis of the variation of the data between BPSK *32 kbit/s* and QPSK *256 kbit/s* according to the available E_b/N_0 for large portions of the simulated pass the high data rate setting can be used.

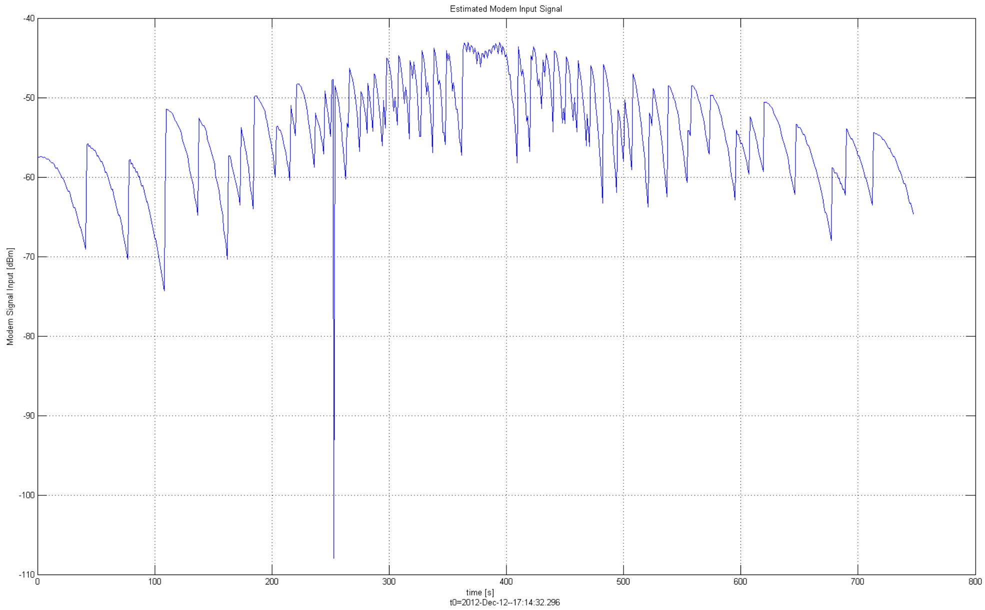

Figure 4.29: Calculated downlink signal for a simulated BRITE-Austria pass. In the calculation, a static modulation and data rate combination of BPSK and *32 kbit/s* was used.

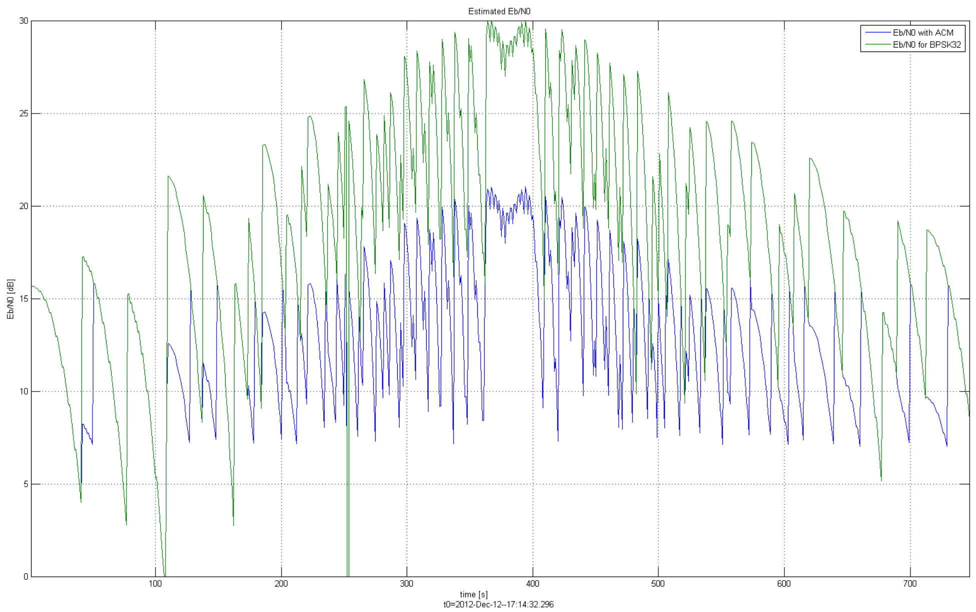

Figure 4.30: Comparison between E_b/N_0 with static data rate and with simple ACM for a simulated BRITE-Austria pass. The ACM scheme sets the modulation and data rate according to an E_b/N_0 threshold of *7 dB* between BPSK *32 kbit/s* and QPSK *256 kbit/s*.

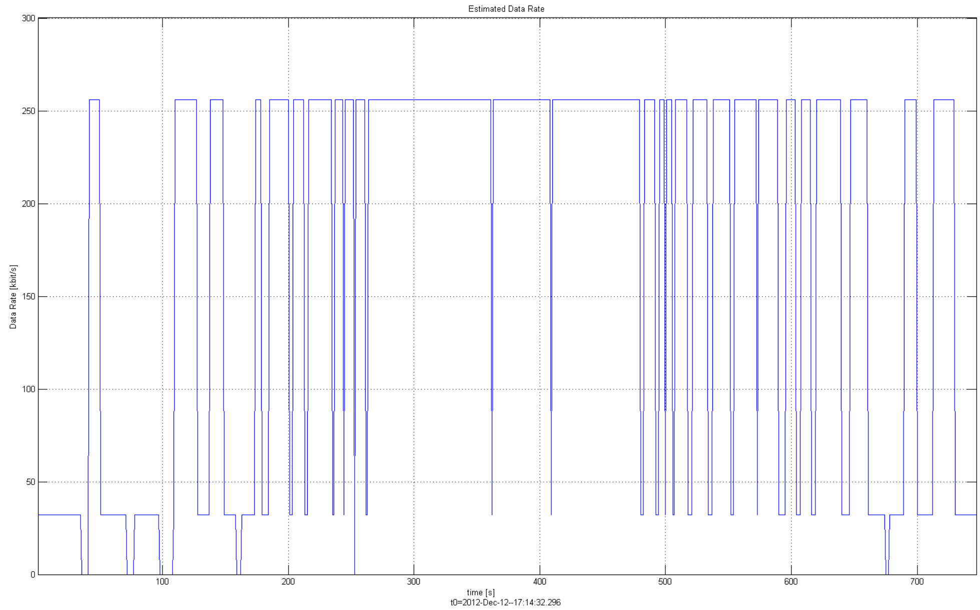

Figure 4.31: Estimated data rate with simple ACM for a simulated BRITE-Austria pass. The modulation scheme and data rate settings are switched between BPSK *32 kbit/s* and QPSK *256 kbit/s* (the minimum and maximum nominal setting). The results show that, for large portions of the contact, the maximum data rate setting can be used.

Table 4.10 shows the pass statistics for a simulated BRITE-Austria contact with the Graz ground station. The total contact time is calculated based on the STK simulated data, while the effective contact time only considers the portion of time during which the E_b/N_0 value is sufficient for allowing data download, based on the E_b/N_0 criterion for the minimum demanded E_b/N_0 of *7 dB*. By using this criterion for the effective contact time, no elevation mask specification is required. For practical reasons, the elevation mask for the Graz ground station defined in the simulation was set to $5°$, as this is the expected worst case for the visual horizon limitation. The comparison between the total and effective contact time of the simulation shows the difference between the theoretical maximum contact time of the ground station and the practical one. The results show that with the selected elevation mask there is no significant variation in the theoretical maximum and effective contact time.

Parameter	**Value**
Total Contact Time	747 s
Effective Contact Time	716 s
Data Download Amount (BPSK 32 kbit/s)	2864 KB
Data Download Amount (ACM)	8136 KB

Table 4.10: Pass statistics for a simulated BRITE-Austria pass over the Graz ground station. The results show that, with simple ACM switching between BPSK *32 kbit/s* and QPSK *256 kbit/s*, the data download amount can be increased by almost 3 times.

In addition, the statistics show the maximum expected data download amount. In this respect, a comparison between the usage of the static default *32 kbit/s* (BPSK) data rate setting and the implementation of simple ACM is provided. This simple ACM is implemented by the ground software, which measures constantly the E_b/N_0 of the modem, and adaptively increases the data rate to *256 kbit/s* with QPSK modulation provided that sufficient E_b/N_0 is available. The simulation results for this particular contact show that switching the data rate according to the link quality theoretically allows the download of almost three times the data amount compared to the static default data rate setting.

Chapter 5

In-Orbit Validation of the BRITE-Austria Nanosatellite and its Ground Station

After the successful launch of a spacecraft, the most critical task is to establish first contact with the satellite from ground. This represents a major milestone and is of great relief among the entire team involved throughout the different phases of the mission. Once contact is established, a first health check of the core satellite system is performed.

Subsequently, the commissioning phase starts, during which the correct functionality of all satellite systems is tested and the overall satellite performance in orbit is verified. This phase comprises a variety of test procedures to be carried out (often manually) at subsystem level by testing the performance of each individual item on the spacecraft. In order to assess the in-orbit behaviour of the spacecraft, tasks are performed sequentially and are usually dependent on each other. For instance, an attempt to control the spacecraft's attitude can only be initiated once correct attitude determination has been verified. The major milestones during this phase are the commissioning of the satellite bus followed by the commissioning of the payload(s). Once the commissioning phase has been successfully completed, nominal mission operations can begin.

From the ground station point of view, the in-orbit validation phase of the satellite represents a crucial phase to verify that the ground station provides the necessary capabilities to operate the mission. No matter how much testing and evaluation of the system performance has been carried out beforehand, only testing with the spacecraft in-orbit can fully verify the performance of the ground station.

This chapter deals with the in-orbit validation of the BRITE-Austria satellite as well as the validation of the design of its master ground station in Graz. After presenting the operations concept for the mission, results from the commissioning and early operations phases are shown, validating the performance of the ground station and operations concept.

5.1 BRITE-Austria Mission Operations Concept

As already mentioned in previous chapters, in the current configuration BRITE-Constellation eventually consists of six planned and five operational satellites. From the operations point of view, having a single ground station for operating all satellites in the constellation would be very challenging. Therefore, a ground station network is used, currently including three participating ground stations. A detailed description of the BRITE ground station network and its operating strategies is provided in Section 5.1.2.

An important aspect to be considered in the operations planning process is the selected satellite orbit, as its characteristics have a substantial impact on mission operations.

5.1.1 The BRITE-Austria Orbit and its Impact on Operations

The orbit of BRITE-Austria is a nearly circular, sun-synchronous polar, dawn-dusk Low Earth Orbit (LEO/SSPO) with a mean altitude of about *775 km*. Therefore, the satellite travels along the day/night boundary and passes the equator at dawn or dusk, yielding typically six contact times with the Graz ground station per day: three in the morning (about 4 to 8 AM local time) and three in the evening (about 6 to 10 PM local time). The above stated typical contact times represent a challenge for manual operations, requiring shift work. The organisation of operations with corresponding operations teams is described in detail in Section 5.4.

The orbital parameters of BRITE-Austria based on the Two-Line Elements (TLEs) are summarised in Table 5.1 for a sample TLE epoch of June, 1st 2013.

BRITE Austria Orbit Parameters	
Inclination	98.6280 deg
Eccentricity	0.001082 km
Right Ascension of Ascending Node	342.4715 deg
Argument of perigee	5.4949
Mean anomaly	354.6353 deg
Mean motion (revolutions/day)	14.3537

Table 5.1: **BRITE Austria orbital parameters.** The orbital parameters shown are provided by the NORAD Two Line Elements - Epoch date (UTC): 2013-06-01 06:18:14

For the TLEs in Table 5.1, the mean altitude of BRITE-Austria is *773.74 km*, yielding a semi-major axis of *7145.73 km*. From the orbital parameters, the orbital period of BRITE-Austria can be derived with Equation 5.1. In addition, the satellite velocity for apogee and perigee can be calculated according to Equation 5.2 and 5.3 [58]. As it can be seen from the calculations, BRITE-Austria has an orbital period of about 100 minutes, travelling at a velocity which varies between *7.4606 km/s* and *7.4768 km/s*.

$$T = 2 \cdot \pi \cdot \sqrt{\frac{a^3}{G \cdot M\oplus}} = 100.32min \quad (5.1)$$

$$v_{apogee} = \sqrt{\frac{G \cdot M\oplus}{a}} \cdot \sqrt{\frac{1-e}{1+e}} = 7.4606km/s \quad (5.2)$$

$$v_{perigee} = \sqrt{\frac{G \cdot M\oplus}{a}} \cdot \sqrt{\frac{1+e}{1-e}} = 7.4768km/s \quad (5.3)$$

with

a ... *semi-major axis*

e ... *eccentricity*

G ... *Earth gravitational constant*

$M\oplus$ ... *Earth mass*

The satellite velocity is an important parameter for the Doppler shift correction required for the transmit and receive frequencies at the ground station.

5.1.1.1 Satellite Range and Doppler Shift

The Doppler shift due to the relative movement of the satellite with respect to the ground station causes a shift in the frequency received by the satellite and the ground station [39], and needs to be corrected for both uplink and downlink frequencies used to ensure proper operations of the communication links.

An important parameter in this respect is the satellite velocity in the direction of the ground station, for which the maximum is at the maximum distance (slant range) of the satellite from the ground station. The maximum distance of the BRITE-Austria satellite to the Graz ground station can be calculated with Equation 5.4 and yields a maximum satellite distance as shown in Equation 5.5 at 0° of elevation from the ground station. The equations used in the following for the calculations related to the Doppler shift for BRITE-Austria are based on the description provided in [43].

$$d_{sat} = -r_E \cdot sin(\Theta) + \sqrt{r_E^2 \cdot sin(\Theta)^2 + r_S^2 - r_E^2} \quad (5.4)$$

with

r_E ... *Earth radius*

r_S ... *distance from centre of the Earth to the satellite*

Θ ... *ground station elevation angle*

$$d_{max}|_{\Theta=0} = 3233.43km \tag{5.5}$$

With the maximum distance of the satellite to the ground station the maximum satellite velocity in the direction of the ground station can be calculated. For this purpose, the angle between the satellite at the horizon β and the ground station is determined according to Equation 5.6 and the satellite velocity is then calculated according to Equation 5.7 [43].

$$\beta = arctan\frac{d_{max}}{r_E} \tag{5.6}$$

$$v_{RX,max} = v_{S,max} \cdot cos(\beta) = 6.6675km/s \tag{5.7}$$

The Doppler shift in the received satellite frequency can then be expressed by Equation 5.8 when the satellite is approaching the ground station, and by Equation 5.9 when the satellite is leaving from the ground station.

$$f_{RX,Doppler} = f_{TX} \cdot (1 + \frac{v_{RX,Sat}}{c}) \tag{5.8}$$

$$f_{RX,Doppler} = f_{TX} \cdot (1 - \frac{v_{RX,Sat}}{c}) \tag{5.9}$$

The Doppler shift can then be calculated accordingly with Equation 5.10 (under consideration of the speed of light c). For BRITE-Austria, the maximum Doppler shift yields ±9.7271 *kHz* (5.11) in the UHF uplink and to ±49.6938 *kHz* (5.12) in the S-band downlink.

$$f_{\Delta} = \pm f_{TX} \cdot (\frac{v_{RX,Sat}}{c}) \tag{5.10}$$

$$f_{\Delta TX} = \pm 9.7271kHz \tag{5.11}$$

$$f_{\Delta RX} = \pm 49.6938kHz \tag{5.12}$$

5.1.2 The BRITE Ground Station Network Operations Concept

The satellites of BRITE-Constellation are operated by the BRITE ground station network. This network has many advantages compared to a single ground station. It increases the link availability, allowing to operate satellites of the constellation in parallel, as well as to perform critical tasks from other stations within the network in case of unexpected behaviour of a particular satellite. In addition, redundancy is an important aspect. In case of unavailability of a ground station, another station in the network can temporarily take over operation tasks until this station is again operative.

Within the network, each satellite has a master ground station which at the same time also acts as mission control centre (MCC). The general operations concept foresees that each master ground station is in charge of its dedicated satellite(s) and tracks other satellites only in case of unavailability of the correspondent master station or in case of emergency. The participating ground stations and their role in the network are listed in Table 5.2.

Ground Station	**Operating Institution**	**Role in the Network**
Graz (Austria)	TU Graz/IKS	BRITE-Austria MCC
Toronto (Canada)	UTIAS/SFL	BRITE-Toronto and UniBRITE MCC
Warsaw (Poland)	SRC	BRITE-PL1 and BRITE-PL2 MCC

Table 5.2: BRITE ground station network. Currently the network includes three participating ground stations for which their role in the network is provided.

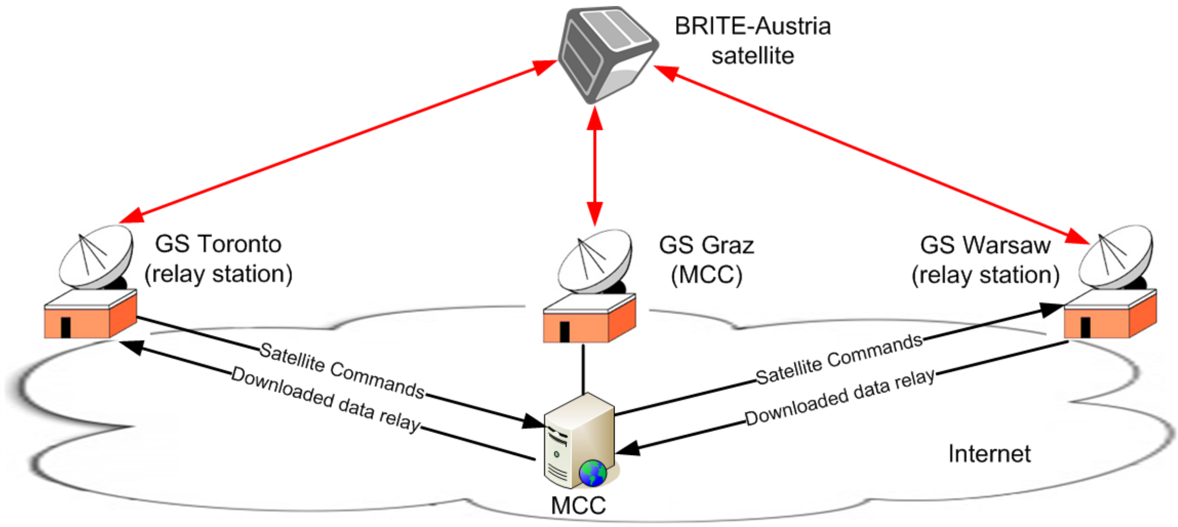

Figure 5.1: BRITE ground station network. The operations concept is shown for the BRITE-Austria satellite. While each ground station can physically establish contact with the spacecraft, the commands to be uploaded to the spacecraft and the downloaded data are handled by the mission control centre in Graz.

Each master station is responsible for its dedicated satellite(s) and is the only one nominally establishing contact and controlling the correspondent spacecraft. If other stations attempt to contact a satellite they are not in charge of, they normally act as relay stations. In this case, they uplink incoming commands from the respective mission control centre (MCC), and forward downloaded satellite data to the MCC without actually having access to the data itself. With this strategy, in case of malfunction of a master station its duties can be temporarily taken over by another station in the network without affecting mission control. An example of the BRITE ground station network operations and data flow is shown in Figure 5.1 for the BRITE-Austria satellite. While all stations can establish contact with the satellite, the entire data flow is handled by the BRITE-Austria MCC in Graz. Hereby, the data flow is handled by a distributed ground software concept. The implementation details for this distributed software architecture are described in Section 5.1.3.

The nominal mission operations concept therefore does not foresee the usage of the ground station network on a regular basis, but only for backup/contingency purposes. However, as BRITE-Constellation grows with more spacecraft in orbit needing to be operated, the ground station network is becoming a key aspect for operations. Practical experience has shown that the capabilities of the network should be increasingly exploited to a reasonable extent for the following purposes [59]:

- For contingency/recovery operations on spacecraft (the way it was planned to be from the beginning)
- To compensate for ground station outages as well as for maintenance or upgrade tasks (also planned originally)
- For commissioning support. This entirely new strategy has been successfully adopted to speed up commissioning procedures, especially during crucial tasks for which increased availability from ground is desirable
- To relieve from backlogs during intensive data collection periods or accumulated data due to ground based interference as described in Section 5.5.4.

With these new considerations the main purpose of ground station network operations within the BRITE mission has recently become to guarantee the maximum uptime of the different spacecraft within the constellation and to maximize the science data return. This can be accomplished by partial exploitation the ground station network, however without planning the network as an available resource on a regular basis.

Mission operations with the ground station network can in principle be handled fully automated thanks to its distributed architecture (see Section 5.1.3), provided adequate scheduling and prioritisation of spacecraft for any ground station in the network is available. This measure especially applies to the Toronto ground station, as it is used for operations of several GNB missions.

As operations over the network were not nominally planned from the beginning, a policy for coordination has been introduced. This policy foresees the formulation of requests to use a particular ground station in the network to the respective flight director and/or operators. In this regard, on-site support can also be requested, if needed. To keep the administrative effort low, permissions are often requested for a certain period (typically for entire shifts, days, or up to a week) and are granted provided conflicts with other spacecraft operations can be avoided.

5.1.2.1 Satellite Ground Segment Access

To characterise the link availability between BRITE-Austria and the ground segment, simulations have been carried out with the software *AGI Systems Toolkit (STK)* ®. Emphasis was put to the access of the spacecraft with the Graz ground station. In addition, an available model of the spacecraft has been used in the simulations to verify the satellite's attitude with respect to the ground station during contacts, as well as to define operational constraints in terms of exclusion angles for different Earth's regions (e.g. Antarctica) or celestial bodies (e.g. Sun or Moon), as shown in Figure 5.2 and Figure 5.3.

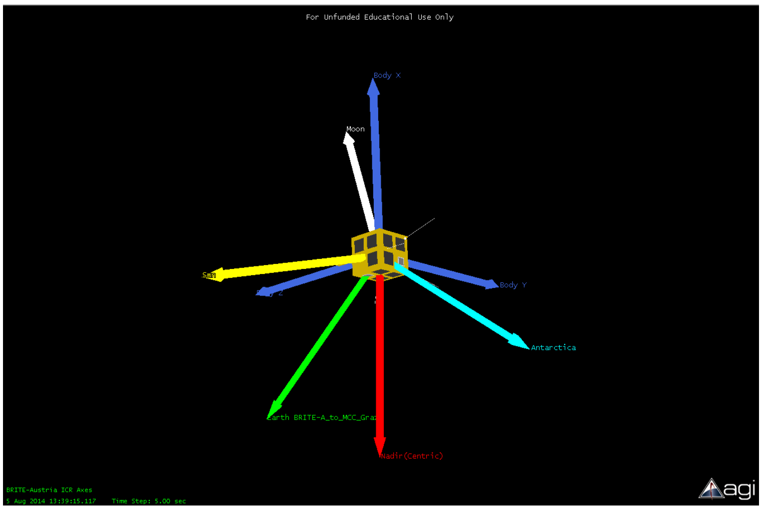

Figure 5.2: Graphical representation of the BRITE-Austria spacecraft's attitude. Different vectors have been defined to determine the spacecraft orientation with respect to Nadir, the ground station, as well as to other regions (Antarctica) and celestial bodies (Sun, Moon) required for the definition of operational constraints (image courtesy:STK)

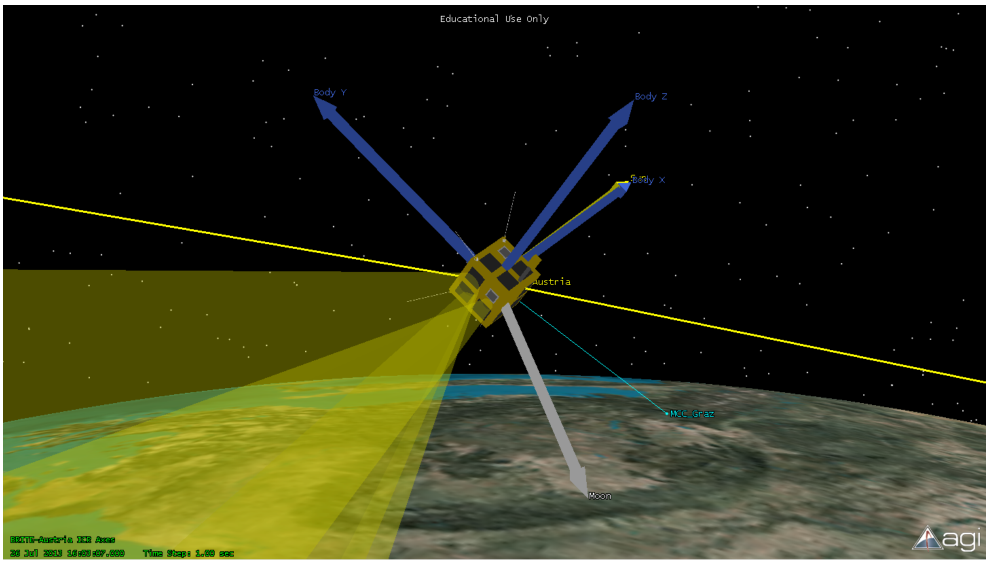

Figure 5.3: BRITE-Austria graphical representation in orbit. The image shows the spacecraft during a contact with the Graz ground station (image courtesy:STK)

A comparison between the coverage of the single Graz ground station and the current BRITE ground station network is shown in Figure 5.4 and Figure 5.5.

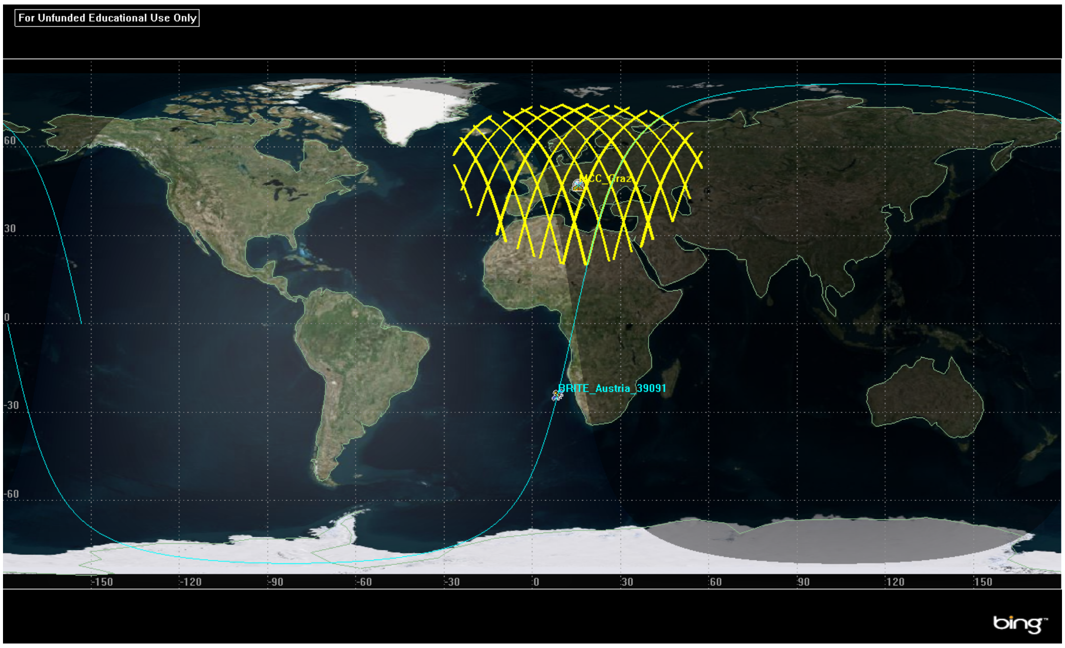

Figure 5.4: Graz ground station coverage. The coverage of the single Graz ground station includes Europe and a small part of Northern Africa. (image courtesy: STK)

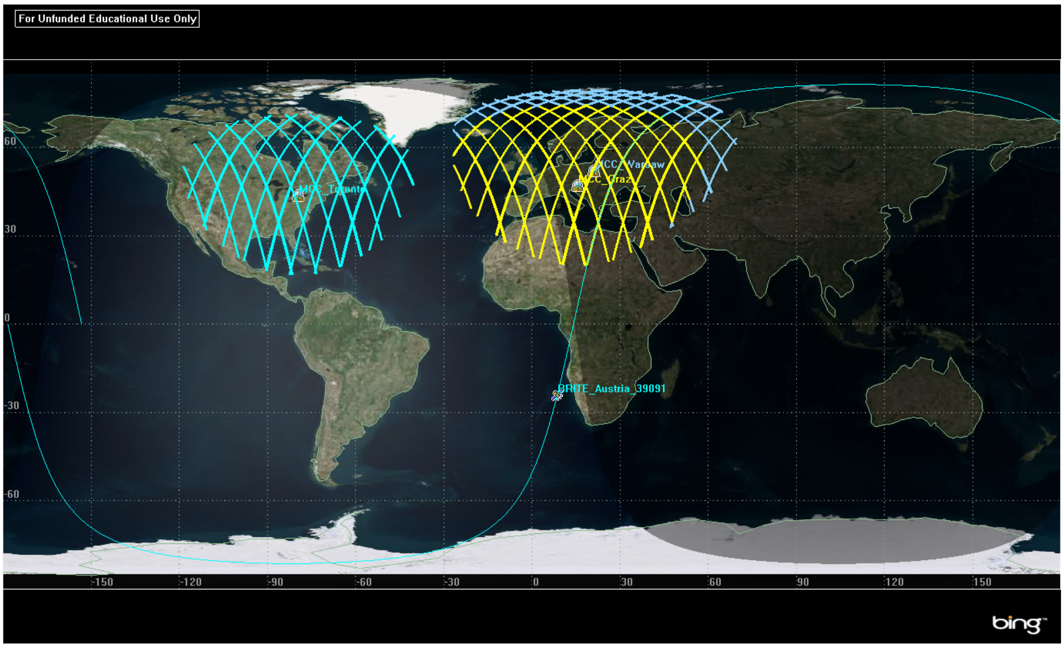

Figure 5.5: BRITE ground station network coverage. The coverage is increased compared to the single Graz ground station, including more Northern latitudes and Eastern longitudes in Europe as well as a large part of Northern America. (image courtesy: STK)

The increased availability of the network compared to the single ground station in terms of available contact time is shown in Figure 5.6 and Figure 5.7. The figures show that by using the ground station network contacts with BRITE-Austria could be established almost at every satellite orbit, while in comparison with the single Graz ground station typically only 6 out of 14 orbits are available per day.

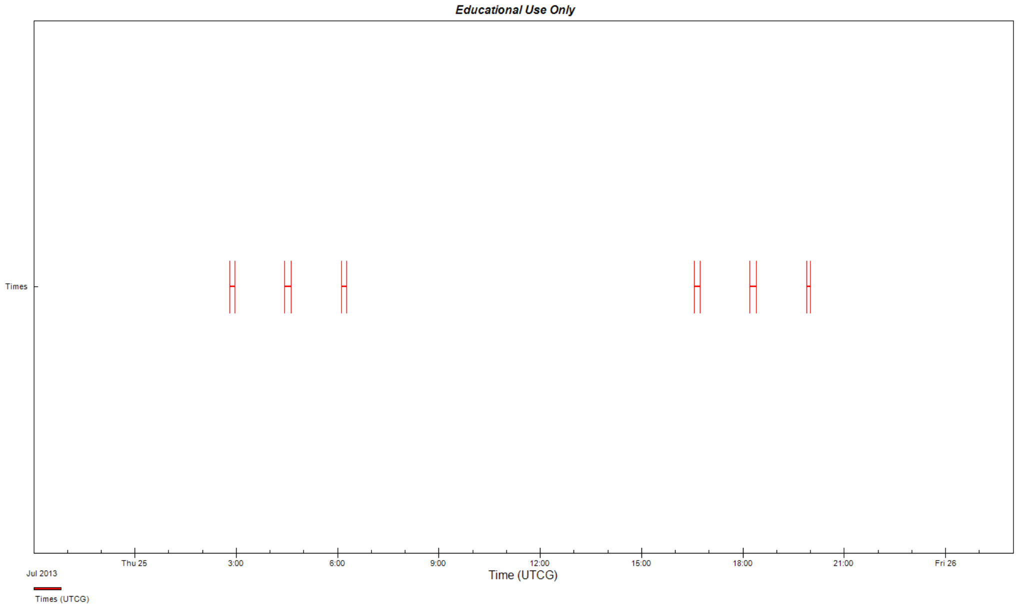

Figure 5.6: Satellite contact time with the single Graz ground station. Typically, six contacts with BRITE-Austria are possible per day in the early morning and late evening local time (image courtesy: STK)

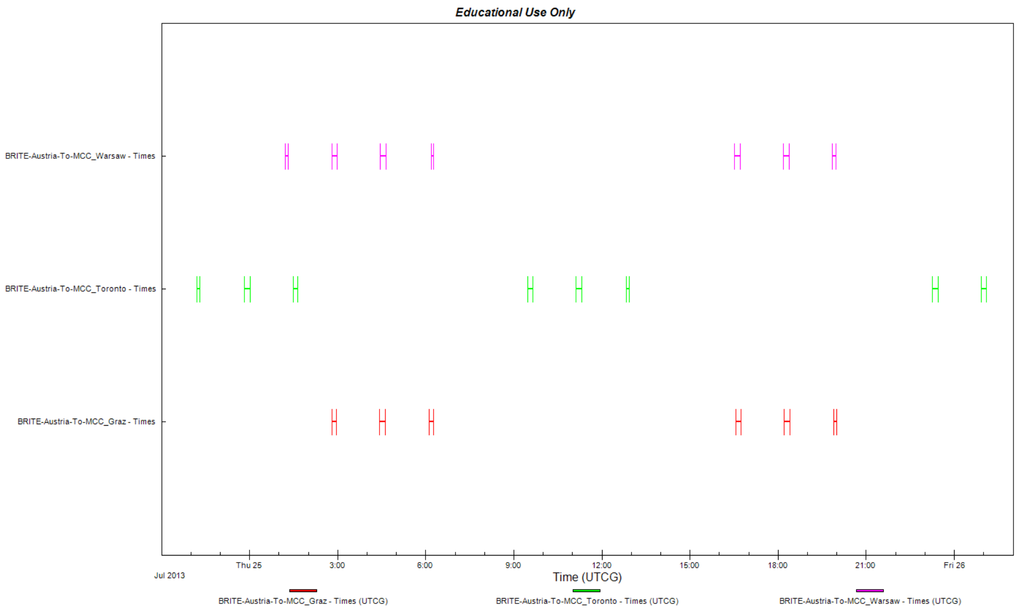

Figure 5.7: Satellite contact time with the BRITE ground station network. With the network, 12 contacts with BRITE-Austria per day would be possible, therefore only two orbits would not be trackable. (image courtesy: STK)

The plots depicted in Figure 5.8 show the azimuth and elevation course for a set of morning and evening passes on the same day of the spacecraft as seen from the Graz ground station. It can be seen that there are typically six contacts available per day. In both set of contacts (morning and evening), there is usually one low elevation Eastern, one high elevation, and one low elevation Western pass. In the morning, the satellite travels from South to North with respect to the ground station in Graz, while in the evening it travels in the opposite direction.

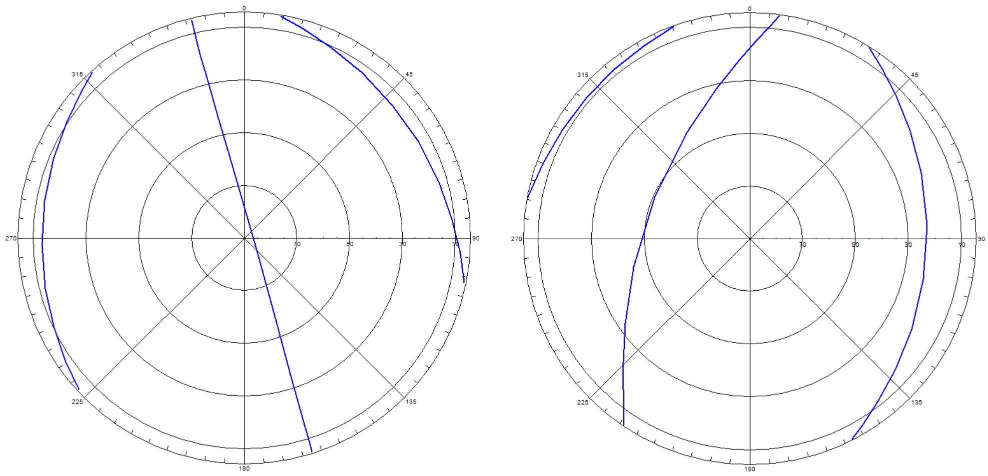

Figure 5.8: BRITE-Austria azimuth/elevation plot for a typical set of contacts with the Graz ground station. The contacts in the morning are shown on the left, the contacts in the evening on the right. In both cases, there is usually one Eastern, one high altitude, and one Western pass. In the morning, the satellite travels from South to North with respect to the ground station in Graz, while in the evening in the opposite direction.

5.1.3 Distributed Ground Software Concept

For operating the BRITE mission, the ground segment software design is based on a distributed software concept [60]. The software draws a distinction between a mission control centre and a ground station. A mission control centre (MCC) implements mission specific software, e.g. control software for the satellite for command upload, housekeeping telemetry analysis software, and payload operations software. For BRITE, the latter includes the science software, allowing for target and regions of interest (ROI) selection, for scheduling of observation periods, as well as for download and processing of the collected science data records. The interface to the ground station hardware (more precisely, the TNC), is accomplished by a packet multiplexing software running at mission control, allowing multiple satellite control and analysis software modules to interact with the spacecraft.

A particular ground station in the network does not need to implement the whole ground segment software suite. All it needs is a client version of the multiplexer software, which connects to an equivalent server instance running at the respective mission control centre via TCP/IP. This way, the client software gets incoming packets to be forwarded to the satellite and relays any kind of downloaded data from the satellite to the corresponding MCC. In addition to this minimal ground segment software configuration, a ground station in the network must have a compatible tracking software running to track the satellite, a compatible TNC as interface to the ground station hardware, and the ground station hardware itself.

Following this concept, mission control and ground stations can be logically separated, allowing mission control to be dislocated from a ground station, without having directly physical access to the satellite. Currently, for practical reasons, this possibility is not exploited by any mission control centre within the BRITE ground station network. However, the advantages of this operations concept become clear for operations over the ground station network. In addition, the concept is scalable to add new relay ground stations to the network.

A rough schematic of the distributed software concept is shown in Figure 5.9. It shows the basic interaction between the ground station hardware, the automated software modules for distributed software operations, acting as a bridge between mission control centres and ground stations (green), as well as generic satellite specific software running at mission control (blue).

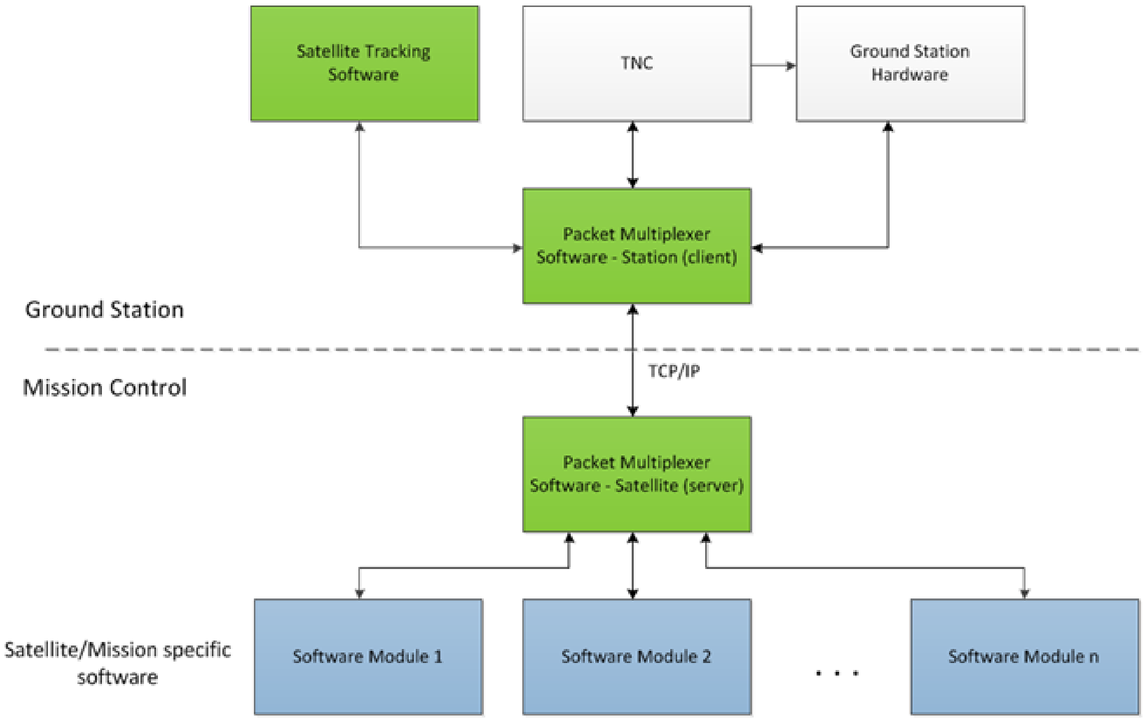

Figure 5.9: BRITE distributed ground software concept. The white boxes describe ground station hardware components, required at every ground station, green boxes represent software modules for different software operations, which allow seamless interconnection of mission control with any ground station in the network, while the blue boxes represent satellite specific software running at the mission control centre only.

5.1.3.1 Automatic Operations and Remote Access

The ground software architecture is conceived such that operations can be performed fully automated [5]. Automated software modules for satellite tracking as well as for command upload and download are used. In case of unexpected behaviour of the spacecraft, automated telemetry validation software generates alarms. An immediate notification along with the complete pass information is sent to the operators via e-mail.

Similarly, remote access for monitoring and control of the ground station is provided to the operators (authorisation provided by the local frequency bureau). For the BRITE-Austria master station in Graz, operators can log in remotely to the ground station PCs used for operations via the remote desktop software *TeamViewer®* from any PC as well as from mobile devices such their smart phones/tablets, as shown in Figure 5.10. For security reasons, the ground station PC accesses are password protected, and in addition operators have to establish a virtual private network (VPN) connection to the TU Graz network to make sure they are (virtually) in the same network as the mission control centre. This remote connection allows operators to have full access to the ground station and perform operations of the satellite remotely, provided that the ground station hardware is running nominally. For most of the ground station hardware, PC software is available to monitor its status so that remotely logged in operators can identify potential issues with the ground station hardware in case of anomalies detected during operations. A camera on the antenna tower is also available to monitor the tracking status as shown in Figure 5.10.

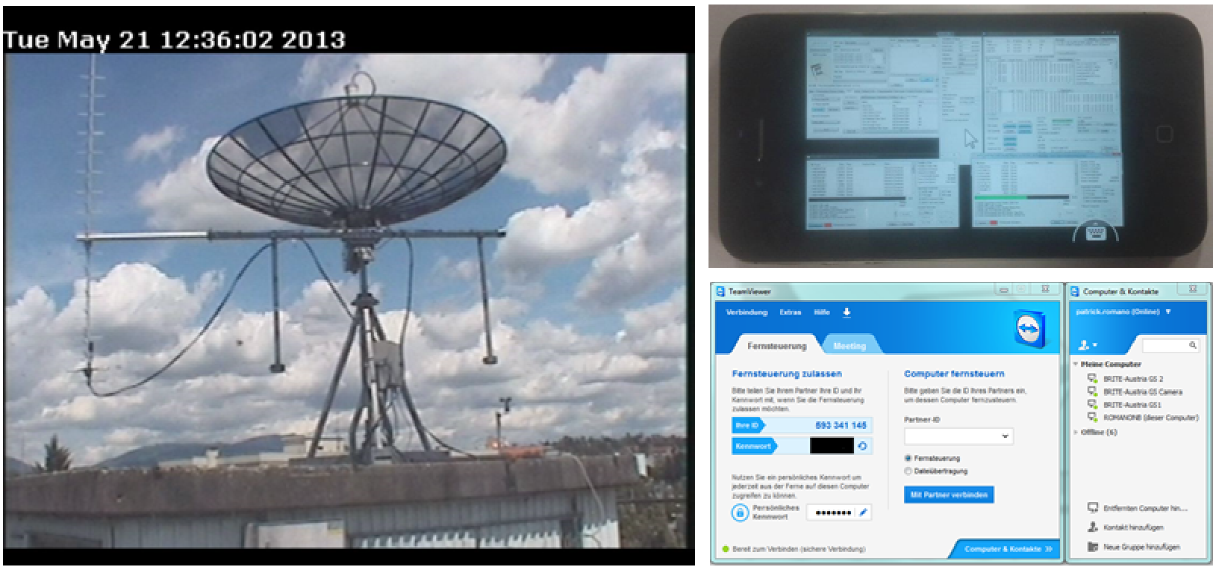

Figure 5.10: BRITE-Austria mission control remote access. Operators can log in from their mobile devices, such as smartphones for remote operations of the spacecraft (top right). A remote view of the antenna tower camera is shown top left, while the *TeamViewer®* login window is shown on the bottom right.

Although the many benefits, these remote operations are not meant as nominal procedures. Critical commissioning tasks have not been performed in this manner. However, this configuration is very practical for remotely monitoring contacts during which only routine tasks have to be performed, especially during morning shifts or weekends. It also provides a simple and quick way for troubleshooting. Besides remote operations as well as regular monitoring of the ground station status, remote access allows operators to assess anomalies in urgent cases without the need of their physical presence.

5.2 BRITE-Austria Ground Segment Software

To operate the BRITE-Austria mission, different types of software are used. As described in Section 5.1, the BRITE-Austria ground segment software (GSS) consists of mission specific software to operate the spacecraft and ground station specific software to operate the ground station. Substantial part of the ground segment software used for operating BRITE-Constellation has been developed for predecessor Generic Nanosatellite Bus (GNB) missions by UTIAS/SFL and has been adapted for the BRITE mission. The BRITE science software has been specifically developed for BRITE to operate the instrument and process the scientific data. While the mission specific software is common for all mission control centres, some of the ground station software has to be customised for each ground station according to the components used.

Figure 5.11 shows the BRITE-Austria ground segment software based on [61], including BRITE mission specific software as well as the Graz ground station specific software. The ground segment software can be basically divided in:

- Automated software (green)
- Real-time software (blue)
- Planning software (yellow)

The following sections give an overview about the main ground segment software modules [62] [61] and describe the new software modules developed in the framework of this thesis to operate the BRITE-Austria mission in more detail.

5.2.1 Common Ground Software Components

Common ground software components describe software modules present at all ground stations and used for operating BRITE satellites, irrespective of whether the ground station acts as mission control centre or just as relay station. These common components include mainly three pieces of software: the satellite tracking software (see Section 5.2.3), the software running on the terminal node controller (TNC), as well as a packet multiplexing software as interface for all other ground segment software.

The software on the TNC is responsible for creating the interface between the ground segment software and the ground station hardware. The TNC consists of a *Linux* based Advanced RISC Machines (ARM) board attached to a custom expansion card which provides the interfaces for the UHF transceiver and S-band modem [62]. In addition, the TNC expansion card has the capability to act as rotator interface, although this functionality is not used by the BRITE-Austria ground station in Graz as the interface is not compatible with the rotators used. The software running on the TNC is *UNIX* based and implements a serial communications controller (SCC) driver, which functions as communications relay between the ground segment software and the spacecraft.

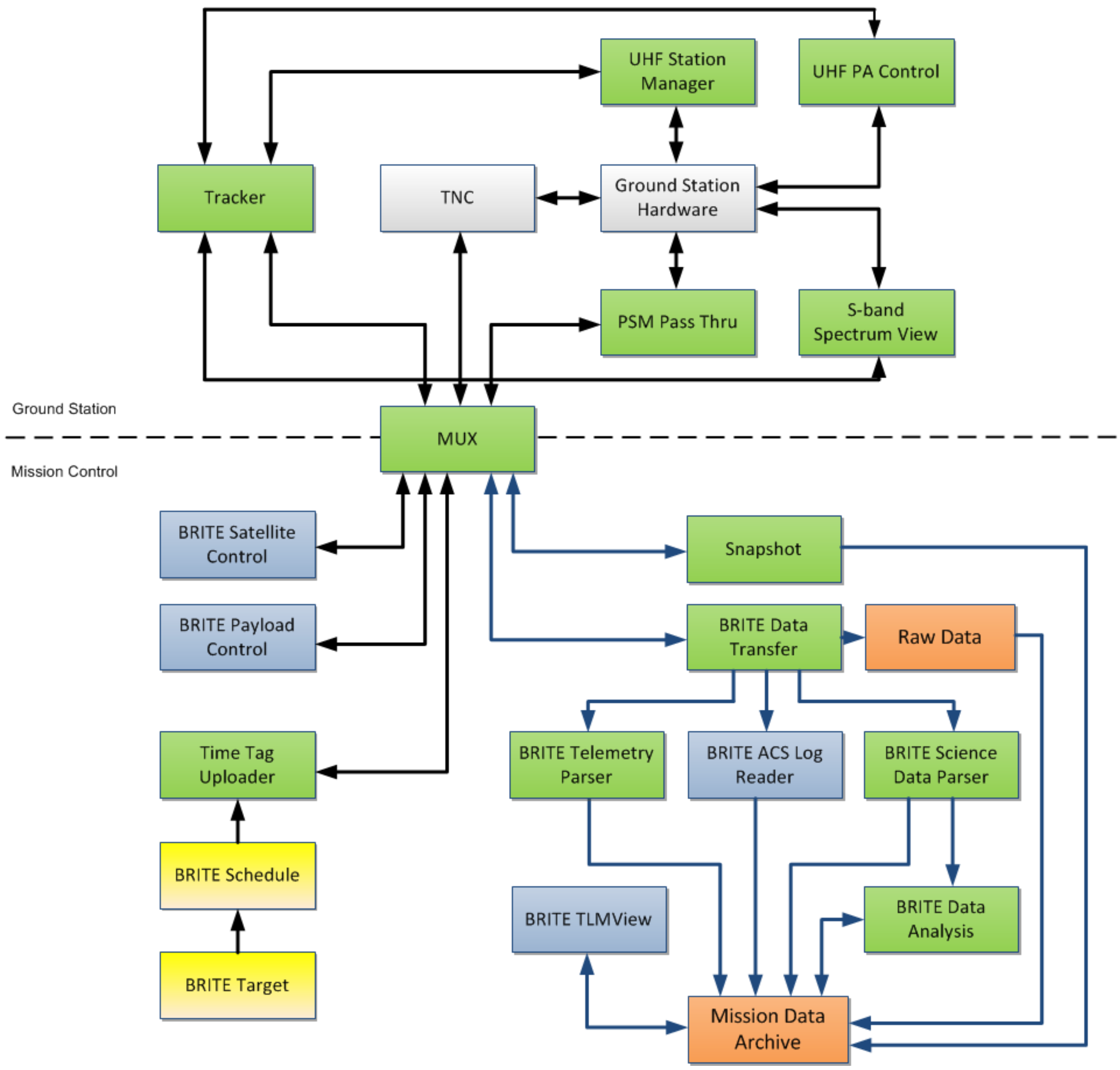

Figure 5.11: BRITE-Austria ground segment software including Graz ground station specific software. The green boxes describe automated software modules, the blue boxes real-time software, while the planning software is shown in yellow boxes.

On the uplink, the TNC gets the multiplexed input packets from the ground software, received by TCP/IP, and provides them as bit stream to the GMSK modem. The modulated baseband signal is then forwarded to the *Yaesu FT897D* transceiver for up-conversion and transmission. On the downlink, the TNC gets the demodulated baseband signal from the satellite modem and encapsulates the received data for transmission via TCP/IP to the ground software. In both directions, the data packet encapsulation is performed using the Nanosatellite Protocol (NSP) developed by UTIAS/SFL, encapsulated in High-Level Data Link Control (HDLC) frames, based on the $AX.25$ link layer protocol commonly used in the radio amateur community [63].

The software module on top of the ground segment software is the *BRITE Multiplexer (MUX)* software [62]. This software module represents the general interface between the TNC - and hence the ground station hardware - and all other ground segment software modules. *MUX* allows connections from different software modules by creating TCP/IP sockets with unique identifiers. The incoming data packets from different modules are multiplexed to command sequences to be uplinked to the satellite. Similarly, on the receiving path, the software demultiplexes the incoming packet stream from the satellite, and redirects the data packets to the correspondent requesting software module by the destination fields specified in the satellite replies.

As already mentioned in Section 5.1.3, the packet multiplexing software can be used in a server-client configuration. In this configuration, a server instance of the software runs at mission control, serving as interface for the different generic and satellite specific software used for operations, while a client instance runs at any ground station in the ground segment network, relaying incoming packets from the server and acting as interface to the respective ground station.

5.2.2 Real-time Satellite Control Software

Real time satellite control software is required for operating the spacecraft during contacts with the ground station, allowing operators to actively interact with the satellite.

The responsible software for establishing contact with the satellite is *BRITE Multiplexer (MUX)*. For that purpose, it sends so-called "$TxSelect$" commands to the S-band transmitter on-board the spacecraft via the selected on-board computer (the housekeeping computer is used as default), including modulation and data rate settings to be used. In addition, for each $TxSelect$ command issued in automatic mode, a timer value in seconds is generated and sent to the S-band transmitter according to the remaining contact time, in order to turn off the S-band transmitter on-board automatically at the end of the pass. This ensures that the S-band transmitter is turned off in any case at the end of a pass. A pre-set modulation and data rate setting is used for satellite acquisition. During a contact, the data rate can be either adapted manually by the operators, or an automatic dynamic data rate adjustment can be used. The latter provides the implementation of simple Adaptive Coding and Modulation (ACM), where, according to the link quality rated by the measured E_b/N_0 values from the satellite modem, the modulation and data rate settings are adapted accordingly for achieving the best performance.

Another crucial functionality provided by the multiplexer software is the implementation of the basic satellite commands for system resets, the so-called "$Firecodes$". These commands are meant to turn on/off or reset the housekeeping or attitude control computer (for first start-up of the system after launch and for contingency/recovery) as well as to perform a general power system reset for emergency, after which the satellite will return to kick-off mode.

Satellite acquisition is usually performed automatically. For that purpose, *MUX* connects to the BRITE tracking software *Tracker* to retrieve the current tracking status, and automatically attempts acquisition of the satellite(s) selected at pass begin at the respective ground station. In addition, the software provides a countdown showing the time left during the pass or the time remaining until the next contact.

The primary user interface to the satellite is the *BRITE Control* software. It includes any possible command understood by the spacecraft, allowing to select the on-board computer to communicate with in bootloader or application software mode.

In bootloader mode, the functionality is mainly limited to basic housekeeping and manual operations, such as setting and querying switches states, sending basic commands (such as ”Ping” or commands to enable communications between OBCs), as well as customised commands or file uploads, including scripts to carry out test routines or to load application code.

In application mode, the software provides the full suite of commands required for satellite operations in different tabs. The whole attitude thread can be controlled via the control software on the attitude control computer. The software not only allows to initialise and run the attitude thread as well as to switch between attitude modes, but it also provides an interface to the array of values to be exchanged between the application code and the attitude software as well as to the attitude settings. In addition, the software allows to read out telemetry from the whole attitude thread as well as any available telemetry from individual sensors/actuators. This functionality is further extended by a customs command tab, through which any specific command can be manually sent to a particular system on the spacecraft by using a destination identifier.

Additional real time satellite software includes *BRITE Payload Control* for manual payload operations, which has been mainly used during testing and commissioning of the payload.

5.2.3 Automated Satellite Operations Software

The BRITE-Austria ground segment software provides capabilities for automatic operations of the satellite. All routine operation tasks can be handled fully automated.

At the beginning of every satellite pass it is crucial to verify the current health state of the spacecraft. For that purpose, a telemetry snapshot is obtained by automated software at the beginning of any pass by reading out the most essential satellite telemetry. After the telemetry readout process has been completed, the software generates an automated e-mail report including alarm notifications, that is forwarded to an operations mailing list accessible to all BRITE-Austria operators.

Unless other actions are required, after checking basic satellite telemetry the normal procedure is to download data collected by the spacecraft. For that purpose, automated data transfer software is used, which continuously checks the circular memory buffers of the different on-board computers on the spacecraft, and downloads any available data. Typically, this includes Whole Orbit Data (WOD), containing all available satellite telemetry, as well as science data in the form of Science Data Records (SDR). Various criteria for prioritisation of file downloads can be defined, e.g. concerning file types or creation dates. For each downloaded file, integrity checks are performed by Cyclic Redundancy Checksums (CRC) and after successful download the file is marked to be deleted. File deletion will be carried out cumulatively once a certain predefined number of files marked for deletion is reached. Next to automatic file download, time tag command uploads can be handled automatically to upload a predefined queue of commands [59]. Time tag commands are used for satellite setup and configuration for long-term planning of observations, as described in detail in Section 5.4.2. Additional automated satellite operations software include science data and satellite telemetry parsers for further manual and/or automated processing and analysis.

5.2.4 Automated Ground Station Operations Software

In order to monitor and control the ground station hardware remotely as well as to allow automatic operations during a contact with the satellite, different software modules interfacing with the ground station hardware are used.

5.2.4.1 Tracking

The most essential automated software interfacing with the ground station hardware is the tracking software to allow automatic satellite tracking during a pass over the ground station. For the BRITE mission, this is performed by the software *Tracker*®. A screenshot of the software is shown in Figure 5.12.

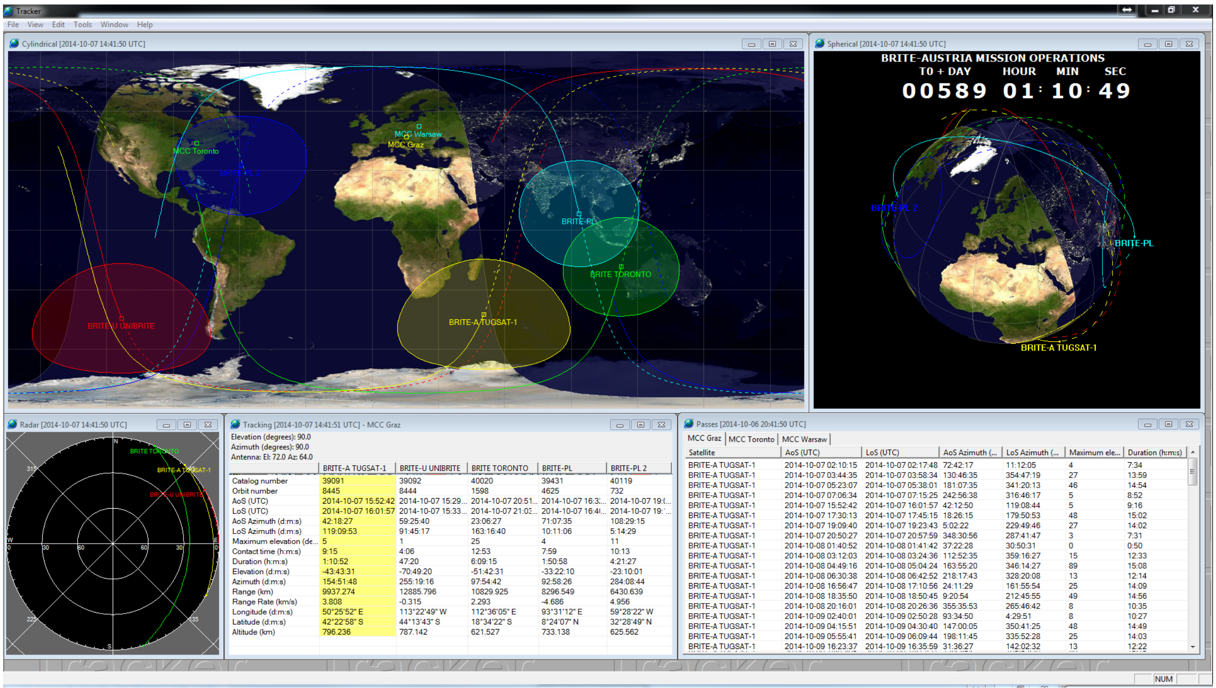

Figure 5.12: Screenshot of the Tracker software used for BRITE-Austria tracking. The software provides a tracking view for different satellites to be tracked, a pass summary, as well as the definition of different graphical visualisations - in the current selection, a 2D and 3D view as well as a radar view are selected.

Tracker controls both azimuth and elevation antenna rotators by communicating with the ERC-M rotator interface described in Chapter 3 and calculates the contact times of the ground station with the spacecraft. In addition, it allows tracking of multiple satellites for operating BRITE-constellation and/or other missions. Furthermore, it allows automatic two line elements (TLE) updates in customisable update intervals (down to a daily basis) as well as to specify the TLE source - either the Celestrak database (free access) [64] or Space-Track [65] by providing a login information. For taking into account special characteristics of a particular ground station, horizon masks can be defined to exclude to track passes below certain elevations if they are not trackable due to certain limitations (e.g., terrain). In addition, tracking offsets can be customised to counteract lags in the tracking or tracking accuracy. The offsets can be defined individually for each rotator and its direction in degrees as well as cumulatively for all rotators in time. For the Graz ground station, fixed offsets have been defined in degrees for both rotators in each of their possible directions as part of the calibration and in addition, time offsets are used to compensate tracking lags. The general trend for time offsets at the Graz ground station is to allow the rotators to point ahead in time typically by 1 to 2 seconds. This parameter can further be tuned in real time during a pass to obtain the best performance.

A crucial functionality provided by *Tracker* is the ability to create TCP/IP sockets, allowing communication to other BRITE ground segment software modules. *Tracker* supports multiple socket connections and provides the current tracking information such as antenna position, tracking status, as well as the identifier of the tracked object. Every ground software module uses this information to start operating automatically when a contact with the ground station starts and to stop when the contact is over.

5.2.4.2 Satellite Uplink Control

In order to establish contact with a BRITE satellite, the S-band downlink of the spacecraft has to be activated by the ground station by sending a so-called "$TxSelect$" command via the *BRITE Multiplexer* software. In order to successfully execute this command, it has to be ensured that the uplink is operating correctly, i.e. the transceiver and power amplifier are generating the expected uplink signal. Therefore, uplink control of the ground station is performed by different software modules having the capability to operate in an automated fashion by retrieving pass information from *Tracker*. This includes two software modules, to interface with the UHF transceiver and the UHF power amplifier, respectively.

The interface to the *Yaesu FT-897D* transceiver used for the uplink is established by a software called *UHF Station Manager* [61]. The software connects to the transceiver via a `COM` port, allowing to perform frequency and output power settings of the transceiver. For operations, it allows setting the Push To Talk (PTT) of the transceiver, both manually or in an automatic fashion. In addition, it performs automatic correction of the transmit frequency according to the Doppler shift at any given time during a pass. The threshold for adjusting the frequency is *1 kHz*. In order to perform this frequency adjustment, the software needs to temporarily unkey the transceiver, as the two commands cannot be sent simultaneously to the transceiver. Therefore, the transceiver is unkeyed for *100 ms* every time a Doppler shift correction is performed.

As already mentioned, the software can be configured to run automated by keying the transceiver when a pass begins and stopping to transmit when a pass is over. For this purpose, the software connects to *Tracker* to retrieve the corresponding tracking information. In addition, multiple satellite identifier can be specified, allowing the software to key the transceiver only if one of the satellites in the list is selected. This prevents to mistakenly contacting another satellite if tracking is enabled.

UHF Station Manager is used in every BRITE ground station, because a *Yaesu FT-897D* transceiver is always used for the UHF uplink, and is therefore part of the BRITE ground segment software architecture [61].

UHF Power Amplifier Control

For the UHF power amplifier, different considerations apply. As the power amplifier does not interface to the TNC and is used to amplify the uplink signal which has been already up-converted and pre-amplified by the Yaesu transceiver, depending on power demands, design choices, and not least budget constraints, the power amplifier used might differ depending on the ground station. As described in Chapter 3, for the BRITE-Austria master ground station in Graz, a *BEKO HLV-550* UHF power amplifier is used. This amplifier provides a remote control interface; however, no standard remote control software is available. Therefore, in the context of this thesis, suitable hardware and software interfaces were developed and configured for remote monitoring and control of the power amplifier as well as for automatic operations during satellite contacts with the Graz ground station.

In order to set the power amplifier switches by remote interface, the concept was to use a hardware interface with compatible relay switches with a simple software interface to develop a GUI. A simple, flexible, and cost effective hardware solution was found in the *National Instruments*® *NI-6008* USB interface, which provides several analogue and digital inputs/outputs with suitable voltage levels to act as relay switches for the power amplifier. This interface is compatible with the *NI LabView*® development software environment, which allows simple implementation of instrument monitoring and control GUIs.

Once the correct behaviour and interfacing of the hardware with the power amplifier was verified, a software module for remote monitoring and control, as well as for automated operations was developed: the *UHF PA Control* software. Figure 5.13 shows the GUI of *UHF PA Control* in action during a BRITE-Austria pass over the Graz ground station.

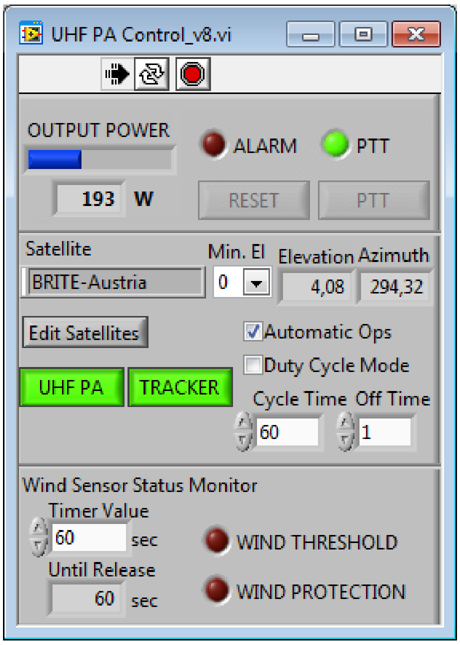

Figure 5.13: ***UHF PA Control* software used for monitoring and control of the UHF power amplifier.** The software in action during a BRITE-Austria contact with the Graz ground station is shown. Automatic operations enables transmission when the satellite is in pass.

The power amplifier monitoring functionality of the software includes telemetry readout of the measured output RF power as well as a global alarm state. As described in Chapter 3, when the power amplifier raises an alarm, three possible causes are specified and displayed on the front panel:

- *Antenna*, in case there is an issue causing power mismatch on the path to the antenna
- *Overdrive*, in case the input power fed into the amplifier is too high
- *Temperature*, in case overheating of the amplifier has occurred

Unfortunately, the remote interface of the power amplifier only reports a general alarm state without specifying the cause, hence this functionality is not available in the software. In case an alarm state is detected, manual inspection of the cause is required by an operator.

The control functionality of *UHF PA Control* allows to turn on and off the `PTT` and `RESET` switches on the power amplifier. The latter can be used to reset the power amplifier after an alarm state has occurred. This function should be used carefully and only after inspecting the cause of the alarm. In particular, this switch should be only commanded by an operator when physically present at the ground station, as the alarm cause is not provided by the software.

For automated operations of the software, an "Automatic Operations" check-box can be set. If selected, a socket connection to the tracking software *Tracker* is established to retrieve tracking information. When in pass, the `PTT` of the power amplifier will be automatically set, and automatically released after pass end. The satellite selected for tracking in the *Tracker* software is automatically operated when in view. *UHF PA Control* keeps a satellite list with entries of the satellites allowed to be operated. By comparison of the entries in this list with the current satellite selection in *Tracker* the software prevents transmitting mistakenly to another spacecraft. The current elevation and azimuth values are also retrieved from the tracking software and displayed. In addition, a minimum elevation threshold can be set, from where on to start/stop transmitting. This is a useful feature to prevent transmitting with high power levels at low elevations when subject to limitations, e.g. due to interference or terrain.

In addition, a duty cycle operations mode is available, allowing to define a duty cycle interval according to which the `PTT` will be periodically turned off for a selected time period. This mode has been implemented to relieve the amplifier and antennas from continuous operations with high power, as prevention from thermal issues as well as overdrive effects.

As already mentioned, the National Instrument USB interface used by *UHF PA Control* provides several analogue and digital inputs/outputs. This interface was also found to be practical for retrieving the status of the wind sensor installed on the antenna tower of the ground station. Therefore, this additional functionality has been implemented in the *UHF PA Control* software module. The wind sensor status monitor utility within the software retrieves the current wind sensor threshold status. If the threshold is reached, it activates a counter for the remaining time of the antenna in the elevation parking position and sets the "Wind Protection" status flag until the counter time has elapsed.

For safety reasons, no control or configuration to the wind sensors is allowed in the software, as this would override the hardware protection implemented. In case the wind threshold is reached and wind protection is activated, an automated email report is generated and sent to the operators mailing list. In addition, the power amplifier's `PTT` is deactivated for the duration of the wind protection activation. The wind sensor monitoring utility therefore represents a useful feature to detect the current wind situation at the ground station especially during remote operations.

5.2.4.3 Satellite Downlink Monitoring and Control

As the downlink is mostly affected by the tracking performance as well as by possible link impairments due to the higher frequency compared to the uplink, it is essential to monitor the receiving signal status at the ground station. In addition, according to the link quality measured by the signal to noise ratio (SNR) of the received signal, the modulation and data rate settings for the downlink can be varied to increase the throughput. Therefore, downlink monitoring and control of the ground station is performed by different software modules interfacing with the satellite modem and with a spectrum analyser for signal measurements.

For interfacing with the satellite modem, the software *PSM Pass Thru* is used. The software retrieves the demodulator status (lock status, input level, frequency, modulation and data rate settings, frequency offset, E_b/N_0) and is able to set modulation/data rate. *PSM Pass Thru* interfaces with the multiplexer software, forwarding the current configuration for visualisation, and accepting configuration inputs to change the modulation and data rate settings. The multiplexer software uses this setting to adapt the data rate automatically according to the link quality rating from the retrieved E_b/N_0.

S-band Spectrum View

In addition to the downlink signal measurements from the satellite modem used for automatic adaptation of the downlink parameters, another important figure to be monitored during pass is the signal spectrum, which is measured by a spectrum analyser. While the spectrum can be read from the analyser directly, visualisation software on the computer screen is more advantageous while operating, and in addition allows monitoring the spectrum during remote operations.

For this purpose, the *S-band Spectrum View* software has been developed in the context of this work. The software connects to the *Rohde&Schwarz®* *FSH3* spectrum analyser, performs the desired configuration settings, collects the current samples of a spectrum analyser sweep and displays the correspondent signal spectrum. The software was realised as *NI LabView®* GUI, as libraries for the used spectrum analyser were already available. These libraries include functions to display the spectrum as well as to perform a variety of configuration settings.

The software combines and extends the available functionality of the standard *LabView* libraries for the spectrum analyser to a GUI tailored for operations of BRITE-Austria, providing the following functionality:

- Configure the basic receive signal settings, such as the centre frequency, span and expected bandwidth of the signal. The expected signal bandwidth is set by selecting the current modulation and data rate setting used. The software calculates the absolute signal bandwidth used for transmission accordingly.
- Configure additional settings of the spectrum analyser, such as the used detector and trace, RF signal reference level, as well as resolution and video bandwidth.
- The satellite to be operated is automatically retrieved from *Tracker* and enabled when in view in automatic operation mode. This way, the software will start to measure and log data only during a pass according to the selected satellite.
- A separate log will be created for every tracked pass, including the average signal level, the average noise level, as well as the calculated signal to noise ratio with the corresponding timestamps, with resolution of one second.
- Retrieve and display tracking information such as elevation and azimuth values whenever the connection to *Tracker* is selected. Note that, when not in pass, the elevation value will be negative; the changing values indicate that the software is still running and the connection to *Tracker* is still operative.
- Read and display the spectrum of the received signal and calculate an estimation for the signal to noise ratio, according to the specified signal bandwidth. For this calculation, every measured power level within the specified bandwidth is averaged and contributes to the measured signal level, while every power level outside this bandwidth is averaged and contributes to the average noise level. It has to be noted that the measured signal level actually corresponds to the signal plus noise power level $S+N$, as the noise power N is superimposed to the signal power. Therefore, the result of the measurement is actually the $(S+N)/N$ instead of the signal to noise ratio S/N. The signal to noise ratio S/N is further calculated and displayed by the software by using Equation 5.13 [53].
- Calculate the Doppler shift for the downlink satellite signal. This is calculated according to the nominal frequency received by the satellite, the satellite's distance, relative velocity as perceived by the ground station, and is determined according to the satellite's position relatively to the ground station during a pass according to the equations described in Section 5.1.1. The latter is performed by taking the current elevation antenna position obtained by the connection with *Tracker*; furthermore, by determining whether the elevation is ascending or descending, the direction of the frequency shift due to the Doppler effect is identified. The Doppler shift calculation is essential for the measurement of the signal to noise ratio, otherwise the detection of the signal bandwidth would be shifted and hence, not accurate.

- Record a snapshot of the current spectrum by collecting all currently displayed samples obtained by the spectrum analyser (301 as default). These values can be used for later processing and for instance to generate plots of the collected spectrum values.

$$(\frac{S}{N})_{dB} = 10 \cdot log_{10} \cdot (10^{\frac{\frac{S+N}{N}dB}{10}} - 1) \tag{5.13}$$

The *S-band Spectrum View* software further provides a calibration mode. To utilise this mode, the control of the rotators need to be deactivated from the *Tracker* software, and the S-band reference calibration transmitter located at the Lustbühel observatory needs to be turned on. The software then takes over control of the rotators and moves the antenna to the predefined position for best signal reception of the calibration transmitter, measures the average received power level and compares it with the expected value for optimal calibration. If the two values differ significantly (i.e. more than 1-2 dB), a new rotator calibration is recommended.

Figure 5.14 shows the GUI of the *S-band Spectrum View* software in action during a BRITE-Austria contact with the Graz ground station, while Figure 5.15 shows the *S-band Spectrum View* software in calibration mode. The latter figure shows an optimal calibration, as the measured signal level matches perfectly with the expected one.

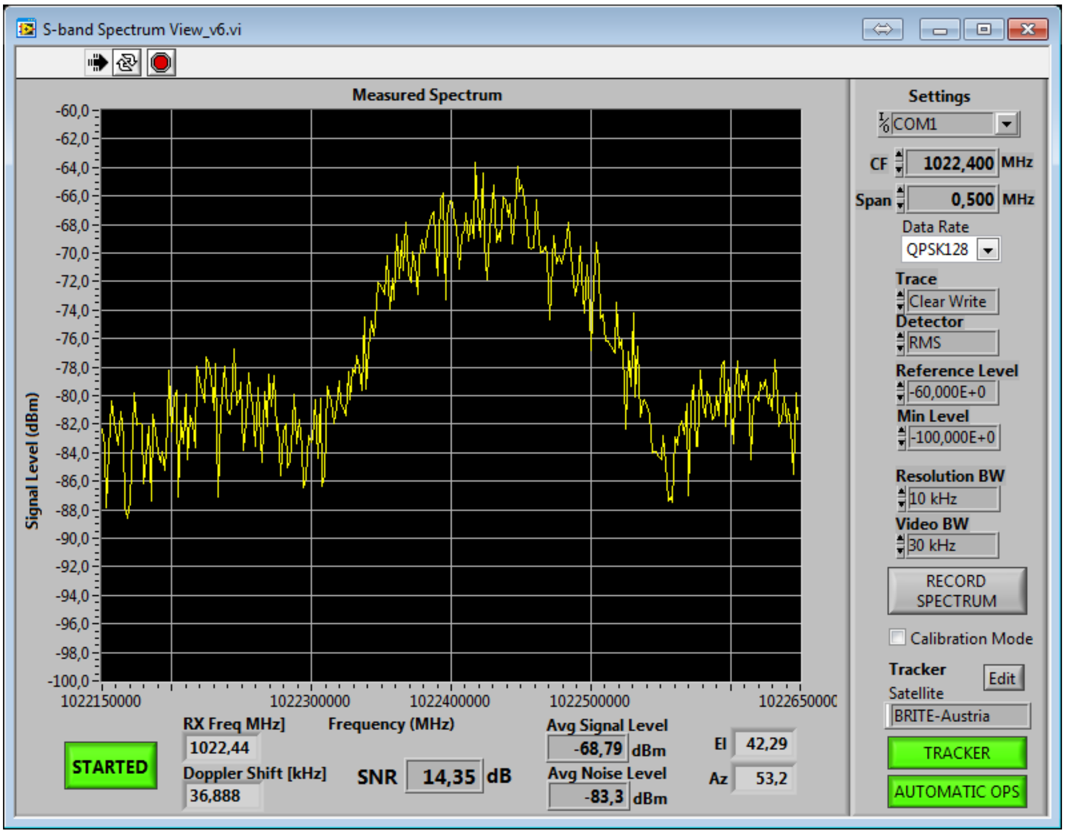

Figure 5.14: ***S-band Spectrum View* software for measuring the downlink signal spectrum.** The software is shown in action during a pass of BRITE-Austria over the Graz ground station measuring the spectrum for QPSK *128 kbit/s*.

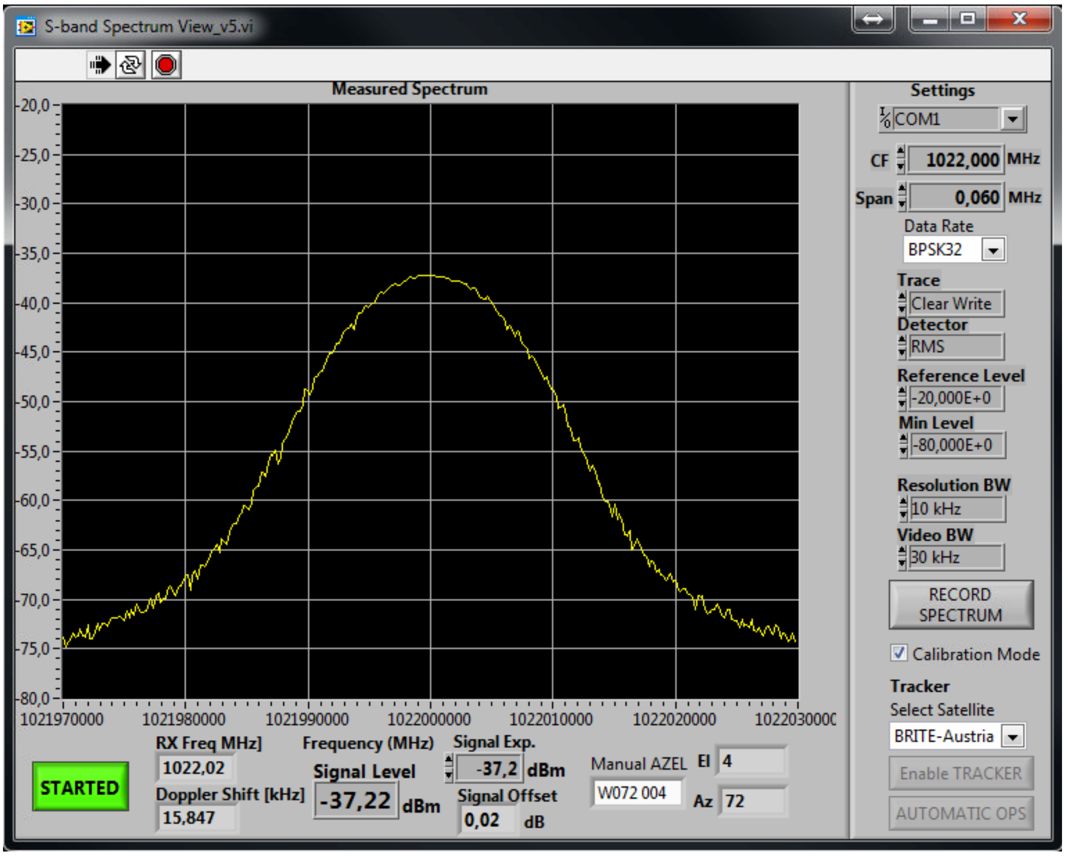

Figure 5.15: ***S-band Spectrum View* software in calibration mode.** This mode is used to verify the antenna rotators calibration with a reference transmitter signal. The plot shows that the calibration is optimal, as the measured signal level value matches with the expected one.

In addition to the standard *S-band Spectrum View* software used for nominal operations of the spacecraft, an extended version has been developed which additionally interfaces with the satellite modem to collect downlink telemetry. This version of the software is shown in Figure 5.16. The modem's input signal level along with the E_b/N_0 and frequency offset from the nominal receive frequency are measured and recorded in parallel with the spectrum measurement of the downlink signal. The advantage of this software is that the frequency offset information measured by the modem is used as input for the spectrum measurement, which uses the actual measured value to set the centre frequency for estimating the signal to noise ratio. Unfortunately, this software has only monitoring capability of the satellite modem, hence, no data rate and modulation settings can be controlled. This limitation makes is not suitable for nominal operations. However, the software is useful for measurements to characterise the downlink performance between the satellite and the ground station, as it collects spectrum measurements from the spectrum analyser and signal measurements from the satellite modem simultaneously. This version of the software has therefore also been used for packet error measurements to characterise the overall link performance of the system.

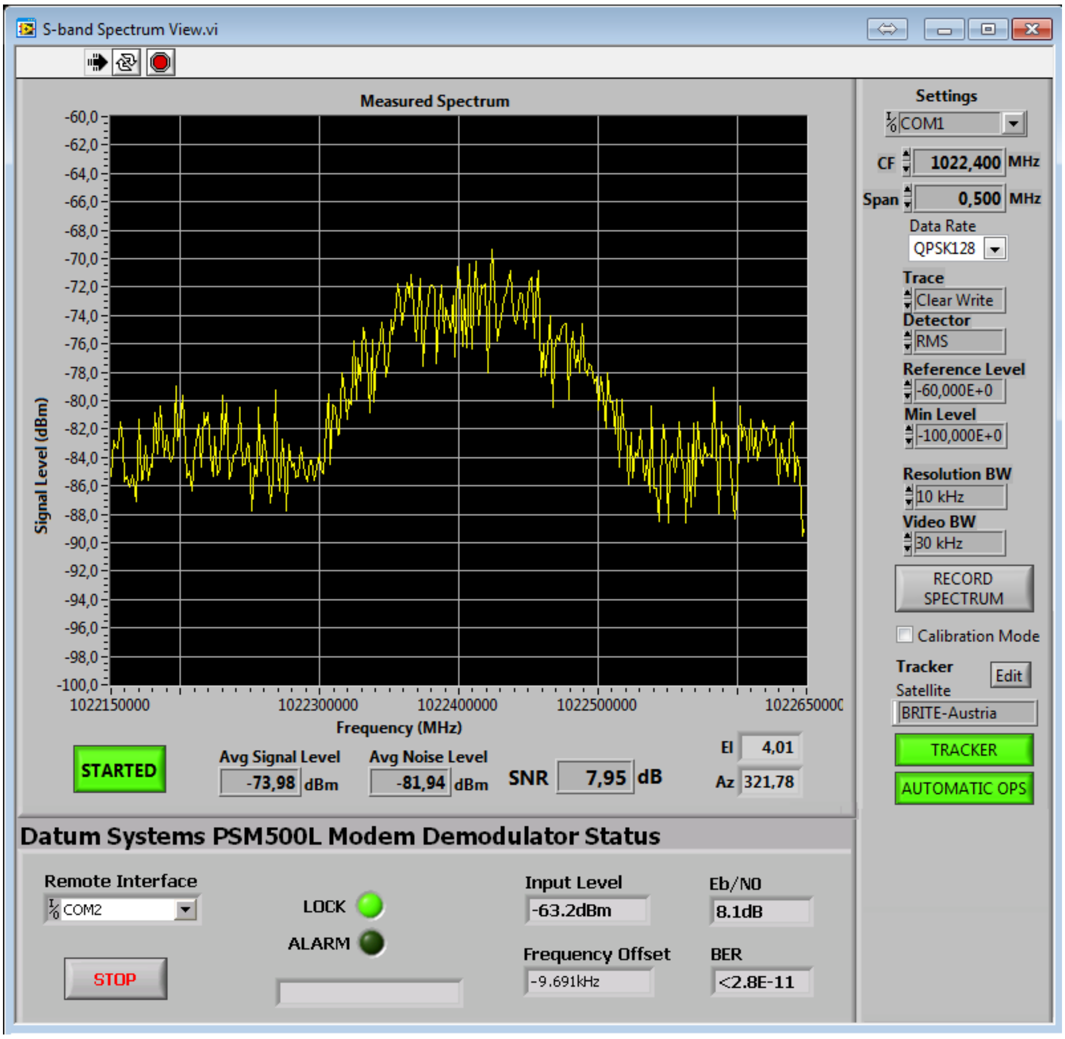

Figure 5.16: Extended *S-band Spectrum View* software. This version of the software allows to measure the downlink signal parameters from the satellite modem in addition to the downlink signal spectrum from the spectrum analyser during a pass of BRITE-Austria over the Graz ground station.

5.2.5 Post-Processing Satellite Data Analysis

Detailed analysis of the downloaded satellite data has to be performed in post-processing. The following section provides a detailed description about post-processing data evaluation strategies focusing on collected satellite telemetry. Science data processing and evaluation is outside the scope of this thesis.

5.2.5.1 Telemetry Analysis with the TLMView Software

Detailed analysis of downloaded satellite Whole Orbit Data (WOD) files can be performed by the *BRITE TLMView* software whenever a WOD file is downloaded. The software has been developed as *Matlab*® GUI for BRITE operations in the context of this thesis.

TLMView takes the parsed WOD files and performs automatic telemetry analysis. It generates alarms according to the limits set for the analysed telemetry points and allows to plot relevant subsets of the telemetry groups for meaningful visualisation and analysis of telemetry values.

TLMView provides the following functionality:

- The selection of individual WOD directories for analysing single WODs or, as WOD telemetry is collected and parsed on a daily basis, daily analysis of WOD files.
- The selection of a WOD analysis period typically of several days for long-term telemetry evaluation and trend analysis
- Individual out of range value analysis for each available telemetry group
- Setting of a criticality factor for the minimum number of out of range values to be detected before triggering an alarm
- Plotting of selected telemetry values (grouped together in a meaningful way). This includes basic telemetry such as voltages, currents, and temperatures, as well as general power statistics of the satellite and attitude control / payload specific telemetry.
- Support of different time intervals for telemetry analysis and plots (sec, min, hours, days)
- For the plots, typical plot functions like zoom, point selection, as well as axis limit settings are supported
- For the alarm analysis, different limit files exist; the correspondent *Matlab .m* file containing the limit definitions for a particular telemetry group can be edited from the GUI.

While detailed analysis of alarms over certain periods of time is required in case of unexpected spacecraft behaviour or anomalies, the plot functions in *BRITE TLMView* represent a powerful tool to quickly assess the performance and analyse the trend of the various subsystems of the satellite. For instance, with *TLMView* the three-axis pointing performance of the satellite can be quickly assessed by analysing the collected state vector telemetry. The state vector includes the body rates of the satellite, as well as the satellite position with respect to its inertial reference frame described by attitude quaternions. The body rates are supposed to be rather low ($< 0.5°/s$ total body rate) when the satellite is stabilised in all three axes, while the attitude quaternions are expected to be fairly stable and match the nominal values of the input quaternion in the three-axis stabilised state. In addition, by looking at the panel currents the pointing relative to the sun can be estimated.

Examples for the assessment of the attitude control performance in three-axis pointing of BRITE-Austria are depicted in the following figures: Figure 5.17 shows the individual body rates for an attitude control period in three-axis pointing, Figure 5.18 shows the quaternion values, and Figure 5.19 shows the correspondent panel currents.

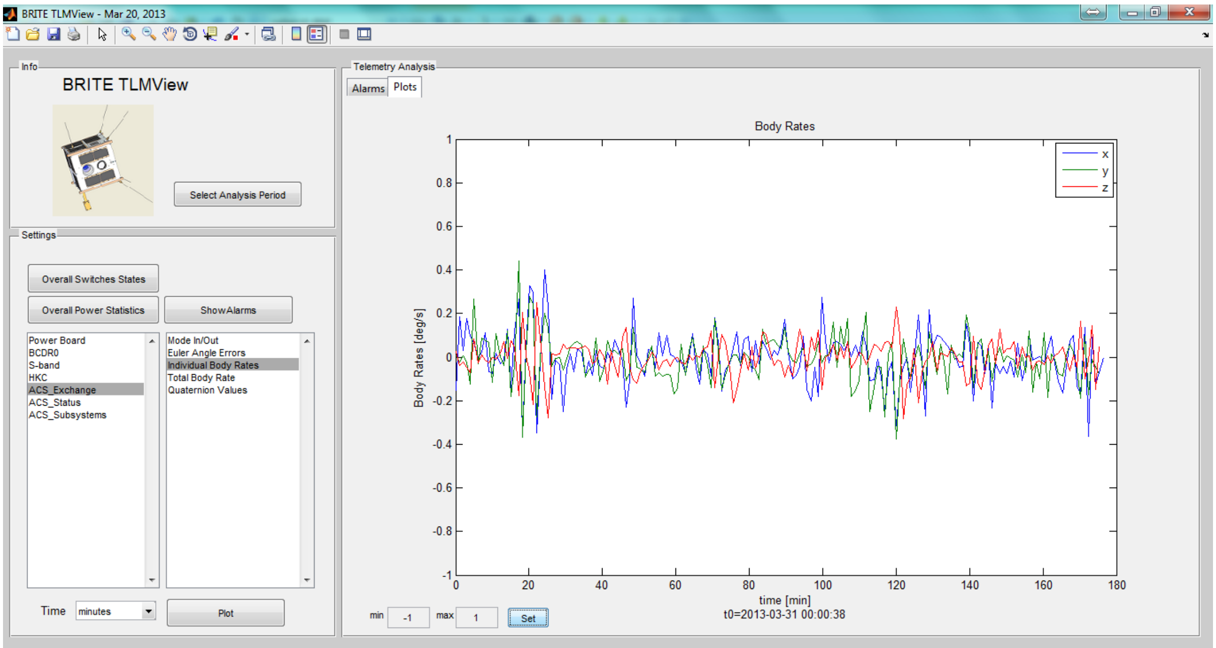

Figure 5.17: ***BRITE TLMView* plot for the measured BRITE-Austria individual body rates during coarse three-axis pointing.** The low and stable body rates indicate that the satellite is stabilised in all three axes, and only little movements are required to keep the desired attitude.

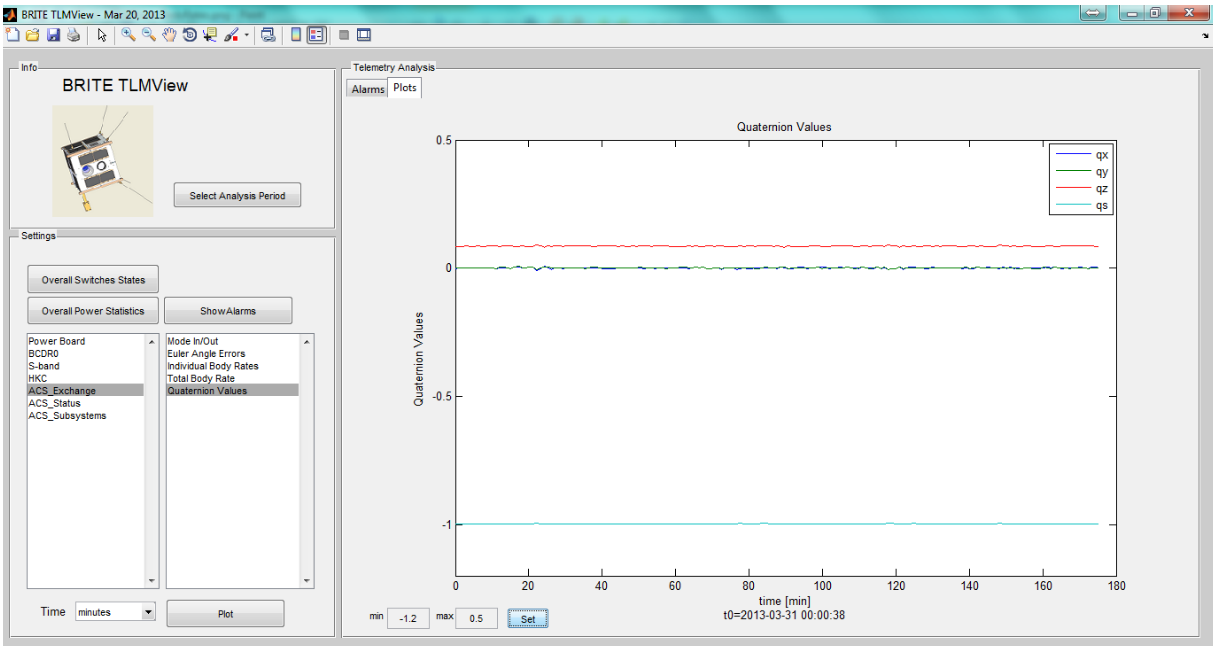

Figure 5.18: ***BRITE TLMView* plot for the measured BRITE-Austria quaternion values during coarse three-axis pointing.** This indicates that the satellite keeps it position stably pointed towards its inertial target.

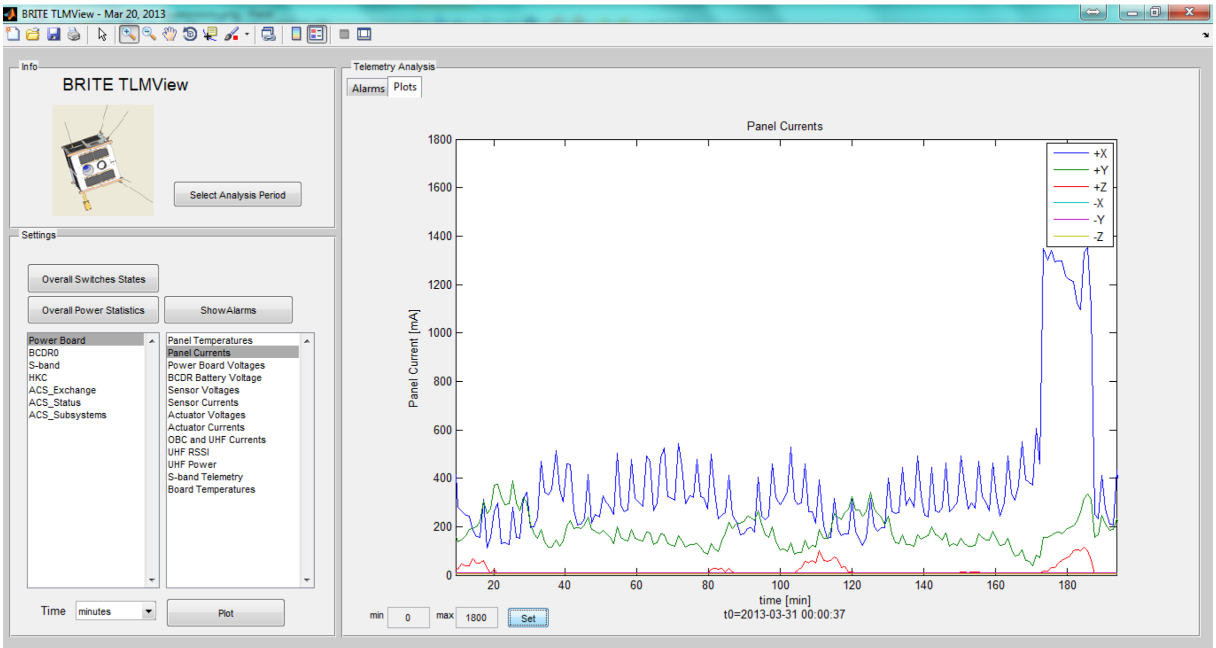

Figure 5.19: ***BRITE TLMView* plot for the measured BRITE-Austria panel currents during coarse three-axis pointing.** The plot shows that the satellite is inertially pointed towards a target facing the Sun mostly with its $+X$ panel and partly with its $+Y$ panel. The panel current increase towards the end of the plot is due to a contact with the ground station that is taking place, as the S-band transmitter requires $4.5\ W$ of electrical power to operate.

It can be seen that the individual body rates are fairly low (mostly $< 0.3°/s$), indicating only small movements of the spacecraft as expected, and that the quaternion values are stable throughout the control period. Furthermore, the panel currents indicate that the satellite is facing the Sun mostly with the +X panel and partly with the +Y panel. This indicates an appropriate pointing direction, as the instrument's aperture is located on the -X face and should not be directly exposed to the Sun. The increase of the currents towards the end of the analysed data set indicates that this telemetry is being collected during a pass, since the S-band transmitter is turned on and is consuming substantial power (*4.5 W*), thus drawing more current from the solar arrays.

An additional plot function useful for assessing the overall satellite state is the overall power statistics plot. It displays the difference between generated and consumed power of the spacecraft for the selected analysis period, specifically indicating how much of the generated power is obtained by the solar arrays and how much from the batteries.

Figure 5.20 shows a sample overall power statistics plot for BRITE-Austria. It can be seen that, as the power consumption increases during the pass since the S-band transmitter is turned on, the battery in use (BCDR0) starts to draw current because it transitions from *"Full"* to *"Fixed"* mode and begins to charge. As a result, the power generation temporarily decreases; after pass end, more power is generated than consumed to charge the battery. As soon as the battery is fully charged, the power generation decreases again to reach the same power level as currently consumed by the satellite.

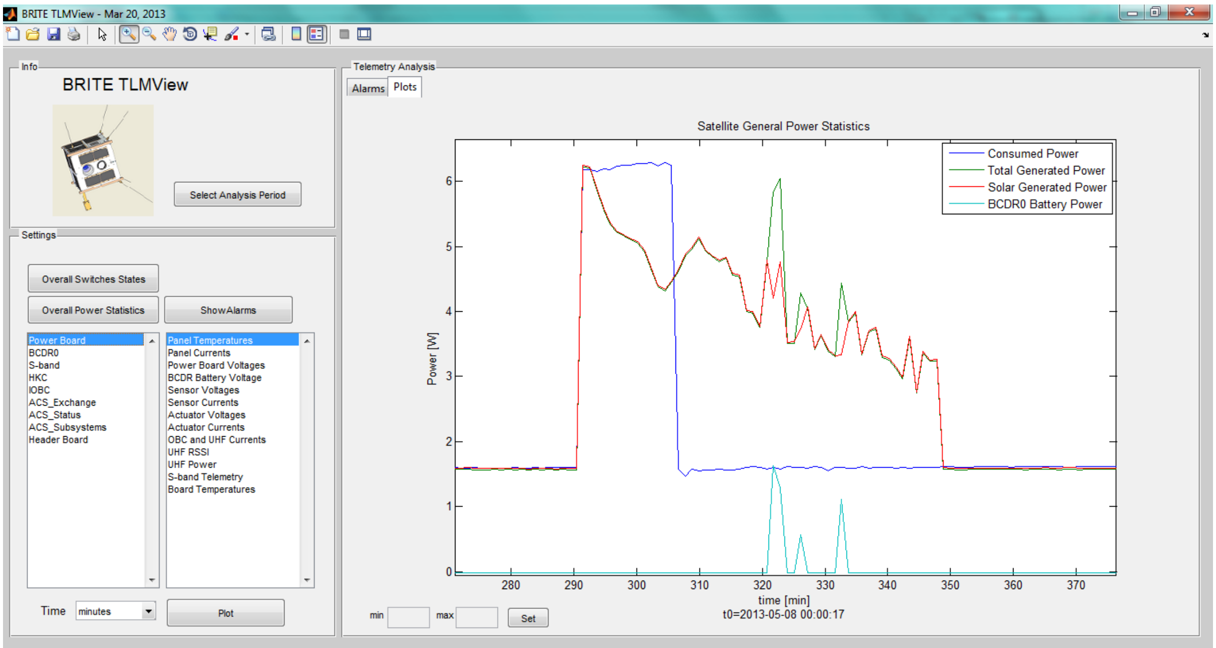

Figure 5.20: ***BRITE TLMView* plot for the measured BRITE-Austria overall power statistics during coarse three-axis pointing.** The power consumption increases during pass and the battery starts to draw current. BCDR0 transitions from *"Full"* to *"Fixed"* mode and begins to charge the battery. As a result, the power generation decreases. After pass end, more power is generated than consumed to charge the battery.

From the communications point of view, the Received Signal Strength Indicator (RSSI) telemetry of the UHF receiver is useful to assess the uplink performance of the ground station. *BRITE TLMView* provides a plot function for the RSSI telemetry, converting the measured voltages to RF power values (in dBm) for better representation. Figure 5.21 shows a plot generated in *BRITE TLMView* for the RSSI at the BRITE-Austria UHF receiver for a single WOD covering the period of an afternoon pass on March 13th, 2013 tracked by the Graz ground station.

The out of range telemetry detection analyses all collected telemetry values per telemetry group (e.g. all power board telemetry). It compares the collected values with the nominal telemetry ranges and raises alarms if the values exceed these limits. It has to be noted that, depending on the telemetry group, spikes might occur in the telemetry readings. If the analysis considered every single out of range value it would mistakenly raise many alarms because of these spikes. Therefore, a criticality factor was introduced to define the minimum number of out-range values to be detected for each telemetry group before triggering an alarm. This value can be customised in the GUI to adapt to the currently analysed data set.

In addition, depending on telemetry group, some alarms may be raised although no anomaly has actually occurred. An example where out of ranges values would be mistakenly detected is when certain switches have already been switched off, but still consume power for some time due to residual capacitance, e.g. the instrument computer switch. In such cases, the mistakenly detected alarms can be avoided by raising the criticality threshold. Other mistakenly detected alarms might occur when the attitude thread is running. For instance, if the attitude thread is commanding the sun sensors to be power cycled, telemetry

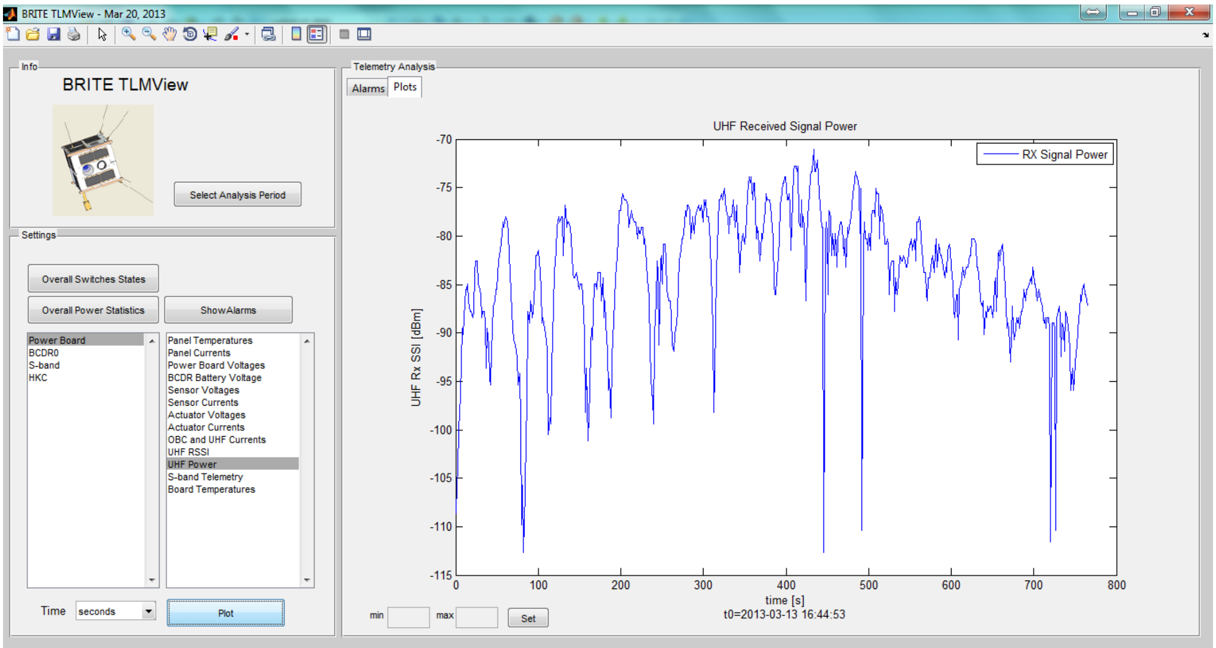

Figure 5.21: ***BRITE TLMView* plot for the measured BRITE-Austria Received Signal Strength Indicator (RSSI) converted to RF power values.** The fluctuations seen in the plot are due to pointing offsets, polarisation effects, as well as due to short intervals of deactivating transmission by the ground software for Doppler correction.

might have been still collected at a specific point in time although the detected switch state signalises that the power switch is already off, causing the ”off” state limits to be used instead of the ”on” state ones, and hence triggering an alarm. These mistaken alarm detections cannot always be avoided by raising the criticality because they might appear in large numbers. In this case it is the operators' duty to recognise that these alarms are actually of no concern.

Figure 5.22 shows the alarm analysis in *BRITE TLMView* for a particular power board telemetry data set without setting a criticality factor. The plot shows that many alarms are raised because of spikes in the telemetry, e.g. the single out of range detected values for the panel temperatures corresponds to the absolute freezing point of $-273.15°$ *C (0K)* , which is the substitution value for temperature telemetry point when a reading cannot be obtained.

To avoid these spikes from being detected as out of range telemetry causing the alarms list to become unnecessarily extensive, the criticality factor can be raised, for instance to a value of 3 as shown in Figure 5.23. In this plot, the alarms list for the same analysed data set has been significantly reduced and can be analysed in detail. The only telemetry values out of range in this list are the sun sensor voltages and magnetorquer currents which are read while the queried switch state at the same point in time is detected to be still off. Therefore, these alarms can be ignored.

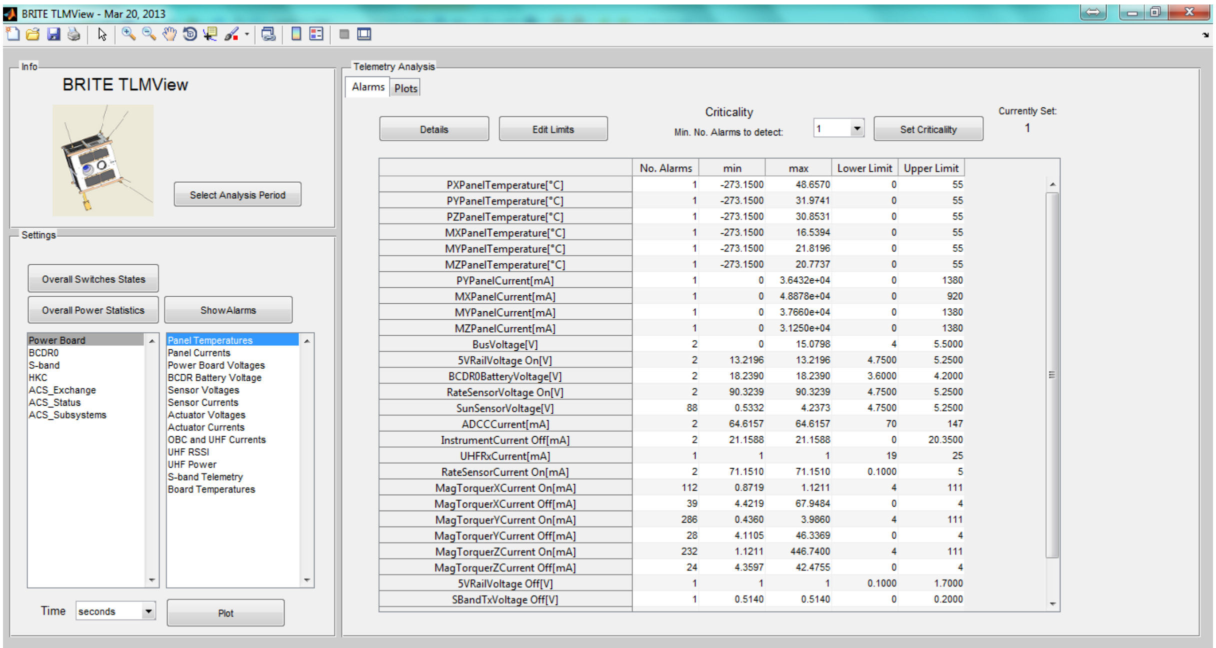

Figure 5.22: ***BRITE TLMView* plot for alarm analysis of power board telemetry without criticality factor.** The plot shows that many alarms are raised because of spikes in the telemetry, e.g. the single out of range detected values.

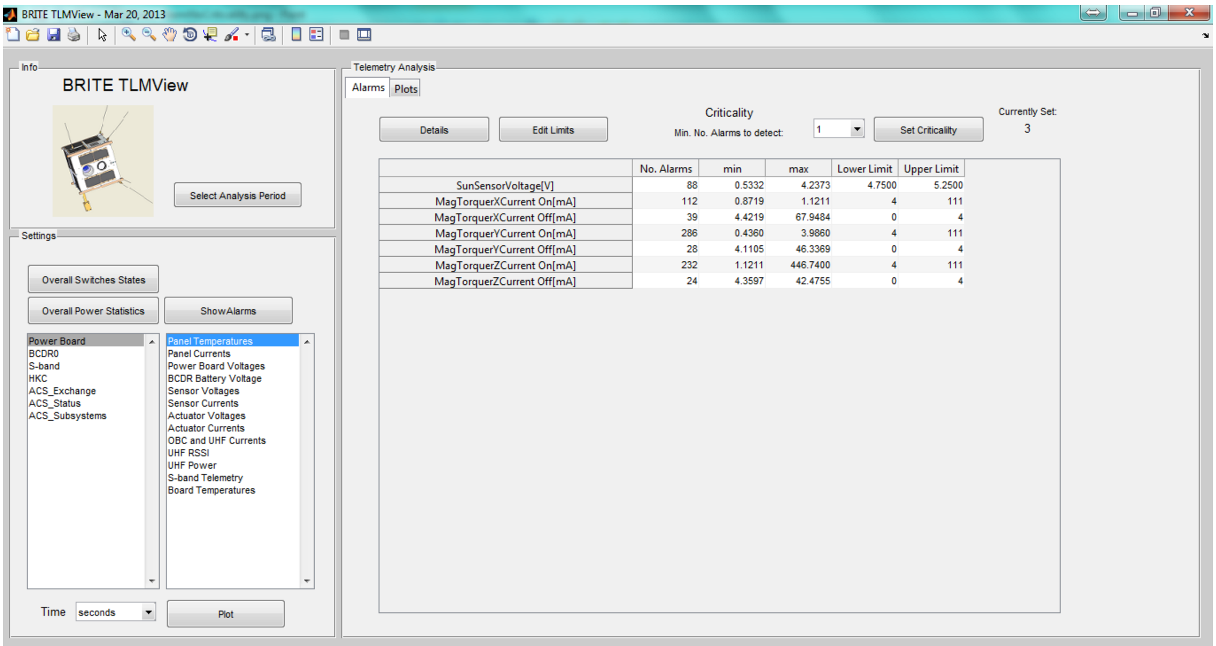

Figure 5.23: ***BRITE TLMView* plot for an alarm analysis of power board telemetry with criticality factor.** For this analysis, the criticality factor has been set to 3. Compared to the plot shown in Figure 5.22 without a criticality factor set, the spikes in the telemetry have been removed.

5.2.5.2 Scripted Ground Segment Procedures for Operations Support

During nominal operations, manual operations of the spacecraft are mostly performed for routine maintenance tasks as well as for contingency and recovery procedures, if needed. For these tasks, pre-defined scripted procedures are available to speed up the process and avoid mistakes/omission of commands.

In a similar way, scripted procedures are applied to the ground segment for various automation tasks. For these tasks, *Python*® scripts are used. The purpose of these scripts is to simplify tasks to the operators and to prevent the occurrence of mistakes. Scripted ground segment procedures include [59]:

- Automatic generation of observation base times according to calculated observation schedules
- Automated compilation of status reports
- Miscellaneous automation tasks such as TLE retrieval and deployment to the satellite propagator database for upload; processing and email forwarding of pass logs/reports, etc.

Figure 5.24 shows sample outputs of a four different Python scripts used for ground segment automation. The top left output shows the automatic retrieval of TLEs from the tracking software which occurs periodically every 2 days. The TLEs are stored in the correct format in the repository used for automated upload to the spacecraft by a satellite script in the ground software. The bottom left window shows the output for email forwarding of pass reports from a ground software module used for file transfer from the spacecraft. The output shown top right retrieves pass information used for the report automatically from the tracking software while at the bottom right the command line utility for automatic compilation of status reports for passes is shown.

5.2.5.3 Ground and On-Board Time Synchronisation

Another important aspect to be considered for satellite operations is time synchronisation. The spacecraft uses the on-board time of the housekeeping computer as time reference. This on-board clock is synchronised with the TNC during contact with the ground station. The on-board time error requirement is < 100 *ms*. On ground, time synchronisation of the ground station is provided by the use of the network time protocol (NTP) [66], by connecting to NTP servers over the wide area network (WAN), which provides a precision of a few tens of milliseconds. This is sufficient to meet the required timing requirements.

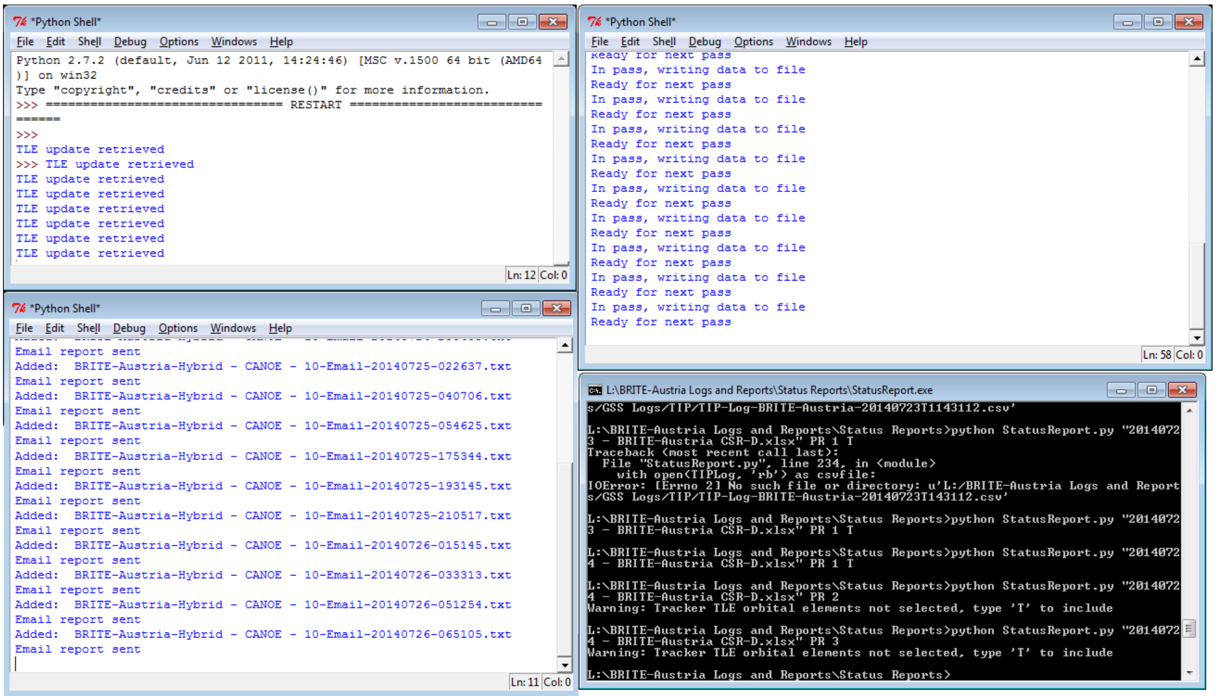

Figure 5.24: **Python scripts used for ground segment automation.** The top left output shows the automatic retrieval of TLEs from the Tracking software which occurs periodically every 2 days. The TLEs are stored in the repository used for upload to the spacecraft in the correct format. The bottom left window shows the output for email forwarding of pass reports from a ground software module used for file transfer from the spacecraft. The output shown top right retrieves pass information used for the report automatically from the tracking software while at the bottom right the command line utility for automatic completion of status reports for passes is shown.

5.3 BRITE-Austria Commissioning

After successful launch of the BRITE-Austria spacecraft on February 25th, 2013, all satellite subsystems had to be verified to ensure their correct functionality in orbit during the satellite commissioning phase. The following in-orbit phases are applicable to the BRITE-Austria spacecraft [67]:

- **Launch and Early Operations Period (LEOP)**
  This phase lasts for about 24 - 48 hours after launch. The major tasks are the verification of communications, positive power and good thermal conditions of the satellite bus.
- **Bus Commissioning**
  Once communications with the spacecraft are stable, verification of all subsystems is performed. The result of this phase is an operative satellite bus with a working ADCS system for three-axis stabilisation of the spacecraft.

- **Instrument Commissioning**
  Only after verification of the correct behaviour of the satellite bus, verification of proper functionality of the optical payload in orbit can be performed. During this phase, the instrument is calibrated and characterised.

- **Science Operations**
  Once the spacecraft (both bus and payload) have been fully commissioned, science operations can be carried out. At this point, the regular operations phase begins.

5.3.1 Commissioning Planning and Tasks

Due to the nature of the BRITE-Austria orbit, two contact windows with the Graz ground station (early morning and late afternoon) with typically up to three consecutive trackable passes of 8-15 minutes each are available. Therefore, shift work is required for manual operations involving different operating teams to accomplish the required tasks. Each operating team needs to document the performed tasks and possible events occurred in the form of status reports and operation logs, in order to allow the next team to take over where the previous team stopped.

During LEOP and the first phases of commissioning, all major actions on the spacecraft were performed manually. Later in the commissioning phase tasks could be more and more automated.

A quite challenging task was represented by the tracking of the satellite during the first two weeks. Initial tracking was based on predicted two line elements (TLEs) and orbital elements from the launch vehicle injection time. With the latter, first contact was successfully established with the BRITE-Austria satellite from the Graz ground station during the first trackable pass, despite a low maximum elevation of 7°. The orbital elements provided by the launch vehicle were so accurate that they could be used up to one and a half days after launch. Meanwhile, the North American Aerospace Defense Command (NORAD) had started to estimate the orbits of all seven objects launched on the Indian Space Research Organisation (ISRO) Polar Satellite Launch Vehicle PSLV-C20 rocket [68], assigning preliminary object numbers. However, as the launch vehicle deploys several payloads in rapid succession, it is unclear at the beginning which object of the cluster is which. For instance, following to the deployment sequence of the PSLV-C20 [69] [70], BRITE-Austria and UniBRITE were deployed with a time interval of 20 seconds and as a result they were only a few seconds apart from the ground station point of view at the beginning. Therefore, the challenge was to determine which object in the list was BRITE-Austria.

As at the beginning the object to track is uncertain and the accuracy of the available two line elements may not be yet optimal, tuning of the tracking parameters needs to be performed at the ground station to establish contact with the spacecraft. This could be achieved by the use of rotator offsets and by scanning forward/backward in time until a downlink lock was obtained. At this stage, even once the right object for the satellite has been identified, there is no guarantee that the spacecraft will be trackable during the upcoming passes by using this object in the list. This is because NORAD attempts re-ordering the objects of a particular launch by ranking them according to their deployment sequence, with the primary payload eventually being the first element in the cluster.

After the launch injection TLEs started to become inaccurate for tracking, first tracking attempts for BRITE-Austria were performed by tracking *"OBJECT E"* of the cluster according to the NORAD listing. As this was the fifth object in the NORAD listing, it would have logically corresponded to BRITE-Austria according to the deployment sequence of the launcher. The tracking of this object was sufficiently accurate at the beginning for communications with BRITE-Austria from the Graz ground station. In the following days, the object selection for tracking was changed back and forth between *"OBJECT E"* and *"OBJECT F"*. As commissioning of UniBRITE was taking place in parallel from the Toronto ground station, tracking experiences were constantly exchanged between operating teams to better distinguish between the two satellites and assign them to the objects in the NORAD listing. For every set of passes tracked, insights in the tracking experiences and the object assumed to be the own spacecraft were forwarded to NORAD to assist in the assignment process of the different spacecraft to each of the tracked objects. As a result, already three days after launch the following preliminary list assigning the identifiers to satellite names was created by the US Joint Space Operations Centre (JSpOC):

- 39086 - SARAL
- 39087 - AAUSAT3
- 39088 - SAPPHIRE
- 39089 - NEOSSAT
- 39090 - STRAND 1
- 39091 - BRITE-AUSTRIA
- 39092 - UNIBRITE
- 39093 - PSLV R/B
- 39094 - PSLV DEB

This should later become the final list assigning the provided identifiers to the satellites on the PSLV-C20 launch. In the final list, the satellite name was changed to *"BRITE-A TUGSAT-1"*, to have both mission and satellite name represented.

5.3.1.1 Commissioning Procedures

For successful commissioning of the BRITE-Austria spacecraft, it was fundamental to develop a suitable commissioning plan with well-defined tasks to be carried out step-by-step, starting from the satellite's launch. After its deployment, the spacecraft enters kick-off mode. This means that only the power subsystem and the UHF receiver are active. The power subsystem generates electrical power from the solar cells, supplies the power board, and charges the batteries. The UHF receiver is also powered by the power board and listens for commands from the ground station. The first task therefore was to turn on the satellite by turning on the transmitter from the housekeeping computer and to get a telemetry snapshot to confirm the satellite's core health. Once this task had been successfully performed, commissioning of the spacecraft could be started.

The commissioning approach for BRITE-Austria was to test all systems sequentially in a rapid fashion to keep the commissioning time short. In case of unexpected behaviour, further debugging was required. The following high-level sequence of commissioning tasks has been performed on the BRITE-Austria satellite [71]:

1. **Satellite start-up and core health check:**
   The satellite was turned on in orbit for the first time by turning on the housekeeping computer and getting a telemetry snapshot. This task was performed on the first trackable pass for BRITE-Austria on its launch day from the Graz ground station at less than 5 degrees of elevation. A core health check of the satellite according to the telemetry obtained revealed that all values were within the expected limits. This first step right after launch represented a major milestone. Figure 5.25 shows an impression of the first contact with the spacecraft.

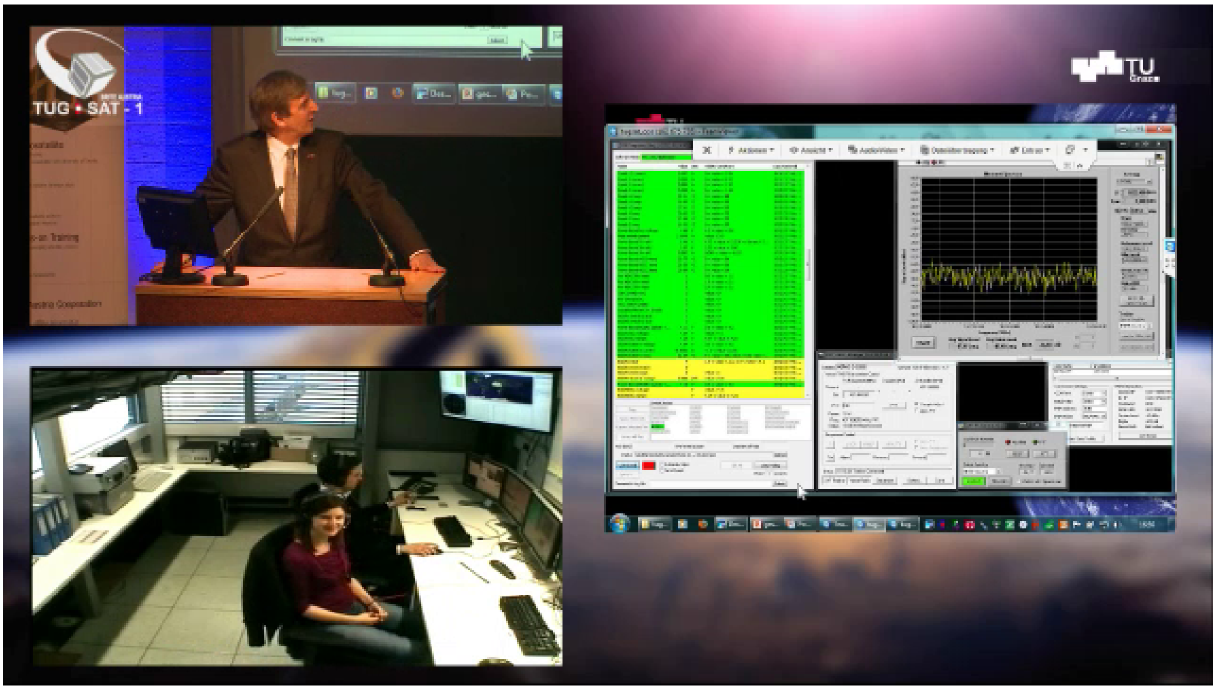

Figure 5.25: BRITE-Austria first contact. Impression of the first contact of BRITE-Austria with the Graz ground station

2. **Commissioning of the housekeeping computer:**
   For commissioning the housekeeping computer (HKC), an automated test routine pre-positioned on the computer's memory had to be executed, checking the core hardware blocks of the computer. Subsequently, the application software could be loaded, telemetry collection in application mode could be started and continuously monitored and analysed for a few orbits.

   For practical reasons, this procedure has been modified for BRITE-Austria. As first contact with the spacecraft was established during a low elevation contact while TLEs were still uncertain, it was decided to load the application code on the HKC right after the successful core telemetry check. This way, the spacecraft was able to collect Whole Orbit Data (WOD) for an entire orbit until the second contact. As the second contact was expected to be better due to higher elevation it was found better suited to commission the HKC. In addition, in this way, better characterisation of the satellite's health status could be performed, as telemetry for an entire orbit was available. During the second contact, the nominal commissioning procedure for the HKC was successfully carried out.

3. **Switching to non-default BCDR and telemetry checks:**
As in case of a system reset the system is restored by running on the default battery and the corresponding BCDR, during nominal operations the non-default BCDR will be used. This way, by assuming correct behaviour of the default BCDR, the system can always be restored in case of unexpected behaviour. After switching to the non-default BCDR, telemetry was collected for a few orbits to check the second battery's health before letting the system run on it.

4. **Commissioning of the attitude control computer and operation of the application software mode in safe mode:**
As the attitude control computer is identical to the housekeeping computer in its hardware design, commissioning of both computers followed the same procedure. The same test routine checking the computer's core hardware modules (tailored to the hardware addresses of the attitude control computer) was executed. Subsequently, the application software for controlling the attitude thread was loaded and verified. At the end of the procedure, the attitude thread was started for the first time by initialising all sensors and actuators (except the startracker) and by starting the attitude cycles. The attitude thread was first put into *"Safe"* mode, in which the sensors and actuators are initialised and turned on, but no attitude determination or control is performed. Telemetry was collected for a few orbits to verify the correct behaviour and stability of the attitude thread.

5. **Commissioning of the coarse attitude sensors (magnetometer and sun sensors):**
Individual commissioning of the coarse attitude sensors is required to verify that they perform as expected in orbit. For that purpose, the magnetometer and all six sun sensors are checked out individually. The in-orbit verification of the coarse attitude sensors is performed in two steps: First, a manual telemetry check is carried out, where the sensor in question is manually power cycled, initialised, and telemetry is queried and analysed. Once the manual response of the sensor has been verified, control over the sensor is left over to the attitude thread. This is required in order to verify the correct interaction between the sensor and the attitude control software and to tune settings. Typically, the attitude thread runs for one orbit collecting so-called Attitude Control System (ACS) logs containing the raw sensor readings. Subsequently, the performance is verified by analysing the collected logs. In case parameters have to be tuned or more data is required, the procedure is repeated. For BRITE-Austria, the magnetometer performance was checked first. Afterwards, all six sun sensors were checked out. During the sun sensor checkout, the default exposure time of the sun sensors was determined to be too long, resulting in partial saturation. Therefore, the exposure time setting was tuned iteratively to achieve the best performance.

6. **Commissioning of passive attitude determination mode:**
Once the coarse attitude determination sensors (magnetometer and sun sensors) have been checked out, passive attitude determination is tested in orbit to verify that the combined measurements of the magnetometer and sun sensors are in agreement and provide correct coarse attitude determination. For that purpose, the attitude thread of the spacecraft was commanded to *"Passive"* mode (attitude determination only), with both the magnetometer and the sun sensors enabled in the device control mask. An ACS log was collected for one orbit in this mode, and the data were analysed subsequently. Unlike for the individual checks of the sensors, where raw data (e.g. sun sensor profiles) are collected, in this mode the attitude thread uses the data actively in its control loop to estimate the satellite's attitude based on the sensor readings.

   The commissioning of the attitude determination mode represents an important step. Once correct determination has been verified, the checkout of the actuators can begin.

7. **Commissioning of the magnetorquers:**
As for the attitude sensor commissioning, attitude actuator commissioning is performed in a similar way by both a manual checkout and a performance check with the attitude thread. However, for the actuators the manual checkout is more critical compared to the sensors checkout, as their activation causes a change in the spacecraft's attitude.

   The first actuators to be checked out on BRITE-Austria were the three magnetorquers. This is because the magnetorquers provide coarse attitude control, as they are used for de-tumbling the spacecraft and they are required for momentum dumping of the reaction wheels. The manual checkout of the magnetorquers foresees turning on each torquer individually, setting different currents up to the maximum to be drawn, and repeating these steps for the other current direction. Subsequently, testing of the magnetorquers with the attitude thread is performed. While for attitude determination the sensors were included in the control mask and integrated in the *"Passive"* mode of the attitude thread, handing it over complete control, the performance check for the magnetorquers still had to be performed manually with the attitude software running. This is because changing to a nominal attitude control mode would impose a risk while the correct interaction and performance of the actuators with the software has not yet been verified in orbit. Therefore, the magnetorquers were activated individually for a short period of time while the attitude thread is running in *"Passive"* and an ACS log was collected. The results of the logs confirmed that the activated magnetorquer affected the spacecraft rates in the orthogonal axes with respect to it while having little effect to the parallel axis. In addition, polarity check testing was performed to ensure that the commanded current directions are correctly processed by the attitude control software.

8. **Satellite de-tumbling:**
Once the magnetorquers had been checked out and their correct interaction with the attitude software had been verified, the spacecraft could be de-tumbled. During this process, the de-tumbling attitude control mode *"B-Dot"* was commissioned, as it may be required later in case the satellite spins up to very high body rates, e.g. due to an unexpected reset or attitude mode transition from control to determination mode.

   The *"B-Dot"* attitude control mode stabilises the satellite by the use of the sole magnetorquers, providing the necessary momentum to lower the body rates of the spacecraft. As the mode is meant for de-tumbling only, no pointing of the spacecraft is supported. For de-tumbling the satellite the attitude thread had the magnetometer, sun sensors, and magnetorquers activated by the device control mask, and was transitioned from *"Passive"* to *"B-Dot"* mode for approximately 10 minutes while an ACS log was collected. The results of the log showed that the spacecraft rates were decreasing and had settled at below $1°/s$, in which case the spacecraft had been sufficiently de-tumbled to transition to coarse pointing mode. If the rates would have been still higher, the spacecraft would have been put to *"B-dot"* mode again until the desired body rates have been reached.

9. **Commissioning of the reaction wheels:**
The three reaction wheels are required for controlling both coarse and fine attitude of the spacecraft in all three axes to fulfil the pointing requirements for achieving the scientific mission objectives. Commissioning of the reaction wheels is required before transitioning to any three-axis attitude control mode.

   As for the magnetorquers, commissioning of the reaction wheels includes manual telemetry checks for each wheel individually as well as performance checks with the attitude control software. For each reaction wheel, an extended manual telemetry health check was performed before spinning it up. The wheel spin-up was performed after manual telemetry check for each wheel as part of the performance check procedure with the attitude control software. For that purpose, each reaction wheel was spun up to *300 rad/s* and let run for about 20 seconds to collect telemetry. Like for the magnetorquers, this step was performed manually while the attitude thread is running in *"Passive"* mode.

   Although the checkout of the reaction wheels is not required for de-tumbling, this step has been performed prior to de-tumbling for BRITE-Austria. The rationale for changing the order in the commissioning sequence is that in this way, after successful de-tumbling of the spacecraft, transition to coarse three-axis pointing could be attempted immediately without checking the wheels out first, and requiring to de-tumble the spacecraft again after the wheels had induced momentum to the spacecraft during their spin-up process.

10. **Commissioning of coarse three-axis pointing mode and attitude stabilisation:**
Once the individual performance of the coarse attitude sensors and all attitude actuators has been verified both at unit level and with the attitude software, after de-tumbling of the satellite transition to coarse three-axis pointing of the spacecraft can be attempted. For BRITE, this is accomplished by inertial pointing with the provision of an attitude quaternion.

    In order to perform this step, some preparatory work needs to be performed. First, an adequate orientation for the spacecraft needs to be determined and the corresponding target quaternion generated. For BRITE-Austria, the first quaternion was generated to allow pointing the -X panel with the instrument aperture on the opposite face with respect to the Sun. In addition to the desired target quaternion, the most recent TLEs need to be retrieved and uploaded to the spacecraft orbit propagator to have accurate knowledge of its orbital parameters.

    As mentioned in the previous commissioning steps, the order of the tasks has been adapted to perform the transition to coarse three-axis pointing right after de-tumbling of the satellite. This is advantageous because the warm-up period of the extended Kalman filter (EKF) used by the attitude thread has already been reached, and the device control mask is configured such that all coarse attitude sensors and all actuators are already included. A transition to the so-called *"Three-axis PID"* mode in the attitude software will convey the satellite in coarse three-axis pointing mode. The attitude software does not inherently draw a distinction between coarse and fine three-axis pointing. The used control mode is the same, the better precision in fine three-axis pointing mode is achieved by including the startracker in the device control mask and enabling its usage in the control loop.

Commissioning of coarse three-axis pointing mode of the spacecraft is a critical task and needs therefore to be examined carefully by the operators. The commissioning procedure therefore required at least two good consecutive passes to carry out the following steps:

- **First pass:**
  First, a verification of the spacecraft attitude status has to be performed to ensure that the spacecraft is successfully running in *"Passive"* mode, that the body rates are sufficiently low ($< 5°/s$) for transitioning to pointing mode, and that no anomalies have occurred. If the status is as expected, the TLEs and target quaternions are uploaded and the spacecraft status is checked again. At this point, while the relevant parameters of the attitude thread are being logged, the transition to *"Three-axis PID"* mode can be manually issued by an operator. Subsequently, the remaining pass time is used to verify the transition success. This is performed by telemetry readouts checking that the implemented attitude software mode matches the three-axis pointing mode, that the body rates are showing a decreasing trend, and that the output quaternion values are settling towards the input quaternion values. In addition, the panel currents are checked to verify that +X is drawing the most current, while -X is constantly pointed away from the Sun. In case of unexpected behaviour, a reset to the attitude control computer operating system will be issued to terminate the attitude thread and induce body rates to the spacecraft while the reaction wheels are idling.
- **Second pass:**
  The ACS log is stopped and its download is started. The same telemetry checks performed during the first pass after transitioning to *"Three-axis PID"* mode are performed (attitude thread status, state vector, and panel currents) and correspondent actions in case of unexpected behaviour have to be taken. If the latter is not the case, the spacecraft has been successfully transitioned to coarse three-axis pointing mode. The log has still to be analysed to assess the performance in detail.

11. **Commissioning of the startracker:**
    The startracker on-board of BRITE-Austria has the capability of providing attitude knowledge better than ± 70 *arcseconds*. It is the most precise attitude sensor on-board the spacecraft and required for fine three-axis pointing. Therefore, the startracker needs to be commissioned before transition to fine three-axis pointing can take place.

    The first step in commissioning the startracker was to find suitable parameters for its operation in orbit, such as amplifier gains and exposure times. Next, full frame images were obtained to verify these parameters and for further tuning, if necessary. Finally, starting from coarse three-axis pointing mode, the startracker was included in the device control mask to perform a so-called warmup test. This is a long term test, where the startracker is activated for 40-50 minutes while the attitude thread is running in coarse pointing mode. The startracker is hereby not included in the control loop, but is only estimating quaternions. An ACS log is obtained during this period and the performance is analysed in terms of reliability of the quaternion readings as well as drop-out rates.

During this phase, potential constraints in the obstruction of the startracker's field of view (FOV) (e.g. obstruction by the Moon, Sun, and Earth within certain angles), as well concerning operations in environments more susceptible to radiation like the Southern Atlantic Anomaly (SAA) have been characterised in detail and the insights were used as inputs for the transition to fine pointing.

12. **Commissioning of fine three-axis pointing mode:**
Fine three-axis pointing (FTAP) is required by the BRITE-Austria spacecraft to perform scientific measurements of bright stars and thus fulfilling the mission goals. Therefore, commissioning of this attitude control mode represents a crucial step for the mission success.

For achieving a transition to fine pointing, the baseline is to have the satellite stable in coarse three-axis pointing (CTAP). Given that assumption, the transition to fine pointing follows the steps that are representative of a nominal operations sequence, except that, during commissioning, observations usually do not take place and ACS logs are collected instead to verify the pointing performance.

The steps to be performed to enter fine pointing can be summarised as follows:

- Ensure the satellite is stable in coarse three-axis pointing with the desired inertial target selected.
- Turn the startracker on by inclusion in the device control mask.
- Set the appropriate parameters for the startracker as determined during the unit's commissioning and wait for a startracker warmup period to complete (typically 3-5 minutes).
- Include the startracker actively in the attitude control loop. From this point on, the attitude thread uses the startracker as sole sensor to determine the spacecraft's attitude. This step denotes the effective transition to fine three-axis pointing mode.
- After a maximum period in fine pointing to be defined according to the different constraints determined during the startracker commissioning, the startracker is disabled from the control loop.
- The startracker is now turned off by exclusion from the device control mask, allowing to save power. The spacecraft is now again in coarse three-axis pointing mode.

During the entire test period, an ACS log is collected and the performance of the pointing is analysed once the log has been downloaded.

The procedure has been repeated several times to fully characterise the fine three-axis pointing performance. After initial verification of the performance, during the time periods in fine pointing, payload activities have been included. Both full frame images and science data records have been obtained, in order to

- preliminarily verify the nominal operations cycle
- additionally assess the fine pointing performance by investigating the pixel variation of target objects within the set rasters of collected science data records

Thanks to the latter, it could be verified that the fine pointing performance is fully compliant with the mission requirement of a pointing accuracy of 2 *arcminutes* for achieving the mission goals. The results showed that the fine pointing root mean square (RMS) error is within 73 *arcseconds*.

13. **Payload commissioning:**
The commissioning of the BRITE-Austria payload represented a complex process, involving a variety of tests for characterising the photometric instrument.

To optimise the test schedule, payload activities have been carried out in between other commissioning activities, starting once coarse three-axis pointing had been achieved.

The first activity in this context was the first full frame image taken by BRITE-Austria on March 23rd, 2013 in coarse three axis pointing, with the attitude set to a target with the solar vector in the satellite's x-axis body frame to have best power conditions and to point the instrument entirely to the opposite face with respect to the Sun. At this target, part of the constellations *Corvus (Crv)*, *Virgoinis (Vir)* and *Crater (Crt)* were in the payload's field of view (FOV). The image, taken with an exposure time of one second, revealed Point Spread Functions (PSFs) of stars down to a visual magnitude of $V = 4$. The PSF of *Delta Corvus B9V* obtained with this image is shown in Figure 5.26. While this image was of limited scientific relevance in the collected data, it confirmed the operational status of the instrument's CCD and optics in orbit, as well as the suitability of the point spread functions for precise photometry in orbit, which revealed to be better than the predictions based on ground testing.

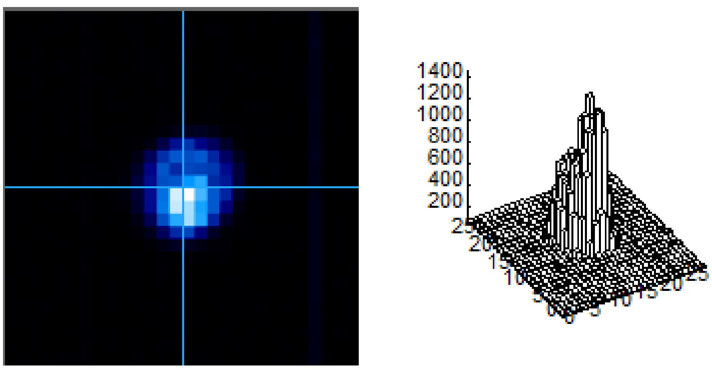

Figure 5.26: Point Spread Function (PSF) of Delta Corvus B9V in the first BRITE-Austria full frame image. Next to the star image on the left, the respective analogue to digital unit (ADU) values are shown. The full frame image has been collected by BRITE-Austria on March 23rd, 2013 (image credit: Dr. R. Kuschnig, Institute of Astrophysics, University of Vienna, 2013)

Since then, several full frame images and science data records have been collected in CTAP. The aim of these tests were to characterise effects in the CCD such as so-called *"hot pixels"* (pixels with very high signal levels not related to any observed object) and to verify the observation cycle when collecting science data records. Based on these data, optimisation of the observation cycle in terms of exposure times, delays between exposures, as well as predictions about the potential increase of hot pixels could be derived.

Once FTAP had been successfully achieved, detailed characterisation of the payload performance in orbit was carried out. In this process, preliminary science data collection already started while testing setup file configurations and timings of the observation cycle. Therefore, at this point first scientific data were collected to a limited extent, and was consistently increased creating a smooth transition towards a nominal operations configuration.

A projection of the BRITE-Austria instrument Field Of View (FOV) as used in a simulation to calculate access to the selected target field is shown in Figure 5.27.

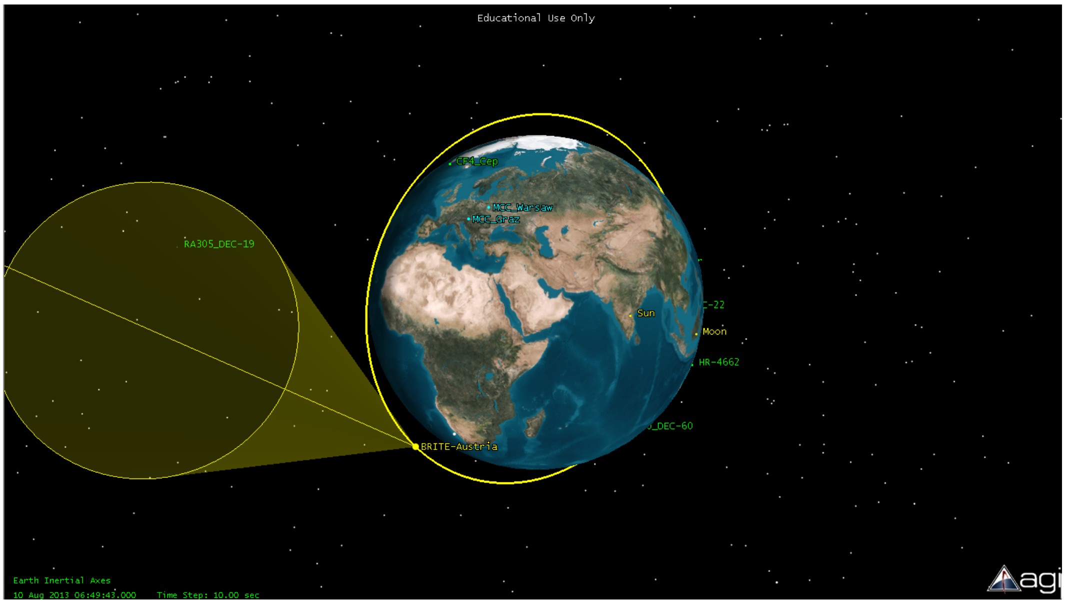

Figure 5.27: BRITE-Austria instrument field of view projection in simulation. The half cone field of view of the instrument is 12° (image courtesy: STK).

General procedures for the commissioning steps described above were already elaborated during the Assembly Integration and Testing (AIT) phase and finalised prior to launch. Detailed procedures could only be finalised once both the on-board and the ground software design and development were frozen, as depending on different software versions the original command sequences might change [8]. In addition, during commissioning, some minor revisions of the command sequences within the existing procedures were performed, and a few changes in the sequence order of some checks were made (e.g. commissioning of de-tumbling mode before reaction wheel checkout). For a better characterisation of some subsystems, additional tests compared to the ones planned in the first place were performed or to obtain more data some test routines were repeated.

5.3.1.2 Contingency and Recovery Procedures

Besides the nominal commissioning procedures covering all required steps and actions to bring the satellite in its nominal operational state, contingency and recovery procedures were prepared to cope with potential unexpected behaviour of both the spacecraft and the ground station, listing possible common problems and a correspondent set of corrective actions. Similar to the commissioning procedures, general contingency and recovery procedures were prepared prior to launch for common known contingency situations that could occur. As commissioning was going on, these procedures were revised/extended according to the behaviour observed on the spacecraft and/or at the ground station. Concerning the ground station, during and post pass corrective actions for contingency had to be adapted from the general procedures to consider the characteristics of the Graz ground station.

An example for a contingency procedure involving both satellite and ground station actions to be taken during and post pass is the procedure covering the inability of spacecraft acquisition during a pass. Most of the times, if contact cannot be established with the spacecraft, the issue will be at the ground station rather than at the spacecraft itself. This procedure is also a good example of the general contingency and recovery strategies for the mission: before taking any action on the spacecraft which represents a critical countermeasure, potential issues on ground are investigated first. The following paragraphs describe the essential steps of this procedure, extracted from the corresponding contingency procedure [72].

Contingency procedures shall be applied if no contact can be established with the spacecraft at elevations of about 10° [72]. The following during pass corrective actions shall be attempted [73] [72]:

- Ground station during pass checks: It shall be checked that both ground station uplink and downlink are operative and configured correctly:
  - Uplink: Check that the Yaesu FT-897D transceiver and the BEKO HLV-550 power amplifier are transmitting and that the measured output power level is reasonable (around *200 W*).
  - Downlink: Check that the satellite modem settings are correct (in the monitoring and control ground software modules), that the power supply for the S-band antenna feed and down-converted is turned on and supplying *12 V DC*, and that the spectrum analyser noise power level is around *-80 dBm*. This ensures that the low noise amplifier and down-converter are power supplied and operative.
  - Tracking: Check that the antenna rotators are working properly by verifying that, according to the rotator interface readings and the video observed from the antenna camera the antenna is moving in the right direction.
- If the issue seems not to be found on the ground station, a firecode to the housekeeping computer to turn it on shall be attempted. This is to check whether an unexpected power system reset has occurred during the time the satellite had no contact with the ground station.
- The firecode shall be attempted several times. If the satellite is responding and indicates that its software state is bootloader, a power system reset has occurred. If the satellite is running in a nominal state and no contact could be established for some other reason, the firecode will be

ignored. In this manner, there is no concern of re-setting the system in an unexpected way by attempting to send a firecode several times.

- If the satellite is still not responding after a firecode has been issued several times, post pass corrective actions have to be taken.
- In case a BCDR fault has occurred it shall be waited for a contact in sunlight so that the satellite is powered by its solar arrays during the pass.

Post passive corrective actions include ground station hardware and software checks to ensure everything is working properly [73]:

- Confirm TLEs: Check if the used TLEs in the Tracker software are the latest available ones from NORAD (Space-Track/Celestrak). If not, perform a manual TLE update in Tracker.
- Confirmation of antenna pointing: The antenna pointing can be verified by pointing at the reference transmitter installed at the Lustbühel observatory and check that the signal can be received when the transmitter is turned on, and that the received signal level is as expected. If that is not the case, recalibrate the rotators and verify the pointing again.
- If after calibration still no signal is received when pointing towards the reference transmitter, check the downlink chain by repeating the measurement at several points in the downlink chain (e.g. on the roof platform at different stages e.g. before and after the down-converter).
- If the downlink performance looks as expected and the pointing is correct, check the uplink performance at several points in the uplink chain (e.g. on the roof at the input of the power splitter or at the inputs of the UHF antenna).
- If the ground station hardware seems to work properly, check if the ground software is operating correctly, i.e. if all software is in-sync, has the correct time information, and is connected to other modules according to its nominal configuration (e.g. multiplexing software connected to the tracking software for automatic acquisition of the spacecraft).
- Check if another station in the network is able to establish contact with the satellite in the next period of time, contact the corresponding operations team and formulate a request for attempting contact from their ground station.

5.4 BRITE-Austria Operations

Once commissioning was completed, the BRITE-Austria nominal operations phase started. This section describes the relevant processes to implement the mission operations concept. After introducing the satellite operational modes, mission planning and execution processes including long term planning of observations as well as satellite set-up and control are introduced. Next, mission evaluation processes are described, with strategies for real-time and post-processing data analysis, as well as for data dissemination and archiving. Finally, operations support processes are presented, including ground station maintenance tasks.

5.4.1 Satellite Operational Modes

For operating the BRITE-Austria mission, different modes have been defined. The BRITE-Austria satellite has four high-level operational modes [71]:

- **Kickoff:** The mode in which the spacecraft enters right after launch. Only the power subsystem and the UHF receiver are active. Besides after deployment, this mode is entered after a power system reset firecode has been received or if an unexpected power system reset has occurred.
- **Safehold:** The on-board computers are turned on and are in bootloader mode. All other units can be turned on manually although control over them may be limited by the OBC Bootloader functionality.
- **Passive Application:** Any unit on the satellite can be active and the OBCs are performing automated tasks (e.g. collecting telemetry), but are not actively in control of power switches
- **Active Application:** The satellite is running software that lets it control any unit on the satellite, i.e. the attitude thread is running and commanding sensors and actuators to control the attitude of the spacecraft according to the control mode implemented.

The vast majority of satellite operations occur in Passive and Active Application mode. Each of these modes has several sub-modes, mainly defined by the ADCS subsystem modes. Where payload operations are possible, a third level of modes is defined. This mode hierarchy is shown in Figure 5.28.

5.4.2 Mission Planning and Execution

After successful completion of the commissioning phase of the BRITE-Austria spacecraft, the nominal operations phase started and is currently on-going. In this phase, operations are largely carried out in an automated fashion, by long-term observation scheduling as well as downloading and analysing both science data and satellite telemetry, without constant supervision by operators.

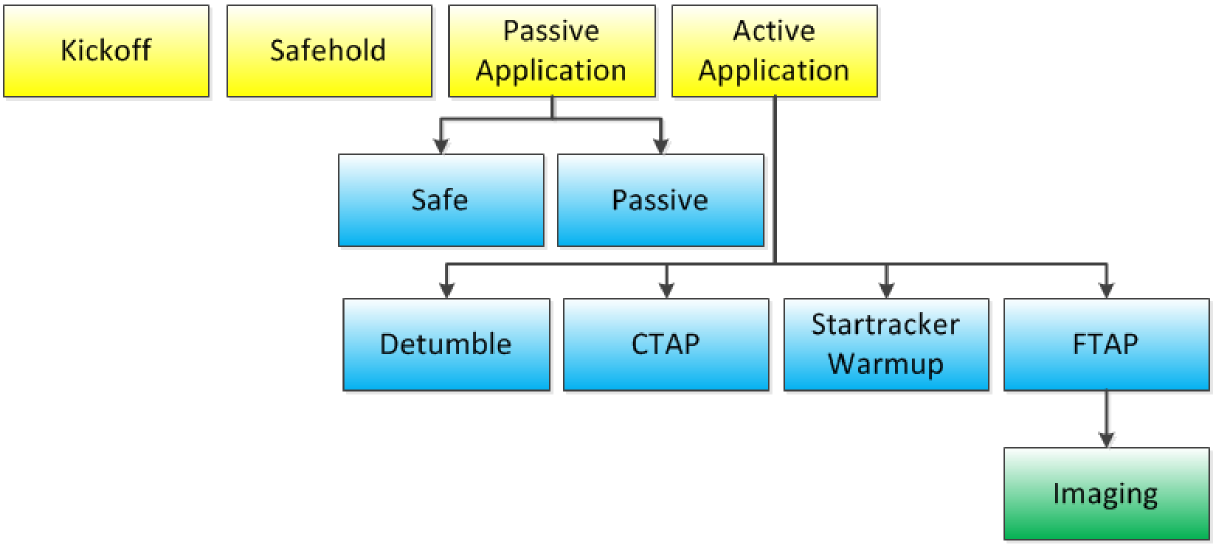

Figure 5.28: BRITE-Austria operational modes hierarchy. The mode hierarchy is shown according to [71]. Besides kickoff and safehold mode, the satellite modes where the attitude software is running (passive and active application modes) implement additional sub-modes.

The primary goal of the spacecraft during nominal operations is to execute the observation plan. For that purpose, observation campaigns of pre-selected targets are carried out, typically lasting for several months. The correspondent satellite configuration involves long-term planning of observations. Therefore, a nominal observation cycle has been defined to be carried out once every orbit. For the observation cycle, it is assumed that the spacecraft is operating nominally in coarse three-axis pointing mode (CTAP) and pointing inertially towards the target to be observed. The observation cycle includes the following high level steps [74] [59]:

- Turn on the startracker by inclusion in the device control mask and await a warm-up period for reliable operation (typically 3-5 minutes)
- Transition to fine three-axis pointing (FTAP) by actively including the startracker in the attitude determination and control loop
- Collection of science data records for typically 15-20 min
- Exclusion of the startracker from the device control mask and transition back to coarse three-axis pointing (CTAP)

5.4.2.1 Long-Term Planning of Observations

Long-term planning of observation is considered in the BRITE-Austria mission planning processes. The planning process starts with the selection of target fields to be observed and the provision of a target coordinate for inertial pointing of the spacecraft towards the desired star field by the science team. According to the selected bright stars in the field, regions of interest on the CCD (so-called rasters) are defined. The exact raster positions are determined by obtaining a full frame image of the target with the satellite while in fine pointing. Currently, rasters of $24x24$ *pixels* are used. Based on these inputs, so-called *"setup files"* are generated. These setup files include all relevant payload settings to carry out observations at the selected target. The key parameters in this respect are the raster positions and size, exposure times, as well as delays between exposures.

The setup files are handed over to mission control for upload to the spacecraft. The setup file hereby serves as input to time tag scripts generated for the implementation of the observation cycle. These time tag scripts contain the command sequence with a base time and time offsets for the nominal observation cycle and are pre-positioned on the spacecraft's on-board memory. With the *BRITE Schedule* software, the commands and base times are generated and exported to the correspondent binary script files for upload to the spacecraft.

A predefined time tag script including the command sequence with a base time and time offsets for the nominal observation cycle is pre-positioned on the spacecraft's on-board memory. While the generated time tag scripts provide the base time for generic implementation of the observation cycle, the correspondent absolute timestamps for starting the scripts have to be determined for observation scheduling. This task is performed by determining the target visibility times for each orbit of the spacecraft under consideration of different operational constraints [74] [75]:

- Suitable exclusion angles for Sun, Moon, and Earth with respect to the Field Of View (FOV) of the instrument and startracker
- Exclusion of startracker operations when passing the South Atlantic Anomaly (SAA) region
- Avoidance of observations while in contact with the ground station
- Special operations procedures with respect to fine pointing during eclipse under consideration of entry/exit times (e.g. avoiding to turn on the startracker while in eclipse)

In this process, start and stop times for the different time tag base scripts used are derived and the correspondent time tag commands are generated for upload to the spacecraft.

The primary purpose of time tagged command scripts is for scheduling observations in the operations phase, however, any satellite command can be time tagged. This feature is useful for executing test procedures exceeding the available contact times with the satellite, as well as for debugging/recovery purposes.

Although the spacecraft autonomy would allow observation scheduling for very long periods of time, automatic observation execution on BRITE-Austria is planned on a biweekly basis. This strategy is pursued for taking into consideration changes in the satellite position in orbit by using always up to date TLEs in the mission planning.

5.4.3 Mission Evaluation Processes

Mission evaluation processes include integrity checks of the downloaded satellite files, as well as real-time and post-processing analysis of the data.

The ground software downloads raw satellite files from the spacecraft. It has the capability of partial file downloading in case a file download cannot be completed during a pass, and carries on with the download automatically during the next contact. In addition, the ground software performs integrity checks of the data by checksum validation and automatically requests any missing or corrupted packets. Only when the complete satellite file has been successfully downloaded it is deployed to the repository and can be parsed. This behaviour applies to both satellite telemetry and payload data [62].

5.4.3.1 Real-Time Evaluation Strategies

Real time evaluation of satellite data is performed at the beginning of each contact with the ground station by retrieving a direct telemetry snapshot of the core satellite subsystem values. For the retrieved telemetry along with pass information an automated report is generated and forwarded via email to the operators mailing list [76]. For each of the basic telemetry points in the list, validity conditions are specified by predefined limits for each single telemetry point. In case of anomalies, alarms are generated and reported in the email. The alarm state is also signalled in the subject to draw the operator's attention.

Additional real-time evaluation strategies include automated email reports of the satellites' on-board mass memory state as well as the download progress during the respective contact [59].

5.4.3.2 Post-Processing Evaluation Strategies

While real-time evaluation of satellite data provides a quick update on the current satellite status during the pass, detailed analysis of the downloaded data is carried out in post-processing. Long-term Whole Orbit Data (WOD) analysis is performed by the software *BRITE TLMView* as described in Section 5.2.5.1. Additional satellite telemetry analysis includes the evaluation of time tag command logs as verification of correct execution of time tag commands on the spacecraft, as well as the evaluation of attitude control system (ACS) logs. The latter provide detailed logging of the satellite's attitude control performance and are not used during nominal operations but only for debugging or testing (e.g. to investigate the fine pointing performance when pointing towards new targets for the first time).

For the scientific output of the mission, extensive post-processing evaluation strategies apply to the collected science data records, including aperture photometry and point spread function (PSF) fitting schemes of the extracted data to obtain brightness measurements of the stars, so-called light curves [77].

5.4.3.3 Data Dissemination and Archiving

The downloaded data are stored on a local repository on the ground station PC, where other software is listening for new files for further processing. For the science data, parsing software is used to extract the different raster images collected during an observation. These images can be further converted into the Flexible Image Transport System (FITS) format used or be viewed by a preview software. For the collected Whole Orbit Data (WOD), a parsing software retrieves each new downloaded raw binary file and parses it to a comma separated value (CSV) file for each collected telemetry group.

Science data parsing and processing is performed by the BRITE science software, which converts the raw data files to FITS files. Satellite telemetry data parsing is performed by the BRITE telemetry parsing software as described in Section 5.2.3 which subdivides the collected whole orbit data (WOD) files into ten different telemetry categories [74]:

- Power board telemetry group
- BCDR0 telemetry group
- BCDR1 telemetry group
- S-band telemetry group
- HKC telemetry group
- IOBC telemetry group
- ACS settings telemetry group
- ACS status telemetry group
- ACS subsystems telemetry group
- Instrument header board telemetry group

Satellite health checks for the downloaded WOD files are performed by the *TLMView* software for WOD analysis as described in Section 5.2.3.

Regarding satellite telemetry there is no time criticality for data dissemination other than for backup purposes, as the data are managed and evaluated by mission control. In contrast, the science data have to be made available to the science team in near-real time. The parsing software for science data retrieves every downloaded Science Data Record (SDR) file immediately after successful download completion, processes the file and disseminates it to the science data repository via FTP within 30 seconds after download. The science team has access to this repository for data retrieval.

For data archiving purposes, the local file repository at the BRITE-Austria MCC is periodically synchronised with the TU Graz/IKS server repository network drive on daily basis. The repository stores all satellite telemetry data (raw and parsed), raw science data, as well as ground software logs and reports.

Operators have access to data repository of raw and parsed telemetry and science data for analysis. All science data, including raw data, processed data, as well as final data products are stored in the BRITE Mission Data Archive (MDA) at the Copernicus Astronomical Centre (CAC) in Warsaw. In addition, mirror sites for the archive are available at the Universities of Vienna and Montreal [59].

For distributed operations over the ground station network, data flow is handled by the BRITE multiplexing ground software as described in Section 5.2.3. A server instance of the software runs at the mission control centre, the other stations in the network run a client instance for the respective spacecraft. In case another station attempts to establish contact with the spacecraft, commands are being relayed via TCP/IP from the mission control centre to the other ground station. This way, the data flow is entirely handled by mission control even though another station has physically access to the spacecraft [62].

5.4.4 Operations Support Processes

Operations support processes for the BRITE-Austria mission include

- Ground segment scheduling and automation
- Operations over the ground station network
- Routine maintenance tasks on the spacecraft and ground station

Ground segment scheduling and automation is provided by the BRITE-Austria mission control centre in a reliable way for fully automated satellite operations. A detailed description of the automatic operations procedures of the spacecraft and ground station along with the software used, as well as operations support for the operators for remote access is provided in Section 5.2.

Operations over the BRITE ground station network represents an added value to the BRITE-Austria mission for maximising the uptime of the spacecraft as well as the science return. Details on the operation strategies over the network are provided in Section 5.1.2.

Routine maintenance tasks on the spacecraft are part of the nominal operations procedures and include scheduled configuration uploads (e.g. setup files or time tag scripts), restart and clean-up procedures, as well as updates e.g. of TLEs for the on-board orbit propagator.

5.4.4.1 Ground Station Maintenance

The ground station in Graz acts as master station for the BRITE-Austria satellite. Therefore, the ground station must be configured and maintained properly in order to ensure regular operations. In addition, remote investigation of the ground station status including environmental conditions is accomplished. Logging and evaluation of passes by automated software ensures correct operation of the ground station. A crucial aspect for operations is to ensure the ground station is always operative.

Therefore, maintenance of the ground station is performed by permanently checking and serving the outdoors equipment (especially mechanical parts e.g. the rotators), by monitoring the indoor equipment (nominal states), as well as by performance checks and corrective actions, if required. Routine maintenance tasks of the ground station include:

- Rotator calibration: since the upgrade to the new rotators the calibration is performed fully automated before every pass
- Loopback testing for TX and RX path are available (although not automated)
- Periodic ground station PC configuration backups (on monthly basis)
- Periodic inspection of the ground station hardware installations (on monthly basis)

5.4.5 Operation Teams

For commissioning of BRITE-Austria, six operators were assigned and trained accordingly to operate the spacecraft. Teams of two people were formed to operate a particular commissioning shift. Two people are better suited for performing critical commissioning tasks, as a single person might overlook something. As during commissioning the overall satellite performance has to be verified before going to nominal operations, many tasks have to be carried out manually, potentially putting the spacecraft in an anomaly state by performing particular actions, and therefore need to be carefully monitored to ensure that mistakes are avoided. In addition, the presence of a second operator is advantageous for checking that all steps in the current procedures are performed correctly as well as for documentation of the steps taken and the behaviour observed. A second operator can further perform telemetry monitoring while the primary operator is performing actions on the spacecraft, as well as monitoring of the ground station status during pass (e.g. signal strengths, tracking performance) or for contingencies, if required [8].

There was no fixed assignment of operating teams prior to commissioning. Instead, the teams were put together for each specific commissioning shift according to the availability of the operators as well as to their expertise, i.e. in the team building process a crucial factor was to have always a more experienced operator in each shift, if possible.

For each commissioning (and later operations) shift, a flight director is assigned. The flight director has absolute authority and takes all relevant operational decisions for the contacts in the shift. This is of particular importance in case any unexpected behaviour is experienced, in which case the flight director has to decide on the contingency procedures to be carried out and can decide to temporarily interrupt operations for the shift he/she is in charge (e.g. in case of malfunction of the ground station). However, the flight director has not inherently the authority to change nominal procedures / task sequences. These decisions have to be discussed with the operations director and/or the satellite systems engineer beforehand.

Given the configuration of the spacecraft as well as the configuration of the ground software, any interaction with the spacecraft itself can only be performed by a single operator at a given time. The flight director can decide whether himself/herself will directly operate the spacecraft or whether to leave the second operator on duty while the flight director coordinates the operations process and assigns / monitors the steps to be taken.

For each manually operated shift, a status report is created to document all relevant steps taken during a particular shift and to allow seamless handover between different operating teams. The common practice foresees operating teams to be at the ground station up to one hour before beginning of the first pass in their shift to prepare according to the actions and or / procedures signalised in the status report as next steps to be performed. The status reports are filled out in a spreadsheet for each shift, containing the following information [75]:

- The team operating, including the flight director assigned for the shift
- Pass information (contact times, elevation, used TLEs, ground station status)
- Identifiers of respective ground software logs
- A description of the actions taken during a particular pass, including the satellites state (software and core telemetry values), downloaded telemetry and science data (including log or file names)
- The spacecraft state during / at the end of the shift
- Actions to be taken during the next shift, allowing the next operating team to prepare accordingly

During the nominal operations phase, the requirements in terms of personnel for operating BRITE-Austria could be largely relaxed thanks to the spacecraft autonomy provided and ground station capability to operate in a fully automated fashion. In addition, the remote access strategies provide additional flexibility to the operators. The main tasks during this phase include mission planning, execution of routine operations procedures (i.e. configuration of the spacecraft), satellite data analysis, as well as contingency / recovery procedures in case of unexpected behaviour. Additional effort is required from the operators to facilitate data download processes to counteract heavy UHF uplink interference effects as described in detail in Section 5.5.4. For operations of the spacecraft, usually a single operator is on duty, including on-call policies and remote operations to basically guarantee a 24/7 service. The purpose of this strategy is to maximise the operational uptime of the spacecraft and as a result the scientific return of the mission.

5.5 Communication Link and Ground Station Performance Evaluation

During commissioning and operations of the BRITE-Austria satellite, several measurements have been carried out to characterise the performance of the communication links between the spacecraft and its master ground station in Graz. For that purpose, measurements of the uplink and downlink signal have been performed to verify the link budget calculations and to characterise the link performance at physical layer. In addition, measurements of the packet error rate and of the downlink data throughput have been carried out to evaluate the overall system performance, considering the nanosatellite protocol (NSP) used for communications with the satellite. Furthermore, since during the operations phase the UHF uplink became heavily affected by ground based interference, additional measurements have been taken on the spacecraft to characterise the interference behaviour. Different countermeasures for the interference have been investigated and implemented. Measurement results and comparisons of the different applied countermeasures are presented.

5.5.1 Signal Performance Measurements

To determine the link performance between the BRITE-Austria satellite and the Graz ground station, signal measurements in both uplink and downlink have been performed during several satellite passes.

5.5.1.1 Uplink Signal Performance Measurements

The performance of the telecommand uplink signal was measured on-board the spacecraft. For that purpose, the Whole Orbit Data (WOD) collection period for the power board telemetry group was increased to the maximum available value (one second instead of the default 60 seconds) to have a more accurate measurement interval of the Received Signal Strength Indicator (RSSI) telemetry point of the UHF receiver, which is logged in the power board telemetry group. In order to obtain uplink signal measurements with this interval from the acquisition of signal (AoS) until the loss of signal (LoS), time tagged commands to set the WOD collection period to one second before pass start and to set it back to default after pass end were prepared and uploaded to the spacecraft beforehand. To better characterise the received signal strength at the spacecraft the transmitted power from the UHF power amplifier was also recorded.

Concerning the uplink it has to be noted that, since the *UHF Station Manager* software used to control the *Yaesu FT-879D* transceiver can only either set the PTT or perform Doppler shift correction, whenever a frequency adjustment is performed according to the current Doppler shift, the PTT is unkeyed for *100 ms*. As the frequency is adjusted every time the offset has reached *1 kHz* and the Doppler shift during a pass for UHF is about ± 10 *kHz*, the transceiver is unkeyed about 20 times for a period of *100 ms* each during a pass. Therefore, if an RSSI value is logged precisely at the time when a Doppler correction is performed, a signal dropout will be detected. The probability of such a detection increases with a shorter telemetry collection period as used during the tests. This behaviour explains the major signal dropouts in the measurement plots presented hereafter.

Figure 5.29 shows the measurement results of the Received Signal Strength Indicator (RSSI) level on the spaceraft, while Figure 5.30 shows the equivalent power levels (in dBm) of the measured RSSI. Finally, Figure 5.31 shows an averaged representation of the received uplink power on the spacecraft for the measurement. Furthermore, all three figures compare the measured uplink signal with the equivalent received signal level on the spacecraft according to the link budget calculations.

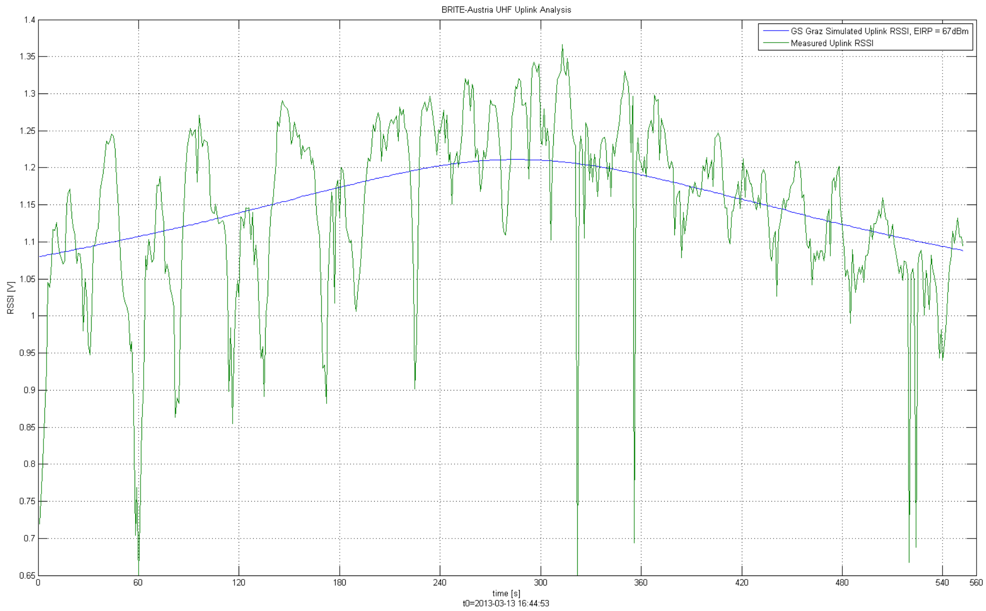

Figure 5.29: Comparison between measured and simulated RSSI for a BRITE-Austria pass over the Graz ground station. The fluctuations seen in the measured signal are due to tracking/pointing offsets (spacecraft inertially pointed), polarisation effects, as well as due to short intervals of deactivating transmission by the ground software for performing Doppler correction.

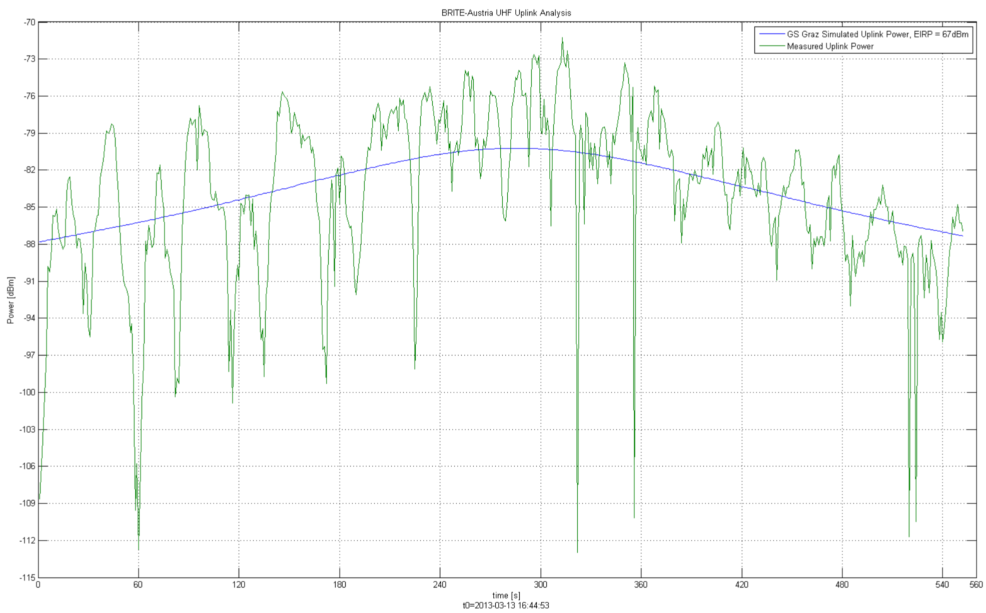

Figure 5.30: Comparison between measured and simulated RF power levels for a BRITE-Austria pass over the Graz ground station. The fluctuations seen in the measured signal are due to tracking/pointing offsets (spacecraft inertially pointed), polarisation effects, as well as due short intervals of deactivating transmission by the ground software for performing Doppler correction.

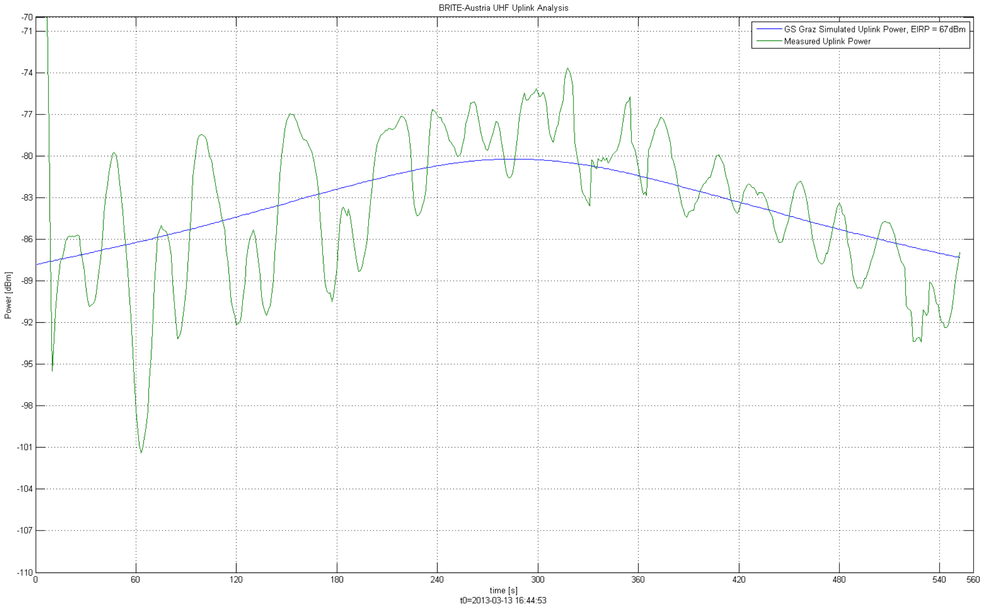

Figure 5.31: Filtered representation of the BRITE-Austria measured uplink power. The measured uplink power for a pass over the Graz ground station and compared with the simulated uplink EIRP is shown.

All calculations were performed by comparing the measured values of the collected RSSI values in the Whole Orbit Data (WOD) files of the spacecraft with the corresponding values from the link budget, with variable distance between the satellite and ground station during the pass according to the access report values generated with the *Systems Toolkit (STK)* software.

For the conversion between raw RSSI values in V to power values in dBm, in the calculations the following extreme values listed in Table 5.3, measured during EMC testing of the integrated spacecraft, were used and the values in between were derived by interpolation.

Parameter	**Value**
Minimum RSSI	0.70 V
Maximum RSSI	1.68 V
Minimum Equivalent Signal Level	-109.8 dBm
Maximum Equivalent Signal Level	-53.1 dBm

Table 5.3: Equivalent RF power levels for the RSSI minima and maxima. The values were obtained by measurement during EMC testing of the integrated spacecraft.

The results show that the measured uplink signal on the spacecraft agrees quite well with the calculated values, apart from signal fluctuations. Apart from the already mentioned dropouts due to Doppler correction, these signal fluctuations can be attributed to tracking/pointing offsets, polarisation effects (the ground station is set to fixed right hand circular polarisation), as well as to unfavourable attitude of the spacecraft with respect to the optimal orientation of the receiving antennas towards the ground station. The latter is due to the fact that the spacecraft is nominal inertially pointed, and hence keeps a fixed orientation towards a fixed target in the sky rather than towards ground as it is the case for nadir pointing.

After the Graz ground station upgrade of the UHF uplink to the configuration with two antennas in March 2014, the measurement was repeated. The purpose of this measurement was to verify the suitability of the new configuration to operate the spacecraft as well as to compare the performance with the single antenna configuration.

Figure 5.32 and Figure 5.33 show the results for a measurement taken during a high elevation pass (78° maximum elevation) over the Graz ground station on August 2nd, 2014, providing a comparison of the measured uplink signal with the equivalent received signal level on the spacecraft according to the link budget calculations for both a single antenna configuration as well as the ideal increase of the antenna gain by *+3 dB*.

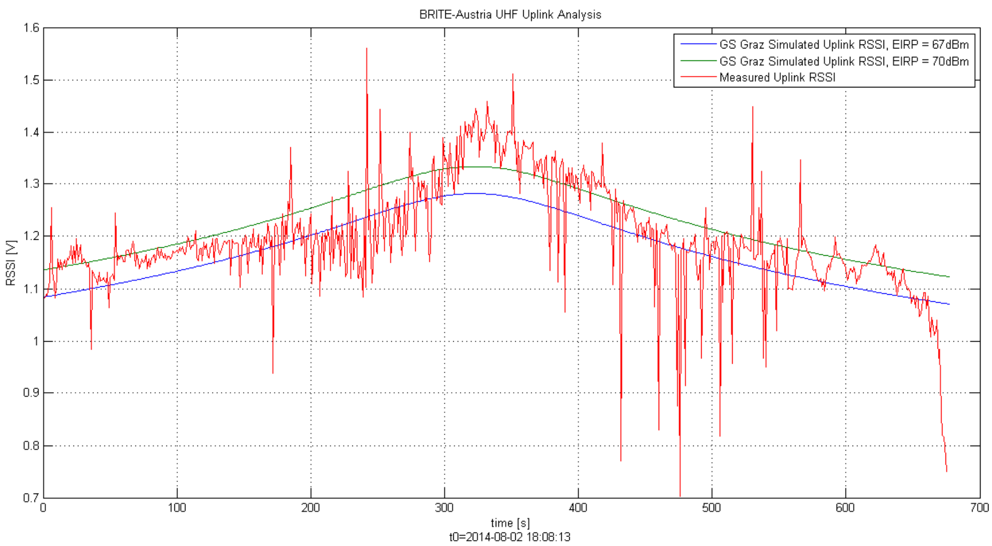

Figure 5.32: Comparison between measured and simulated RSSI for a BRITE-Austria pass over the Graz ground station after upgrade to a dual UHF antenna configuration. The measurement was performed on August 2nd, 2014. The measured values are compared with the simulated available uplink EIRP for a single antenna configuration as well as the ideal increase of 3 dB by the second antenna.

It has to be noted that the measurements for the dual antenna configuration were taken with the spacecraft tracking nadir instead of pointing inertially. Details for the nadir tracking implementation and rationale are described in Section 5.5.4. The results show therefore better stability of the received signal on the spacecraft compared to the single antenna measurements (i.e. less signal fluctuations / dropouts), as the orientation of the receiving UHF antennas on the spacecraft was nearly constant during the measurement. A few very high signal peaks can also be seen and can be attributed to UHF signal interference.

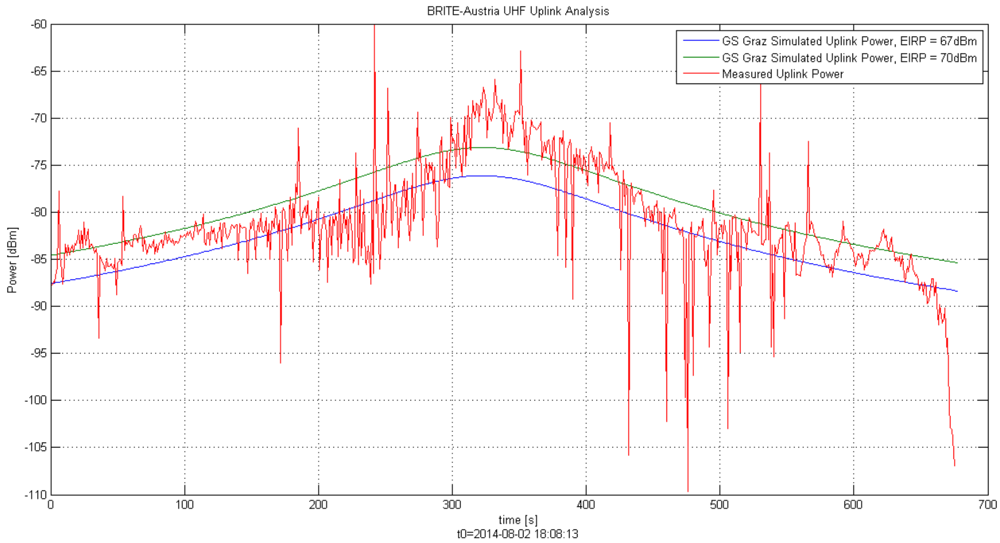

Figure 5.33: Comparison between measured and simulated RF uplink power for a BRITE-Austria pass over the Graz ground station after upgrade to a dual UHF antenna configuration. The measurement has been performed on August 2nd, 2014. The measured values are compared with the simulated available uplink EIRP for a single antenna configuration as well as the ideal increase of *3 dB* by the second antenna.

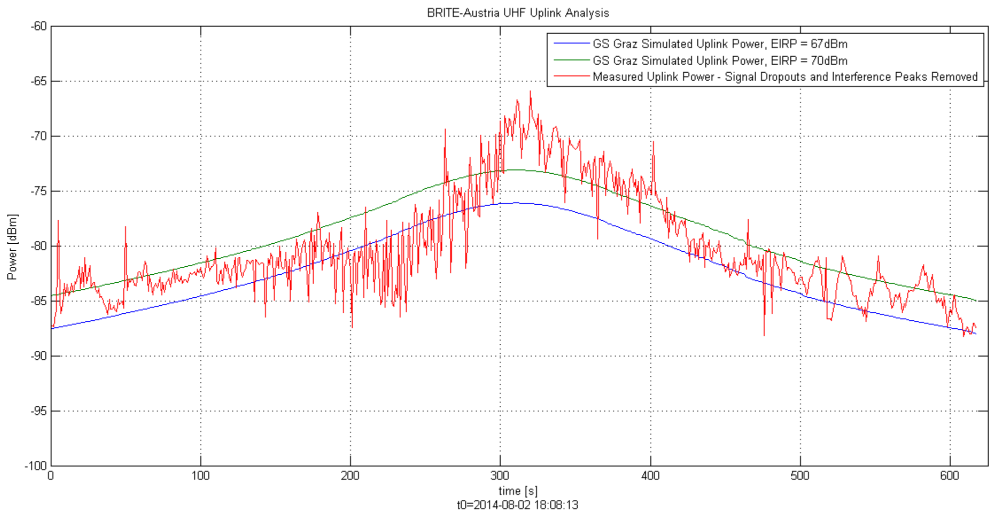

Figure 5.34: Adjusted representation of the BRITE-Austria measured uplink power after the ground station upgrade to two UHF antennas. A representation of the BRITE-Austria measured uplink power after the ground station upgrade to two UHF antennas with the signal dropouts removed for a pass over the Graz ground station on August 2nd, 2014 and comparison with the simulated available uplink EIRP for a single antenna configuration as well as the ideal increase of *3 dB* by the second antenna is given. These data have been used for mean value calculations and comparison between the measured and calculated values.

The results show that for the majority of the measurement the uplink signal is higher than the expected signal level for the single antenna configuration, and often reaches the expected signal level for an ideal increase of the EIRP by *+3 dB*. On the highest elevations, the measured signal even exceeds the signal level expected for the dual antenna configuration. While it is difficult to determine the exact ground station EIRP from these measurements, an estimate has been derived by comparing the mean values of the calculated vs. measured EIRP, removing the dropouts in the measured signal as well as the interference signal peaks. A corresponding plot of this representation is shown in Figure 5.34. The results show that the mean value for the measured EIRP is *1.94 dB* higher than for the calculated EIRP value of the single antenna configuration and as a result, *1.06 dB* lower than for the calculated EIRP value of the dual antenna configuration under assumption of an ideal EIRP increase by *3 dB*. Therefore, as a first estimation, the EIRP of the dual antenna configuration has increased by *1.94 dB* compared to the single antenna configuration.

5.5.1.2 Downlink Signal Performance Measurements

Concerning the received downlink signal from the BRITE-Austria satellite, measurements at the ground station are basically performed during every contact with the spacecraft. The receiving parameters of the S-band downlink are recorded from the satellite modem at the ground station, including the received signal level, frequency offset, and E_b/N_0. In addition, the signal spectrum along with the corresponding signal to noise ratio are recorded from the spectrum analyser. For better analysis of the downlink signal measurements, the enhanced *S-band Spectrum View* software as described in Section 5.2, combining the measurements of the satellite modem and the spectrum analyser has been used on a subset of passes mainly dedicated to communication link tests. Finally, to determine the tracking performance, the actual antenna positions in azimuth and elevation during the pass were logged from the tracking software and compared with the ideal positions obtained from *STK* simulations for the respective pass.

For the downlink, the measured signal has been compared with the expected values according to the *Matlab* simulations described in Chapter 3. Figure 5.35 shows this comparison for an afternoon pass of BRITE-Austria over the Graz ground station on March 13$^{\text{th}}$, 2013. The plot shows that the measured values agree quite well with the expected values from the simulation, which also takes into account the characteristics of the ground station. In addition, Figure 5.36 shows a filtered representation for better comparison, confirming the results. The fluctuations in the measured downlink signal can be mainly attributed to tracking lags of the ground station rotators as well as to variations in the orientation of the S-band antennas of the spacecraft with the respect to the ground station due to inertial pointing.

5.5.2 Packet Error Rate Measurements

In addition to the signal measurements, the link performance between the BRITE-Austria satellite and its master ground station in Graz has been assessed by measurements of the packet error rate for different modulation and data rate configurations.

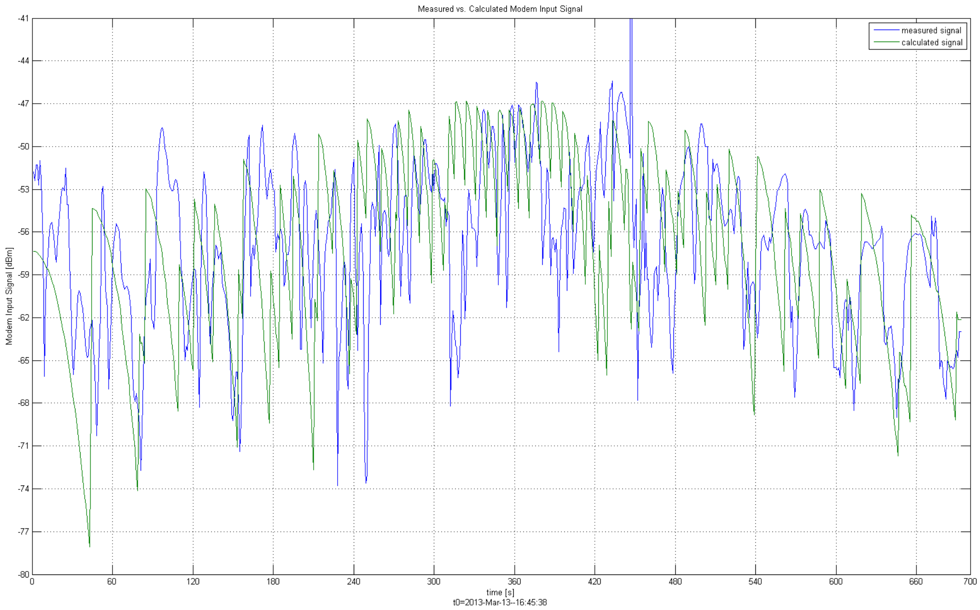

Figure 5.35: Comparison between measured and simulated downlink signal levels for a BRITE-Austria pass over the Graz ground station. The measurement was performed on March 13th, 2013. The plot shows that the measured and simulated signal agree quite well.

For measuring the packet error rate (PER), a test script of 1000 so called *"Ping"* commands was generated and uploaded to the spacecraft. A "Ping" command is an essential command to which the spacecraft will reply with a *"Pong"* command, independently from its current software state from either the bootloader or the application code. The *"Pong"* command includes an identification of the responding on-board computer, the current software state, as well as the OBC time stamp. Both *"Ping"* and *"Pong"* commands correspond to a single Nanosatellite Protocol (NSP) packet [78].

The test script was issued from the Graz ground station via the UHF uplink to the BRITE-Austria housekeeping computer (HKC). The HKC is the device that communicates directly with the communication system on-board, receiving commands from the UHF receiver, routing them to other computers/devices, and forwarding all data to be downloaded to the S-band transmitter. Therefore, by performing the test with the HKC it was ensured that the measurements were not influenced by additional packet delays, timeouts, or transmission errors due to inter-OBC communication.

The script is only completed after a *"Pong"* response is received for the last *"Ping"* command; if a timeout occurs while sending the packet, another attempt to retransmit the packet is made until it has finally been received and acknowledged by a *"Pong"* reply. At the end, for the 1000 *"Ping"* commands in the script, 1000 *"Pong"* replies are obtained from the HKC. By comparing the number of transmitted *"Ping"* packets with the 1000 *"Pong"* packet responses received, the packet error rate for the specific test period can be determined. The packet errors are therefore determined by the number of retransmissions for a *"Ping"* packet, and the packet error rate can be calculated according to Equation 5.14.

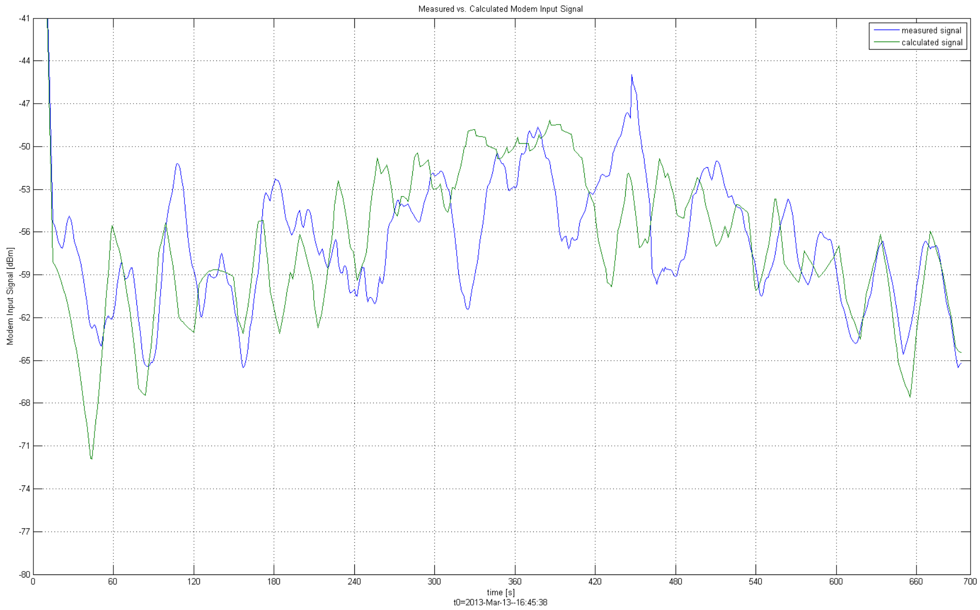

Figure 5.36: Comparison between measured and simulated downlink signal levels for a BRITE-Austria pass over the Graz ground station - filtered representation. The measurement has been performed on March 13th, 2013. This representation again shows a good match between measured and simulated signal.

$$PER[\%] = \left(1 - \frac{Packets_{RX}}{Packets_{TX}}\right) \cdot 100 \tag{5.14}$$

The packet error rate was measured for the following different modulations and data rates:

- BPSK 32kbit/s
- BPSK 128 kbit/s
- QPSK 256 kbit/s

It has to be noted that during all performed measurements, the link quality varied according to the satellites distance to the ground station, its orientation towards the ground station, the tracking accuracy of the ground station rotators, as well as potential ground based interference in both communication paths. This behaviour affects both the uplink and the downlink, but due to the different frequencies, antennas, and RF-front end used different effects can occur for the uplink and the downlink at different times during the measurements. Therefore, the measured packet error rate does not describe the link performance of the overall system in absolute terms, but always in dependence of the current boundary conditions for a particular ground station pass.

To consider all the additional effects affecting the link, additional parameters were recorded while performing the packet error measurements. These parameters include the received signal strength at the spacecraft UHF receiver with 1 second measurement interval along the transmitted signal strength from the UHF power amplifier on ground, the receiving S-band downlink parameters of the satellite modem and spectrum analyser at the ground station, as well as the tracking information logged from the tracking software.

Figure 5.37 shows the packet errors which occurred for a particular BRITE-Austria pass while transmitting with BPSK *32 kbit/s* (zeros in the plot indicate packet errors).

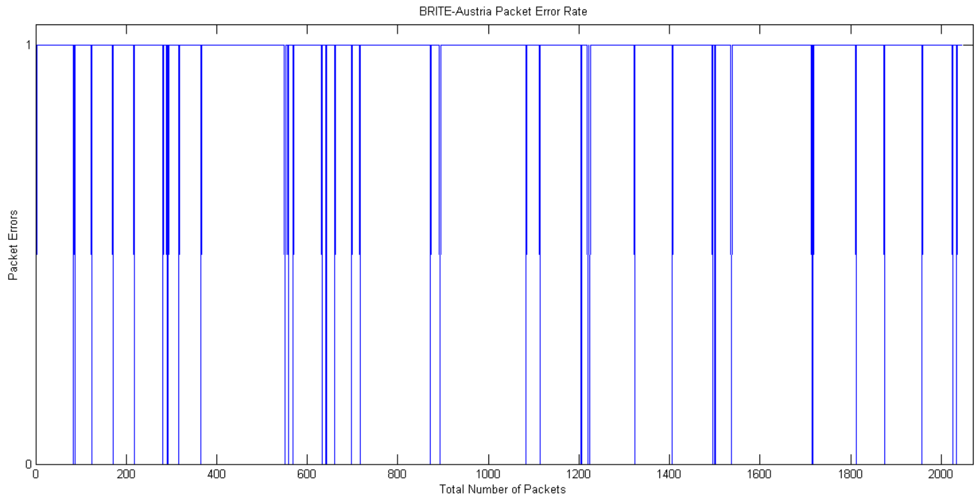

Figure 5.37: BRITE-Austria packet error rate. The packet error rate has been measured while transmitting with the BPSK *32 kbit/s* setting. A "1" in the plot denotes a packet success, while a "0" in the plot describes a packet failure.

By performing several measurements and a comparison of the results, the link performance for operating the BRITE-Austria satellite from the Graz ground station has been characterised. Table 5.4 shows the results of the packet error measurements for different modulation and data rate combinations.

Configuration	Measurement	TX Packets	RX Packets	Packet Success	Packet Errors
BPSK 32	Total	10,452.00	9,768.00	93.46%	6.54%
BPSK 32	Individual Avg.	653.25	610.5	93.88%	6.12%
BPSK 128	Total	6,000.00	5,411.00	90.18%	9.82%
BPSK 128	Individual Avg.	857.14	773.00	90.51%	9.49%
QPSK 256	Total	4,607.00	4,333.00	94.05%	5.95%
QPSK 256	Individual Avg.	767.83	722.67	94.41%	5.59%

Table 5.4: Packet error measurement results between BRITE-Austria and the Graz ground station. The results for different modulation and data rate configurations are shown. The performance is comparable between the different schemes, except for BPSK *128 kbit/s*, where the measured packet error rate is significantly higher.

The results show that the packet error rates for the communication link between BRITE-Austria and the Graz ground station including all occurring link impairments vary between 5.59% and 9.49%. Concerning the different data rate configurations and modulation schemes, the performance is comparable, except for BPSK *128 kbit/s*, where the measured packet error rate was significantly higher.

As already mentioned, during the operations phase nadir tracking of the spacecraft was implemented during contacts with the Graz ground station to improve the link performance. Unfortunately, packet error measurements could not be repeated for this new configuration due to heavy impairments of the UHF uplink by interference for the time being as described in Section 5.5.4.

5.5.3 Data Throughput Measurements

In addition to the packet error rate, another important measure for determining the link performance is the data throughput. Throughput measurements were performed by analysing the data amount downloaded during passes mainly dedicated to data downloads. This was performed in both manual operations and automated operations configuration with ACM. For the considered downloads in manual operations mode the data rate was varied manually by an operator according to the observed downlink quality. In the automated configuration with ACM, modulation and data rate are adapted automatically by the ground software according to the current link quality rated by the measured E_b/N_0 from the satellite modem.

Measurements of the BRITE-Austria downlink throughput were performed by analysing the packet logs of the relevant passes over the Graz ground station. The logs contain the raw packets exchanged between the satellite and the ground station.

For analysing the logs, it is necessary to know the contained packet format. The logs contain the Nanosatellite Protocol (NSP) packets as sent to or received by a client. The BRITE-Austria NSP packet format with HDLC framing is shown in Figure 5.38 and consists of the following [78]:

- HDLC start and end flag
- HDLC satellite address
- NSP destination and source address
- NSP command
- data field of variable length (including address bytes)
- cyclic redundancy check (CRC) field

HDLC Start Flag	HDLC Satellite Addr.	NSP Dst Addr.	NSP Src Addr.	NSP Command	Data (variable)	CRC	HDLC Stop Flag
1 Byte	2 Bytes	1 Byte	1 Byte	1 Byte	n Bytes	2 Bytes	1 Byte

Figure 5.38: BRITE-Austria Nanosatellite Protocol (NSP) packet format with HDLC framing. The HDLC frames are encapsulated with NSP packets at network layer.

The log analysis was therefore performed by identifying the relevant downloaded packets and by summing up the individual packet lengths to obtain the total downloaded information data. In addition, by determining the start and end timestamps of the download, the average information data rate for the pass can be calculated by dividing the total amount of data downloaded (in bits) with the duration of the download (in seconds). In addition, the packet overhead was subtracted for each packet to obtain the correspondent average user data for the pass.

The analysis therefore takes into account potential link impairments or signal outages during the measuring period and provides a good estimation for the system performance under real link conditions.

Figure 5.39 shows the manual data rate variation on the downlink according to the link conditions for a BRITE-Austria pass over the Graz ground station on March 14th, 2013.

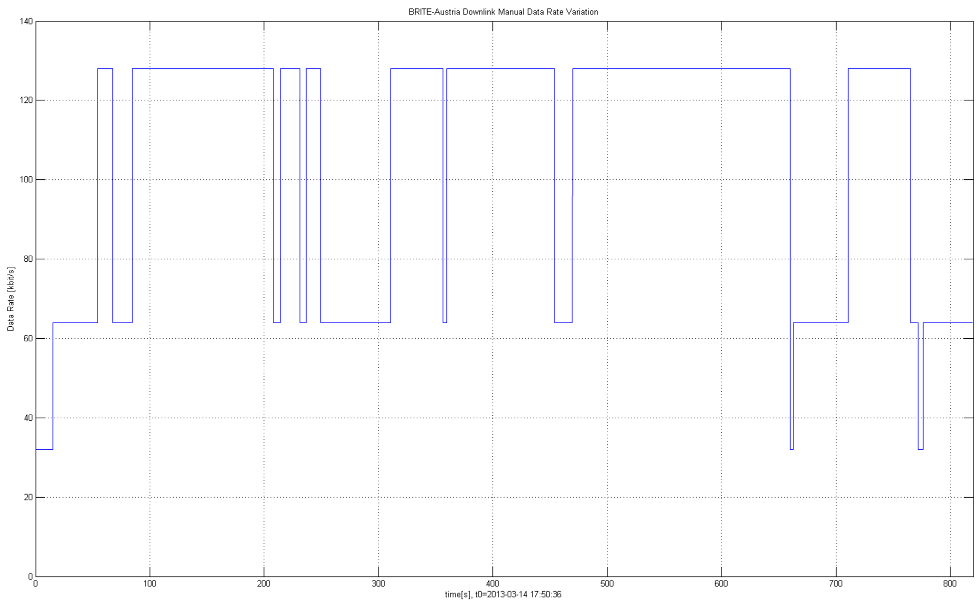

Figure 5.39: BRITE-Austria downlink manual data rate variation. The values were recorded for a contact with the Graz ground station on March 14th, 2013. The plot shows that, due to the good signal conditions, the data rate could be raised to *128 kbit/s* for large portions of the pass.

Table 5.5 shows the details for the sample contact of BRITE-Austria with the Graz ground station on March 14th, 2013, comparing the information data rate with the user data rate resulting from the occurring packet overhead during the download. During this contact, an ACS-log was downloaded while the spacecraft was in passive attitude determination mode. The maximum elevation for the contact was 67°.

Table 5.6 shows the overall throughput statistics for over 50 manually operated BRITE-Austria contacts with the Graz ground station. For the analysed contacts, the data rate was manually varied mostly between *32 kbit/s* and *128 kbit/s* using BPSK modulation, and during a few contacts also by using QPSK modulation with data rates up to *256 kbit/s*. The results show that the average information data rate lays at about *55 kbit/s*, for which about 94.5% is user data and 5.5% is NSP packet overhead.

Duration [s]	Information Data [Byte]	User Data [Byte]	Information DR [bit/s]	Overhead [%]	User DR [bit/s]
819.00	5,313,362	5,018,852	51,901	5.54	49,024

Table 5.5: BRITE-Austria throughput measurement details for a single pass. The measurement was performed during an afternoon pass over the Graz ground station on March 14th, 2013. The average available user data rate (DR) for the pass was 50 *kbit/s*.

For obtaining the correspondent user data, only the overhead needs to be removed, as the incoming data has already been decoded by the satellite modem with the code rate $1/2$. The average available user data rate is around *50 kbit/s*. This yields an average available user data download amount for a single pass (*573 s* on average) of *3.5 MByte* and an estimated daily user data download amount of *18.1 MByte* (assuming *60 min = 3000 s* of average contact time).

	Duration [s]	Information Data [Byte]	User Data [Byte]	Information DR [bit/s]	Overhead [%]	User DR [bit/s]
Total	27,334	187,256,048	176,988,788			
Avg. p. Pass	573	3,66,812	3,463,919	51,160	5.45	48,329
Avg. Total				54,805	5.48	51,800
Daily Stats	3,000	19,184,984	18,123,435			

Table 5.6: Throughput measurement results between BRITE-Austria and the Graz ground station. The results show that the average available user data rate for a contact is > 50 *kbit/s*, yielding an average data download amount of 3.5 *MByte* per *10 minutes* pass. Assuming 60 *minutes* of contact per day, the available data download amount is 20 *MByte/day*.

A data download volume of around *13-14 MByte/day* is required for downloading satellite telemetry data (around *1 MByte/day*) and science data for 20 minutes observations every orbit of a single target field with 15 science rasters defined (around *900 kByte/file*). These sample figures are already beyond the nominal mission requirements and the results show that these requirements can be met with an additional substantial margin of *4 MByte/day*. This excess capacity can further be used to increase the science data collection. The rationale derives from the fact that the in-orbit validation of the instrument has shown that the performance is better than specified, allowing to observe stars with visual magnitudes down to $+4.5$ (compared to the $+3.5$ as specified in the requirements). Science data collection can be increased in the following different ways [77]:

- Increase the number of stars to be observed in the FOV (up to 30 has been successfully demonstrated on the Centaurus observation campaign)
- Extend the overall observation time per orbit (up to 30 minutes has been successfully demonstrated)
- Reduce the delay/processing interval between exposures

- Observe an additional secondary target field (successfully demonstrated on BRITE-Austria, UniBRITE, and BRITE-Toronto)

Although the results show that the achievable data throughput is well-suited to operate the mission, there is still room for improvement. The intermittent connectivity due to link disruption has an impact on the transmission efficiency and throughput. Better tracking precision of the ground station and nadir tracking of the spacecraft could bring further improvements.

In addition, from October 2013 strong ground based interference signals were detected affecting the UHF uplink, requiring improvements in the communication link design. A detailed description of the UHF interference along with possible countermeasures is provided in the next section.

5.5.4 UHF Uplink Interference Measurements

Starting from the beginning of October 2013, BRITE-Austria has been affected by strong ground based interference over Europe, significantly limiting operations of the spacecraft. The interference signal affects operations by inhibiting the upload of spacecraft commands as well as by limiting the downlink performance due to missing acknowledgements to the data download transmissions in the return channel.

In the five months from the beginning of October 2013 up to the beginning of March 2014, the UHF uplink interference was completely absent for only about 3 weeks in total, randomly spread over the period (except for almost one week in a row at the beginning of November). The interference signal typically affects 4-5 out of 6 trackable passes a day, where the most Eastern contact is occasionally not affected particularly when at low elevations with respect of the Graz ground station (< 10 *deg* max.). During contacts with the Graz ground station when interference is detected, typically only two minutes towards South are not affected. This is consistent for both morning passes (from South to North) and evening passes (from North to South). These two minutes led to the first assumption that the primary interference source must be located at Northern European latitudes.

After the launch of the first Polish BRITE satellite Lem at the end of November 2013, it was discovered that also Lem is heavily affected by interference in the UHF uplink. Since Lem was placed in a different orbit and has little overlap with BRITE-Austria with respect to contact times from ground, a coordinated effort of a specific type of service (e.g. space radar) was suspected to be the possible source of interference. This further led to the assumption that also UniBRITE, the third BRITE satellite already in orbit at that time, which was launched together with BRITE-Austria in the same orbit, could be affected as well, but had not been noticed previously as the spacecraft is only operated from Toronto. It was verified that on UniBRITE the same interference effects were present while the spacecraft was operated over Europe.

Apart from the BRITE-Constellation satellites, valuable additional information about the interference signal uplink frequency has been obtained during discussions with other CubeSat teams with spacecraft on the same launch with BRITE-PL1 at the end of November:

The UWE-3 spacecraft from the University of Würzburg, Germany [79] is affected by interference in its UHF uplink in a similar manner as the BRITE spacecraft. In particular, there seems to be a correlation between the periods/contacts affected vs. unaffected by interference with the BRITE spacecraft. UWE-3 uses the frequency slot next to BRITE in the allocation (437.380 MHz).

The GOM-X1 spacecraft from GOMSpace, Denmark, is not affected by interference in its UHF uplink. The UHF uplink frequency of the satellite is, however, 115 kHz apart from the BRITE uplink frequency (437.250 MHz) [80].

The FUNcube satellite from AMSAT-UK is affected in the UHF uplink, but only at low elevations due to a known terrestrial radar service in the UK, but has no interference issues at higher elevation angles. The uplink frequencies of FUNcube are far from the ones of the other spacecraft (435.130 to 435.150 MHz) [81].

The conclusion of this survey with other CubeSats suggests that the uplink frequency of the interference source must be located very close to the uplink frequencies of BRITE (437.365 MHz) and UWE-3 (437.380 MHz).

In order to confirm the assumptions stated above and to characterise the interference signal, several measurements have been performed on all three BRITE spacecraft in orbit at that time. For that purpose, during overflights of BRITE-Austria, BRITE-PL1, as well as UniBRITE over Europe, the received signal strength of the receiver was measured on all three spacecraft. For these measurements, the collection period of the power board whole orbit data (WOD) was increased to one second (instead of the default 60 seconds).

The results show that an interference signal was detected on all three spacecraft with identical properties which can be characterised as follows:

- The signal is pulsed, for which the pulse duration cannot be fully characterised as the measurement interval is only one second and the pulses could be shorter than that
- The signal level of the pulses is very high, often larger than the available EIRP from the BRITE ground stations, and has occasionally reached the saturation level of the receivers on the spacecraft (-60 dBm)
- The signal level increases and decreases in accordance to increasing and decreasing elevation of the spacecraft over Europe, hence a directive terrestrial service can be excluded; the source is either omnidirectional (in this case with very high gain) or (more likely) tracking the spacecraft intentionally

A graphical representation of the interference signal on BRITE-Austria in a period where a contact with the spacecraft from the Graz ground station would have been possible is shown in Figure 5.40. The plot shows a comparison between the measured interference signal on the spacecraft (green line) with the equivalent signal that would have been received on the spacecraft from the Graz ground station during the possible contact time (blue line), based on the maximum available ground station EIRP. The plot clearly shows that, the interference signal is detected on the spacecraft starting from around two minutes before the visibility with the Graz ground station and stops two minutes before exiting the visibility from the ground station. As this measurement was taken during an afternoon pass, when the spacecraft travels from North to South, this confirms the first assumption of the geographical location of the interference source towards Northern Europe. It can be seen that the last 2 minutes of the pass are interference-free. In addition, some of the interference signal peaks are significantly higher than the available ground station EIRP.

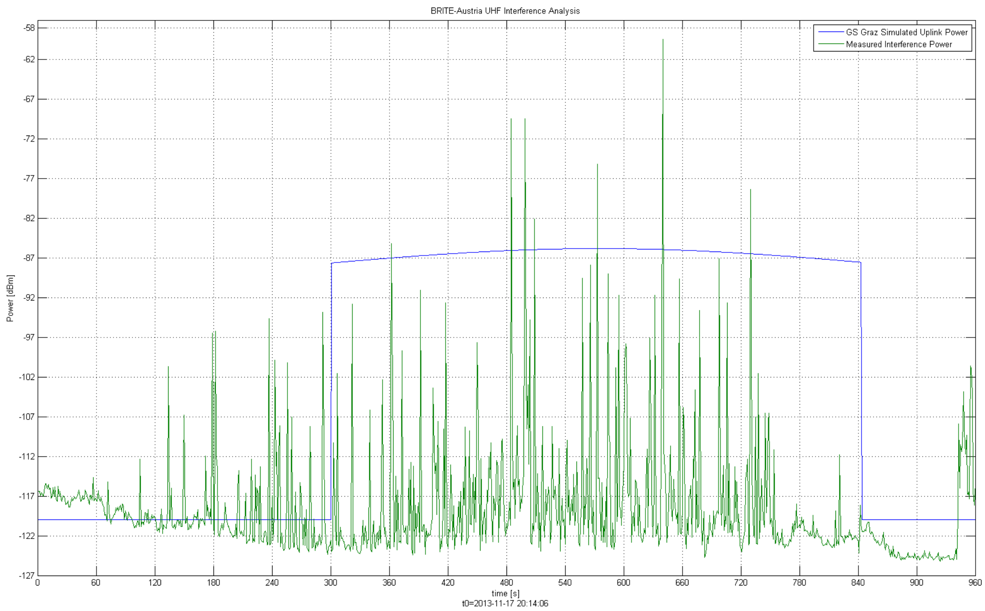

Figure 5.40: BRITE-Austria UHF uplink interference. The plot shows the UHF interference signal measured by the BRITE-Austria spacecraft and a comparison with the expected received uplink signal from the Graz ground station. The interference signal consists of short, high power signal pulses. Compared to the available uplink power of the ground station, the pulses significantly exceed the power level, and the signal peaks reach the saturation level of the satellite receiver (*-60 dBm*).

Another major purpose of the performed interference measurements was to determine whether the interference source is tracking an object on purpose or if it is a signal of rather omnidirectional characteristic. For that purpose, simultaneous signal measurements have been performed on BRITE-Austria and BRITE-PL1 during overlaps in the ground track over Europe. During this test, BRITE-Austria was the first of the two spacecraft flying over Europe, from North to South, and crossing the ground track with BRITE-PL1 coming from South, shifted by a few minutes in time.

A graphical representation of the results of this test is shown in Figure 5.41. The measured interference signal on BRITE-Austria is shown in green, while the measured interference signal on BRITE-PL1 is shown in red. The blue line shows the equivalent signal which would have been received on the BRITE-Austria spacecraft from the Graz ground station during the possible contact time (blue line), based on the maximum available ground station EIRP (68 dBm). The plot shows that from around 2 minutes

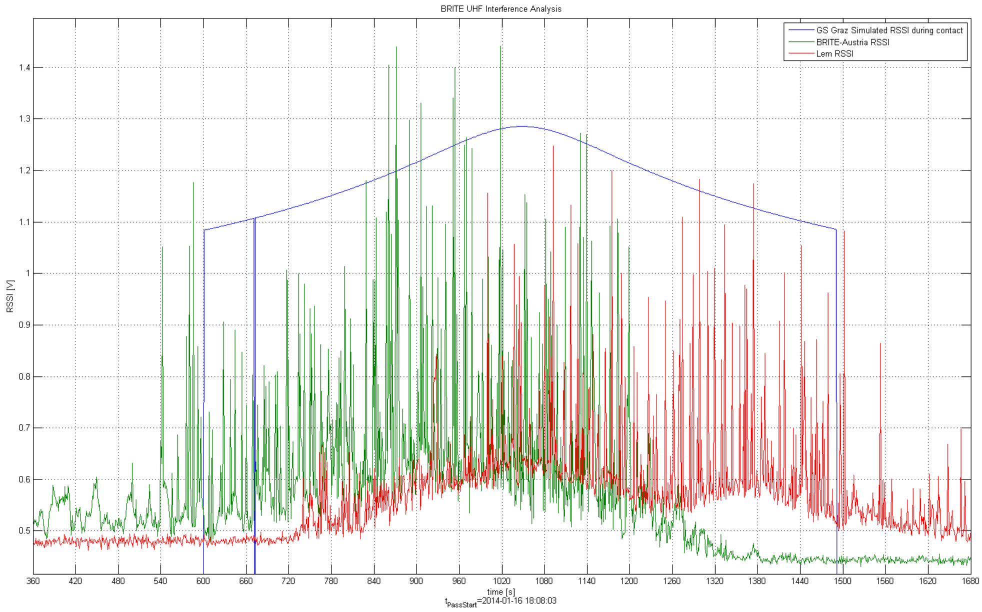

Figure 5.41: BRITE-Austria and BRITE-PL1 UHF uplink interference overlap. The plot shows a collected UHF uplink interference measurement for overlapping BRITE-Austria and BRITE-PL1 passes over Europe. Starting from two minutes before the upcoming contact with the Graz ground station, only BRITE-Austria was affected by interference. With BRITE-PL1 approaching BRITE-Austria, there is an overlap of the interference signal on both spacecraft. Unlike for other passes, five minutes before exiting the visibility from the Graz ground station, the interference signal disappeared on BRITE-Austria and from then on was only detected on BRITE-PL1. These results show that the interference source is tracking.

before the upcoming contact with the Graz ground station, BRITE-Austria was affected by interference. With BRITE-PL1 approaching BRITE-Austria, some interference signal can also be seen on BRITE-PL1, probably due to the still wide beamwidth of the transmitted signal. Unlike for other passes, five minutes before exiting the visibility from the Graz ground station, the interference signal disappeared on BRITE-Austria. At that point the two spacecraft had crossed their ground tracks and were moving apart and from then on the interference signal was only detected on BRITE-PL1. Therefore this measurement suggests that the interference source is tracking and switching from one spacecraft to the other one on purpose.

Consecutive measurements over several BRITE-Austria orbits over Europe were performed to investigate possible interference source locations. Results from four consecutive measurements over four orbits of BRITE-Austria in the afternoon of November 17th 2013 (the spacecraft is coming from East and travelling from North to South) are shown in Figure 5.42. The blue lines depict the orbit track of BRITE-Austria for the four investigated orbits. The yellow lines show the access of the satellite with the ground station in Graz. The red dots denote the start (North) and end (South) points of the detected interference signal. The red lines show the phases when interference was detected on the spacecraft.

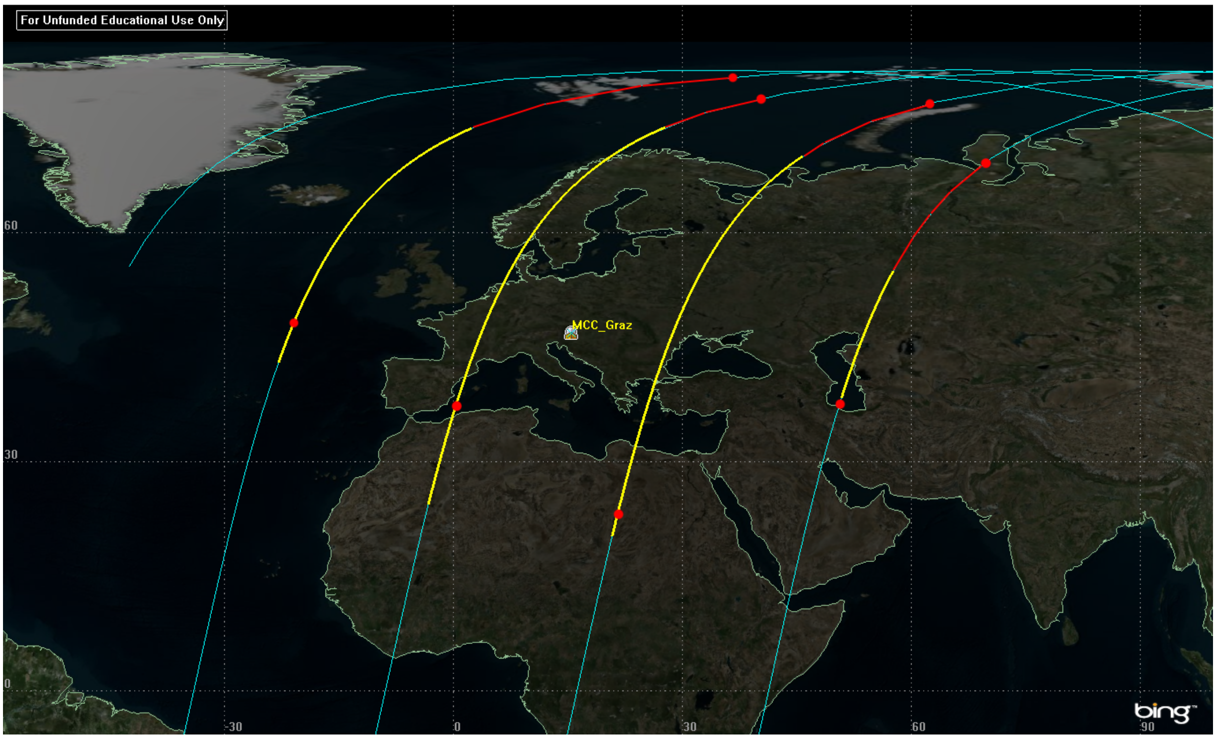

Figure 5.42: BRITE-Austria UHF uplink interference ground track. Ground track and coverage of UHF interference signal measured on the BRITE-Austria spacecraft for 4 consecutive orbits crossing Europe. The blue lines show the orbit track of BRITE-Austria for the four investigated orbits. The yellow lines show the access of the satellite with the ground station in Graz. The red dots denote the start (North) and end (South) points of the detected interference signal. The red lines show the phases when interference was detected on the spacecraft, while the red dots denote the respective start and end of the interference signal on the track.

The access of the interference signal source could come from a single source. However, as shown in Figure 5.43, it is unusual to observe that the measured interference signal level increases from East to West, with the maximum during the last of the four measured orbits (assuming the source is always transmitting with the same transmit power).

To summarise the results from the different measurements performed it can be stated:

- The interference source(s) are located in Northern Europe
- Not only a single source of interference is involved
- The interference source(s) are tracking
- The interference signal consists of short pulses with high power, typical for a radar signal

Based on these results, the interference sources are believed to be military early warning radar stations for space situational awareness in Northern Europe, which constantly monitors the strategic air and space sectors.

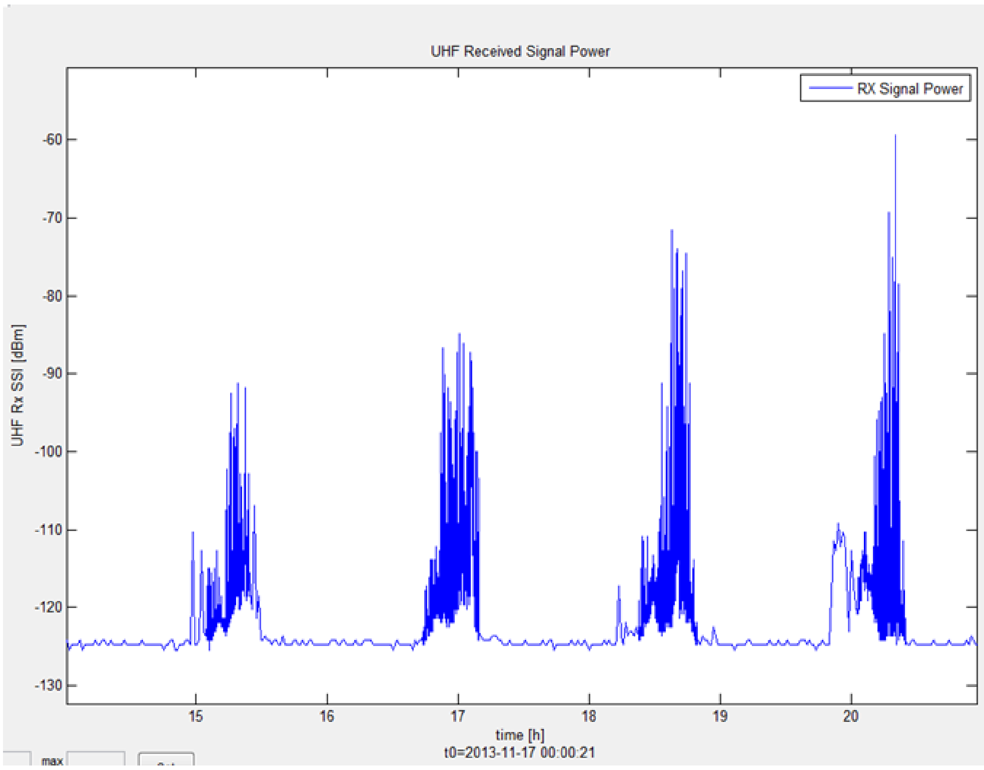

Figure 5.43: BRITE-Austria UHF uplink interference RSSI analysis. Equivalent received signal strength of UHF interference signal on the BRITE-Austria spacecraft for 4 consecutive orbits crossing Europe. For this measurement, the interference signal level increases from pass to pass, reaching its maximum during the last measurement, for which the satellite was already crossing the Atlantic ocean.

While the possibilities to characterise the UHF interference with BRITE constellation are limited to RSSI measurements and overlapping ground tracks due to the static UHF RX frequency, the *70 cm* amateur radio has been characterised in detail by the *UWE-3* picosatellite by measuring the received signal at different frequencies. The results of these measurements presented in [82] show that central European regions are mainly affected by interference between *437.000 MHz* and *437.600 MHz*.

5.5.4.1 Interference Uplink Analysis and Countermeasures

To characterise the impact of the interference effects on the uplink path with respect to command or file uploads, a quantitative analysis of the interference effects has been performed at packet level based on the following assumptions:

- A pulsed radar interference source with a pulse duration of *1 ms* (typical for pulsed radars)
- The tracking range of the radar lies between *1000 km* and *4000 km* (typical pulsed radar range), yielding a pulse repetition rate between *150 Hz* and *37 Hz*, respectively.

For the uplink bit rate of *9600 bit/s* used this means that every 64^{th} / 256^{th} bit is affected, respectively.

Packet Payload Size	256	32	8	Byte
Total Packet Size	268	44	20	Byte
Number of Packets	2	10	39	
Total Upload Data Volume	330	426	774	Byte
Overhead	7.84	39.22	152.94	%
Max. Bit Errors per Packet	34	6	3	bit

Table 5.7: Comparison between different packet sizes for file uploads. The comparison shows that, while for small packet sizes the number of bits affected by the radar pulses decreases, the overall upload data volume increases due to the additional overhead.

Commands and files are uploaded to the spacecraft in NSP packets as described in Section 5.5.2. The shortest command that can be sent to the spacecraft (”Ping” command) is *7 Bytes* long including the packet overhead (only *6 Bytes* overhead as it is a pure NSP command without the HDLC frame overhead). For this command, already *1 bit* is affected by the laser pulse.

For file uploads, such as time tagged scripts or instrument setup files, NSP packets encapsulated in HDLC frames are used. Therefore, in this case the packet overhead is *12 Bytes*. In the typical ground software setup for file uploads, the files are divided in packets of *256 Bytes* length. For this packet length, *34 bits* are affected by a laser pulse (for *1000 km* distance) and hence, it is very unlikely that these packets can be delivered successfully.

As countermeasure, the packet size can be reduced. The key in this respect is to find a good compromise between packet size and additional upload data volume due to packet overhead. Table 5.7 shows a comparison between payload packet sizes of *256 Byte*, *32 Byte*, and *8 Byte* for uploading an instrument setup file of *306 Byte*.

The results show that for packets of *8 Byte* payload only *3 bit* are maximal affected by interference and hence there is a good chance that the packets can be uploaded without too many retry attempts. The drawback is clearly the large packet overhead (1.5 times the payload), which leads to uploading 2.5 times data compared to the actual file size. A packet size of *32 Bytes* payload represents a compromise between small packet size and overhead.

Under operational conditions in the presence of interference, the following observations have been made:

- File uploads in *256 Bytes* long packets are nearly impossible to upload
- File uploads in *32 Bytes* long packets perform quite well
- File uploads in *8 Bytes* perform best despite the large packet overhead

A key aspect in the analysis of the interference effects on the uplink signal is the impact on the acknowledgement packets during file downloads from the spacecraft. The overall size of an acknowledgement packet is *27 Bytes*; therefore, based on the presented considerations, *4 bits* are affected by the interference pulses.

The analysis showed that, based on the assumed interference signal pulse duration and repetition rates, only single bits are affected by interference. Therefore, the implementation of forward error correction (FEC) would allow the correction of these bit errors and improve the uplink performance significantly.

5.5.4.2 Interference Downlink Analysis and Countermeasures

To characterise the impact of the interference effects on the downlink performance, an analysis of the throughput has been performed and compared with the results for passes unaffected by interference. The results are shown in Table 5.8 and Table 5.9. It can be seen, that, for an estimated daily contact duration of 50 minutes (3,000 seconds), the downloaded daily data amount in presence of interference is only $1/6$ compared to the amount without interference. According to the current data collection, the daily data amount to be downloaded is estimated with about *15 MByte*, which means that only $1/5$ of the required daily volume would be feasible to download if all passes were affected by interference in the uplink.

	Duration [s]	**Information Data [Byte]**	**Information DR [Byte/s]**
Total	8,104	7,622,912	
Average	675	692,992	7,964
Daily Stats(est.)	3,000	3,078,444	

Table 5.8: Throughput measurement results between BRITE-Austria and the Graz ground station with UHF interference. The available downloaded data amount is significantly reduced to *3 MByte/day*, which is less than what can be downloaded in average during a single pass.

	Duration [s]	**Information Data [Byte]**	**Information DR [Byte/s]**
Total	7,482	46,413,793	
Average	623	3,867,816	47,218
Daily Stats(est.)	3,000	18,610,182	

Table 5.9: Throughput measurement results between BRITE-Austria and the Graz ground station without UHF interference. The results show that the ground station is capable of downloading *18.6 Mbyte/day* without interference.

A quick countermeasure to improve the downlink throughput was to increase the maximum number of packets per request in the downloading ground software from 32 packets to large numbers (i.e. 512 or more). This way, when a larger number of packets is requested, larger bulks of data are downloaded at once, and the missing packets are requested in a later step.

An analysis of the throughput making use of this countermeasure shows, that the throughput can be almost doubled, allowing to download around $1/3$ of the required daily data volumes. Detailed results are shown in Table 5.10.

	Duration [s]	**Information Data [Byte]**	**Information DR [Byte/s]**
Total	7,545	13,352,112	
Average	629	1,112,676	13,640
Daily Stats(est.)	3,000	5,308,991	

Table 5.10: Throughput measurement results between BRITE-Austria and the Graz ground station with UHF interference by increasing the maximum packet requests. With this workaround, the downloadable daily data amount is increased to *5.3 MByte/day*.

While this quick countermeasure of increasing the maximum number of packets per request brought some improvement, the overall performance is still unacceptable for nominal operations of the missions.

Therefore, the following possible improvements have been identified:

- On-board countermeasures
  - Science on-board data compression
  - Nadir tracking of the spacecraft during contacts with the ground station
  - Communication protocol improvements to implement data streaming
  - Implementation of Forward Error Correction (FEC)
- Ground-based countermeasures
  - Ground software improvement to allow data transfer in streaming mode (only filling holes)
  - Ground station uplink upgrade to increase the EIRP
  - Extension of the ground station network

The science on-board data compression turned out not to be a valuable option due to the hot pixels variations on the CCD, introducing uncertainties to perform a distinction between science data and noise/artefacts.

An upgrade of the ground station towards higher Effective Isotropic Radiated Power (EIRP) would bring some improvements. While the interference signal will still limit operations, higher EIRP allows packet requests and acknowledgements to get through easier, improving the data throughput in the downlink. What this upgrade will not solve is the ability to upload large files to the spacecraft (e.g. for software upgrades).

Since mid March 2014, the Graz ground station uplink has therefore been upgraded to increase the available EIRP by the following:

- A second UHF antenna to increase the EIRP by *3 dB* due to the combined directivity
- An upgrade in the UHF power amplifier to operate with up to *1 kW* of RF-power compared to the *500 W* previously used.

Therefore, the maximum EIRP of the ground station has been increased by around *+6 dB*. A detailed description of the upgrade is given in Chapter 3.

Further improvements of the downlink performance when operating with interference can be obtained by manual file transfer optimisation by the operators. For that purpose, the operators selectively transfer files of different sizes according to the current downlink quality. For instance, when the link quality is good and expected to remain so for the next minutes, the downlink data rate is increased, and a large file transfer is started. If the link quality does not degrade to create holes in the transfer, the file can often be completely downloaded without the need of intermediate acknowledgements. This can be achieved by a cumulative request for all file packets at the beginning, provided that the file size is reasonable (< 1 *MByte*). This allows file transfers to be unaffected by interference, however, it is not always possible and represents quite an effort for the operators to manually operate contacts that could be handled fully automated.

Almost at the same time of the ground station UHF uplink upgrade, the ground software feature for automatic adaptation of the data rate according to the measured link quality was implemented. This feature allows to improve the data throughput also during automatic operations.

Another countermeasure to improve the performance of the BRITE-Austria downlink performance is the implementation of nadir tracking of the spacecraft during contacts with the Graz ground station. As during nominal operations the spacecraft is inertially pointed towards the currently selected target field for observations, the spacecraft attitude does not necessarily allow favourable orientation of the S-band patch antennas towards the ground station. Although the combined antenna characteristic of the two S-band patches is nearly omnidirectional, a signal fluctuation of several dB occurs between the maximum (perpendicular facing one of the Z panels) and the minimum.

The BRITE-Austria spacecraft has the capability of nadir tracking as a derivation of inertial pointing, by continuously updating the target quaternion when enabled. Nadir tracking can be implemented for any face of the spacecraft by specifying rotation angles along the roll, pitch, or yaw axis. The spacecraft has been configured to rotate by 90° along the roll axis to achieve the following configuration:

- Set $+Z$ to zenith direction: this will orient $-Z$ to nadir and hence, towards the ground station during contact
- Set $+Y$ to velocity vector direction
- Set $-X$ (payload face) to orbit normal direction, and hence, anti-sun for the dawn-dusk SSO

Throughput measurements have been performed with the spacecraft tracking nadir to analyse improvements of the link performance while operating in the presence of interference. The measurements consider 10 entire days of operations (all contacts) dedicated exclusively to data download. Besides the nadir tracking, the measurements also reflect the EIRP upgrade of the ground station, the automatic data rate variation, as well as manual download effort of the operators on a few of the considered contacts (typically 2 per day).

The results of these measurements are presented in Table 5.11, showing that the download data volume has significantly increased by using these countermeasures to cope with the uplink interference. The average download data volume achieved of *14.3 MByte/day* corresponds to about $3/4$ of the download data volume capacity measured without interference.

	Duration [s]	**Information Data [Byte]**	**Information DR [Byte/s]**
Total	22,950	110,068,985	
Average	555	2,640,633	35,640
Daily Stats(est.)	3,000	14,278,969	

Table 5.11: Throughput measurement results between BRITE-Austria and the Graz ground station with UHF interference countermeasures. The measurements have been performed after UHF TX power upgrade while implementing nadir tracking and adaptive data rate variation during contact. It can be seen that the countermeasures for operations with interference significantly increased the throughput. The result show that the average downloaded data volume is *14.3 MByte/day*, about $3/4$ of the downloaded data volume without interference.

Further improvements have been achieved by the upgrade of the antenna rotators as described in Chapter 3. As expected, the better tracking performance has increased the data throughput statistics despite the impairments imposed by the interference.

Long-term analysis and comparison between the throughput of the configuration before and after the rotators upgrade has been performed. For meaningful comparison, the analysis for the old rotator configuration hereby only considers the period after the various implemented UHF interference countermeasures (UHF TX power upgrade, nadir tracking and adaptive data rate variation during contact). The results of this analysis is shown in Table 5.12.

The in-orbit performance of the BRITE instruments have shown capabilities beyond the original scientific requirements. These capabilities allow to further increase the science return of the mission by collecting additional data compared to the anticipated amounts. As a result, the demand for download capabilities by the ground segment has significantly increased.

The results presented in Table 5.12 show that the improved performance of the Graz ground station can provide average download capabilities of *16.3 MByte/day* even while operating in persistent presence of interference. Compared to the original data download requirements of at least *2 MByte/day*, an improve-

	Old Rotator	New Rotator	
Days	96	119	
Science Data Records	1,028.0	1,798.1	MByte
Full Frame Images	76.4	45.1	MByte
Whole Orbit Data	94.2	61.1	MByte
ACS Logs	104.4	4.6	MByte
TTC Logs	11.9	28.8	MByte
Total	**1,314.9**	**1,937.5**	**MByte**
Peak Daily Amount	**26**	**37**	**MByte**
Average Daily Amount	**13.7**	**16.3**	**MByte**

Table 5.12: Throughput comparison between old and new rotator configuration in the presence of interference. The analysis for the old rotator configuration only considers the period after the various implemented UHF interference countermeasures (UHF TX power upgrade, nadir tracking and adaptive data rate variation during contact). The result show that the average downloaded data volume with the new rotators is increased by *2.6 MByte/day* compared to the old rotator configuration.

ment by > 8 times can be provided. This performance allows for nominal science data collection of up to *20 minutes* every orbit for target fields with 15 stars (data volumes 800 *KByte/file*; about *0.5 MByte/day* satellite telemetry collection has also to be considered).

As the scientific data collection could be even more extended compared to the figures presented above, to further increase the download capabilities, it would be desirable to have other ground stations in the network available. Recently, the use of the existing BRITE ground station network has been intensified, for among other reasons, to relieve from accumulated backlogs in case the Graz ground station cannot handle the downloads on its own. The procedures for the usage of the BRITE ground station network are described in detail in Section 5.1.2.

A long-term solution would be an extension of the ground station network to include other ground stations. From the operational point, this would not only help counteracting interference problems, but also relieving loads of the current participating ground stations in the network and provide substantial data download margins. Different organisations have already expressed their interest in participating, and the inclusion of ground stations other than on the Northern hemisphere would bring some additional benefits when looking at the observations cycles of the BRITE spacecraft. The major drawbacks of this approach remain the establishment, maintenance, and operations effort of the ground stations, implicating substantial costs, as well as the time line for the ground stations readiness, since at present five BRITE spacecraft are operational in orbit and the nominal minimum lifetime of each mission is two years.

While the presented countermeasures provide acceptable performance results, in the long-term, an effective countermeasure is the implementation of a streaming mode for the downlink to increase the data throughput, as well as FEC in the uplink. Implementation options and solutions are discussed in detail in Chapter 6.

This page is intentionally left blank.

Chapter 6

Ground Station Enhancements and Outlook

The BRITE-Austria master ground station in Graz has demonstrated successful operations of the BRITE-Austria mission. The current configuration of the ground station is compatible in hardware and software with the standards used by Generic Nanosatellite Bus (GNB) missions developed by UTIAS/SFL. To serve nanosatellite missions different from GNB, the ground station hardware and software needs to be adapted to other standards.

6.1 Ground Station Interoperability with Other Satellite Communication Standards

The two following possible approaches have been identified to extend the current ground station design to serve other small satellite missions:

1. Ground station compatibility with communication standards for CubeSat missions
2. Compatibility with the Consultative Committee for Space Data Systems (CCSDS) standards for operating state of the art missions based on well established space communication standards

The next sections provide a detailed description of these two approaches.

6.1.1 Ground Station Extension to Operate CubeSat Missions

The present configuration of the Graz ground station hardware could be extended to be CubeSat compatible quite easily. Most of the upgrades hereby are generic to support the different radio amateur frequencies used and hence applicable to generic CubeSat missions.

The major steps in this regard include:

- Installation of a VHF antenna on the antenna tower
- Extension of the existing UHF configuration for bidirectional use
- Extension of the S-band frequency range to include the target radio amateur frequencies in the S-band amateur radio allocation (at about *2.4 GHz*)
- Installation of CubeSat compatible transceiver and TNC in the mission control room

The installation of a VHF antenna on the same tower can easily be achieved, as there is still space available on the antenna tower opposite to the mounted UHF antennas. A suitable VHF crossed-Yagi antenna for the amateur radio band is already available in-house. Appropriate polarisation switching as well as feed lines to the mission control room would need to be installed.

Concerning the extension of the existing UHF configuration for bidirectional use, the major modification includes the installation of a diplexer for allowing both transmit and receive with the same antennas, as well as a UHF low noise amplifier for amplification of the downlink signal.

Alternatively, the establishment of a dedicated UHF/VHF antenna tower separated from the S-band antenna tower could also be pursued as described in Section 6.2.1.

For extending the S-band frequency range there are basically two options:

- Replacing the existing receive filter with a broadband filter allowing signal reception in both the SRS and amateur radio band
- Adopting a dual feed solution to operate separately on both frequency ranges

Finally, a CubeSat compatible transceiver and TNC are required. The BRITE transceiver is compatible with generic CubeSat communication standards and could be used for UHF/VHF communications, or a dedicated transceiver can also be used. In addition to the transceiver, a compatible TNC running the mission specific software is required. A generic TNC compatible with CubeSat missions based on communications with the AX-25 protocol is already available in-house.

Figure 6.1 shows a block diagram for a possible extension of the current Graz ground station hardware design to be CubeSat compatible for the dual S-band feed solution. The items in the yellow boxes denote the CubeSat specific components or the components which would have to be added to the current design. The correspondent modified signal paths are highlighted in red. It has to be noted that, since the present considerations are only at conceptual level and the exact interfaces have not been yet defined, detailed interfaces are not included.

The extension of the ground station hardware to support the amateur radio frequency bands typically used to operate CubeSats (VHF, bidirectional UHF, S-band) will represent an adequate solution to operate generic CubeSat missions. Depending on the operations concept and standards, the respective specific ground segment software configuration needs to be implemented.

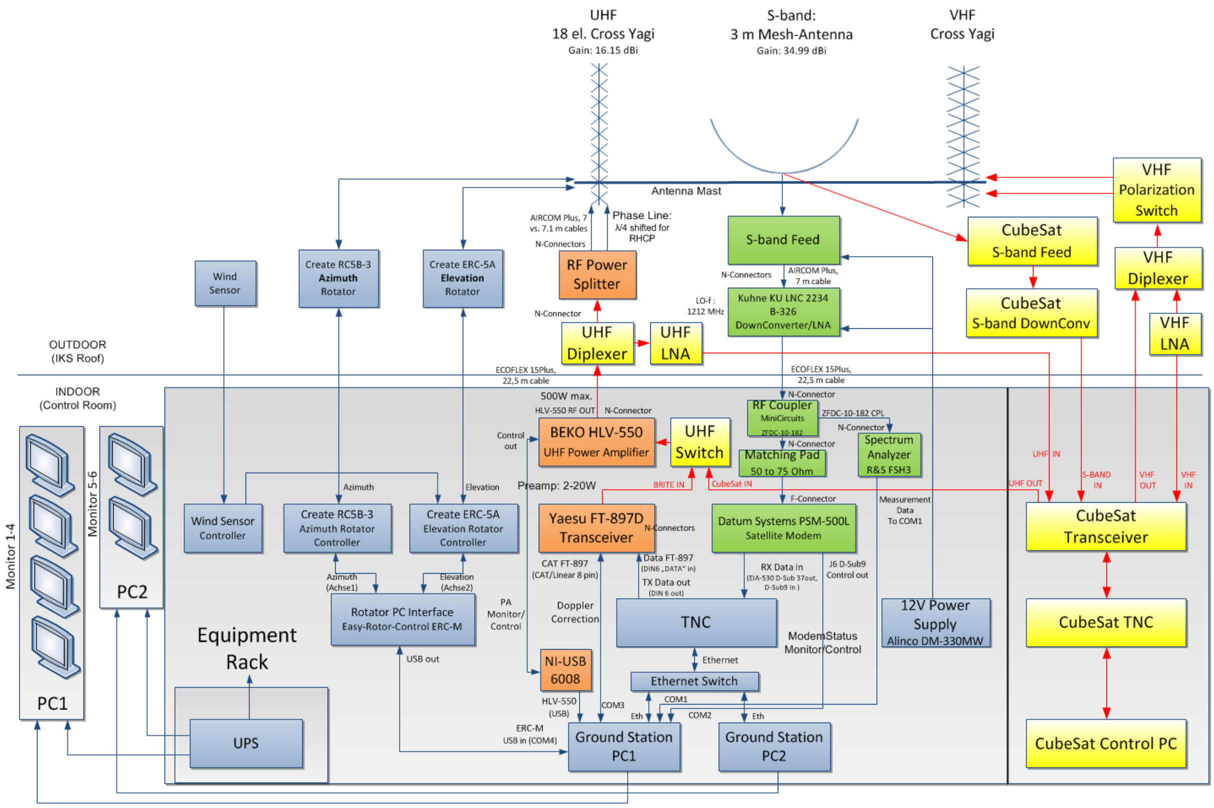

Figure 6.1: Graz ground station extended block diagram for CubeSat operations. The extensions include CubeSat compatible components in the S-band downlink, as well as an upgrade of the UHF chain for bidirectional communications, and the introduction of a VHF downlink chain.

6.1.2 Interoperability with CCSDS Standards

A different approach is to make the ground station compatible with well established space communication standards to serve as generic ground station for professional small satellite missions. For that purpose, compliance with the communication standards recommended by CCSDS [83] is required.

A cheap and simple approach to make the Graz ground station CCSDS compliant is the implementation of a software defined radio (SDR) front end, based on the solution adopted by the ESA NGS-1 ground station [84].

The basic idea in this context is to use a commercial off-the-shelf SDR hardware (e.g the USRP system from *National Instruments* ® [85]) as radio frequency front-end and implement the signal processing on a PC with a suitable software development toolkit (e.g. GNU Radio [86]).

The modifications required to the Graz ground station to implement CCSDS affect the S-band chain. The satellite modem used for BRITE is CCSDS compliant in the physical layer, therefore the implemented CCSDS engine could interface directly with the modem. In addition, the modem provides data rates up to *10 MBit/s* which is in line with state of the art S-band small satellite TT&C systems. The main signal processing task required would be the provision of CCSDS compliant encoding and framing of the data packets for the modem.

Furthermore, an extension of the S-band chain to a bidirectional communication system (i.e. the implementation of the transmit path) is required to serve upcoming nanosatellite missions using S-band in both uplink and downlink.

6.2 Multi-Mission Ground Station Operations Concept

The baseline implementation of the BRITE-Austria ground station in Graz has been realised in a way to have a combined antenna tower for uplink and downlink, and to be co-located with the mission control centre.

The BRITE ground segment concept however provides a logical separation between ground station and mission control. For supporting multiple mission operations, this characteristic can be exploited to create a distributed operations environment, allowing access to ground segment resources to different missions as needed. The concept foresees an extension of the current configuration in two steps:

- An abstraction in hardware, by separation of S-band and UHF / VHF antenna towers
- An abstraction in software, by virtualisation of the mission control centres

6.2.1 Ground Station Design with Separate Antenna Towers for UHF/VHF and S-band

As described in the previous sections, upgrades of the current ground station configuration to serve generic CubeSat missions as well as to provide CCSDS compatibility require several hardware installations, in particular on the antenna tower. A possible solution to relieve overload of the existing antenna tower configuration is to set up a second dedicated antenna tower for UHF/VHF communications and to keep the current antenna tower for S-band only. This solution is feasible as TU Graz/IKS has a second building available which can be used to set up the UHF/VHF tower on its roof with a co-located control room nearby for accommodating the correspondent equipments rack. This second location is the neighbouring building next to the main TU Graz/IKS building at the TU Graz Inffeld Campus. This solution brings several advantages:

- It relieves operations of the existing S-band antenna tower and increases the tracking performance as there are no longer additional antennas on the tower which need to be counterbalanced or which introduce additional movements or wind loads.
- On the UHF/VHF tower, an UHF antenna group of four antennas can be accommodated to increase the available uplink power by additional *+3 dB*.
- With the separated antenna towers, the UHF uplink is no longer obstructed by an S-band antenna mounted nearby and can achieve better performance.

Concerning the S-band antenna tower, the configuration for operating BRITE-Austria remains unchanged. Additional upgrades to introduce an S-band transmit path as well as the baseband adaptations for CCSDS compatibility can be achieved without major redesigns.

An additional upgrade of the antenna rotators of the existing antenna tower to achieve better tracking precision has been performed in January 2015. The new rotators provide a tracking precision of $0.5°$ to $1°$ in both azimuth and elevation, increasing the tracking performance substantially. Having only a single S-band antenna on the antenna tower will additionally facilitate the operations of the new rotators.

For the new UHF/VHF antenna tower, an additional BRITE TNC is required to accept packets to be uploaded to the spacecraft from the ground software. The ground software MUX can logically separate TX and RX, allowing to connect different TNCs for the respective direction of the communication path. As the TNC is connected via TCP/IP, it can be commanded independently of its physical location, thus allowing to be located at the neighbouring building in the same room where the equipments rack for the UHF/VHF station is installed.

Concerning the modifications for the operations of generic CubeSat missions, the new UHF/VHF ground station can be made available; the necessary RF and baseband equipment required can be installed in the same equipments rack as the BRITE specific components.

In addition, underneath the possible UHF/VHF antenna tower location, next to the container accommodating the equipments rack an additional control room is available that could be set up as generic mission control room with direct access to the UHF/VHF ground station. Concerning the utilization of the S-band antenna tower for serving missions different than BRITE, a solution to access the correspondent baseband equipment installed in the S-band ground station from the generic mission control room can be conceived.

6.2.2 Ground Segment Virtualisation for Multi-Mission Operations

With separate ground stations and potentially multiple mission operations based on different hardware / software configurations, a powerful and flexible solution is provided by the use of a virtual machine environment. Virtual machines introduce an additional abstraction layer, allowing to logically separate the hardware interfaces from the ground station and mission control software. A high level architecture concept has been elaborated for the planned UHF/VHF and S-band ground stations at TU Graz/IKS and includes the following hierarchy:

1. A virtual machine host for each ground station, providing interfaces to the respective ground station hardware as well as the necessary resources for the virtual machine clients

2. Baseband equipment interface converters to Ethernet, allowing the virtual machines to access the hardware without relying on the host machine

3. Ground station control virtual machines, implementing the respective ground station specific software to access the ground station hardware for the different systems used for mission operations

4. Mission control virtual machines for each mission / spacecraft with the respective ground segment software

Since January 2015, the BRITE-Austria ground station is already running successfully on the virtual machines shown in Figure 6.2. To operate the mission, dedicated mission planning, mission control, and ground station control virtual machines are used, which operate independently from each other. The current BRITE-Austria ground station with the combined S-band/UHF antenna tower is being used.

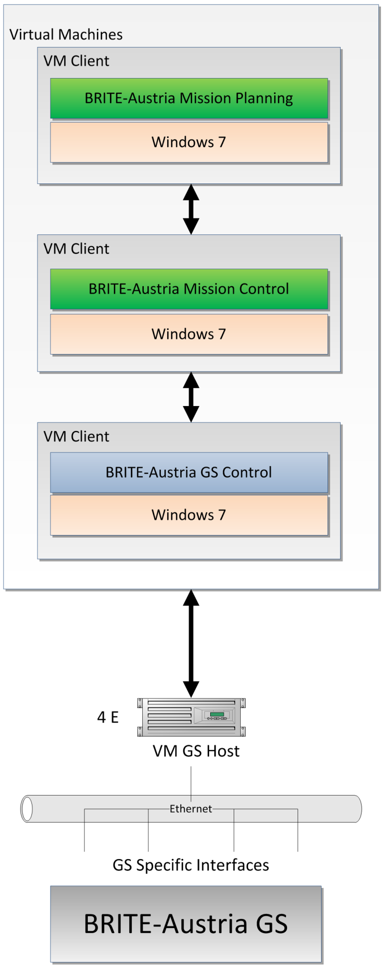

Figure 6.2: Current Graz ground station virtualisation hierarchy. BRITE-Austria uses dedicated mission planning, mission control, and ground station control virtual machines which are independent from each other.

The high level architecture and hierarchy for a possible future configuration is shown in Figure 6.3. Next to the virtual machines for operating the BRITE-Austria mission, this example considers the implementation of a generic CubeSat mission operations system based on UHF/VHF only, as well as an external connection for providing access to the ground station for the ESA OPS-SAT mission control system located at ESOC in Darmstadt.

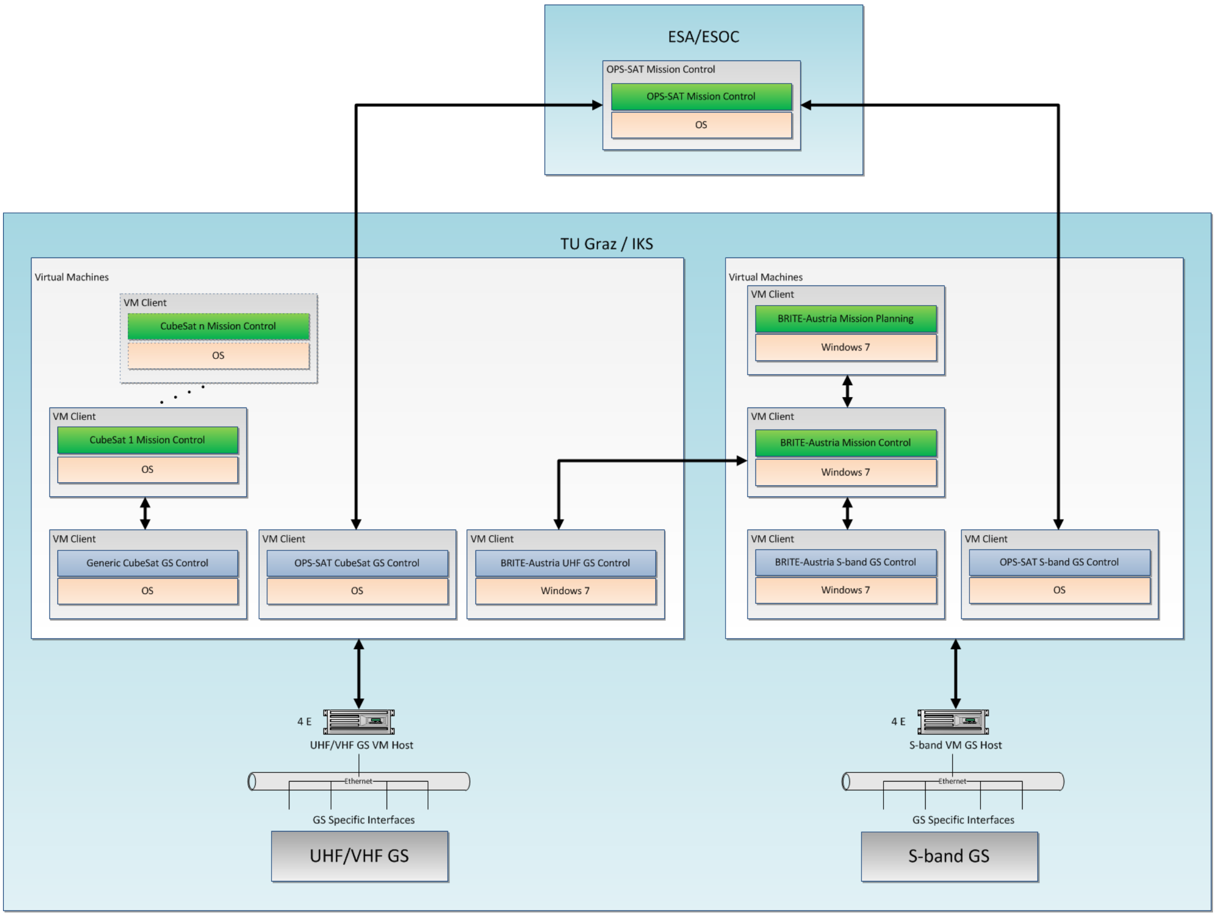

Figure 6.3: Graz ground station virtualisation hierarchy outlook. The high level architecture and hierarchy for virtualisation of the ground stations at TU Graz / IKS are shown. Mission specific ground station control virtual machines (VMs) are running at the respective ground station host. Mission control virtual machines connect to the respective ground station control virtual machines for accessing the ground stations. The depicted architecture considers three types of missions to be operated: BRITE-Austria, a generic CubeSat mission operations system based on UHF/VHF only, as well as the external connection for the ESA OPS-SAT mission control system.

The virtualisation concept provides high flexibility and scalability of the system. Hardware interfaces can be added and removed/replaced at the different ground stations as desired, their access and specific software for operations is implemented in the ground station control virtual machines. Therefore, the hardware access is completely independent of the operating system or interfacing software and can be quickly established by executing the respective virtual machine. The only element to be considered is to ensure exclusive access to a particular ground station control virtual machine to the respective ground station at any given time to avoid access conflicts with the ground station hardware (in case the same hardware is used).

Mission control resides logically one layer above in the hierarchy, bringing several advantages. Each operating team can access the respective mission control virtual machine

- at any given time
- at any given location
- without causing conflicts with other missions / systems

Merely the access to the ground station virtual machine(s) / ground station has to be determined by scheduling processes according to available resources and priorities. This could be implemented at the respective ground station host as it grants resources to the different hosted virtual machines.

6.3 BRITE-Austria Communication Protocol Enhancements

To increase the transmission efficiency and the data throughput for BRITE-Austria operations, enhancements in the used communication protocols would be desirable. As described in Chapter 5, the data packets used by the BRITE-Austria mission use the Nanosatellite Protocol (NSP) format, which is a network layer protocol on top of HDLC encapsulation at data link layer.

The envisaged enhancements mainly affect the transport layer functionalities of the used protocols with regard of the used transmission window sizes and the acknowledgement modes of received packets via the UHF return link from ground. Besides optimising the data transmission efficiency, these enhancements will also help to cope with impairments in the UHF uplink due to interference.

To counteract the experienced UHF uplink interference as described in Chapter 5, enhancements on both on-board and ground segment software have been identified to improve the data throughput, including enhancements of the communication protocols used.

The improvement in the ground segment software do not affect the communication protocols itself, but rather the data transmission mode. As already described in Chapter 5, the increase of the maximum packet number per request to a large number brought some improvements compared to the default 32 packets, as acknowledgements are only required for larger bulks of data. A new approach would be to implement a ”streaming” mode in the downloading ground segment software modules, with the following functionalities:

- Activation of a ”streaming” mode in the ground software
- Allow to perform prioritisation of files to be downloaded
- Get a file listing and determine file(s) to be streamed (according to prioritisation and only for files not already partly downloaded)
- Initiate file transfer; data rate can be varied dynamically during download according to the link quality, maximising the efficiency

- Wait for the end of the file to be reached (wait for end character/sequence) without acknowledging any packets in between;
- Determine holes in the downloaded files and request missing packets

The advantages of this approach include the full automation of the streaming functionality, as it is handled by the ground segment software without requiring planning, and provides high efficiency, because even though data are being streamed, unknowns such as link availability, satellite state, and ground station state are eliminated. Therefore, this approach could represent a long-term solution for operations, and in general a potential countermeasure for impairments in the uplink.

For modifications of the on-board software on the spacecraft, different considerations apply, as modifications in the communication protocol stack are required. In this respect, for increasing the transmission efficiency, a Delay/Disruption Tolerant Networking (DTN) [87] [88] approach would be suitable. This would allow counteracting for link disruptions due to signal fluctuations, tracking uncertainties, as well as noise signal interference.

Requirements for the on-board communication protocol enhancements include [89] [90]:

- supporting large transfer windows (large number of packets per request)
- avoiding positively acknowledging bulks of data and instead using selective negative acknowledgements (SNACKs) for indicating only missing or corrupted data packets
- allowing cumulative SNACKs or to requesting the missing/corrupt packets at the end of the file transmission rather than in between

However, it was decided not to pursue this approach due to the additional complexity that would be introduced in the used communication protocol and as a result, in the entire on-board software implementation.

A third approach is the enabling of a ”downlink heavy” mode for scheduled on-board data streaming triggered by the spacecraft during scheduled contacts with the ground stations. For that purpose, the satellite will determine the files on-board that need to be downloaded and begin broadcasting the selected data automatically on pass under assumption of a ground station in listening mode by time tagged commands. The ground software will then reassemble the downloaded data stream to the correspondent original files. After the completion of the file transfers, the ground software will request any missing packets that have not been received in broadcast mode and send requests to the spacecraft to fill holes. In addition, multiple missing packet requests are foreseen with single ground commands. This approach involves minor modifications in both the on-board and ground software. The major advantage of this concept is that only the downlink needs to be supported by the ground station when this mode is activated, thus being unaffected by any uplink impairments. Therefore, it would also allow to use downlink-only ground stations to clear large backlogs while the holes can be filled later from a ground station with bidirectional link capabilities.

The final solution which has been selected and implemented accordingly consists of a downlink-heavy transmission mode with additional control functionalities from the ground software . For that purpose, the new BRITE-Austria on-board software defines different dedicated threads for data download purposes, including:

- A bidirectional communication thread, which basically allows bidirectional acknowledged data transmission as used in previous versions of the software
- An auto-download thread: This thread implements the described streaming functionality. It retrieves all files selected for auto-download and initiates file transfers (also in parallel) until the file is completed without encountering for packet losses during the transmission. The auto-download thread therefore allows to optimally exploit the available downlink data rate.
- A hole filling thread: This thread is dedicated to retrieve missing packets due to transmission holes occurred while auto-downloading files from the spacecraft. As this thread runs on its own, it can be executed in parallel with the auto-download thread to maximise the efficiency.

Each file being auto-downloaded obtains a sequence number for identification by the auto-download thread. In order to avoid complex scheduling, the automatic operations sequence of the ground software interfacing with the new on-board software includes a ”start auto-download” command. This command uploads first a time-tag command to the spacecraft to disable auto-download after loss of contact (LoS) based on a predefined time span, and only enables auto-download after successful acknowledgement of this command by the spacecraft. The auto-download start command can also be used in a time-tagged configuration to allow streaming of data for scheduled contacts with downlink-only ground stations.

The hole filling strategy is implemented in the correspondent ground software used for file transfer, providing maximum flexibility to optimise the implementation according to the observed performance behaviour of the filling hole functionality without the need for changes in the on-board software.

Figure 6.4 shows a screenshot of the ground segment software module used for file transfer during a pass with the auto-download thread active, downloading files and filling holes in parallel. It can be seen that two files are being auto-downloaded, and in parallel the hole-filler thread is active and filling holes of another file, while other files with holes are waiting for the hole-filler thread in the queue.

Preliminary assessment of the auto-download performance has been carried out by throughput measurements in the presence of interference. For the tests, all previously described improvements (increased uplink power with dual antenna configuration, dynamic data rate adjustment, and nadir tracking of the spacecraft) were applied. The detailed results of the auto-download performance measurements are presented in Table 6.1.

The results of the auto-download performance assessment show that the throughput increases significantly compared to the standard bidirectional communication scheme. The estimated total daily data download volume has more than doubled from *14 MByte/day* to *39 MByte/day*.

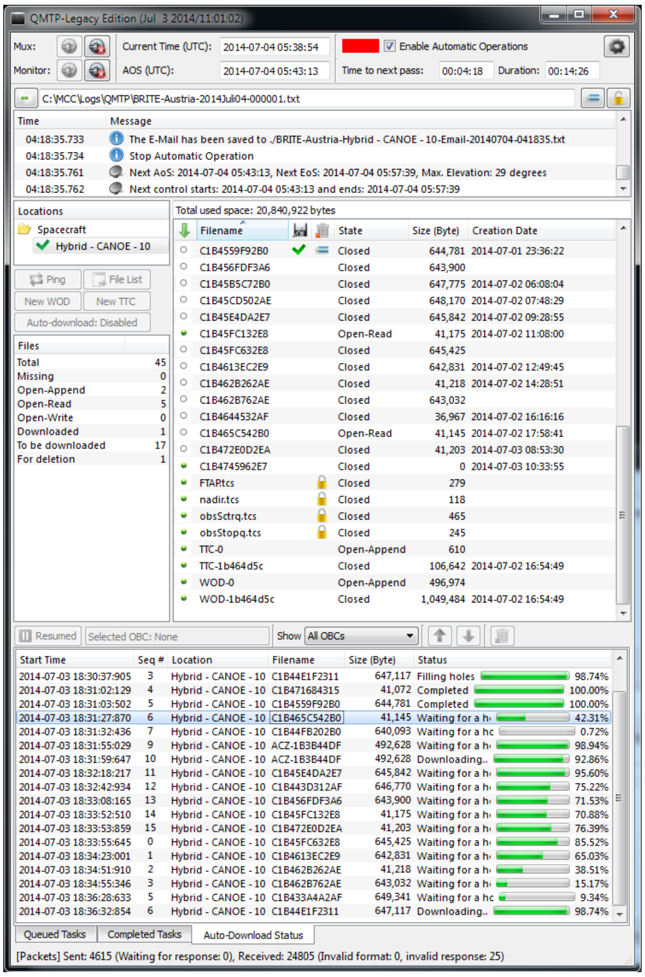

Figure 6.4: BRITE-Austria ground segment software during auto-download. The auto-download thread is active and downloading files (currently two). In parallel, the hole-filler thread is active and filling holes of the file with sequence number "3". All other files with holes are pending in the queue waiting for a hole filler. Completed file transfers are marked as "completed".

	Duration [s]	Information Data [Byte]	Information Data Rate [Byte/s]	File Downloads Completed
Total	3,595	47,049,238		30
Average	599	7,841,540	111,348	5
Daily Stats(est.)	3,000	39,262,229		

Table 6.1: BRITE-Austria throughput measurement results with auto-download. The results of the auto-download performance assessment show that the throughput increases significantly compared to the standard bidirectional communication scheme. The estimated total daily data download volume has more than doubled from *14 MByte/day* to *39 MByte/day*. However, download completion could be achieved only on about half of the downloaded files (based on an average file size of around *900 kByte*.

These results can be attributed to the improved downlink conditions due to nadir tracking and adaptive downlink data rate variation. However, the results show that, despite the large data download volumes, download completion could be achieved only on about half of the downloaded files (based on an average file size of around *900 kBbyte*.

The preliminary conclusion therefore is that the auto-download functionality avoids large backlogs in terms of download volumes, but would require from time to time access to the spacecraft unaffected from interference to allow hole-filling and completion of file downloads. Therefore, additional stations in the BRITE ground station network would be of great benefit.

6.4 Extension of the BRITE Ground Station Network

In addition to the communication protocol and transmission mode enhancements, the long term plan is to extend the BRITE ground station network by adding more ground stations for increasing availability.

Several organisations have expressed their interest to contribute to the BRITE project with additional ground stations, including the following locations:

- Vancouver, Canada
- Stromlo, Australia
- Santa Cruz, Aruba
- Cape Town, South Africa
- Svalbard, Norway

The Vancouver station is basically an extension of the existing MOST ground station and will become available for BRITE operations in late 2015. The setup of all other ground stations is currently under investigation. Needless to say, the Svalbard ground station would bring a major benefit to the mission, as it allows tracking of all passes of sun-synchronous polar orbits as used by the BRITE satellites.

All these potential ground stations to be included would be used as relay stations instead of master ground stations. Therefore, basically a core and extended ground station network could be set up. Figure 6.5 shows the core and possible extended BRITE ground segment network with the participating stations, while Figure 6.6 shows the coverage of the possible extended ground station network.

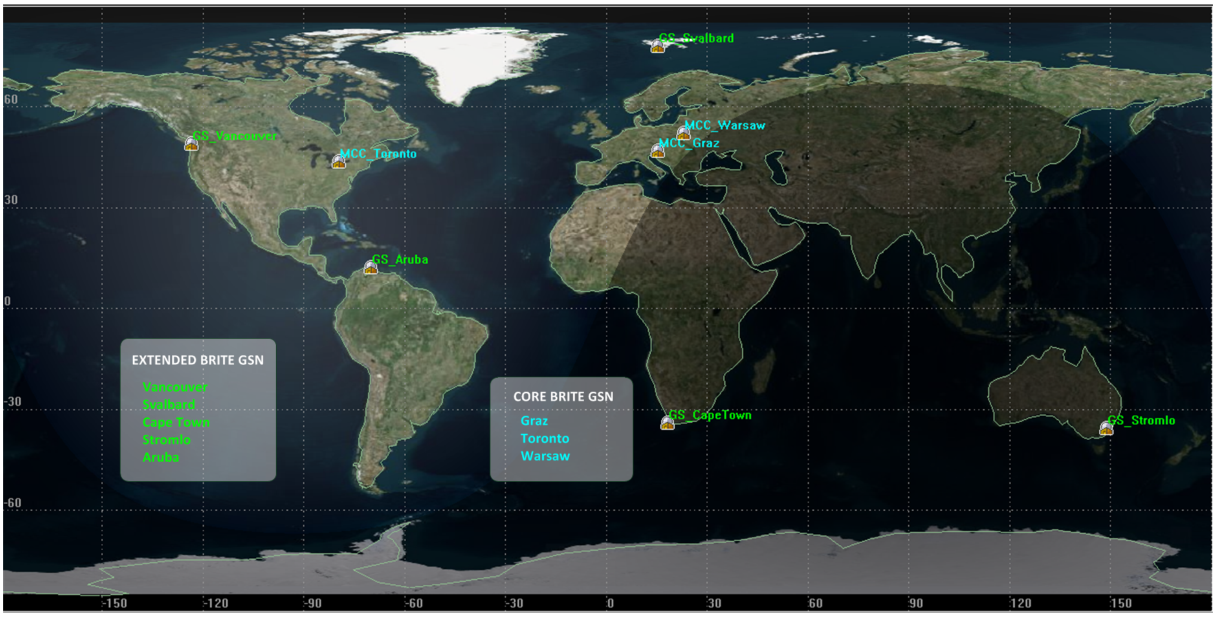

Figure 6.5: Possible extension of the BRITE ground station network. The core and possible extended BRITE ground station network with the participating stations is shown. In addition to the core ground stations in Graz, Toronto, and Warsaw, possible additional stations include Vancouver (Canada), Santa Cruz (Aruba), Stromlo (Australia), Cape Town (South Africa), and Svalbard (Norway).

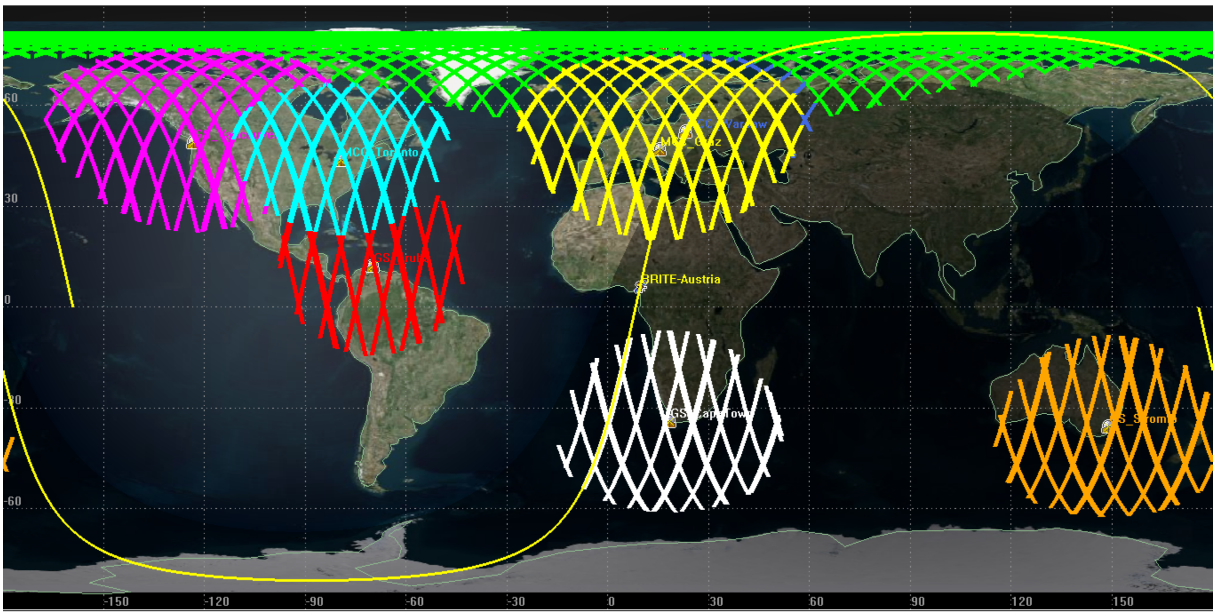

Figure 6.6: Coverage of the extended BRITE ground station network. The coverage of the possible extended BRITE ground station network including the ground stations presented in Figure 6.5 is shown. The extension of the network would significantly increase the coverage and contact times, and would therefore be of great benefit for BRITE Constellation operations (image courtesy: STK).

This page is intentionally left blank.

Chapter 7

Conclusions and Lessons Learned

In this chapter, concluding remarks for the doctoral thesis are presented, summarising the achievements and addressing lessons learned.

The thesis dealt with the establishment, assessment, and operations of a ground station for nanosatellite missions. The presented ground station has been realised to operate the BRITE-Austria mission.

First, an introduction to the topic was given by explaining the role of the ground segment for generic space mission, and then narrowing the topic down to ground segments for nanosatellite missions.

Next, in Chapter 2 the BRITE-Austria mission was introduced. An overview of the BRITE Constellation and the consortium was provided, and the focus was laid on BRITE-Austria/TUGSAT-1, the first Austrian satellite. A description of the satellite's communication subsystem as the space-to-ground interface was provided. Functional tests of the communication subsystem at unit and system level were presented, as well as relevant parts of the integrated spacecraft environmental testing, along with the respective test results.

Subsequently, the established master ground station, which also acts as mission control centre for operating BRITE-Austria, was presented in Chapter 3. An overview of the ground station requirements and a detailed description of the ground station design were provided. Design choices were explained as well as possible improvements to the ground station and respective constraints were illustrated.

To verify the performance of the ground station and to determine its adequateness for operating the BRITE-Austria mission, several simulations and measurements were carried out and compared with each other. This performance evaluation of the ground station was presented in Chapter 4. The focus was hereby laid on (but not limited to) the S-band downlink design as the main design driver, since substantial amounts of science data need to be downloaded during mission operations. The measurements included antenna patterns in both up- and downlink, the system noise temperature of the S-band communication chain in dependence of elevation angles and weather conditions, the antenna gain and figure of merit of the S-band chain, as well as the determination of the S-band radio horizon of the ground station by measuring interference signals from the surroundings affecting the receiving performance. Link budgets have been calculated, including the measured values whenever available, to obtain an estimation of the overall system performance. Furthermore, modelling of the ground station has been carried out with *Matlab*® simulations including the measurement results to estimate the link performance for simulated satellite passes over the ground station and derive long term statistics. In addition, measurements with comparable spacecraft (NTS for the uplink, MOST for the downlink) were carried out for the full assessment of the ground station link performance in both directions.

After the BRITE-Austria launch, the performance of the ground station has been verified during satellite commissioning and early operations. The setup, planning, and execution of BRITE-Austria operations has been part of this work and was presented in Chapter 5. The operations concept with the BRITE ground station network was introduced, and an overview of the ground segment software used was provided. In this respect, the software modules developed in the context of this work to evaluate the satellite housekeeping telemetry, as well as for operating the ground station (power amplifier and RX signal measurements) were explained in detail. A description of the top level commissioning tasks performed as well as an overview about nominal operations and contingency procedures were provided. Furthermore, to verify the link performance between the BRITE-Austria spacecraft and the master ground station several measurements have been performed and were presented. These included signal measurements, measurements of the packet error rate determined by bidirectional ping tests, data throughput measurements for several contacts primarily used for data download, as well as an assessment of detected signal interference in the UHF uplink. Applied countermeasures and strategies to improve the download capabilities despite these inevitable limitations in the return channel were detailed along with results, showing that the achieved improvements allow to operate the mission without limiting the scientific output according to the requirements.

Finally, Chapter 6 gave an overview about possible enhancements to the current ground station design and an outlook. Concepts for extending the ground station to serve multiple missions were presented, including:

- Extension of the current ground station hardware configuration to be compatible with generic CubeSat missions standards as well as missions based on professional space communication standards such as CCSDS.
- Separation of the current UHF/S-band ground station for BRITE-Austria to a dedicated UHF/VHF and an S-band ground station.
- Virtualisation of the ground segment for serving multiple missions based on a virtual machine host at each ground station and virtual machine clients with abstraction levels for ground station control and mission control.

Additional enhancements presented focused on operations of the BRITE-Austria mission. Enhancements of the communication protocols were introduced for increasing the data throughput and counteracting for potential link impairments such as the UHF interference. In addition, the possible extension of the existing BRITE ground station network including additional ground stations was presented.

7.1 Achievements

The BRITE-Austria master ground station in Graz has demonstrated successful operations of the BRITE-Austria mission. The current configuration of the ground station is compatible in hardware and software with the standards used by Generic Nanosatellite Bus (GNB) missions developed by UTIAS/SFL. In this context, the ground station has served as backup station for maintenance of other nanosatellites within the BRITE Constellation, including UniBRITE, BRITE-PL1 (Lem), and BRITE-Toronto. Furthermore, the ground station has been successfully used for establishing first contact with the following satellites:

- BRITE-Austria
- UniBRITE
- BRITE-Toronto
- CanX-4
- CanX-5

As another achievement, parts of the S-band downlink design of the Graz ground station have been selected as baseline for the ESA/ESOC NGS-1 nanosatellite ground station in Darmstadt, which will be used for OPS-SAT [91]. The OPS-SAT mission objective is to provide a reconfigurable platform for in-orbit demonstration of new operations concepts and technologies for upcoming ESA missions [92].

The established BRITE-Austria ground station represents a professional approach for operations of a scientific small satellite mission. The ground station has proven to provide high performance, high availability, and high reliability. Furthermore, the high level of automation of the ground station allows operations to be carried out in a fully automated manner. The achievements in terms of performance are provided in the next sections.

High Performance

The BRITE-Austria mission has been very successful so far, collecting scientific data of very high quality. The spacecraft has already exceeded the nominal mission lifetime of 2 years. In the first 27 months in orbit, the following observation campaigns have been carried out:

- Orion (two observation campaigns)
- Centaurus
- Perseus
- Vela/Puppis
- Scorpius (ongoing)
- Cygnus (ongoing)

Performance Figure	**Requirement**	**Achievement**
Pointing accuracy	< 2 arcmin	70 arcsec
Star magnitude	$+3.5$	$+4.5$
Instrument ROI pixel size	$32x32$	down to $24x24$
No. of stars observed in FOV	> 2	up to 30
Data download capabilities	at least *2 MByte/day*	*16.3 MByte/day* avg.; *37 MByte/day* peak

Table 7.1: BRITE-Austria comparison between requirements and achieved performance. The performance achievements show that the performance of the mission has significant exceeded the original requirements. The ground station has proven to provide on average > 8 times the original data download capabilities compared to the requirement.

The in-orbit performance of the BRITE-Austria spacecraft has shown capabilities far beyond the original scientific requirements. These capabilities allow to further increase the science return of the mission by collecting additional data compared to the anticipated amounts. As a result, the demand for download capabilities by the ground segment has significantly increased. Table 7.1 shows a comparison between the original mission requirements and the achievements.

The results presented in Table 7.1 show that the Graz ground station can provide average download capabilities of *16.3 MByte/day* even while operating in persistent presence of interference. Compared to the original data download requirements of at least *2 MByte/day*, this represents an improvement by more than a factor of 8. It has to be noted that this statistic includes also ground contacts dedicated to maintenance tasks (such as configuration updates) or contingency, during which the data collection is also reduced. Therefore, the average data download capabilities in the nominal data collection periods will even exceed this number. Furthermore, the peak download performance of the ground station provides 18.5 times the capabilities compared to the original requirement.

In absolute numbers, in 27 months of operations (20 of which in the nominal operations phase) BRITE-Austria has collected $240,000$ science data records and $5,3$ *GB* of raw data.

High Availability and Reliability

Table 7.2 shows the availability figures for the BRITE-Austria ground station. In the first 27 months of BRITE-Austria operations, the Graz ground station has proven to provide high availability by operating 97.47% of all possible ground contacts, which in turn cover almost half of all orbits of the spacecraft (i.e. ground contact can be established from Graz every second orbit on average). The outages are due to environmental limitations (e.g. high wind loads) or maintenance.

The only longer outage of the ground station occurred in August 2013 (elevation rotator motor failure). Due to the limited personnel availability, as the issue occurred in the main holiday period, the replacement of the rotator with the redundant spare took five days. In the remaining time, the ground station was not operative for a total period of 7 days, including the two main upgrades (UHF dual antenna system and rotator upgrade). Therefore, the ground station has proven high reliability for mission operations.

Figure	Value	Percentage	
Total Orbits	11,998		
Total Passes	5,966	49.72%	of orbits
Maintenance	80	1.34%	
Wind/other outages	71	1.19%	
Operated Passes	**5,815**	**97.47%**	of passes

Table 7.2: Graz ground station availability. In the first 27 months of BRITE-Austria operations, the Graz ground station has proven to provide high availability by operating 97.47% of all possible ground contacts. The outages are due to environmental limitations (e.g. high wind loads) or maintenance.

Another strategy to increase the reliability is the provision of redundancy in the ground station configuration whenever possible, allowing quick equipment replacement in case of failure. The following ground station spare equipment is available (in cold redundancy):

- Antenna rotators
- UHF antenna dipoles
- UHF transceiver and power amplifier
- S-band feed, LNA, bandpass filter, and downconverter
- S-band modem
- TNC
- Ground station servers and clients (running in parallel, the redundant server performs virtual machine replication in real time and full backups in regular intervals.)

Furthermore, the reliability is increased by the use of an un-interruptible power supply (UPS) providing power margins in case of power outage to prevent unavailability of the ground station, as well as the use of a dedicated fibre optics backbone for operating the virtual machine environment.

High Level of Automation

The BRITE-Austria ground segment provides a high level of automation allowing satellite operations in a fully automated manner. The BRITE-Austria ground station software automatically establishes contact with the spacecraft, and the BRITE-Austria mission control software automatically performs operational tasks on the spacecraft. Pass notifications are automatically sent to the operators via e-mail at the end of each operated contact, providing a core telemetry snapshot as well as a summary of the tasks performed, the file system status on the OBCs, and download statistics. In case of unexpected behaviour of the spacecraft, alarms are generated and included in the automated pass report.

In addition, the BRITE-Austria ground segment allows remote access to authorised operators for fully remote operations of the spacecraft during pass as well as to perform planning and evaluation tasks.

High Scalability

The BRITE-Austria distributed ground software concept provides high flexibility and scalability of the system. The distinction between ground station and mission specific software allows parallel operations of multiple missions.

The virtualisation concept described in Chapter 6, already successfully implemented for BRITE-Austria operations, introduces an additional hardware abstraction level, allowing different missions to implement their specific ground station configuration (hardware and software). With proper scheduling and orchestration of the access to the ground station resources, this concept makes the ground station well-suited for multi-mission operations.

7.2 Lessons Learned

The excellent in-orbit performance of the spacecraft exceeding the requirements and hence the scientific capabilities have significantly increased the data download requirements. As the BRITE-Austria ground station has been designed to provide high performance and capabilities far beyond the original data download requirements, these demands could be fulfilled. The lesson learned in this context is to consider substantial performance margins in the ground station system design to provide additional capabilities.

Even though the high ground station capabilities, the persistent presence of interference in the UHF uplink, as described in detail in Chapter 5, represented a challenge for mission success. Although effective countermeasures could be implemented for BRITE-Austria, the lesson learned in this context is that some satellite amateur radio bands (in particular UHF) are susceptible to interference which cannot be avoided due to the non exclusive/secondary use allocation, thus imposing a risk to mission success.

The recommendation is therefore to move towards coordinated frequency bands to avoid such circumstances. The frequency allocation request process for coordinated ITU bands does not represent a significantly larger effort compared to a request for an amateur radio frequency, as in any case an ITU filing needs to be submitted. The only difference is that coordination of the amateur radio frequency goes through IARU, avoiding the ITU coordination review process by the member states.

The main advantage in obtaining a frequency allocation in a coordinated ITU band is the grant of exclusive use and protection. In case the use of an amateur radio band cannot be avoided, it is strongly recommended to implement forward error correction (FEC) to mitigate potential interference effects. Future TU Graz nanosatellite missions will pursue this strategy for amateur radio bands.

Appendix A

Abbreviations and Acronyms

ACM	Adaptive Coding and Modulation
ACS	Attitude Control System
ADCC	Attitude Determination and Control Computer
ADCS	Attitude Determination and Control System
AIS	Automatic Identification System
AIT	Assembly Integration and Testing
AIV	Assembly Integration and Verification
AM	Anti Meridian
AMSAT-UK	Radio Amateur Satellites - United Kingdom
ANT	Antenna
AoS	Acquisition of Signal
ARM	Advanced RISC Machine
ASAP	Austrian Space Applications Programme
BCDR	Battery Charge and Discharge Regulator
BER	Bit Error Rate
BMVIT	Bundesministerium für Verkehr, Innovation und Technologie
BNC	Bayonet Neill-Concelman
BPSK	Binary Phase Shift Keying
BRITE	BRIght Target Explorer
BRITE-PL	BRIght Target Explorer - Poland
C/N	Carrier to Noise Ratio
C/N_0	Carrier to Noise Power Density Ratio
C-QPSK	Coded Quadrature Shift Keying
CAT	Computer Aided Transceiver
CCD	Charge Coupled Device
CCDF	Complementary Cumulative Distribution Function
CCSDS	Consultative Committee for Space Data Standards
CCW	Counter Clockwise

CD	Cumulative Distribution
COM	Communication Port
COTS	Commercial Off The Shelf
CR	Code Rate
CRC	Cyclic Redundancy Check
CSV	Comma Separated Value
CTAP	Coarse Three-Axis Pointing
CW	Clockwise
DC	Direct Current
DIN	Deutsches Institut für Normung eV
DTN	Delay/Disruption Tolerant Networking
DUT	Device Under Test
Eb/N0	Bit Energy per Noise power density
EIRP	Effective Isotropic Radiated Power
EMC	Electromagnetic Compatibility
EMI	Electromagnetic Interference
ERC	Easy Rotor Control
ESA	European Space Agency
ESOC	European Space Operations Centre
ESTRACK	European Space Agency TRACKing station network
EVM	Error Vector Magnitude
FEC	Forward Error Correction
FFG	Forschungs Förder Gesellschaft
FITS	Flexible Image Transport System
FOV	Field of View
FP7	Seventh Framework Program for Research of the European Commission
FPGA	Field Programmable Gate Array
FTAP	Fine Three-Axis Pointing
FTDI	Future Technology Devices International
FTP	File Transfer Protocol
G/T	Gain over System Noise Temperature (Figure of Merit)
GENSO	Global Education Network for Satellite Operations
GFSK	Gaussian Frequency Shift Keying
GMSK	Gaussian Minimum Shift Keying
GNB	Generic Nanosatellite Bus
GND	Ground
GNU	GNU's not Unix
GS	Ground Station
GSS	Ground Segment Software
GUI	Graphical User Interface
HDLC	High-Level Data Link Control
HEMT	High Electron Mobility Transistor

HKC	Housekeeping Computer
HSPA	High Speed Packet Access
IARU	International Amateur Radio Union
IF	Intermediate Frequency
IfA	Institute for Astrophysics
IKS	Institute of Communication Networks and Satellite Communications
IOBC	Instrument On Board Computer
IP	Internet Protocol
ISRO	Indian Space Research Organisation
ITC	Institute of Telecommunications
ITU	International Telecommunication Union
JSpOC	Joint Space Operations Centre
LED	Light Emitting Diode
LEO	Low Earth Orbit
LEOP	Launch and Early Operations Period
LFFT	Long Form Functional Test
LNA	Low Noise Amplifier
LNC	Low Noise Converter
LO	Local Oscillator
LTAN	Local Time of Ascending Node
LTDN	Local Time of Descending Node
MB	Mega Byte
MCC	Mission Control Centre
MCS	Mission Control System
MDA	Mission Data Archive
MOST	Microvariability and Oscillations of STars
MUX	BRITE Multiplexer
NF	Noise Figure
NORAD	North American Aerospace Defense Command
NSP	Nanosatellite Protocol
NTP	Network Time Protocol
NTS	Navigation Technology Satellite
OASYS	On-orbit Attitude SYStem software
OBC	On Board Computer
OSI	Open Systems Interconnection
PA	Power Amplifier
PC	Personal Computer
PCB	Printed Circuit Board
PCI	Peripheral Component Interconnect
PEP	Peak Envelope Power
PER	Packet Error Rate

PID	Proportional Integral Derivative
PSF	Point Spread Function
PSLV	Polar Satellite Launch Vehicle
PTT	Push To Talk
QB50	International Network of 50 double and triple CubeSats
QPSK	Quadrature Phase Shift Keying
RCV	Receive
RF	Radio Frequency
RG	Radio Guide
RHCP	Right Hand Circular Polarisation
RISC	Reduced Instruction Set Computing
RMS	Root Mean Square
ROI	Region Of Interest
RS	Recommended Standard
RSSI	Received Signal Strength Indicator
RX	Receive
S/C	Spacecraft
S/N	Signal to Noise Ratio
SAA	South Atlantic Anomaly
SCC	Serial Communication Controller
SDR	Science Data Record
SDR	Software Defined Radio
SFL	Space Flight Laboratory
SNACK	Selective Negative ACKnowledgement
SNR	Signal to Noise Ration
SRC	Space Research Centre of the Polish Academy of Sciences
SRS	Space Research Space-to-Earth
SSO	Sun Synchronous Orbit
SSPO	Sun Synchronous Polar Orbit
STK	Systems Tool Kit
SWR	Standing Wave Ratio
TCP	Transmit Control Protocol
TIP	Terminal Interface Program
TLE	Two Line Element
TNC	Terminal Node Controller
TT&C	Telemetry Tracking and Control
TTC	Time Tag Command
TTL	Transistor Transistor Logic
TU Graz	Graz University of Technology
TUV	Vienna Unversity of Technology
TVAC	Thermal Vacuum
TX	Transmit

UHF	Ultra High Frequency
UMTS	Universal Mobile Telecommunication System
UPS	Uninterruptible Power Supply
USB	Universal Serial Bus
UTC	Universal Time Coordinate
UTIAS	University of Toronto Institute for Aerospace Studies
UWE-3	University Würzburgs Experimentalsatellit 3
UV	University of Vienna
VHF	Very High Frequency
VKI	von Karman Institute of Fluid Dynamics
VM	Virtual Machine
VPN	Virtual Private Network
VSWR	Voltage Standing Wave Ratio
WAN	Wide Area Network
WOD	Whole Orbit Data

Bibliography

[1] W. Larson and J. Wertz, ed., *Space Mission Analysis and Design*. Space Technology Series, Space Technology Library, Third ed., 1999. (Cited on page 1 and 2.)

[2] European Space Agency, "ESA Tracking Stations," 2013. http://www.esa.int/Our_Activities/Operations/Estrack_tracking_stations. (Cited on page 2.)

[3] W. Larson and V. Alonsoperez and R. Qedar, ed., *Small Satellite Program Guide*. Space Technology Series, Space Technology Library, First ed., 2014. (Cited on page 3.)

[4] V. Alosoperez et al., "Guidebook on Small Satellite Programs," 2011. Final Report. International Space University, Space Studies Program 2011. (Cited on page 3.)

[5] P. Romano, M. Unterberger, and O. Koudelka, "BRITE-Austria Ground Segment and Distributed Operations Concept," in *Proceedings of the IAF Congress 2012*, 10 2012. (Cited on page 4, 10 and 115.)

[6] ITU, "International Telecommunication Union Web Page," 2013. http://www.itu.int/. (Cited on page 4.)

[7] IARU, "International Radio Amateur Union Web Page," 2013. http://www.iaru.org/. (Cited on page 4.)

[8] P. Romano and M. Unterberger and M. Bergmann, *Small Satellite Program Guide*, Chapter 9: BRITE-Austria/TUGSAT-1: First Austrian Nanosatellite - Case Study, pp. 200–250. Space Technology Series, Space Technology Library, First ed., 2014. (Cited on page 4, 147 and 156.)

[9] GENSO, "Global Education Network for Satellite Operations," 2012. http://www.genso.org. (Cited on page 4.)

[10] H. Page, M. Gil, P. Beavis, and F. Aguado, "GENSO: A Report on the Early Operational Phase," in *Proceedings of the IAF Congress 2010*, 09 2010. (Cited on page 4.)

[11] European Space Agency, "ESA's New VEGA Launcher Scores Success on Maiden Flight," 2012. http://www.esa.int/Our_Activities/Launchers/Launch_vehicles/Vega3/ESA_s_new_Vega_launcher_scores_success_on_maiden_flight. (Cited on page 4.)

[12] QB50, "The QB50 Project," 2012. http://www.qb50.eu. (Cited on page 5.)

[13] S. Billeter, M. Richard, "Satellite Control Software (QB50 SCS)," Presented at the 7th QB50 Workshop in Brussels, Belgium, 2014. (Cited on page 6.)

[14] P. Beavis, "ESOC CubeSat Ground Station Network," Presented at the 7th QB50 Workshop in Brussels, Belgium, 2014. (Cited on page 6.)

[15] O. Koudelka, G. Egger, B. Josseck, N. Deschamps, C. Grant, D. Foisy, R. Zee, W. Weiss, R. Kuschnig, A. Scholtz, and W. Keim, "TUGSAT-1/BRITE-AUSTRIA - The first Austrian Nanosatellite," in *Proceedings of the IAF Congress 2006*, 10 2006. (Cited on page 9.)

[16] BRITE-Constellation Web Page, "BRITE-Constellation: Nanosatellites for Astrophysics," 2013. `http://brite-constellation.at/`. (Cited on page 9 and 15.)

[17] BRITE Poland, "BRITE-PL First Polish Scientific Satellite Web page," 2013. `http://www.brite-pl.pl/pliki/main_en.html`. (Cited on page 9.)

[18] UTIAS/SFL, "Canada adds two satellites to BRITE Constellation," 2012. `http://www.utias-sfl.net/RecentNews/news-20110119.html`. (Cited on page 9.)

[19] A. Moffat, W. Weiss, S. Rucinski, R. Zee, M. van Kerkwijk, S. Mochnacki, J. Matthews, J. Percy, P. Ceravolo, and C. Grant, "The Canadian BRITE NanoSatellite Mission," in *38th COSPAR Scientific Assembly*, 07 2010. (Cited on page 9.)

[20] W. W. Weiss, S. M. Rucinski, A. F. J. Moffat, A. Schwarzenberg-Czerny, O. F. Koudelka, C. C. Grant, R. E. Zee, R. Kuschnig, S. Mochnacki, J. M. Matthews, P. Orleanski, A. Pamyatnykh, A. Pigulski, J. Alves, M. Guedel, G. Handler, G. A. Wade, K. Zwintz, and the CCD Photometry Tiger Teams, "BRITE-Constellation: Nanosatellites for Precision Photometry of Bright Stars," in *Proceedings of the International Astronomical Union, IAU Symposium, Volume 301, pp. 67-68*, 02 2014. (Cited on page 9.)

[21] M. Unterberger, P. Romano, and O. Koudelka, "New Telemetry System Design for Future Nanosatellite Missions," in *Proceedings of the IAF Congress 2010*, 10 2010. (Cited on page 9.)

[22] Austrian Research Promotion Agency, "Austrian Space Applications Programme Web Page," 2013. `http://www.ffg.at/austrian-space-applications-programme`. (Cited on page 9.)

[23] TUGSAT-1/BRITE-Austria, "TUGSAT-1/BRITE-Austria Web Page," 2013. `http://www.tugsat.at/`. (Cited on page 10.)

[24] M. Unterberger, B. Jossek, O. Koudelka, "BRITE-Austria Detailed Design Document," 2009. (Cited on page 10.)

[25] A. S. Tanenbaum, *Computer Networks*. Prentice Hall, Fourth Edition, 2003. (Cited on page 11.)

[26] M. Unterberger, B. Jossek, O. Koudelka, "BRITE-Austria: Communication Systems Design Critical Design Document," 2008. (Cited on page 13.)

[27] P. Romano, M. Unterberger, "BRITE-Austria UHF Receiver Rev.4 Unit Level Test Results," 2012. (Cited on page 17.)

[28] P. Romano, M. Unterberger, "BRITE-Austria S-band Telemetry Transmitter Unit Level Test Results," 2011. (Cited on page 20.)

[29] A. Steinkellner, M. Unterberger, P. Romano, "BRITE-Austria: Flatsat Qualification Test Report," 2011. (Cited on page 24.)

[30] C. Grant, "BRITE Assembly Integration, and Test (AIT) Plan," 2009. (Cited on page 25.)

[31] M. Unterberger, P. Romano, "BRITE-Austria: Electromagnetic Compatibility Test Procedure & Results," 2011. (Cited on page 26.)

[32] M. Unterberger, P. Romano and R. Kuschnig, "BRITE-Austria: Open Field Test Procedure & Results," 2011. (Cited on page 31.)

[33] M. Unterberger, B. Jossek, O. Koudelka, "BRITE-Austria Ground Station Requirements Document," 2007. (Cited on page 36 and 37.)

[34] A. Maini and V. Agraval, *Satellite Technology: Principles and Applications*. Wiley, 2007. (Cited on page 36.)

[35] M. Unterberger, B. Jossek, O. Koudelka, "BRITE-Austria: Ground Station Hardware Design Critical Design Document," 2008. (Cited on page 38.)

[36] P. Romano, "BRITE-Austria/TUGSAT-1 Ground Station Hardware Manual," 2012. (Cited on page 38.)

[37] K. Rothammel and A. Krischke, *Antennen Buch*. DARC Verlag Baunatal, 12. aktualsierte Auflage, 2001. (Cited on page 58.)

[38] L. Ippolito, *Satellite Communications System Engineering*. Wiley, 2008. (Cited on page 67, 70 and 87.)

[39] G. Maral and M. Bousquet, *Satellite Communications Systems: Systems, Techniques and Technology*. Wiley, fifth ed., 2009. (Cited on page 67, 87 and 107.)

[40] S. Saunders and A. Zavala, *Antenna and Propagation for Wireless Communication Systems*. Wiley, 2nd Edition, 1999. (Cited on page 67.)

[41] S. Cakaj and K. Malaric, "Rain attenuation modelling for low earth orbiting satellite ground station at S-band in Europe," in *The 18th IASTED International Conference on Modelling and Simulation*, 05 2007. (Cited on page 67.)

[42] S. Cakaj, B. Kamo, I. Enesi, and O. Shurdi, "Antenna Noise Temperature for Low Earth Orbiting Satellite Ground Stations at L and S Band," in *Proceedings of The Third International Conference on Advances in Satellite and Space Communications (SPACOMM 11)*, 04 2011. (Cited on page 67.)

[43] W. Keim, "Scientific Satellite Ground Station at 2GHz in Urban Environment," 2004. Doctoral Thesis. (Cited on page 67, 93, 107 and 108.)

[44] A. V. Kantak, S. D. Slobin, “Atmosphere Attenuation and Noise Temperature Models at DSN Antenna Locations for 145 GHz,” 2009. NASA JPL Publication. (Cited on page 69.)

[45] S. Cakaj, W. Keim, and K. Malaric, “Sun Noise Measurement at Low Earth Orbiting Satellite Ground Station,” in *47th International Symposium ELMAR-2005*, 06 2005. (Cited on page 70.)

[46] Rohde & Schwarz, “The Y Factor Technique for Noise Figure Measurements,” 2012. Application Note. (Cited on page 70.)

[47] Australian Government - Radio and Space Weather Services, “Learmonth Observatory - Quiet Solar (IFLUX),” 2012. http://www.ips.gov.au/Solar/3/4/2. (Cited on page 73.)

[48] R. Heine, “Elektrische Feldstärke und Antennenfaktor,” 2013. METRIX Electromagnetics Ltd. AN011: http://www.metrix-em.de/AN011.pdf. (Cited on page 75.)

[49] DSN Document Release, “DSN Telecommunications Link Design Handbook - 104, Rev. F 34-m BWG Stations Telecommunications Interfaces,” 2010. (Cited on page 76.)

[50] G. Hörack, “Modellierung des TUGSAT-Kommunikationssystems,” 2013. Bachelor Thesis. (Cited on page 81 and 83.)

[51] Rundfunk und Telekom Regulierungs-GmbH (RTR-GmbH), “2100 MHz paired Spectrum,” 2014. https://www.rtr.at/en/tk/Spectrum2100MHzFDD. (Cited on page 83.)

[52] O. Koudelka, *Nachrichtensatelliten - Skriptum zur Lehrveranstaltung*. Skriptenreferat der Hochschülerschaft an der TU Graz GmbH, 1999. (Cited on page 87.)

[53] E.Türkyilmaz, M.Bergmann, and W.Gappmair, “Nachrichtentechnik Labor - Digitale Modulationsverfahren und Kanalcodierung: Grundlagen,” 2013. Laborskriptum. (Cited on page 87 and 126.)

[54] K.Carroll, R.Zee, and J.Matthews, “The MOST Microsatellite Mission: Canadas First Space Telescope,” in *12th AIAA/USU Conference on Small Satellites*, 08 1998. (Cited on page 93.)

[55] H. Helvajian and S. Janson, *Small Satellites: Past, Present, and Future*. AIAA, 2009. (Cited on page 93.)

[56] UTIAS/SFL, “The CanX-6 - NTS Mission,” 2011. http://www.utias-sfl.net/nanosatellites/CanX6/. (Cited on page 95.)

[57] Datum Systems, “PSM-500 Series Programmable SCPC/VSAT Modem Feature Matrix,” 2008. (Cited on page 99.)

[58] O. Montenbruck and E. Gill, *Satellite Orbits: Models, Methods, and Applications*. Springer, 2000. (Cited on page 106.)

[59] P. Romano, M. Unterberger, R. Kuschnig, and O. Koudelka, “BRITE-Austria Mission Operations Phase - First Results and Lessons Learned,” in *Proceedings of the IAF Congress 2014*, 10 2014. (Cited on page 110, 120, 136, 151, 153 and 155.)

[60] M. Unterberger, B. Jossek, O. Koudelka, “BRITE-Austria Ground Segment Software Architecture and Design - Critical Design Document,” 2008. (Cited on page 114.)

[61] D. Kekez, “BRITE Ground Segment Software Architecture,” 2012. (Cited on page 117 and 122.)

[62] P. Romano, M. Unterberger, O. Koudelka, “BRITE-Austria Ground Segment Software Architecture and Design - Software Design Document,” 2008. (Cited on page 117, 118, 153 and 155.)

[63] T. Tuli, N. Orr, and R. Zee, “Low Cost Ground Station Design for Nanosatellite Missions,” in *Proc. of 24th AMSAT North American Space Symposium*, 10 2006. (Cited on page 118.)

[64] Celestrak Web Page, “NORAD Two-Line Element Sets Current Data,” 2013. `http://celestrak.com/NORAD/elements/`. (Cited on page 121.)

[65] Space-Track, “Space-Track Web Page,” 2013. `https://www.space-track.org/`. (Cited on page 121.)

[66] D. L. Mills, “Internet Time Synchronization: the Network Time Protocol,” in *IEEE Transactions on Communications (Volume:39, Issue: 10)*, 10 1991. (Cited on page 136.)

[67] D. Kekez, “BRITE Constellation Operation,” 2012. (Cited on page 137.)

[68] Indian Space Research Organisation (ISRO), “Polar Satellite Launch Vehicle (PSLV),” 2013. `http://www.isro.org/launchvehicles/PSLV/pslv.aspx`. (Cited on page 138.)

[69] Indian Space Research Organisation (ISRO), “PSLV-C20/SARAL Mission Brochure,” 2013. `http://www.isro.org/pslv-c20/pdf/brochure.pdf`. (Cited on page 138.)

[70] Nanosatellite Launch Services 8 Web page, “BRITE-Constellation: Nanosatellites for Astrophysics,” 2013. `https://www.utias-sfl.net/NLS-8/`. (Cited on page 138.)

[71] C. Grant, M. Dwyer, K. Sarda, D. Kekez and J. Lifshits, “BRITE Commissioning and Operations Overview,” 2012. (Cited on page 140, 150 and 151.)

[72] P. Romano, M. Unterberger, “TUGSat-OPS-RP001 Power System Reset Recovery,” 2013. (Cited on page 148.)

[73] UTIAS/SFL, “BRITE Contingency and Recovery Procedures,” 2012. (Cited on page 148 and 149.)

[74] M. Unterberger, P. Romano, “BRITE-Austria: ASAP7 - WP04 Report Satellite Operations,” 2013. (Cited on page 151, 152 and 154.)

[75] M. Unterberger, P. Romano, M. Bergmann, R. Kuschnig, and O. Koudelka, “Experience in Commissioning and Operations of the BRITE-Austria Nanosatellite,” in *Proceedings of the IAF Congress 2013*, 9 2013. (Cited on page 152 and 157.)

[76] M. Unterberger, P. Romano, “BRITE-Austria: ASAP7 - WP03 Report Satellite Commissioning,” 2013. (Cited on page 153.)

[77] P. Romano, M. Unterberger, R. Kuschnig, “BRITE-Austria: ASAP7 - WP04 Report Attitude and Payload Performance, Calibration and Optimization,” 2014. (Cited on page 153 and 169.)

[78] D. Kekez, "Nanosatellite Protocol (NSP) Versions 3 and 4," 2013. (Cited on page 164 and 167.)

[79] Universität Würzburg, "UWE-3 News," 2014. http://www7.informatik.uni-wuerzburg.de/forschung/space_exploration/projects/uwe_3/uwe_3_news/. (Cited on page 171.)

[80] GomSpace, "GomSpace GOMX-1," 2014. http://gomspace.com/index.php?p=gomx1. (Cited on page 171.)

[81] AMSAT-UK, "FUNcube-1 Mission Overview," 2014. http://funcube.org.uk/. (Cited on page 171.)

[82] S. Busch, P. Bangert, S. Dombrovski, and K. Schilling, "UWE-3, In-Orbit Performance and Lessons Learned of a Modular and Flexible Satellite Bus for Future Picosatellite Formations," in *Proceedings of the IAF Congress 2014*, 10 2014. (Cited on page 175.)

[83] The Consultative Committee for Space Data Systems, "The Official Web Site," 2013. http://public.ccsds.org. (Cited on page 185.)

[84] M. Lülfl, "NGS-1 Baseband," 2013. ESA/ESOC TN, Issue 1.1. (Cited on page 185.)

[85] National Instruments, "USRP," 2015. http://www.ni.com/sdr/usrp/. (Cited on page 185.)

[86] GNU Radio, "GNU Radio," 2013. http://gnuradio.org/. (Cited on page 185.)

[87] V. Cerf, S. Burleigh, A. Hooke, L. Torgerson, R. Durst, K. Scott, K. Fall, H. Weiss, *Delay-Tolerant Network Architecture*. IETF RFC 4838, Informational, 2007. (Cited on page 191.)

[88] DTNRG, "Delay tolerant networking research group - web site," 2009. http://www.dtnrg.org. (Cited on page 191.)

[89] P. Romano, M. Unterberger, and O. Koudelka, "Next-Generation Communication Protocol Concepts for Future Nanosatellite Constellations," in *Acta Astronautica, Volume 67, Issues 9-10, November December 2010, Pages 1126-1131*, 12 2010. (Cited on page 191.)

[90] P. Schrotter, P. Romano, "Current Developments of Interplanetary Internet," 2009. Interplanetary Communication - Action 1: Requirements Analysis, Technical Note. (Cited on page 191.)

[91] European Space Agency, "OPS-SAT," 2014. http://www.esa.int/Our_Activities/Operations/OPS-SAT. (Cited on page 199.)

[92] European Space Agency, "OPS-SAT Mission Requirements Document," 2014. DHSO-MIS-RS-1001. (Cited on page 199.)